수의학박사학위논문

Cross-talks between Nuclear factor erythroid-2-related factor 2 signaling and peroxisome activity in porcine oocyte and embryo by treatment with melatonin and phytanic acid

멜라토닌과 피탄산 처리에 따른 돼지 난자 및 배아 내
Nuclear factor erythroid-2-related factor 2
기전 및 퍼옥시좀 활성의 관계 분석

2021 년 2 월

서울대학교 대학원
수의학과 임상수의학(수의산과·생물공학) 전공
김의현

Cross-talks between Nuclear factor erythroid-2-related factor 2 signaling and peroxisome activity in porcine oocyte and embryo by treatment with melatonin and phytanic acid

A THESIS SUBMITTED TO THE GRADUATE SCHOOL OF SEOUL NATIONAL UNIVERSITY IN PARTIAL FULFILLMENT OF THE REQUIREMENT FOR THE DEGREE OF DOCTOR OF PHILOSOPHY IN VETERINARY CLINICAL SCIENCE

Major in Veterinary Clinical Sciences
(Theriogenology and Biotechnology)
College of Veterinary Medicine
Graduate School of Seoul National University

By

Eui Hyun Kim

December 2020

Declaration

This thesis is submitted by the undersigned for examination for the degree of Doctor of Philosophy to the Seoul National University. This thesis has not been submitted for the purposes of obtaining any other degree or qualification from any other academic institution.

I hereby declare that the composition and experiment of this thesis and the work presented in it are entirely my own.

Eui Hyun Kim

멜라토닌과 피탄산 처리에 따른 돼지 난자 및 배아 내 Nuclear factor erythroid-2-related factor 2 기전 및 퍼옥시좀 활성의 관계 분석

지도교수 윤 화 영

이 논문을 수의학 박사학위논문으로 제출함

2020 년 10 월

서울대학교 대학원

수의학과 임상수의학(수의산과·생물공학) 전공

김의현

김의현의 박사학위논문을 인준함

2020 년 12 월

위 원 장 위 한 상 (인)

부위원장 윤 화 영 (인)

위 원 박 세 창 (인)

위 원 김 건 아 (인)

위 원 정 진 영 (인)

Cross-talks between Nuclear factor erythroid-2-related factor 2 signaling and peroxisome activity in porcine oocyte and embryo by treatment with melatonin and phytanic acid

Major in Veterinary Clinical Sciences
(Theriogenology and Biotechnology)
College of Veterinary Medicine
Graduate School of Seoul National University

We hereby approve the thesis of Eui Hyun Kim for the Degree of Doctor of Philosophy in Veterinary Clinical Science

HAN SANG YOO
육 화 영
박 시 창
김 건 아
정 진 영

December 2020

Cross-talks between Nuclear factor erythroid-2-related factor 2 signaling and peroxisome activity in porcine oocyte and embryo by treatment with melatonin and phytanic acid

Eui Hyun Kim

(Supervised by Prof. Hwa Young Youn, D.V.M., Ph.D.)

Major in Veterinary Clinical Sciences

(Theriogenology and Biotechnology)

College of Veterinary Medicine

Graduate School of Seoul National University

ABSTRACT

Pigs have been dedicated to biomedical research for models of human disease and xenotransplantation because they share similarities with humans, such as sizes of organs, physiology, as well as diets. Moreover, pigs are a multiparous species that make simple approaches for researchers applicable in *in vitro* production (IVP). IVP is the fundamental step for producing transgenic animals and *in vitro* maturation

(IVM) of oocytes and *in vitro* culture (IVC) of embryos, which are the main procedures used during IVP. However, successful IVM and IVC remain unaccomplished. Although well-controlled culture conditions and environments, as well as quality of oocytes and handling are pivotal for improving success rates of IVM and IVC, damages from oxidative stress (OS) on gametes and embryos are considered a major task for research. Numerous trials for preventing OS such as antioxidative chemical treatments or genetic modifications by assisted reproduction techniques have been implemented. Recently, some studies suggested the importance of signaling pathways and their regulations in mammalian oocytes and embryos. The signaling pathways that regulate OS are receiving attention from research and among them, the nuclear factor erythroid-2-related factor 2 (Nrf2) signaling pathway is known to be one of the strongest antioxidative pathways.

Another aspect for improving the success rate of IVM and IVC is lipid metabolism regulations within oocytes and embryos. Chemicals such as melatonin and phytanic acid (PA) are known to regulate lipid metabolism in porcine species. It is reported that upregulation of lipid oxidation leads to increased oocyte maturation and embryonic development, in the meantime, producing ATP. Peroxisomal activities such as Peroxin family activation, α- and β-oxidation of fatty acids (FAs), short-chained FA transportation to mitochondria and defense mechanisms against OS are also known to reduce OS and increase ATP production. In addition, there are reports that the Nrf2 signaling pathway is involved not only in antioxidant mechanisms, but also in lipid metabolism in mammalian gametes and embryos. Therefore, this study attempted to investigate a possible synergistic relationship

between the Nrf2 signaling pathway and peroxisomal activities in porcine oocytes and embryos.

First, in order to investigate whether the Nrf2 signaling pathway is involved in porcine embryos, IVM of porcine oocytes along with *in vitro* fertilization (IVF) was performed. Melatonin was treated during IVC of porcine embryos and activation of the Nrf2 signaling pathway was evaluated by real time PCR and immunocytochemistry. In addition, brusatol, an *Nrf2*-specific inhibitor, was also treated during IVC to validate the signaling pathway. As a result, 10^{-7} melatonin significantly increased the embryonic development and upregulated the Nrf2 signaling pathway ($P < 0.05$), which was verified by gene and protein expressions in porcine embryos. Therefore, it can be concluded that melatonin mediates the Nrf2 signaling pathway and the pathway is regulated significantly in porcine embryos.

Next, the peroxisomal activities in porcine oocytes were investigated. PA is a long and branched FA, which is digested by α- and β- oxidation in peroxisomes, resulting in FA shortening. Subsequently, the short-chained FAs are transported to mitochondria for ATP synthesis. In this experiment, IVM and IVF were performed and real time PCR, immunocytochemistry, staining of reactive oxygen species (ROS) and glutathione (GSH), BODIPY, and mitochondrial membrane potential (MMP) were employed to evaluate the peroxisomal activities in porcine oocytes. Through the selection of optimal PA concentration during IVM, it was found that 40 μM PA significantly increased the maturation rate of oocytes and the cumulus cell expansion rate ($P < 0.05$). Moreover, PA significantly upregulated the activities of peroxisomes in porcine oocytes, which was tested by gene and protein expressions related to the

peroxisomal activities ($P < 0.05$). Furthermore, lipid metabolism, MMP, and ATP contents were also upregulated by PA ($P < 0.05$). Therefore, it can in part be concluded that there was strong participation of peroxisomal activities were found in porcine oocytes.

The actions of Nrf2 signaling along with peroxisomal activities in porcine oocytes were then investigated. The study was done using IVM with melatonin and brusatol treatment and parthenogenetic activation. Then, real time PCR, immunocytochemistry, ATP and ROS/GSH staining, RNA sequencing, and western blot were used to verify the mechanism. Primarily, the inhibitory effect of brusatol was tested during porcine IVM and it was found that 12 nM brusatol was the optimal concentration. Thereafter, 10^{-9} M melatonin and 12 nM brusatol were treated on porcine oocytes and then, the embryonic development was evaluated. Gene (including sequencing) and protein expression analysis showed that the peroxisomal activities were significantly upregulated by melatonin and the signal of Nrf2 was also influenced by the activities of peroxisomes ($P < 0.05$). Thus, it can be concluded that the connection between Nrf2 signaling and peroxisomal activities might be significant in porcine oocytes.

For the last experiment, the cross talk between Nrf2 signaling and peroxisomal activities in porcine embryos was investigated. A combination of melatonin and PA was used as treatment during IVC of porcine embryos and *Pex19*-targeted siRNA was applied to knockdown the peroxisome actions. IVM, parthenogenetic activation, immunocytochemistry, real time PCR, and BODIPY staining were employed in this experiment. As a result, the combination group showed a sharp increase in rates of

embryonic development ($P < 0.05$). Moreover, the knockdown of the peroxisomal activities was clearly observed by gene and protein expressions ($P < 0.05$). Most importantly, when the combination group was treated with a siRNA-injected group, an effect of recovery was significantly observed by gene and protein expressions ($P < 0.05$), including staining of ATP, FA, and MMP.

In conclusion, it was demonstrated that melatonin and PA treatments mediated the cross talk between the Nrf2 signaling pathway and the peroxisomal activities in porcine oocytes and embryos. Moreover, they influenced lipid metabolism, ATP synthesis, and MMPs. Additionally, the cross talk was found to be effective against OS. Therefore, the regulation of cross talk between the Nrf2 signaling pathway and peroxisomal activities might be indispensable for improvements of porcine oocyte maturation and embryonic development.

……

Key word: Antioxidant, embryo development, lipid metabolism, Nrf2 signaling, peroxisome, pig, oocyte maturation

Student Number: 2018-25700

TABLE OF CONTENTS

ABSTRACT..... **i**

TABLE OF CONTENTS..... **vi**

LIST OF TABLES..... **ix**

LIST OF FIGURES..... **xi**

LIST OF ABBREVIATIONS..... **xv**

PART I. GENERAL INTRODUCTION..... **1**

1. Introduction..... **2**

2. Literiture review..... **12**

PART II. GENERAL METHODOLOGY..... **32**

1. Animals and chemicals..... **33**

2. *In vitro* maturation..... **33**

3. Parthenogenetic activation..... **34**

4. *In vitro* fertilization..... **35**

5. Real time PCR..... **36**

6. Statistical analysis..... **37**

PART III. THE ROLES OF NRF2 SIGNLAING AND PEROXISOMAL ACTIVITIES IN PORCINE OOCYTES AND EMBRYOS..... 38

Chapter I. Involvement of Nrf2/ARE signaling through regulation of melatonin and brusatol in porine embryos..... **41**

1. Introduction..... **41**

2. Materials and methods..... **44**

3. Results..... **49**

4. Discussion..... **64**

Chapter II. Involvement of phytanic acid-induced peroxisomal activity in porcine oocytes and embryos..... **70**

1. Introduction..... **70**

2. Materials and methods..... **73**

3. Results..... **86**

4. Discussion..... **110**

PART IV. CROSS-TALK BETWEEN NRF2 SIGNALING AND PEROXISOMAL ACTIVITY IN OOCYTES AND EMBRYOS **117**

Chapter I. Melatonin-induced Nrf2 signaling influences peroxiosmal activities in porcine oocytes **120**

1. Introduction **120**

2. Materials and methods **123**

3. Results **131**

4. Discussion **165**

Chapter II. Peroxisome-derived lipid metabolism influences Nrf2 signaling via the co-treatment of melatonin and phytanic acid in porcine embryos **171**

1. Introduction **171**

2. Materials and methods **174**

3. Results **183**

4. Discussion **205**

GENERAL CONCLUSION **210**

PUBLICATION LISTS **214**

REFERENCES **219**

국문초록 **260**

LIST OF TABLES

Table 1. **The use of pig organs and survival of organs from transgenic pigs into non-human primates** **3**

Table 2. **Demonstrated signaling pathways that are regulated in mammalian reproductive cells, gametes and embryos** **7**

Table 3. **A list of genetically modified pigs** **14**

Table 4. **A list of treated chemicals during mammalian IVM** **18**

Table 5. **The composition of modified Tris-buffered medium (mTBM)** **22**

Table 6. **Information on primer sequences for real-time PCR** **48**

Table 7. **Effect of melatonin during IVC on embryonic development after IVF** **53**

Table 8. **Effect of brusatol during IVC on embryonic development after IVF** **54**

Table 9. **Co-treatment effects of melatonin and brusatol during IVC on embryonic development after IVF** **55**

Table 10. **Primer sequences related to oocyte competence and cumulus expansion** **81**

Table 11. **Primer sequences related to antioxidant and apoptosis** **82**

Table 12. Primer sequences related to peroxisome activities..... 83

Table 13. Primer sequences related to lipid metabolism..... 84

Table 14. Primer sequences related to mitochondria..... 85

Table 15. Primers used for quantification of differential expressed transcripts..... 130

Table 16. Raw data of sequencing from mature COCs..... 147

Table 17. Trimmed data of sequencing from mature COCs..... 148

Table 18. Result of mapped data from cDNA fragments..... 149

Table 19. List of candidate siRNAs targeting Pex19 and scramble siRNA..... 180

Table 20. Sequence-specific primers used for quantification of differential expressed transcripts..... 181

LIST OF FIGURES

Figure 1.	**The outline of the thesis**	**11**
Figure 2.	**A brief flow of the Nrf2 signaling pathway with basal and stressed conditions**	**28**
Figure 3.	**A schematic illustration of the peroxisomal activity and its influences on lipid metabolism and antioxidant mechanism**	**31**
Figure 4.	**Effect of 10-7 M melatonin on expression of Nrf2/ARE signaling pathway related genes in IVF-derived porcine blastocysts**	**56**
Figure 5.	**Immunocytochemical analysis of MT2 in porcine blastocysts**	**58**
Figure 6.	**Immunocytochemical analysis of Nuclear factor erythroid 2-related factor 2 in porcine blastocysts**	**60**
Figure 7.	**Immunocytochemical analysis of Kelch-like ECH-associated protein 1 in porcine blastocysts**	**62**
Figure 8.	**Optimization of phytanic acid (PA) concentration through the assessment of oocyte maturation, cumulus expansion assessment, and mRNA transcript expressions**	**92**
Figure 9.	**Assessment of the effect of 40 μM PA on IVF-derived embryonic development, oocyte antioxidant, and apoptosis level**	**94**
Figure 10.	**Evaluation of the peroxisomal activities in matured porcine oocytes**	**96**
Figure 11.	**Assessment of lipid metabolism in porcine oocytes. oocytes**	**98**
Figure 12.	**Evaluation of mitochondrial potentials in porcine oocytes**	**100**

Figure 13. **Several genes related to apoptosis (BCL2 and BAX), antioxidant (CAT), peroxisomal activities (PHYH, PEX3, PEX5, PEX12, PEX19, PPARα, and PPARγ), (d) lipid metabolism (ATGL, HSL, MGLL, CGI58, and PLIN2), and mitochondria (NRF1, PGC-1α, and TFAM) were analyzed in porcine CCs from two experimental groups (control vs. 40 μM PA) by real time PCR** **102**

Figure 14. **The effect of PA was tested during IVC of porcine embryos and concentrations of PA was ranged 0, 20, 40, and 80 μM** **105**

Figure 15. **The effect of PA was tested during IVC of porcine embryos** **108**

Figure 16. **Selection of optimal brusatol concentration via the assessment of embryo development and cumulus expansion. Brusatol concentrations: 0, 50, 200, and 400 nM (first concentration range); 0, 6, 12, and 25 nM (second concentration range)** **139**

Figure 17. **Evaluation of treatments with melatonin and brusatol on porcine COCs and their competences. With the treatment of 10^{-9}M melatonin and 12 nM brusatol, their effects on the CC expansion and subsequent embryonic development were evaluated** **142**

Figure 18. **Determination of ATP production and GSH and ROS levels in porcine oocytes** **145**

Figure 19. **Raw data and trimmed read counts in porcine COCs from RNA sequencing** **150**

Figure 20. **General gene expressions in porcine COCs from the four experimental groups (control, melatonin, brusatol, and co-treatment)** **152**

Figure 21. **Evaluation of sample reproducibility and results of the top 10 terms of GO functional analysis..... 154**
Figure 22. **Assessments of genes of interest by qRT-PCR and protein expression analysis by immunocytochemistry in porcine COCs..... 159**
Figure 23. **Protein analysis of protein of interest in porcine COCs by immunocytochemistry and western blotting..... 161**
Figure 24. **A schematic illustration of the cross-talk between Nrf2 signaling and peroxisomes activated by melatonin in porcine COCs..... 163**
Figure 25. **Assessments of porcine embryonic development treated with melatonin, phytanic acid (PA), and injected with Pex19-targeted siRNAs..... 189**
Figure 26. **Gene expression evaluations of melatonin/PA treatment and Cnd3-injection on porcine 2-cell embryos..... 191**
Figure 27. **Gene expression evaluations of melatonin/PA treatment and Cnd3-injection on porcine blastocysts..... 193**
Figure 28. **Immunocytochemical analysis of NRF2 in porcine 2-cell embryos and blastocysts. Fluorescence microscopy was applied to obtain images of embryos..... 195**
Figure 29. **Immunocytochemical analysis of PEX19 in porcine 2-cell embryos and blastocysts. Fluorescence microscopy was applied to obtain images of embryos..... 197**
Figure 30. **Immunocytochemical analysis of PHYH in porcine 2-cell embryos and blastocysts. Fluorescence microscopy was applied to obtain images of embryos..... 199**
Figure 31. **BODIPY staining analysis of ATP contents and fatty acids in blastocysts. Fluorescence microscopy was applied to obtain images of the blastocysts..... 201**

Figure 32. JC-1 mitochondrial membrane potential (MMP) staining in blastocysts. Fluorescence microscopy was applied to obtain images of the blastocysts..... **203**

LIST OF ABBREVIATIONS

ANOVA	**Analysis of variance**
AI	**Artificial insemination**
ARE	**Antioxidant responsive elements**
ART	**Assisted reproduction technology**
BSA	**Bovine serum albumin**
cDNA	**Complementary DNA**
COC	**Cumulus oocyte complex**
DC	**Direct current**
DMSO	**Dimethyl sulfoxide**
eCG	**Equine chorionic gonadotropin**
ELISA	**Enzyme-linked immunosorbent assay**
FA	**Fatty acid**
FBS	**Fetal bovine serum**
GPCR	**Guanine nucleotide binding protein protein-coupled receptors**
GSH	**Glutathione**
h	**Hour**
hCG	**Human chorionic gonadotropin**
HEPES	**Sodium hydroxide, 10 mM N-piperazine-N'-[2-ethanesufonic acid]**
IACUC	**Institutional Animal Care and Use Committee**
ITS	**Insulin-transferrin-selenium**

IVC	***In vitro* culture**
IVF	***In vitro* fertilization**
IVM	***In vitro* maturation**
mTBM	**Modified Tris-buffered medium**
Nrf2	**Nuclear factor erythroid 2-related factor 2**
OS	**Oxidative stress**
PA	**Phytanic acid**
PFF	**Porcine follicular fluid**
PVA	**Polyvinyl alcohol**
PZM	**Porcine zygote medium**
qRT-PCR	**Quantitative real time polymerase chain reaction**
ROS	**Reactive oxygen species**
SCNT	**Somatic cell nuclear transfer**
TALP	**Tyrode's albumin lactate pyruvate**
TCM-199	**Tissue culture medium-199**
ZP	**Zona Pellucida**

PART I

GENERAL INTRODUCTION

1. Introduction

The roles of pigs have been fundamental in agriculture through their use in meat production, monetary management, and marketing throughout numerous countries. Moreover, ways of reducing the production costs and improving systemic environments are being attempted (Nagai, Funahashi et al. 2006; Crespo 2009). However, new and creative applications using the porcine species outside of the pig industry has been gaining attention, including their use in biomedical research and human medicine. About the continuous and severe shortage of human organs for transplantation, many hypotheses and suggestions have been made that claim organs from pigs may be used as a replacement for human organs (Shimokawa, Tomoike et al. 1983; Cooper 1991). The promises of the usage of pigs was proposed by researchers in this field who were conducting research mainly with lungs, livers, and hearts, as well as many other accessory organs. (Ramirez, Chavez et al. 2000; Tseng, Kuwaki et al. 2005; Bush, Barbas et al. 2011; Mohiuddin, Singh et al. 2016; Shah, Navarro-Alvarez et al. 2016; Iwase, Hara et al. 2017). This trend insinuates that the use of pigs as disease models and xenotransplantation may now be expanding in animal industries. The history of the use of pig organs transplanted to non-human primates has been given in Table 1.

In order to improve the success rates of the production of genetically modified pigs, assisted reproduction techniques (ARTs) such as somatic nuclear transfer

Table 1. The use of pig organs and survival of organs from transgenic pigs into non-human primates.

Type of graft	Type of genetic modification	Longest survival time (Days)	Year
Heart (heterotopic transplantation)	GTKO, CD46, TM	945	2016
	GTKO, CD46	236	2012
	GTKO	179	2005
Heart (orthotopic transplantation)	CD46	57	2011
	GTKO, CD46, TM	40	2017
Kidney	GTKO, CD55	310	2016
	GTKO, CD46, CD55, EPCR, TFPI, CD47	237	2017
	CD55	229	2003
	GTKO, CD46, CD55, TM, EPCR, CD39	136	2015
	CD55	39	2000
Liver (orthotopic transplantation)	GTKO	25	2016
	CD55	8	2000
Lung (orthotopic transplantation)	vWF-KO	109 h	2007
	GTKO, CD46	48 h	2011

Adopted from (Hryhorowicz, Zeyland et al. 2017)

(SCNT), microinjection, intracytoplasmic sperm injection (ICSI), and *in vitro* fertilization (IVF) had been developed and are gaining ground. With ARTs, researchers are provided accurate methodologies and appropriate environments to produce genetically modified or cloned pigs. Before the ARTs can be improved, there are basic cornerstones of the technique that need to be refined, including *in vitro* culture (IVC) of oocytes and embryos. Therefore, manipulations techniques using oocytes and embryos *in vitro* have been gaining attention. Mukherji et al. first suggested the possibility of maturing mice oocytes *in vitro* (Mukherjee. 1972), there have been numerous trials of *in* vitro manipulation in pig oocytes and embryos, which resulted in the production of an *in vitro*-manipulated piglet in 1989 (Mattioli, Bacci et al. 1989). However, the *in vitro* system still had numerous problems pertaining to culture conditions, oxidative stress (OS) and media compositions (Polejaeva & Campbell 2000; Nakano, Kato et al. 2012; Ma, Li et al. 2017; Ma, Liang et al. 2018; Kim, Kim et al. 2019). In regard to these problems, it is suggested that the production of high quality blastocysts and their transfer to surrogates can be done using a low oxygen IVC system (Kikuchi, Onishi et al. 2002); moreover, studies that followed suggested the success of porcine IVC systems by treating the systems with antioxidant chemicals to reduce reactive oxygen species (ROS) (Do, Shibata et al. 2015; Jin, Lee et al. 2017; Kim, Lee et al. 2017a; Lee, Jin et al. 2017; Liang, Jin et al. 2017; Lee, Jin et al. 2018b; Kim, Kim et al. 2019; Kim, Kim et al. 2020).

Regarding the suggested gas composition during the development of IVC in the 20th century, oxygen was used at up to 20% of the total gas composition when

IVC was first developed, which is most definitely higher than the composition of the oxygen *in vivo* (Wright 1977). A subsequent study reported that reducing the oxygen composition from 5% to 20% could be more helpful for the development of embryos (Iwamoto, Onishi et al. 2005). . Most researchers in the field use a gas composition comprising of 5% CO_2, 5% O_2, and 90% N_2. Using this gas composition, porcine embryos are cultured for approximately seven days. During this process, cells or embryos can be impaired by free radicals produced by ROS, which cause lipid peroxidation and inactivation of related enzymes (Ribarov & Benov 1981; Kikuchi, Onishi et al. 2002). Therefore, numerous studies have tried to reduce ROS by treating the systems with antioxidant chemicals such as melatonin, resveratrol, spermine, and phytanic acid (PA) (Jin, Lee et al. 2016; Lee, Jin et al. 2017, 2018a; Kim, Kim et al. 2020). The reported studies showed great improvements of *in vitro* maturation and culture systems in porcine species and even showed success of *in vitro* culture-induced piglets. These results suggest that a strong and confirmed protocol that led oocytes and embryos to be more competent by avoiding ROS is extremely fundamental to proceed to subsequent steps of research.

ATP is another important factor that has crucial roles in mammalian oocyte maturation and embryo development (Sturmey & Leese 2003; Kim, Ridlo et al. 2020). ATP is produced in many organelles, though mechanisms occurring inside the cytoplasm, and even from outer environments or circumstances (Jansen & Wanders 2006; Wanders & Waterham 2006). Among the mechanisms that produce ATP, it is suggested that ATP is mainly produced by the metabolism of lipids and fatty acids (FAs) (Wanders, Waterham et al. 2015). Some studies suggested that lipid

metabolism in porcine oocytes is significant in oocyte maturation during *in vitro* maturation (IVM) and IVC of porcine embryos (Prates, Nunes et al. 2014; Jin, Lee et al. 2017; Lowe, Bathgate et al. 2019). Moreover, it is partly suggested that the lipid metabolism and subsequent ATP production may be processed by peroxisomal activities (Figueroa, Kawada et al. 2000; Dunning, Cashman et al. 2010; Kim, Kim et al. 2020). According to several studies that suggest roles of the peroxisomal activities, β-oxidation and lipid metabolism, it was deduced that their connected roles might also occur in the cytoplasm of mammalian oocytes and embryos. In addition, there are numerous reports suggesting that some signaling might interplay with this lipid metabolism (Lee 2017). For example, the nuclear factor erythroid 2-related factor 2 (Nrf2) signaling pathway, glucagon receptor signaling, and hedgehog signaling are known to regulate lipid metabolism in mammalian cells (Matz-Soja, Rennert et al. 2016; Galsgaard, Pedersen et al. 2019; Kim, Ridlo et al. 2020). Therefore, it is important for research to corroborate exact mechanisms and cascades that mediate the lipid metabolism. A list of demonstrated signaling that are commonly known for significant intervention in reproductive cells, oocytes and embryos is shown in Table 2. Nrf2 signaling is especially powerful at signaling for the regulation of lipid metabolism. However, Nrf2 signaling is also known to mediate or be mediated by ROS and free radicals (Dong, Sulik et al. 2008; Akino, Wada-Hiraike et al. 2018). Thus, the significant roles of the Nrf2 signaling pathway are still gaining attention in research.

Table 2. Demonstrated signaling pathways that are regulated in mammalian reproductive cells, gametes and embryos.

Signaling pathway	Related factors	Cell type	Species	Year	Reference
Nrf2 signaling	Brusatol	Embryo	Cattle	2014	(Amin, Gad et al. 2014)
	Brusatol	Oocyte	Mouse	2017	(Ma, Li *et al.* 2017)
	Melatonin, Brusatol	Oocyte	Pig	2019	(Kim, Kim *et al.* 2019)
	Phytanic acid, Melatonin	Embryo	Pig	2020	(Kim, Ridlo *et al.* 2020)
Hedgehog signaling	-	Ovary	Mouse	2007	(Russell, Cowan et al. 2007)
	Sonic hedgehog supplementation	Embryo	Pig	2011	(Nguyen, Lo et al. 2011)
	Cyclopamine	Oocyte and Embryo	Mouse	2014	(Liu, Wei et al. 2014)
	Melatonin, Sonic Hedgehog	Oocyte	Pig	2017	(Lee, Jin *et al.* 2017)
PI3K signaling	RhoA	Embryo	Mouse	2014	(Liu, Wang et al. 2014)
	AKT (Protein Kinase B)	Oocyte	Cattle	2017	(Andrade, da Silveira et al. 2017)
	Follistatin	Embryo	Cattle	2018	(Ashry, Rajput et al. 2018)
	Melatonin, SH6	Oocyte and Embryo	Cattle	2019	(El Sheikh, Mesalam et al. 2019)
	PS48	Oocyte	Pig	2020	(Jiao, Zhu et al. 2020)
Wnt signaling	-	Embryo	Cattle	2013	(Denicol, Dobbs et al. 2013)
	Embryonic stem cells	Embryo	Mouse	2015	(Muñoz-Descalzo, Hadjantonakis et al. 2015)
	IWP2	Embryo	Pig	2017	(Huang, Yuan et al. 2017)
	Klotho	Oocyte	Pig	2020	(Kim, Taweechaipaisankul et al. 2020)

MAPK signaling	PD98059	Oocyte	Mouse	2003	(Kalous, Kubelka et al. 2003)
	DOC1R	Oocyte	Mouse	2003	(Terret, Lefebvre et al. 2003)
	Thermal stress	Oocyte	Pig	2014	(Yen, Tseng et al. 2014)
	ERK1/2	Oocyte	Mouse	2015	(Zhang, Liu et al. 2015)
mTOR signaling	Rapamycin	Oocyte	Pig	2014	(Lee, Kim et al. 2014)
	-	Oocyte	Mouse	2018	(Guo, Zhang et al. 2018)
	Rapamycin, Telomere	Oocyte	Cattle	2020	(Kordowitzki, Hamdi et al. 2020)
FGF signaling	Inhibition of FGF signaling	Oocyte	Cattle	2012	(Zhang & Ealy 2012)
	Inhibition of FGF signaling	Embryo	Pig	2016	(Li, Li et al. 2016)
TGFβ signaling	Inhibition of TGFβ	Embryo	Mouse	2015	(Ghimire, Heindryckx et al. 2015)
	SMAD4 feedback	Granulosa Cell	Pig	2018	(Du, Pan et al. 2018)
Notch signaling	-	Ovary	Mouse	2001	(Johnson, Espinoza et al. 2001)
	Jag1	Oocyte	Mouse	2019	(Hubbard, Prasasya et al. 2019)
	-	Embryo	Mouse	2020	(Batista, Diniz et al. 2020)

The two major roles (lipid metabolism and antioxidative response) in Nrf2 signaling can also be found in peroxisomal activities (Lee 2017). This is to say that these activities can also produce ATP through FA consumption and the implementation of the defense mechanism against self-induced ROS using hydrogen dioxides existing in- and outside of the peroxisomes (Cho, Gladwell et al. 2010). Therefore, it is quite plausible that these two mechanisms (Nrf2 signaling and peroxisomal activities) have germane roles to each other. In summary, detailed and sophisticated technics are required for IVM and IVC systems to improve subsequent steps such as embryo transfer to a surrogate, implantation, gestation, and piglet delivery. Due to this, there were numerous trials conducted to enhance these *in vitro* systems. It is currently becoming necessary to investigate and specify the exact mechanisms that are occurring in mammalian oocytes and embryos during improvements being made to IVM and IVC systems, and some studies raise the importance of the Nrf2 signaling and peroxisomal activities respectively in terms of antioxidative mechanism and peroxisomal activities.

The purpose of this study was to investigate the cross talk between the Nrf2 signaling pathway and peroxisomal activities during maturation of oocytes and the development of embryos in pigs. Therefore, in Part I, the general background of this thesis is described in detail and is followed by common methodologies of the related experiments being enumerated in Part II. In Part III, investigations on the roles of the Nrf2 signaling pathway and peroxisomal activities were performed in porcine oocytes and embryos respectively, thereby establishing each of the roles of both mechanisms that are significant in porcine oocytes and embryos. Then, in Part IV,

the cross-talk between the Nrf2 signaling pathway and the peroxisomal activity in both porcine oocytes and embryos was investigated and their connection was re-confirmed by RNA sequencing and partially by protein analysis. Moreover, investigation on incidental mechanisms including lipid metabolism and antioxidative mechanism was performed. A schematic outline of this thesis is summarized in Figure 1.

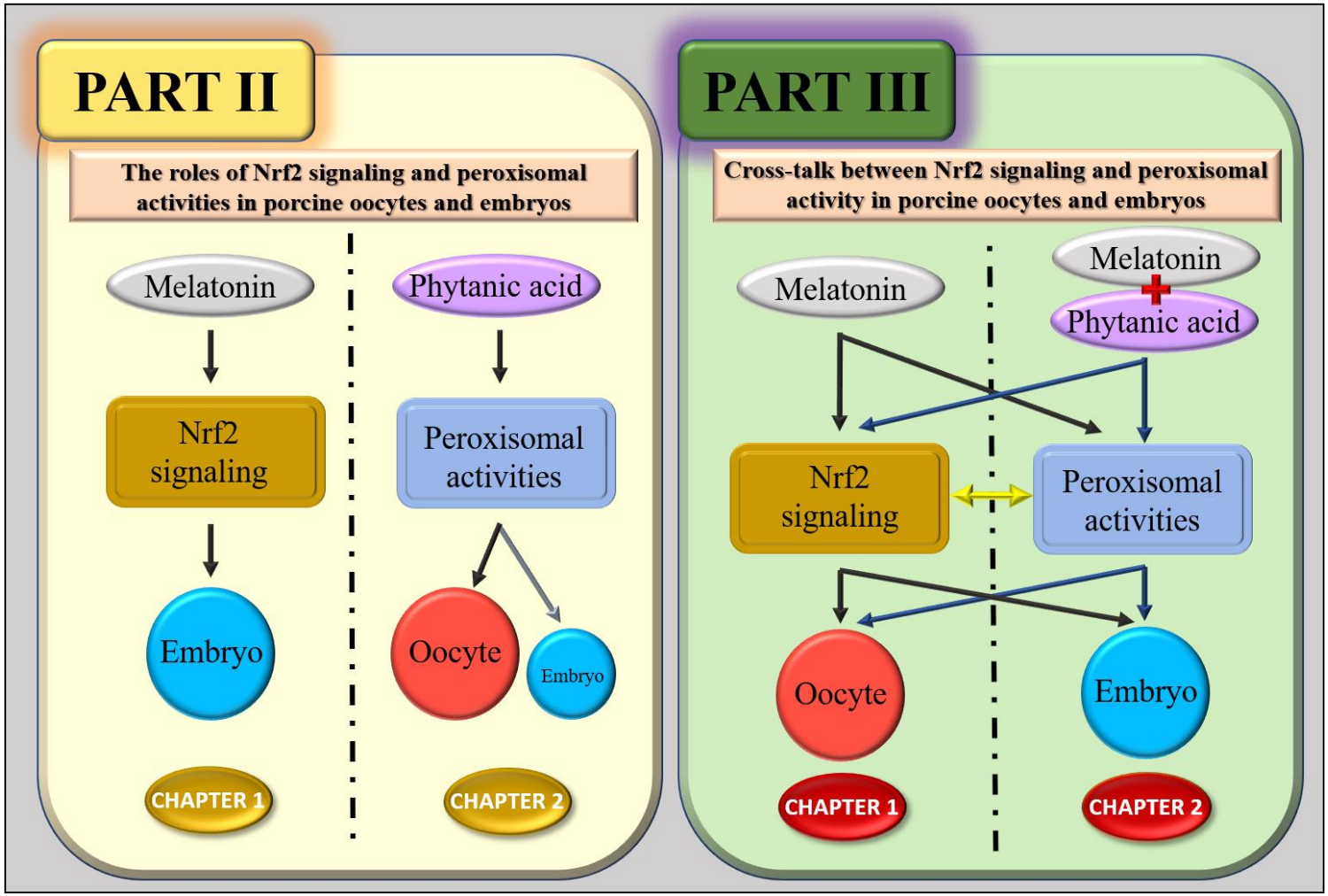

Figure 1. The outline of the thesis

2. Literature review

1.1. Pigs in research

The use of animals in research had been drastically increased ever since the beginning of modern biomedical research in the twentieth century (Ericsson, Crim et al. 2013). The most commonly used model until the present time has been mice as they provide diverse approaches to functional studies and mapping of genes (Keffer, Probert et al. 1991; Uysal, Wiesbrock et al. 1997) and a series of heredities within generations can easily be observed as their life span is relatively shorter than other mammalian species (Yuan, Peters et al. 2011). However, there are also a number of major limitations in mice such as shortcomings of applications to clinical studies (Perleberg, Kind et al. 2018) and physiological differences (Cibelli, Emborg et al. 2013). Instead, pigs have been gaining attention in the field of disease models, because they are found to have fundamental similarities with humans in organ size, physiology, as well as diet, and are suitable for biomedical research (Kararli 1995; Heinritz, Mosenthin et al. 2013). The porcine species had not only been of service and use to human beings in the food supply and livestock industries, but has become of use in research on human health and diseases. Therefore, among numerous biomedical and clinical trials on pigs, genetic modification for disease models and xenotransplantation are of important focus in order to overcome incurable human diseases.

Successful approaches to disease models and xenotransplantation require basic concepts of controlling environments and conditions of germ cells that are cultured *in vitro* (Ferreira & Allard 2015). In pigs, some studies demonstrated that diseases such as foot-and-mouth disease, reproductive and respiratory syndrome virus, and enterovirus could be transmitted to pigs or their litters by artificial insemination (AI) as pathogenic viruses were found or detected by isolation in porcine semen (Phillips, Foley et al. 1972; McVicar, Eisner et al. 1977; Shin, Torrison et al. 1997). Furthermore, poor quality or aged oocytes are also suggested to have downregulation of fertilization ability, embryo developmental potential, and cause protein secretion, all of which may lead to failure of implantation and gestation (Miao, Kikuchi et al. 2009; Powell, Manandhar et al. 2010). Until now, there have been numerous trials and productions of genetically modified pigs using ARTs. Genetic modifications in pig disease models had been performed in various fields such as mutation of Huntington disease (Yang, Wang et al. 2010), cardiovascular disease (Whyte, Samuel et al. 2011), breast cancer (Luo, Li et al. 2011), and diabetes (Renner, Fehlings et al. 2010). A summarized table of human disease-targeted genetically modified pig disease models is shown in Table 3. It is especially evident that an appropriate control and culture of the oocytes may also result in competence of subsequent embryonic development. Therefore, on the basis of this concept, which maintains that improving the quality of germ cells are pivotal for pig reproduction, the complete process of IVM of porcine oocytes and subsequent embryonic development remains unclear and it is suggested to be of focus in future research.

Table 3. A list of genetically modified pigs.

Disease	Modified target	Technic	Reference
Huntington's disease	Mutant Huntington (*HTT*)$^{+}$	SCNT	(Yang, Wang *et al.* 2010) (Yan, Tu et al. 2018)
Alzheimer's disease	Amyloid precursor protein (*APP*) K670Nt/M671L^{+}	SCNT	(Kragh, Nielsen et al. 2009)
	Multi-cistronic vector		(Lee, Hyun et al. 2017)
Spinal muscle atrophy	Survival motor neuron (*SMN*)$^{+/-}$	SCNT	(Lorson, Spate et al. 2011)
Cardiovascular disease	Endothelial nitric oxide synthase 3 (*eNOS3*)$^{+}$	SCNT	(Whyte & Laughlin 2010)
	Peroxisome proliferator-activated receptor-γ (*PPAR-γ*)$^{-/-}$	SCNT	(Yang, Yang et al. 2011)
	Catalase (*CAT*)$^{+}$	SCNT	(Whyte, Samuel *et al.* 2011)
	Apolipoprotein CIII (*ApoCIII*)$^{+}$	SCNT	(Wei, Ouyang et al. 2012)
Diabetes mellitus	Hepatocyte nuclear factor-1 homeobox A, dominant negative (*HNF1α*^{dn})$^{+}$	SCNT	(Umeyama, Watanabe et al. 2009)
	Glucose-dependent insulinotropic polypeptide receptor (*GIPR*^{dn})$^{+}$		(Renner, Fehlings *et al.* 2010)
	Insulin deficient / (Insulin) INS gene$^{-/-}$		(Cho, Kim et al. 2018)
	Mild maternal hyperglycemia / INS^{C93S}		(Renner, Martins et al. 2019)
Retinitis pigmentosa	Rhodopsin, mutant P23H (*RHO* P23H)$^{+}$	SCNT	(Ross, Fernandez de Castro et al. 2012)
Breast cancer	Breast cancer associated gene 1(*BRCA1*)$^{+/-}$	SCNT	(Luo, Li *et al.* 2011)
Polycystic kidney disease	pCMV-PKD2 vector	SCNT	(He, Ye et al. 2013)
Xenotransplantation	GGTA1$^{-/-}$	SCNT	(Hauschild, Petersen et al. 2011)
	CMAH$^{-/-}$/GT$^{-/-}$/shTNFRI-Fc/HO-1		(Kim, Lee et al. 2017b)
	GGTA$^{-/-}$ / TNFRI-Fc and HO-1 expression		(Kim, Lee et al. 2019)

Partially Adopted from (Perleberg, Kind et al. 2018)

1.2 *In vitro* maturation

Indeed, it is necessary that pig production for biomedical research purposes, xenotransplantation, or disease models be developed consistently; however, in order to implement this, controlling favorable conditions of porcine gametes and embryos are fundamental. Natural mating or AI could be solutions for pig reproduction; moreover, studies of gamete cryopreservation and IVP of porcine embryos are being continued (Niemann & Rath 2001). However, it is challenging in that *in vivo* embryos are not able to be harvested consistently resulting in unstable consequences. Therefore, IVM systems have been acknowledged a better alternative to obtain fair quality of oocytes (Kim, Lee *et al.* 2017a). Moreover, tailored and controlled conditions for IVM such as gas compositions, environment, and culture conditions are feasible compared to *in vivo* studies (Paredes, Terron et al. 2007; Choi, Park et al. 2008; Nakano, Kato *et al.* 2012; Do, Shibata *et al.* 2015). In addition, *in vitro* studies of gametes and embryos are gaining more attention in that it is much easier for researchers to assess quality of gametes, investigate gamete-related mechanisms, and produce a number of embryos within a relatively short time and with less costs compared to producing *in vivo* embryos in pigs (Gil, Cuello et al. 2010). However, the *in vitro* environment is not able to provide the same conditions as *in vivo*, and therefore it is necessary to improve IVM system that may mimic the system *in vivo*.

1.2.1. Enhancement of IVM systems

Although IVM is preferred by researchers for use in *in vivo* studies, there are specific problems that occur during the use of IVM of porcine oocytes. Some well-known infamous causes are OS, as well as gas compositions, exposure to contaminants, and control of temperature. In addition, the unexpected toxic effect of some chemicals, environments, or even the oocyte itself may also contribute to the failure of porcine IVM (Beall, Brenner et al. 2010). The entire process involved in an IVM system includes immature oocyte collection from ovaries, oocyte culture for maturation, embryo production through the ARTs, and IVC of the embryos. Numerous factors may influence the process throughout IVM systems; therefore, it was necessary for research to focus on troubleshooting the problems that can cause the failure of the entire IVM process.

Trials and changes for improving efficiencies of porcine IVM either by modifications of genes, culture conditions, or environments have been performed and as the result, numerous achievements of such improvements were reported. The most common method for the improvement of IVM systems is chemical treatment. Toxicity or improvements during the process of IVM are critical for researchers when optimizing the culture system. For example, the toxicity effect of butylparaben was tested on porcine oocytes (Jeong, Lee et al. 2020) and deficiency in Zinc was found to cause embryonic developmental failure tin these porcine oocytes (Jeon, Yoon et al. 2015). Additionally, retinoids improved IVM of porcine oocytes and its subsequent embryonic development (Alminana, Gil et al. 2008). Therefore, the

improvement of porcine IVM can surely be implemented through chemical treatments, including the assessment of toxicity or inhibitory effects. Table 4 shows the representative chemicals that were used frequently in mammalian IVM.

Another method is to alter culture conditions such as the medium or co-culture system during IVM. As culture time is part of the processes included in IVM systems, changing the compositions of the IVM medium or culture system can have critical consequences. Yuan et al. demonstrated that changing combination of the culture medium showed a dramatic increase in porcine oocyte maturation (Yuan, Spate et al. 2017). In addition, Lee et al., showed improved maturation of porcine oocytes when co-cultured with canine oviduct cells (Lee, Oh et al. 2018). Likewise, IVM systems for successful maturation of porcine oocytes remain to be improved to advance IVP of disease models and biomedical research.

Table 4. A list of treated chemicals during mammalian IVM.

Chemical	Type of chemical	Effect of chemical	Species	Year	Reference
Melatonin	Antioxidant	Embryonic development	Cattle	2014	(Tian, Wang et al. 2014)
		Melatonin receptor, OM	Ewe	2017	(Tian, Wang et al. 2017)
		DNA protection	Mouse	2019	(Leem, Bai et al. 2019)
		Clathrin-mediated endocytosis	Human	2019	(Li, Liu et al. 2019)
		Antioxidant, OM, Peroxisome	pig	2020	(Kim, Ridlo *et al.*)
Rapamycin	Immunosuppressor	Developmental capacity rescue	Pig	2014	(Lee, Kim *et al.* 2014)
		Oocyte maturation	Pig	2015	(Lee, Park et al. 2015)
		IVF, Autophagic activation	Mouse	2016	(Lee, Shin et al. 2016)
		Telomere maintenance	Cattle	2020	(Kordowitzki, Hamdi *et al.* 2020)
Resveratrol	Dietary supplement	IVM and IVC system	Cattle	2014	(Wang, Tian et al. 2014b)
		Synergy with melatonin	Pig	2018	(Lee, Jin et al. 2018c)
		Oocyte maturation	Pig	2018	(Wang, Zhu et al. 2019)
		Aging prevention	Mouse and Human	2018	(Liu, Sun et al. 2018)
		Oocyte maturation system	Ewe	2019	(Zabihi, Shabankareh et al. 2019)
Retinoic acid	Vitamin	Fertilization improvement	Mouse	2011	(Nasiri, Mahmoudi et al. 2011)
		Antioxidant	Cattle	2018	(Gad, Abu Hamed et al. 2018)
		Oocyte maturation system	Camel	2019	(Saadeldin, Swelum et al. 2019)

1.2.2. Procedures of oocyte maturation

Oocytes are composed of several layers: zona pellucida (ZP), perivitelline space, plasma membrane, and lastly, cytoplasm and a nucleus. ZP is a glycoprotein that encompasses the inner layers of the oocyte and prevents polyspermy, during the process of fertilization, (Gupta, Bansal et al. 2009) and perivitelline space, a hollow space where polar bodies are positioned in which cortical granules are deposited after maturation of the oocyte (Hassa, Aydin et al. 2014). Most importantly, the cytoplasm and nucleus undergo two aspects of maturation: cytoplasmic and nuclear maturation. Dramatic changes that are pivotal for fertilization are progressed during cytoplasmic maturation (Nagai, Funahashi et al. 2006) and the incomplete maturation of the cytoplasm can cause a loss of developmental competence of an oocyte (Appeltant, Somfai et al. 2016). Nuclear maturation initiates with a resumption of meiosis in order to leave a haploid of chromosomes from the diploid state, which it reaches to metaphase II (Conti & Franciosi 2018). Apart from IVM failures caused from *in vitro* conditions, failures can also follow during the series of stages that occur for oocyte maturation and several signaling pathways, which appear to be abnormal, can be attributed to failure during the process (Schmitt & Nebreda 2002). Therefore, the study of signaling in the process of oocyte maturation is necessary to uncover the unsolved obstacles regarding IVM systems.

1.3. *In vitro* culture of porcine embryos

The processes involved in the porcine IVC system start from ARTs such as parthenogenesis, IVF, SCNT, ICSI, and microinjection with matured oocytes. Then, the activated oocytes are cultured for seven days in IVM medium. While they are cultured in the medium, they undergo a series of cleavage stages, morulae, and then a blastocyst stage, which is called the preimplantation embryo. The control of IVC systems is as important as that of IVM systems, both are extremely sensitive to culture conditions and the surrounding environment (Hamdoun & Epel 2007), and the embryos must undergo substantial changes in both their cytoplasm and nucleus. However, attempts to overcome several obstacles during the embryo development are still unsatisfiable.

In the case of proper fertilization of a matured oocyte and sperm, they first form pronucleus. Here, most of the embryos in pigs including many species have to confront the most challenging stage during the embryo development, which is a drastic transition of developmental control from maternal to zygote itself. When zygotes initiate development, they depend on maternal transcripts, and then progress to zygotic genome activation as the maternal transcripts degenerate (Schier 2007). In pigs, it is reported that porcine embryos undergo the transition of zygotic genome activation at the four-cell stage (Xie, Chen et al. 2010). However, some embryos still fail to develop up to the blastocyst stage and it is mainly due to '*in vitro* developmental block' of the embryos (Machaty, Day et al. 1998). In this thesis, Tris-

buffered medium (mTBM) was modified for fertilization using the IVF process. The compositions of the media are listed in Table 5.

Table 5. The composition of modified Tris-buffered medium (mTBM).

Component	Catalog No.	M.W.*	Concentration
NaCl**	S5886	58.44	113.1 mM
KCl***	P5405	74.55	3 mM
CaCl2*2H2O****	C7902	147.01	7.49 mM
TRIS*****		121.14	19.99 mM
Glucose	G8270	180.16	10.99 mM
Na-pyruvate******	P4562	110.04	4.99 mM
Caffeine	C0750	194.19	8.59 mM
BSA*******	A4161		8 % (w/v)

* Molecular weight
** Sodium chloride
*** Potassium chloride
**** Calcium chloride dihydrate
***** Tris base (TRIS-RO, Roche)
****** Sodium pyruvate
******* Bovine serum albumin

1.3.1. Enhancement and application of IVC system

Similar to the improvement of IVM systems, there are numerous studies suggesting possible enhancement of IVC systems by chemical treatments. Lee et al. demonstrated that resveratrol treatment during IVC could improve the development of porcine embryos (Lee, Wang et al. 2010), in the same manner, Oxamflatin, an HDACi, treatment also increased porcine embryonic development and nuclear reprogramming (Mao, Zhao et al. 2015). Moreover, toxicity of specific chemicals can be tested by treating the chemical during IVC of embryos. For example, Weber et al. investigated the toxicity of cryoprotectants on porcine embryos and found an optimal concentration of the cryoprotectant that is feasible to be used as treatment on embryos.

In addition, IVP of porcine embryos contribute significantly to biomedical research by ARTs that can be applied to generating transgenic pigs, such as those used as disease models and clones, by genetic modification. As this is one of the fundamental stages for producing the genetically engineered models, ongoing research is gaining more attention currently. At first, transgenic pigs were produced by pronuclear DNA microinjection (Hammer, Pursel et al. 1985), however, problems were also reported concomitantly with the unexpected mistargeting of genes, size of the pig, and inappropriate activation of signals or high lipid content surrounding oocyte causing failure of pig production (Logan & Martin 1994; Uchida, Shimatsu et al. 2001).

Another way to produce transgenic pigs is using SCNT. Since the first cloned pig was produced in 1980's (Prather, Sims et al. 1989), many trials for producing cloned or disease model pigs have been implemented. In 2000, Polejaeva and Campbell claimed that SCNT with appropriate gene modification is considered to be an effective way to produce transgenic animals (Polejaeva & Campbell 2000) and that this might make a breakthrough regarding limitations of studies on embryonic stem cells and human diseases (Kim, Kim et al. 2010). As numerous trials and achievements for improving IVM and IVC are being reported, other focuses in this field are emerging such as those related to the signaling pathways during maturation of mammalian gametes or the development of mammalian embryos.

1.3.2. Signaling pathways during embryo development

Numerous studies suggest the importance of specific signaling pathways that mediate development of porcine embryos. Indeed, many indispensable factors such as culture conditions and environment must be maintained and well-controlled; however, the signaling pathways that are significantly involved in porcine embryo development could not be neglectable. Hence, continuous reports on signaling pathways during porcine embryonic development are being published. For instance, regulations of Wnt signaling was suggested to be vital to porcine parthenogenetically activated embryos (Huang, Ouyang et al. 2013) and the Nrf2/ARE signaling pathway was found to be involved in the antioxidant mechanism in IVF-derived porcine preimplantation embryos (Kim, Kim et al. 2019). Furthermore, the activation of the

phosphatidylinositol 3-kinase/AKT signaling pathway was suggested to have roles in porcine embryonic development and influence the downstream of the signaling (Jeong, Yoon et al. 2017).

Interestingly, some signaling pathways not only affect the embryonic development, but also influence downstream cascades or phenomenon of the pathways such as the antioxidant mechanism (Dong, Sulik et al. 2008), lipid metabolism, or implantation (Wang & Dey 2005; Kajdasz, Warzych et al. 2020). In specific, the Nrf2 signaling pathway is one of the representatives signaling in antioxidant mechanism and along with Nrf2 signaling, numerous signaling pathways such as Wnt signaling, Hedgehog signaling, and PI3K signaling are continuously reported in the field of reproduction (Amin, Gad et al. 2014; Lee, Jin et al. 2018a; El Sheikh, Mesalam et al. 2019; Kim, Taweechaipaisankul et al. 2020). However, detailed studies on signaling pathways related to embryos, specifically in pigs, are yet to be sufficient.

1.4. Nrf2 signaling

In cellular defense mechanisms, Nrf2 is a transcription factor that mediates functions of antioxidants (Lee & Johnson 2004; Wells 2015), cytoprotection (Akino, Wada-Hiraike et al. 2018), and reproduction processes (Hu, Roberts et al. 2006). In a basal state, Nrf2 is retained by Kelch-like ECH-associated protein 1 (Keap1), a natural cytosolic inhibitor, which resides in cells (Zipper & Mulcahy 2002). When Keap1 inhibits Nrf2, it becomes an activator of the Cullin3/Ring Box 1/E3 ubiquitin ligase complex, and then the complex, which resides in the cytosol leads to degradation of Nrf2 through proteasomes (Cullinan, Gordan et al. 2004; Kobayashi, Kang et al. 2004; Zhang, Lo et al. 2004). On the contrary, when OS is occurring in a cell, it causes dissociation of Nrf2 from Keap1, then Nrf2 translocates into the nucleus for transcription of ARE-related genes, which prevents ROS (Kaspar, Niture et al. 2009). The overall flow of the pathway is illustrated by Liu et al (Liu, Locascio et al. 2019).

This signaling pathway is famously known for its defense mechanism against OS; however, it has been reported as having additional functions and involvement in oocytes and embryos. Lin et al. demonstrated that an inhibition of the Nrf2 signaling pathway caused impaired cell cycle progression during mouse embryo development (Lin, Sui et al. 2018) and Amin et al. suggested that the regulation of the Nrf2 signaling pathway has a germane relationship with embryo survival in response to OS and has a possible connection with lipid metabolism in bovine species (Amin, Gad et al. 2014). Recently, a study conducted by Ma et al. suggested that the Nrf2

signaling pathway is also involved in the anti-aging process in mouse embryos (Ma, Liang et al. 2018). With continuous updates on Nrf2 functions in oocytes and embryos, new discoveries of Nrf2 in functions and connections with other signals are still ongoing.

According to the studies suggested previously, the Nrf2 signaling pathway can be activated or inhibited by chemical treatments to culture media and mediates various metabolisms in mammalian oocytes and embryos. This may also be applicated in porcine oocytes and embryos in that they are extremely sensitive to OS (Dennery 2007) and a high level of OS occurrence in oocytes and embryos leads to degeneration or a loss of maturation and developmental potentials (Guerin, El Mouatassim et al. 2001). However, studies of involvement of the Nrf2 signaling pathway in porcine oocytes and embryos are still scarce and this study partially aims the involvement of the Nrf2 signaling pathway through an antioxidant mechanism, lipid metabolism, maturation, and development of the porcine oocytes and embryos. A schematic illustration of the Nrf2 signaling pathway is shown in Figure 2.

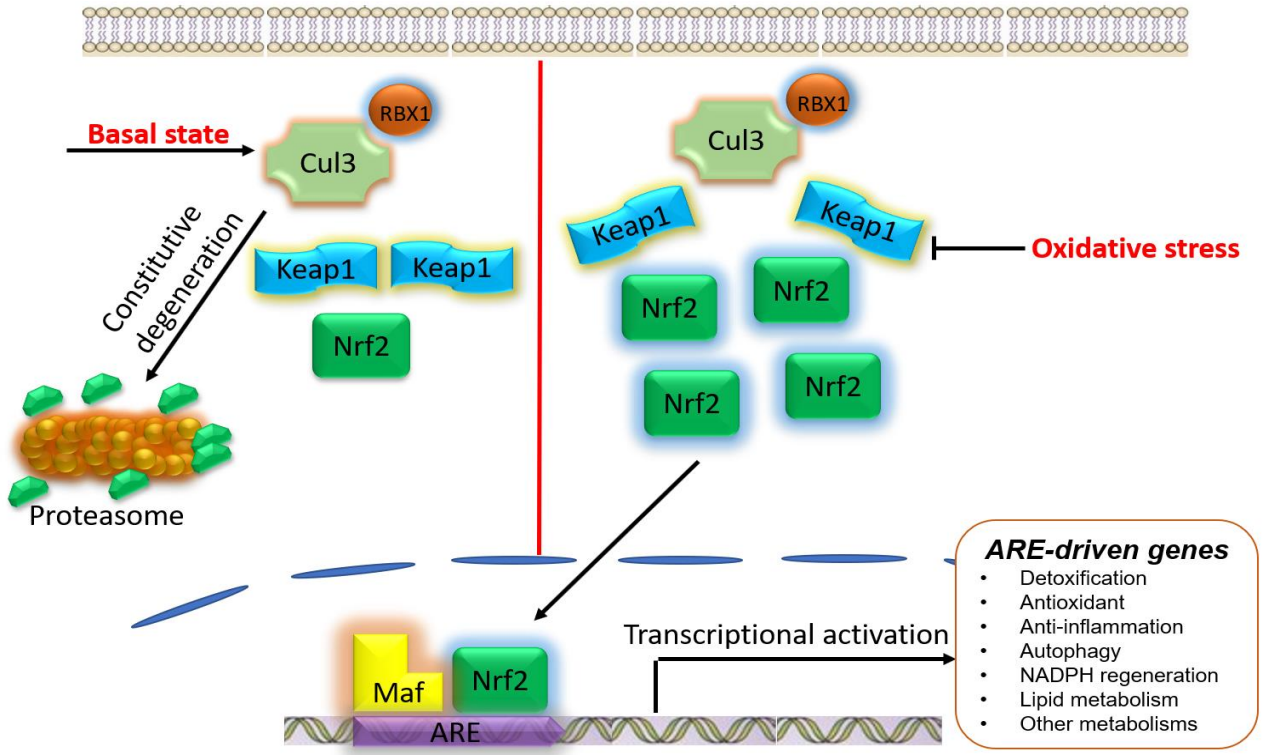

Figure 2. A brief flow of the Nrf2 signaling pathway with basal and stressed conditions. The figure was modified from the study of Liu, Locascio et al. **(Liu, Locascio et al. 2019)**

1.5. Peroxisomal activity

Peroxisomes are dynamic subcellular organelles residing ubiquitously in most eukaryotic cells (Schrader & Fahimi 2006) and have flexible abilities to alter their functions and morphologies in accordance with environments or signals within cells (Schrader, Grille et al. 2013). They have canonical and fundamental roles such as OS detoxification (Kao, Gonzalez et al. 2018), antioxidant mechanisms (Antonenkov, Grunau et al. 2010), FA breakdown via a battery of oxidation (Lodhi & Semenkovich 2014), and catabolism of amino acids (Manivannan, Scheckhuber et al. 2012). When the peroxisomes undergo particular metabolic procedures, they produce byproducts called 'hydrogen peroxides (H_2O_2)', which trigger OS-like mechanisms, thereby causing damage to the surroundings. However, the study conducted by Pavelka et al. suggested that in the meantime, oxidases and catalases are produced concomitantly together with H_2O_2 preventing any damages that might occur (Pavelka, Goldenberg et al. 1976).

There are numerous reports on peroxisomal activities and biogenesis involved in lipid metabolism using lipid droplets or long/branched-chain FAs. Apart from the functions that prevent OS and control toxicity in cells, the peroxisomes have an additional role in β-oxidation of FAs, the degradation of lipids (Mannaerts & van Veldhoven 1996). Interestingly, the β-oxidation that occurs in the peroxisomes only functions to reduce the length of FA chains which will later be sent to mitochondria for completion of FA digestion (Wanders, Waterham et al. 2015). Therefore, the FA digestion through peroxisome-mitochondria contact results in ATP generation via

the citric acid cycle. Contact between peroxisome and mitochondria was proven in that the location of peroxisome was proximal to the sites of mitochondria. Specifically, some peroxisomal biogenesis factors (Pex) such as Pex 3 and Pex 34 had pivotal roles in connecting membrane contact sites between peroxisome and mitochondria (Shai, Yifrach et al. 2018).

These findings leave questions as to whether the peroxisomes are involved in mammalian reproduction. A few studies suggest influences of peroxisomes on reproduction. Kim et al. reported that peroxisomal activities influenced lipid metabolism in porcine oocytes (Kim, Kim et al. 2020), Figueroa et al. found peroxisome-like structures and presumed peroxisome-derived catalase activities were occurring in rat gametes and ovaries (Figueroa, Kawada et al. 2000), and Brauns et al. found that peroxisomal dysfunction impairs spermatogenesis in mice (Brauns, Heine et al. 2019). Along with the significance of the Nrf2 signaling pathway, there may be cross talk with the peroxisomal activities and other related factors in porcine oocytes and embryos, which would contribute to valuable research in the field of IVP and reproduction. In Figure 3, hypothesized lipid metabolism and an antioxidant mechanism by the peroxisomal activity are illustrated.

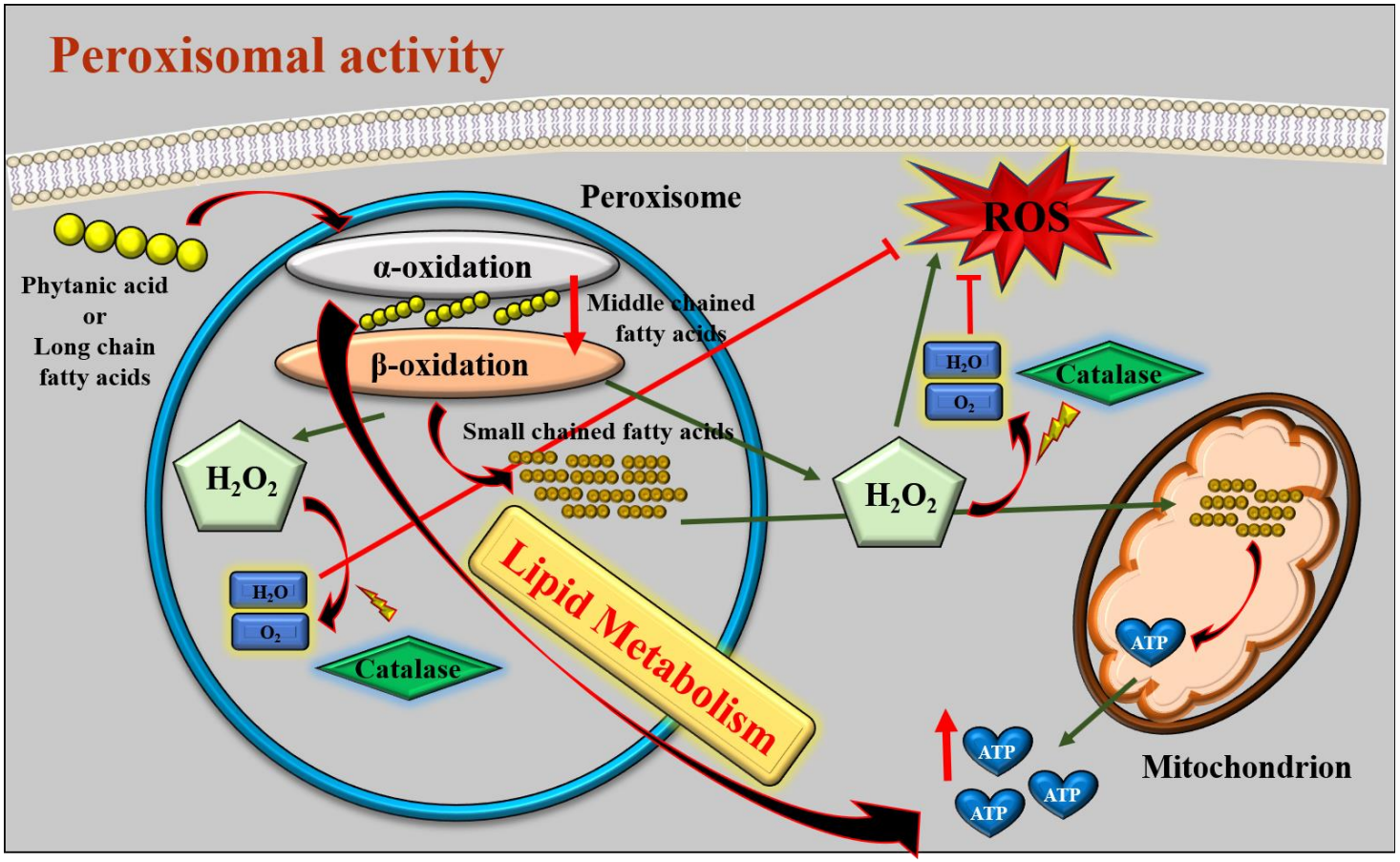

Figure 3. A schematic illustration of the peroxisomal activity and its influences on lipid metabolism and antioxidant mechanism.

PART II

GENERAL METHODOLOGY

1. Animals and chemicals

The pig ovaries used in this study were obtained after slaughtering and manufacturing processes. In terms of the research ethics regarding the use of these ovaries, the Institutional Animal Care and Use Committee (IACUC) of Seoul National University carried out ethical screening, then approved the ovaries for research use (No. SNU-190621-2-1 and SNU-171212-2). All reagents and chemicals used in this study were obtained from Sigma-Aldrich Chemical Company (St. Louis, MO, USA), unless otherwise indicated.

2. *In vitro* maturation

Porcine ovaries were obtained from prepubertal gilts at a local abattoir and sent the laboratory. Cumulus-oocyte complexes (COCs) were retrieved by aspiration of 3-8 mm sized follicles with an 18-gauge needle fitted on a disposable 10 mL syringe, then washed two times in washing medium comprising 9.5g/L of tissue culture medium-199 (TCM-199; Invitrogen, Carlsbad, CA, USA), 2 mM sodium bicarbonate, 0.3% polyvinyl alcohol (PVA), 5 mM sodium hydroxide, 10 mM N-piperazine-N'-[2-ethanesufonic acid] (HEPES), and 1% penicillin-streptomycin (Invitrogen). COCs with homogenous cytoplasm and three or more layers of cumulus cells were carefully selected under a stereomicroscope. They were cultured in IVM medium comprising TCM-199, 0.91mM sodium pyruvate, 10 μL/mL insulin-transferrin-selenium solution (ITS-A) 100X (Invitrogen), 10 ng/mL epidermal growth factor, 0.57 mM cysteine, 10 IU/mL human chorionic

gonadotropin (hCG), 10 IU/mL equine chorionic gonadotropin (eCG), and 10% porcine follicular fluid (vol/vol). The COCs were incubated at 39°C under 5% CO_2 in 95% humidified air. After 20 to 22 h of maturation culture with hormones, the COCs were washed in hormone-free IVM medium, then cultured again in IVM medium without hormones for additional 20 to 22 h.

3. Parthenogenetic activation

After 44 h of IVM, COCs were denuded with 0.1% hyaluronidase. Denuded oocytes were washed and selected in Tyrode's albumin lactate pyruvate (TALP) medium. Oocytes exhibiting the first polar body with distinct cellular membranes and homogenous cytoplasm were equilibrated gradually in activation medium containing 0.28 M mannitol, 0.1 mM $MgSO_4$, 0.5 mM HEPES, and 0.1 mM $CaCl_2$. The oocytes were transferred to the activation medium in a 3.2 mm double electrode chamber, then activated through 60 μs electric stimulation with a direct current pulse of 1.5 kV/cm using a BTX Electro-Cell Manipulator 2001 (BTX Inc., San Diego, CA). Subsequently, the activated oocytes were washed and stabilized in porcine zygote Medium-5 (PZM-5; CSR-CK024; Waco Chemicals, Japan). Finally, they were transferred to 40 μL droplets of PZM-5, covered with mineral oil, and cultured at 39°C in a humidified atmosphere of 5% CO_2, 5% O_2, and 90% N_2 for 7 days.

4. In vitro fertilization

After 44h of IVM, matured oocytes were denuded with 0.1% hyaluronidase by gently pipetting and washed in TALP medium. Then, oocytes that had homogeneous cytoplasm and clear membranes with polar bodies were selected, and moved to 40 μL of pre-incubated mTBM drops, consisting of 113.10 mM NaCl, 3 mM KCl, 7.50 mM $CaCl_2$, 11 mM glucose, 1 mM caffeine, 0.57 mM L-cystein, 20 mM Tris, and, 8% Bovine Serum Albumin (BSA) (w/v) in a 60 × 10 mm Petri dish (Falcon; Becton Dickinson Labware, Franklin Lakes, NJ). Ejaculated spermatozoa were obtained from DARBY Pig Breeding Co. (Anseong, Korea). The semen was centrifuged at 1000 g for 2 min, and the sperm pellet was resuspended with prewarmed porcine semen extender (Navibiotech, Cheonan, Korea). Then, the spermatozoa were centrifuged again at 1000 g for 2 min. Immediately before the next process, sperm motility was evaluated and >90% motile spermatozoa were used in each replication. Swim-up procedures were performed at 39°C in Sp-TALP medium, then spermatozoa were injected into mTBM droplets at a final concentration of 5×10^5 cells/mL. After 6 h co-incubation of oocytes and spermatozoa, zygotes with second polar bodies were washed in mTBM droplets by gently pipetting, then transferred to 40 μL droplets of PZM-5, covered with prewarmed mineral oil, and cultured at 39°C in a humidified atmosphere of 5% O_2, 5% CO_2, and 90% N_2 for 7 days.

5. Real time PCR

Samples were stored at -80°C until RNA was extracted, then total RNA was isolated by the RNAqueous^{TM} Micro Kit (Invitrogen, Vilnius, Lithuania). The total RNA was quantified on a NanoDrop 2000 Spectrophotometer (Thermo Fisher Scientific, Wilmington, DE, USA), and then immediately used for synthesizing complementary DNA (cDNA) using amfiRivert cDNA synthesis Platinum Master Mix 0 (genDEPOT, Houston, TX, USA) according to the manufacturer's protocol. For quantitative real-time PCR, each reaction mixture contained 1 μL cDNA, 0.4 μL (10 pmol/μL) forward primer, 0.4 μL (10 pmol/mL) reverse primer, 10 μL SYBR Premix Ex Taq (Takara, Otsu, Japan), and 8.2 μL of Nuclease Free Water (NFW) in a PCR plate (Micro-Amp Optical 96-Well Reaction Plate, Applied Biosystems, Singapore). The mixture was amplified using the Applied Biosystems StepOneTM Real-Time PCR Systems (Applied Biosystems, Waltham, MA, USA). For each sample, at least three replications were done in a plate. Forty cycles of reactions were performed with the following parameters: denaturation for 15 s at 95°C, annealing for 1 min at 60°C and extension for 1 min at 72°C. The expression of each target gene was quantified relative to that of the endogenous control gene (*GAPDH*) (Lee *et al.*, 2017). Genes of interest verified through Efficiency (%) = $(10^{-1/slope} - 1) \times 100$, ranged from > 8 to < 35 and R^2 value > 0.98 were considered as available data. The relative expression of each target genes was calculated using the following equation (Jin, Lee *et al.* 2017):

$$R = 2^{-[\Delta Ct\ sample - \Delta Ct\ control]}$$

6. Statistical analysis

All experiments in this study were performed in triplicates at least. Statistical analysis was performed using GraphPad PRISM 5.01 (PRISM 5, GraphPad Software, Inc., San Diego, CA 92108, USA). To determine significant differences between experimental groups, all data were expressed in terms of mean ± S.E.M, and analyzed using a one-way analysis of variance (ANOVA) with Tukey's Multiple Comparison Test. P values < 0.05 represented significant differences.

PART III

THE ROLES OF NRF2 SIGNALING AND PEROXISOMAL ACTIVITIES IN PORCINE OOCYTES AND EMBRYOS

Abstract

In general, OS is a major problem during *in vitro* culture of embryos. Numerous studies have shown that melatonin, which is known to have antioxidant properties, prevents the occurrence of OS in embryos. However, the molecular mechanisms by which melatonin prevents OS in embryos are still unclear. The present study suggests a possible involvement of the Nrf2/antioxidant-responsive element (Nrf2/ARE) signaling pathway, which is one of the prominent signals for OS prevention through Nrf2 activation, connecting melatonin, OS prevention and porcine embryonic development. The aim of chapter I was to investigate the effects of melatonin (10^{-7} M) on porcine embryonic development *via* the Nrf2/ARE signaling pathway; brusatol (50 nM; *Nrf2* specific inhibitor) was used to validate the mechanism. Treatment of porcine embryo with melatonin significantly increased formation rates of blastocysts and their total cell numbers and also upregulated the expression of Nrf2/ARE signaling and apoptosis-related genes (*MT2*, *NRF2*, *UCHL*, *HO-1*, *SOD1* and *BCL-2*). Furthermore, the expression of proteins (NRF2 and MT2) was also upregulated in the melatonin-treated group. Concomitantly, brusatol significantly inhibited these effects, upregulating the expression of *KEAP1* and *BAX*, including the expression level of KEAP1 protein. These results provide evidences that melatonin prevents OS through Nrf2/ARE signaling pathway in porcine *in vitro* fertilization -derived embryos.

Lipid metabolism plays an important role in oocyte maturation. The peroxisome is the fundamental mediator for this mechanism. In chapter II, the

peroxisomal lipid metabolism in porcine oocytes was investigated. Phytanic acid (PA) was chosen as an activator of alpha-oxidation in peroxisomes. Oocyte maturation, embryo development, immunocytochemistry of peroxisomal lipid activities, and staining of mitochondrial potentials were assessed. I found that 40 mM PA not only increased porcine oocyte maturation and embryonic development, but also upregulated the expression of genes and proteins related to activities of the peroxisomal lipid metabolism (PHYH, PEX19, and PEX subfamilies) and mitochondrial potentials (NRF1 and PGC1a). Moreover, PA upregulated the lipid droplet and fatty acid content in the oocytes. Moreover, mitochondria were activated and the mitochondrial membrane potential was increased after PA treatment, resulting in the production of more ATPs in the oocytes. The findings suggest that the degradation of PA via alpha-oxidation in the peroxisome may potentiate oocyte maturation processes, peroxisomal lipid oxidation, and mitochondria activities.

Chapter I. Involvement of Nrf2/ARE signaling through regulation of melatonin and brusatol in porcine embryos

1. Introduction

Melatonin (N-acetyl-5-methoxytryptamine), a natural hormone, is synthesized by the mammalian pineal gland and peripheral reproductive organs, as well as being a byproduct from plants (Stehle, Saade et al. 2011). As is widely known, the functions of melatonin include regulating the circadian rhythm (Stehle, Saade *et al.* 2011), steroidogenesis (MacPhee, Cole et al. 1975) and mammalian reproduction (Tamarkin, Baird et al. 1985). In addition, Reiter et al. postulated that, because melatonin was found to be a direct free radical scavenger, it stimulates antioxidative enzymes, thereby quenching free radicals (Reiter, Mayo et al. 2016). Moreover, melatonin acts as an antioxidant *via* ARE activities (Nguyen, Nioi et al. 2009). Numerous studies have already demonstrated that treatment with an optimal concentration of melatonin during IVP of embryos critically improves the quality of oocytes and determines subsequent embryonic development in various mammalian species, including mice (Tamura, Takasaki et al. 2008), cattle (Wang, Tian et al. 2014a) and pigs (Rodriguez-Osorio, Kim et al. 2007; Jin, Lee et al. 2017; Lee, Jin et al. 2018b). Although some studies identified intracellular mechanisms of melatonin action by evaluating oocyte maturation and embryo development, thereby improving

IVP outcomes *(Amin, Gad et al. 2014; Lee, Jin et al. 2017*), it is still uncertain how this hormone works. Furthermore, no study has studied the enhancement of porcine embryonic development by melatonin *via* the Nrf2/ARE signaling pathway.

Nuclear factor erythroid 2-related factor 2, also known as NFE2L2 or Nrf2, a potential therapeutic agent in various medical conditions such as chronic diseases, neurogenerative diseases and brain injuries, including treatment of chronic neurodegeneration, chemically-induced cellular damage, and even reduction of OS in granulosa cells by *Nrf2* activation (Lee & Johnson 2004; Wells 2015; Akino, Wada-Hiraike et al. 2018). From these studies, it is generally accepted that Nrf2 translocates from the cytoplasm to the nucleus, binds to ARE sites, then upregulates various enzymes responsible for producing cytoprotective compounds and proteins such as superoxide dismutase-1 (SOD1) and heme oxygenase-1 (HO-1) (Magesh, Chen et al. 2012). Such compounds that are activated by Nrf2 are also responsible for antioxidative functions related to cellular defense mechanisms (Lee & Johnson 2004; Magesh, Chen et al. 2012; Wells 2015). Some factors that are related to the Nrf2/ARE signaling pathway regulate Nrf2 under numerous stimuli.

Among these, Keap1 is one of the fundamental factors. As a natural inhibitor of Nrf2, Keap1 in part mediates Nrf2 activity by repressing it, through ubiquitylation that leads to proteasomal degradation. However, under OS conditions, Keap1 releases Nrf2 by altering its conformation, thereby activating it and initiating transcription (Nguyen, Nioi et al. 2009; Kansanen, Kuosmanen et al. 2013; Ma 2013). However, this mechanism can be ceased by brusatol, a specific inhibitor of *Nrf2*. It is a quassinoid isolated from the fruit of *Brucea javanica* and found to reduce

burdens of tumor, mitigate chemoresistance in in vitro and in vivo cancer models (Ren, Villeneuve et al. 2011; Tao, Wang et al. 2014; Wu, Harder et al. 2015), and most importantly, specifically inhibit Nrf2 via Keap1-dependent ubiquitination and proteasomal degradation, thereby promotes a rapid depletion of Nrf2 (Olayanju, Copple et al. 2015).

Several studies have demonstrated that melatonin plays a critical role in regulation of the Nrf2/ARE signaling pathway by modulating various mechanisms involved with OS *via* Nrf2 cascades (Tripathi & Jena 2010; Negi, Kumar et al. 2011; Chen, Renn et al. 2017). However, up to date, a few studies have been demonstrated the links between antioxidation-related signaling pathways and porcine embryonic developments. (Amin, Gad et al. 2014; Ma, Li et al. 2017; Lin, Sui et al. 2018). Therefore, the aim of this study was to investigate if there is a direct impact and activation of Nrf2 transcripts by melatonin *via* the Nrf2/ARE signaling pathway in IVF-derived porcine preimplantation embryos.

2. Materials and methods

2.1. Animals and chemicals

Procedures for animals and chemicals were described in general methodology.

2.2. Chemical preparation

Melatonin (Cat No. M5250) and brusatol (Cat No. SML1886) was purchased from Sigma Aldrich and shipped as a powder from. Dimethyl Sulfoxide (DMSO) was used as a solvent for melatonin and brusatol. Melatonin was dissolved in DMSO to make a stock solution at the concentration of 10^{-2} M, then diluted 10^{-3}, 10^{-5}, 10^{-7}, and 10^{-9}M and brusatol at the concentration of 800nM, then diluted 50, 200, and 400 nM. Each concentration was treated in PZM-5 (Funakoshi Corporation, Tokyo, Japan) and for the exact comparison, the same amount of DMSO was treated in the control groups.

2.3. *In vitro* maturation

Procedures for IVM were described in general methodology.

2.4. *In vitro* fertilization

Procedures for IVF were described in general methodology.

2.5. Embryo evaluation and total cell count after IVF

The day of IVF, when presumptive zygotes were transferred to IVC medium, PZM-5, was considered Day 0. Evenly cleaved embryos were monitored under a stereomicroscope on Day 2 (48 h). Blastocyst formation was evaluated on Day 7 (168 h) after IVF and total cell numbers were counted. ZP digestion was performed with 0.5% pronase to remove remaining attached spermatozoa. After washing in TALP medium, zona-free blastocysts were stained with 5 μg/mL of Hoechst 33342 for 8 min. After a final wash in TALP medium, stained blastocysts were mounted on a glass slides in 100% glycerol drops, compressed with a cover slip, and observed under a fluorescence microscope (Nikon Corp.) at 400 × magnifications.

2.6. Immunofluorescence staining

Indirect immunofluorescence staining was performed in order to evaluate and compare the expression levels of Nrf2, Keap1, and MT2 among treatment groups after IVF. IVF porcine blastocysts were selected and ZP was removed with 0.5% pronase in order to remove remaining attached spermatozoa. Then, washed in PBS

containing 1% PVA, then, fixed with 4% paraformaldehyde (w/v) in PBS for at least 2 h, permeabilized with 1% Triton X-100 (v/v) in distilled water (DW) for 1 h at 39°C, washed 4 times in 1% PVA in DW, and incubated in DW containing 2% BSA for 2 h in order to block non-specific sites. Then, blastocysts were directly transferred into 2% BSA containing primary antibody for Nrf2 (1:200; 70R-50116; Fitzgerald Industries International, Acton, MA, USA), Keap1 (4 μL/mL; ab218815; Abcam, Cambridge, UK), and MT2 (1:200; ARP64072_P050; Aviva Systems Biology, San Diego, CA, USA) and incubated at 4°C, overnight. Subsequently, they were washed three times in PBS with 1% PVA and incubated with a secondary fluorescein isothiocyanate-conjugated anti-rabbit polyclonal antibody (1:200, ab6717, Abcam. Cambridge, UK) at 37°C for 1.5 h in darkness. The blastocysts were washed three times in PBS with 1% PVA, then counterstained with 5 μg/mL Hoechst-33342 for 8 min. They were mounted on glass slides, and observed under a fluorescence microscope. The fluorescence measurements were performed using ImageJ software (version 1.46r; National Institute of Health, USA) and at least 10 blastocysts from each group were used for the staining.

2.7. Analysis of gene expression by quantitative real-time PCR

Procedures for Real time PCR were described in general methodology. The primers used in this experiment are listed in Table 6. Specifically, at least 40 porcine blastocysts from each experimental group were used for RNA extraction.

2.8. Statistical analysis

Procedures for statistical analysis were described in general methodology

Table 6. Information on primer sequences for real-time PCR.

Genes	Primer sequences (5'- 3')	Product size (bp)	Accession No.
GAPDH	F: GTCGGTTGTGGATCTGACCT	207	NM_001206359
	R: TTGACGAAGTGGTCGTTGAG		
MT2	F: AGCTGCCTTAACGCCATCAT	219	XM_021063941.1
	R: ATTGTCGCCCAGTCAGTGAG		
Nrf2	F: GCCCAGTCTTCATTGCTCCT	115	XM_013984303
	R: AGCTCCTCCCAAACTTGCTC		
Keap1	F: ACCCAATTTCTGCCCCTGAG	214	NM_001114671
	R: ACTTGACCTGCAGCGTAACA		
UCHL1	F: CCCTTCGCTTTATCCCCGTT	117	NM_213763
	R: CGCTTATCTGCAGACCCCAA		
SOD1	F: TGACTGCTGGCAAAGATGGT	133	NM_001190422
	R: TTTCCACCTCTGCCCAAGTC		
HO-1	F: ACCCAGGACACTAAGGACCA	227	NM_001004027
	R: CGGTTGCATTCACAGGGTTG		
Bax	F: CATGAAGACAGGGGCCCTTT	181	XM_003127290
	R: CATCCTCTGCAGCTCCATGT		
Bcl-2	F: AGGGCATTCAGTGACCTGAC	193	NM_214285
	R: CGATCCGACTCACCAATACC		

F, Forward primer; R, Reverse Primer

3. Results

3.1. Effect of melatonin treatment during IVC

In the first experiment, several concentrations (0, 10^{-3}, 10^{-5}, 10^{-7} and 10^{-9} M) of melatonin were included during IVC to determine the optimal concentration. Melatonin treatment showed no significant differences on cleavage rate among the groups. However, there were significant differences in blastocyst formation rate and total cell numbers. Treatment with 10^{-7} M melatonin significantly increased the porcine blastocyst formation rate compared to the control, 10^{-3}, 10^{-5} and 10^{-9} M melatonin concentrations (29.5% vs. 15.7%, 11.0%, 18.3%, and 16.9%, respectively, $P < 0.05$, Table 2). Total cell numbers of blastocysts were also significantly increased when embryos were treated with 10^{-5}, 10^{-7} and 10^{-9} M melatonin compared to control and the 10^{-3} M melatonin (84.3, 83.3, 87.0 vs. 65.0 and 44.0, $P < 0.05$, Table 2). However, 10^{-3} M melatonin group showed the lowest number of cells in blastocysts among all groups ($P < 0.05$). Consequently, 10^{-7} M melatonin was chosen as the optimal concentration for subsequent experiments because it showed the highest blastocyst formation rate among the groups (Table 7).

3.2. The inhibitory effect of brusatol treatment during IVC

In the second experiment, the concentrations of brusatol used were 0, 50, 200 and 400 nM according to a previous study on brusatol treatment of mouse embryos

(Lin, Sui et al. 2018). Treatment with brusatol significantly decreased every steps of the porcine embryo development – cleavage rate, blastocyst formation rate, and total cell number of blastocysts. The 400 nM brusatol-treated group showed the lowest cleavage rate compared to control, 50 and 200 nM (73.7% vs. 93.4%, 84.6%, and 81.4%, respectively, $P < 0.05$, Table 8). Moreover, the effect of brusatol was evaluated on blastocyst formation rate, and all treatment groups (50, 200 and 400 nM) showed a significant decrease compared to control (5.6%, 1.5% and 1.8% vs. 14.8%, respectively, $P < 0.05$). Lastly, total cell numbers of blastocysts were significantly decreased in all brusatol-treated groups (50, 200 and 400 nM) compared to control (38.3, 29.3 and 28.7 vs. 56.5, respectively, $P < 0.05$). Therefore, 50 nM brusatol was considered as the optimal concentration of inhibiting Nrf2 transcription factor for the subsequent experiment.

3.3. Inverse effects of melatonin and brusatol treatment during IVC

To my knowledge, melatonin and brusatol have opposite functions when regulating *Nrf2*, therefore, to investigate the inverse effects of melatonin and brusatol, they were co-treated during IVC on subsequent embryonic development after IVF. The melatonin-treated group showed a significant increase in blastocyst formation rate compared to the control and brusatol groups (24.65% vs. 15.55% and 10.13%, respectively, $P < 0.05$, Table 5). Moreover, embryos treated with melatonin showed a significant difference in blastocyst total cell number compared to the control, brusatol and co-treated groups (78.80 vs. 52.60, 48.00 and 57.40, respectively, $P <$

0.05). However, there were no differences in cleavage rate. This result demonstrates the inverse effects of melatonin and brusatol on blastocyst formation rate and a possible effect of restoration in the co-treated group (Table 9).

3.4. Effect of melatonin and brusatol treatment during IVC on gene expression in IVF-derived porcine blastocysts

The expression of genes shown in Table 6 was investigated in IVF-derived porcine blastocysts. Figure 4A shows gene expression levels related to the melatonin receptor and the Nrf2/ARE signaling pathway and melatonin significantly increased mRNA transcript levels of *MT2*, *Nrf2* and *UCHL1* with no expression difference of *Keap1* in porcine blastocysts compared to control ($P < 0.05$). Unlike in other groups, the co-treatment group showed the same increase of *UCHL1* as the melatonin-treated group and the highest increase in *MT2* transcript level. In the brusatol-treated group, expression of *Nrf2* gene was significantly downregulated and expression of *Keap1* upregulated compared to control. Additionally, mRNA transcript levels related to ARE were examined (Fig. 4A). The expression levels of *HO-1* and *SOD1* were significantly increased in the melatonin-treated group, and *SOD1* was decreased in the brusatol treated-group compared to control; however, no difference was observed in *HO-1* expression. Lastly, as shown in Figure 4, the expression levels of *Bax* and *Bcl-2*, the apoptosis related gene, were evaluated in porcine blastocysts. The mRNA transcript level of *Bax* was significantly increased in the brusatol-treated and co-treated groups compared to control ($P < 0.05$), although the co-treated group was

significantly lower than the brusatol-treated group. Lastly, the expression level of *Bcl-2* was observed to be the highest in the melatonin and co-treated groups.

3.5. Assessment of MT1, Nrf2, and Keap1 levels by immunofluorescence staining

To elucidate effects of these agents at the protein levels, the presence of specific proteins related to the Nrf2/Keap1 signaling pathway was analyzed in porcine blastocysts. In Figure 5, MT2 was detected in all experimental groups and the highest intensity was observed in the melatonin-treated group compared to the control, brusatol and co-treated groups ($P < 0.05$). As shown in Figure 6, there was a significant increase of Nrf2 protein intensity in melatonin-treated blastocysts compared to other groups ($P < 0.05$). Protein expression level of Keap1 was also examined by immunocytochemistry (Fig. 7A). The intensity of the brusatol-treated and co-treated groups were significantly increased compared to the other groups ($P < 0.05$, Fig. 7B).

Table 7. Effect of melatonin during IVC on embryonic development after IVF.

Chemicals (M)	No. of embryos cultured	No. of embryos developed to (mean ± SEM*, %)		Total blastocyst cell number (mean ± SEM*)
		≥ 2 cells	Blastocyst	
Control (0)	185	145(76.67±5.30)	22(15.73±1.39)[a]	65.00±4.79[a]
10^{-9}	190	158(83.07±5.28)	32(16.87±2.28)[a]	87.00±3.08[c]
10^{-7}	188	161(84.03±3.92)	56(29.48±1.66)[b]	83.25±3.68[c]
10^{-5}	184	139(76.33±4.69)	31(18.25±3.72)[a]	84.25±2.93[c]
10^{-3}	185	139(74.40±3.21)	20(11.00±0.80)[a]	44.00±2.48[b]

* Six replicates were carried out.

* [a,b] Values with different superscripts in the same column are significantly different ($P < 0.05$).

* ANOVA

Table 8. Effect of brusatol during IVC on embryonic development after IVF.

Concentrations	No. of embryos cultured	No. of embryos developed to (mean ± SEM*, %)		Total blastocyst cell number (mean ± SEM*)
		≥ 2 cells	Blastocyst	
Control (0 nM)	177	165(93.40±1.29)[a]	24(14.86±1.59)[a]	56.50±1.56[a]
50 nM	180	155(84.58±3.39)[a]	10(5.56±1.07)[b]	38.25±2.18[b]
200 nM	181	149(81.42±3.72)[a]	3(1.48±0.92)[b]	29.33±3.76[b]
400 nM	185	138(73.70±5.92)[b]	3(1.80±1.30)[b]	28.67±1.45[b]

* Five replicates were carried out.

* [a,b] Values with different superscripts in the same column are significantly different ($P < 0.05$).

* ANOVA

Table 9. Co-treatment effects of melatonin and brusatol during IVC on embryonic development after IVF.

Chemicals	No. of embryos cultured	No. of embryos developed to (mean ± SEM*, %)		Total blastocyst cell number (mean ± SEM)
		≥ 2 cells	Blastocyst	
Control	187	163(86.99±2.52)	29(15.55±1.13)[a]	52.60±4.73[a]
Melatonin	183	162(88.35±2.83)	45(24.65±1.65)[b]	78.80±3.04[b]
Brusatol	197	157(79.41±3.25)	20(10.13±1.26)[c]	48.00±2.21[a]
Mtn+Bru	193	167(86.42±1.22)	29(14.98±1.09)[ac]	57.40±1.57[a]

* Five replicates were carried out.

* [a,b] Values with different superscripts in the same column are significantly different ($P < 0.05$).

* Ctrl, control; Mtn, 10^{-7} M melatonin; Bru, 50 nM brusatol

* ANOVA

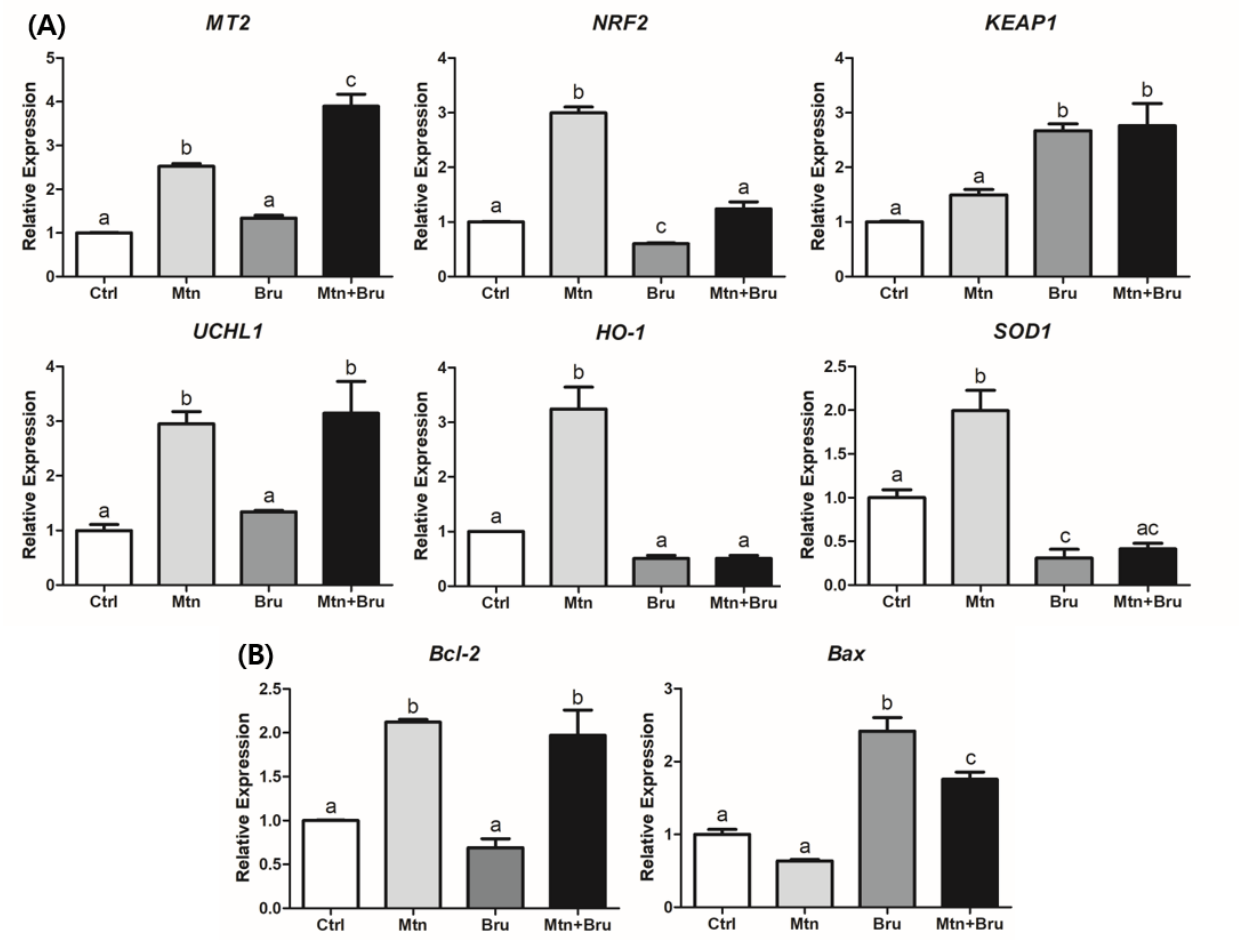
(A)
MT2
NRF2
KEAP1
UCHL1
HO-1
SOD1
Relative Expression
Ctrl
Mtn
Bru
Mtn+Bru
(B)
Bcl-2
Bax

Figure 4. Effect of 10^{-7} M melatonin on expression of Nrf2/ARE signaling pathway related genes in IVF-derived porcine blastocysts. (A) Nrf2/ARE signaling pathway-related genes (*MT2, Nrf2, Keap1, UCHL1, SOD1,* and *HO-1*). (B) Apoptosis-related genes (*Bax* and *Bcl-2*). Within the same mRNA, bars with different alphabetical letters are significantly different among the groups ($P < 0.05$). The experiment was replicated at least three times.

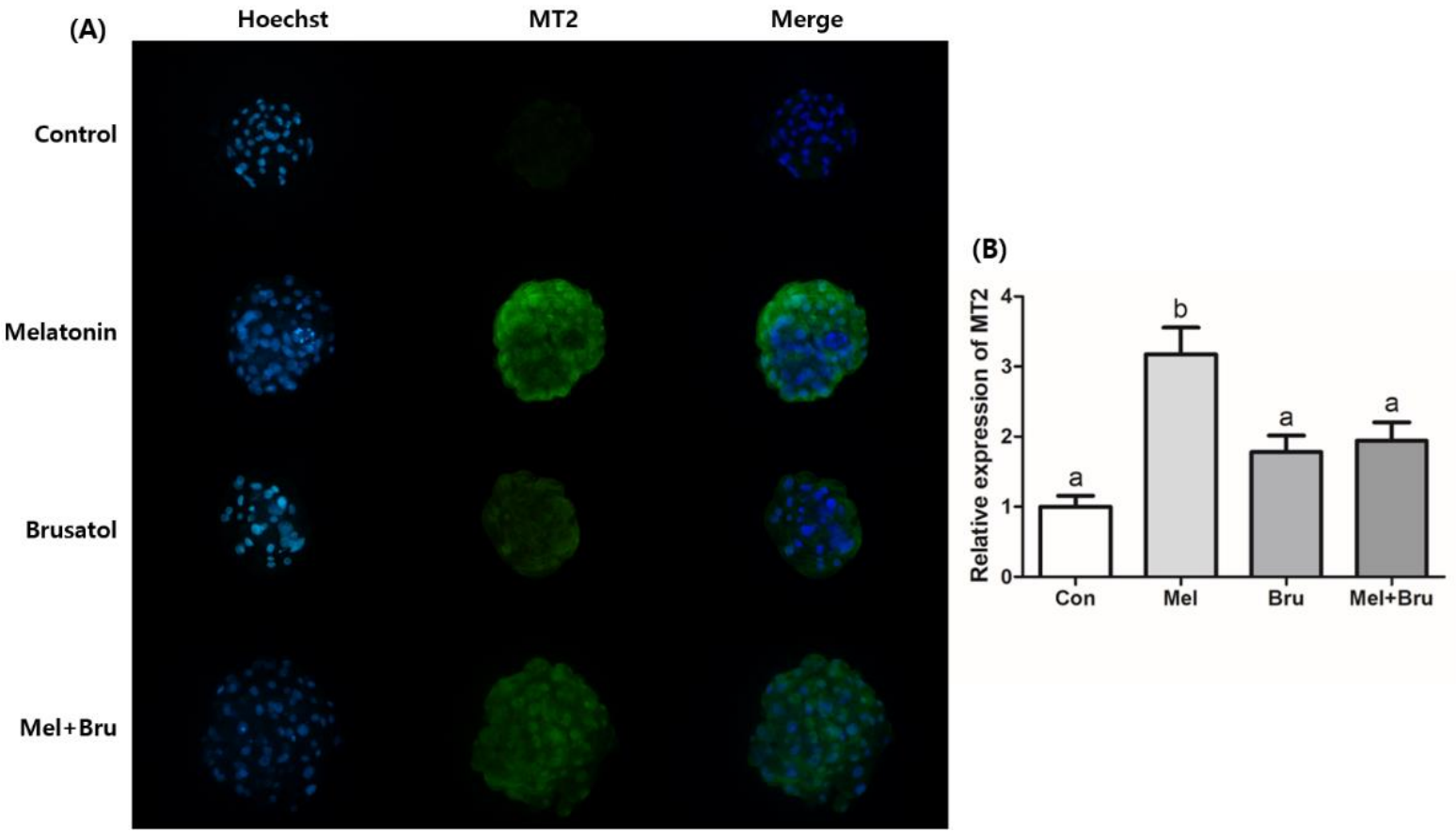
(A)
Hoechst
MT2
Merge
Control
Melatonin
Brusatol
Mel+Bru
(B)
Relative expression of MT2
0
1
2
3
4
a
b
a
a
Con
Mel
Bru
Mel+Bru

Figure 5. Immunocytochemical analysis of MT2 in porcine blastocysts. (A) Images of blastocysts were obtained by fluorescence microscopy. Representative *in vitro* fertilized porcine blastocysts in each group were stained with MT2 and counterstained with Hoechst 33342 (B) Statistical analysis of 10^{-7} M melatonin, 50 nM brusatol, and co-treatment effects on MT2 protein expression in porcine blastocysts. Five replicates were carried out for this experiment. Data are shown as the means ± S.E.M. Groups marked with different alphabetical letters are significantly different ($P < 0.05$). Mel, 10^{-7} M melatonin; Bru, 50 nM brusatol. Original magnification 200×.

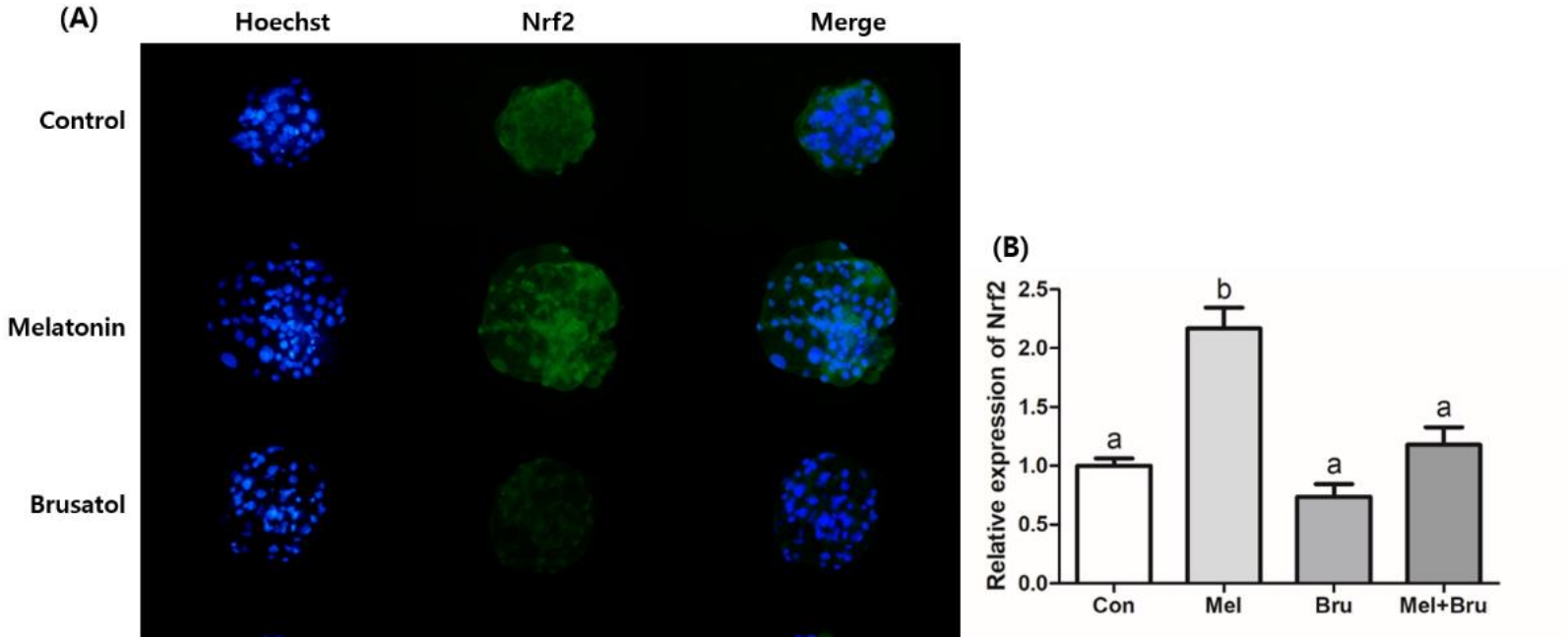
(A)
Hoechst
Nrf2
Merge
Control
Melatonin
Brusatol
Mel+Bru
(B)
Relative expression of Nrf2
2.5
2.0
1.5
1.0
0.5
0.0
a
b
a
a
Con
Mel
Bru
Mel+Bru

Figure 6. Immunocytochemical analysis of Nuclear factor erythroid 2-related factor 2 in porcine blastocysts. (A) Representative *in vitro* fertilized porcine blastocysts in each group were stained with Nuclear factor erythroid 2-related factor 2 and counterstained with Hoechst 33342. (B) Statistical analysis of 10^{-7} M melatonin, 50 nM brusatol, and co-treatment effects on Nuclear factor erythroid 2-related factor 2 protein expression in porcine blastocysts. Six replicates were carried out for this experiment. Data are shown as the means ± S.E.M. Groups marked with different alphabetical letters are significantly different ($P < 0.05$). Mel, 10^{-7} M melatonin; Bru, 50 nM brusatol. Original magnification 200×.

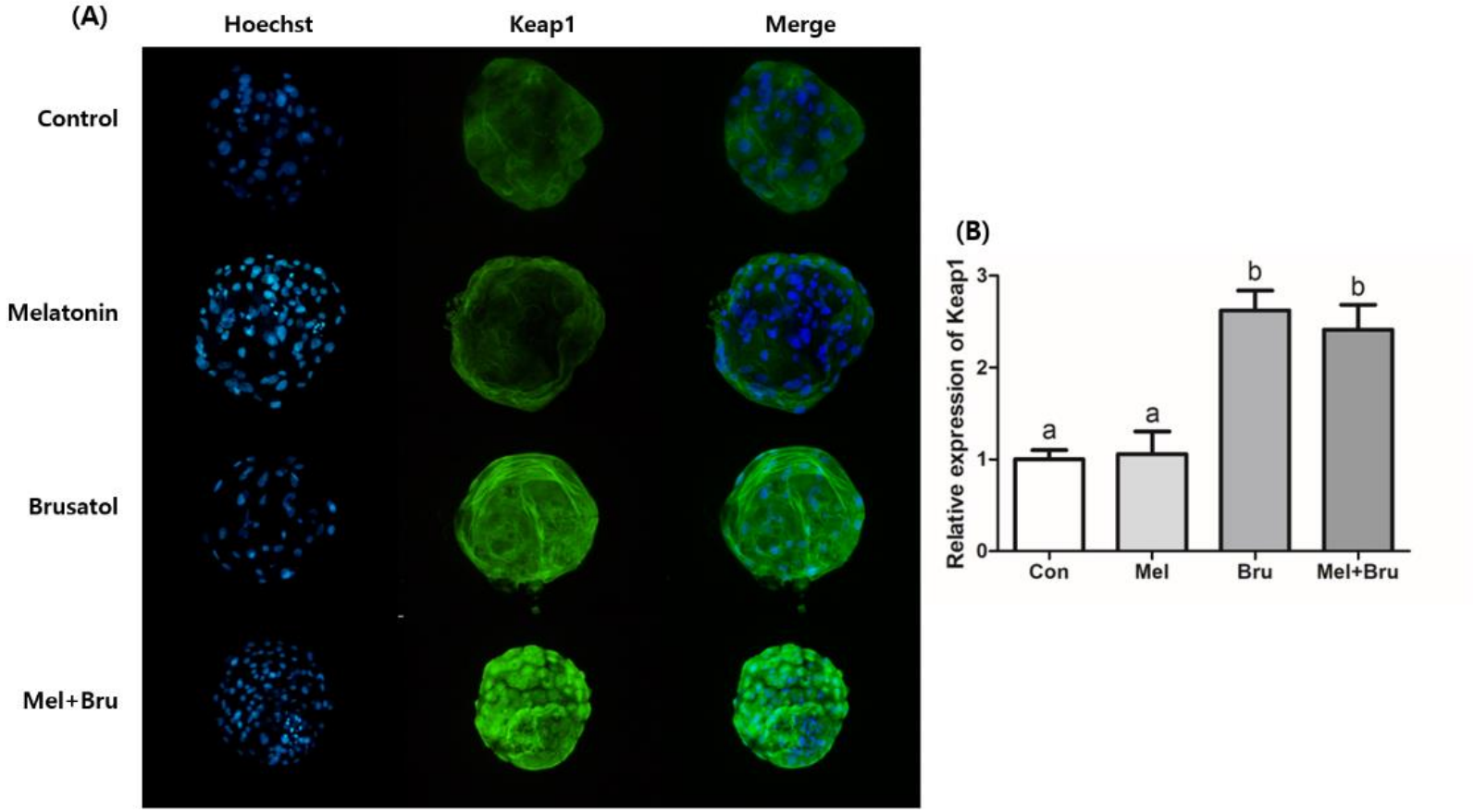
(A)
Hoechst
Keap1
Merge
Control
Melatonin
Brusatol
Mel+Bru
(B)
Relative expression of Keap1
0
1
2
3
a
a
b
b
Con
Mel
Bru
Mel+Bru

Figure 7. Immunocytochemical analysis of Kelch-like ECH-associated protein 1 in porcine blastocysts. (A) Representative *in vitro* fertilized porcine blastocysts in each group were stained with Kelch-like ECH-associated protein 1 and counterstained with Hoechst 33342. (B) Statistical analysis of 10^{-7} M melatonin, 50 nM brusatol, and co-treatment effects on Kelch-like ECH-associated protein expression in porcine blastocysts. Five replicates were carried out for this experiment. Data are shown as the means ± S.E.M. Groups marked with different alphabetical letters are significantly different ($P < 0.05$). Mel, 10^{-7} M melatonin; Bru, 50 nM brusatol. Original magnification 200×.

4. Discussion

For the first time, the current study examined the role of the Nrf2/ARE signaling pathway in development of porcine preimplantation embryos by treating them with melatonin. The results provide evidences that communications between melatonin and the Nrf2/ARE signaling pathway improved porcine embryo IVC, regulation of the Nrf2 cascade-related gene transcript levels, and subsequent protein expression in the blastocysts. Moreover, increased mRNA transcript levels were prevented by the Nrf2 specific inhibitor, brusatol. This implies that melatonin improves embryonic development, and increases expression of Nrf2/ARE signaling genes and protein expression levels in accordance with the hypothesis.

Previous studies suggesting that the role of melatonin during porcine embryo development is pivotal and optimized concentrations of melatonin were treated during IVC in order to prove its effects (Rodriguez-Osorio, Kim et al. 2007; Choi, Park et al. 2008; Nakano, Kato et al. 2012; Do, Shibata et al. 2015). Possible reasons for the inconsistencies might be different experimental methods, gas conditions during incubation or culture conditions such as media compounds and even differences within species (Rodriguez-Osorio, Kim et al. 2007; Nakano, Kato et al. 2012; Do, Shibata et al. 2015). Therefore, the melatonin concentration was optimized to establish the appropriate concentration in the experimental environment. In the results, 10^{-7} M melatonin was considered to be the optimal concentration for subsequent experiments. This is consistent with the fact that melatonin is effective at antioxidation during porcine IVC (Rodriguez-Osorio, Kim et al. 2007; Choi, Park

et al. 2008; Nakano, Kato et al. 2012; Do, Shibata et al. 2015). In contrast, 10^{-3} M melatonin decreased the total cell number of blastocysts compared to control (Table 7) and this, being consistent with a previous study, supports the idea that 10^{-3} M melatonin treatment during IVC of IVF-derived porcine embryos may be detrimental for embryo development partially due to high concentration-induced toxicity (Rodriguez-Osorio, Kim et al. 2007).

Positive effects of melatonin treatment during IVM have also been reported: 10^{-9} M melatonin was the most effective concentration for oocyte maturation, cumulus cell expansion, lipid content and even subsequent embryonic development *via* several signaling pathways such as sonic hedgehog signaling and the pentose phosphate pathway (Shi, Tian et al. 2009; Alvarez, Ferretti et al. 2013; Jin, Lee et al. 2017; Lee, Jin et al. 2017; Lee, Jin et al. 2018b). On the other hand, investigations on modulation of specific pathways by melatonin during porcine IVC still need further details and clarification. Nrf2 is generally accepted as having crucial roles in up-regulating the expressions of cytoprotective enzymes, cellular antioxidant defense system, and reproduction processes. (Leung, Kwong et al. 2003; Lee & Johnson 2004; Hu, Roberts et al. 2006; Wells 2015; Akino, Wada-Hiraike et al. 2018). When activated, it in turn activates AREs to prevent OS (Nguyen, Nioi et al. 2009; Wells 2015; Akino, Wada-Hiraike et al. 2018). In addition, blastocyst formation is a critical indicator for the efficiency of embryo development and culture conditions (Nomura, Iwase et al. 2007) and the total cell number of blastocysts is a standard criterion for evaluating the quality of embryos (Knijn, Gjorret et al. 2003). Consequently, the results showed that melatonin was effective on increasing porcine

embryonic development and regulated *Nrf2* and its related genes (*Keap1*, *UCHL1*, *SOD1*, and *HO-1*) in porcine blastocysts in the experiment. The results may support the fact that melatonin activates the Nrf2/ARE signaling pathway as demonstrated in previous studies (Tripathi & Jena 2010; Negi, Kumar et al. 2011; Chen, Renn et al. 2017; Guo, Sun et al. 2017).

Here, brusatol, the *Nrf2* specific inhibitor, was applied to the current study to specify whether melatonin truly functions as an antioxidant by regulating the Nrf2/ARE signaling pathway. Brusatol inhibits *Nrf2* directly and specifically in many types of cells and oocytes by inducing a rapid depletion of Nrf2 (Olayanju, Copple et al. 2015; Ma, Li et al. 2017). Moreover, it is proved that brusatol with micromolar concentrations inhibits protein synthesis of Nrf2, and also it inhibits *Nrf2* transcription specifically with nanomolar concentrations (Ren, Villeneuve et al. 2011). In Table 8, the negative effect is clearly shown and also the result is supported by the study of Lin et al which showed that 50 nM brusatol also had negative effects during IVC of mouse embryos (Lin, Sui et al. 2018). This supports the results shown in Table 8 and Figure 4A, and these results indicate that treatment with brusatol is detrimental for embryonic development in a dose-dependent manner. Therefore, the study demonstrated that brusatol inhibited the actions of Nrf2.

The hypothesis was that melatonin would activate this pathway through melatonin receptor 2 (MT2), subsequently preventing OS during porcine IVP. At present, including MT2, other melatonin receptors are known such as MT1, in mammals, and MT3 in amphibians and birds (Reppert, Weaver et al. 1996; Sugden, Davidson et al. 2004). Moreover, they appear to be part of the superfamily of guanine

nucleotide binding protein (G protein)-coupled receptors (GPCR) (Reppert 1997). It was suggested that the mechanism and abilities of melatonin to enhance the expansion of cumulus cells in COCs and oocytes independently and to enhance subsequent embryonic development is mediated by MT2 (Danilova, Krupnik et al. 2004; Lee, Jin et al. 2018b) which implies that functions of MT2 is pivotal for melatonin mechanism during embryonic development. In Figure 4A and 5, MT2 was also expressed in the control and brusatol-treated groups. This can be explained by the study of Pala et al that MT2 bindings can be achieved through non-specific hydrophobic interactions (Pala, Lodola et al. 2013); moreover, brusatol is suitable for binding with MT2 because it is also known to have poor aqueous affinity (Zhou, Tan et al. 2017). To sum up, it is presumed that IVF-derived porcine blastocysts took up melatonin *via* MT2, and a result the blastocyst formation rate and total cell number of blastocysts were increased.

In Figure 6, the results may support the idea that melatonin is infused through MT2 into developing embryos, thereby activating AREs *via* the Nrf2/ARE signaling pathway. In particular, *HO-1* and *SOD1* are genes that are responsible for antioxidative mechanisms related to the Nrf2/ARE signaling pathway (Ma 2013; Akino, Wada-Hiraike et al. 2018; Lin, Sui et al. 2018). According to Figure 4A, brusatol is closely related to *SOD1* and downregulates its function. Although *HO*-1 has a close relationship with the Nrf2/ARE signaling pathway, further studies of the possible cross-talk between brusatol and *HO*-1 are needed because opposite effects on *HO*-1 by brusatol have been reported in some studies (Xu, Li et al. 2015; Liu, Xu et al. 2019). Therefore, it is speculated that brusatol has no effect on *HO*-1 at least in

porcine preimplantation blastocysts, but affects *Nrf2* and *SOD1* regulation. Connections between melatonin and the Nrf2/ARE pathway may partially be explained by the expression of *Nrf2*, because its expression level was inversely regulated in each treatment.

According to the results, because melatonin up-regulated mRNA and protein expression level of *Nrf2*, it was subsequently assumed that melatonin would also affect ubiquitination in Nrf2 and keap1 interaction. Therefore, along with the proteasomal degradation, Ubiquitin C-terminal hydrolase L1 (*UCHL1*) can be a potential marker for deubiquitylation of enzymes from the proteasome system using ubiquitin because its decrease is related to decreased cell proliferation (Sanchez-Diaz, Chang et al. 2017). It is known that OS and apoptosis have mutual interactions (Kannan & Jain 2000) and also the antioxidative mechanism of melatonin is closely involved in apoptosis of cells and embryos (Zhao, Hao et al. 2016; Lan, Han et al. 2018). Therefore, *Bcl-2* and *Bax*, apoptosis related genes, were selected for analysis. Figure 4B demonstrates that the apoptosis related genes are regulated by both melatonin and brusatol.

Ren and colleagues have stated that cell lines had different statuses of *Keap1*, and in part, brusatol promoted Nrf2 degradation in a keap1-dependent manner depending on the types of cells (Ren, Villeneuve et al. 2011). However, there are no studies on brusatol-Keap1 interaction in gametes or zygotes. Interestingly, as shown in figure 4A and 7, the results may support the partial dependence of brusatol on *Keap1*. In brief, the actions of brusatol may depend directly on *Keap1* at least in

porcine blastocysts in accordance with the result. However, the mechanism by which brusatol depends on *Keap1* warrants further investigation.

In this experiment, it is hypothesized that through the uptake of melatonin by porcine embryos, melatonin directly activates and translocates *Nrf2*, then AREs are produced. However, brusatol (the *Nrf2* specific inhibitor) was applicated in order to verify that the activation of *Nrf2* is truly affected by melatonin. It was found that melatonin up-regulated mRNA and protein expression level of MT2 in the porcine embryos (Fig. 4A and 5) and also up-regulated mRNA and protein expression level of Nrf2 (Fig. 4A and 6). Additionally, the inhibitory works of brusatol on *Nrf2* was also observed in the porcine embryos after the uptake of melatonin. Altogether, the current study suggested a plausible interaction between a direct impact of melatonin through the Nrf2/ARE signaling pathway on porcine preimplantation embryos during IVC. The MT2 receptor, as one of the GPCRs, communicates with numerous pathways that activates antioxidative responses (Han, Wang et al. 2017; Lee, Jin et al. 2017) and among them, the Nrf2/ARE signaling pathway could be one of the potential pathways for embryo researches. As this is the first research into the mechanism of the Nrf2/ARE signaling pathway in porcine IVF-derived preimplantation embryos, further studies should be initiated in order to elucidate this mechanism.

Chapter II. Involvement of phytanic acid-induced peroxisomal activity in porcine oocytes and embryos

1. Introduction

Peroxisomes are widely known to be essential dynamic organelles for most eukaryotic cells (Gabaldon 2010). Their copy numbers, activities, and morphologies differ depending on the organ and tissue types as well as on nutrition (Fransen, Lismont et al. 2017). The main functions of the peroxisome are as follows: (i) the enzymatic breakdown of long-chain FA complexes via alpha-, beta-, and omega oxidation mechanisms, (Wierzbicki 2007) (ii) ether-phospholipid biosynthesis, (Wanders & Waterham 2006) (iii) amino acid catabolism, (Manivannan, Scheckhuber et al. 2012) and (iv) reactive oxygen species-related cellular defense systems (Antonenkov, Grunau et al. 2010). The significance of peroxisomes was first demonstrated by Goldfischer et al. in Zellweger syndrome, which is an inherited lethal disorder in humans, caused by the lack of peroxisomes in the kidney and liver (Goldfischer, Moore et al. 1973). Moreover, peroxisome dysfunction causes several other diseases such as X-linked adrenoleukodystrophy and Refsum disease (Van Veldhoven 2010). However, the importance of this organelle in germ cells, such as oocytes, remains to be elucidated.

Alpha-oxidation occurs solely in the peroxisomes and requires phytanic acid (PA) as a source for subsequent metabolic processes (van den Brink & Wanders

2006). Alpha-oxidation is initially activated by the decomposition of the long-chain fatty acid PA into pristanic acid to deliver shortened FAs for subsequent oxidation, such as beta-oxidation in mitochondria and even the peroxisome itself, to produce energy (Wanders, Jansen et al. 2001). Additionally, inhibition of beta-oxidation in mouse and bovine oocytes decreased the nuclear maturation rates and negatively affected subsequent embryonic development (Ferguson & Leese 2006; Dunning, Cashman et al. 2010). It was recently reported that lipids are a potential energy source for the oocytes, wherein the amount of ATP produced by lipids is several times greater than that of the complete oxidation of glucose (Lowe, Bathgate et al. 2019). It has also been reported that ATP usage is fundamental for porcine oocyte maturation (Yuan, Liang et al. 2016). Lipid metabolism has been previously demonstrated to play an important role in porcine oocytes, reinforcing their competence and providing the potential for subsequent embryonic development (Dunning, Russell et al. 2014; Prates, Nunes et al. 2014; Jin, Lee et al. 2017). Additionally, several studies have indicated that lipid metabolism plays a significant role in oocyte maturation (Somfai, Kaneda et al. 2011; Jin, Lee et al. 2017). However, studies on the specific interactions between the peroxisome and lipid metabolism in porcine oocytes are currently lacking. Therefore, this study aimed to characterize the metabolism of peroxisomal lipids and the diversity of its functions in porcine oocytes.

To date, the understanding of peroxisomal action in mammalian oocytes, including its role in oocyte maturation potential, embryonic development, and self-defense mechanisms, is scarce. Since the action of the peroxisome on lipid metabolism, ATP production, and cellular defenses against ROS and apoptosis are

significant in eukaryotic cells (Titorenko & Terlecky 2011; Manivannan, Scheckhuber et al. 2012; Waterham & Wanders 2012; Del Rio & Lopez-Huertas 2016), the role of peroxisomes in oocytes also merits further investigation. The hypothesis was narrowed to the fact that peroxisomes may also be involved in the mechanisms of porcine oocyte maturation, competence, and energy production processes. The aim of this study was to investigate the peroxisomal lipid metabolism in porcine oocytes after treatment with PA during IVM.

2. Materials and methods

2.1. Research ethics and chemicals

Procedures for research ethics and chemicals were described in general methodology.

2.2. Oocyte recovery and IVM

Procedures for oocyte recovery and IVM were described in general methodology.

2.3. Assessment of nuclear maturation

After 42-44 h of IVM, the matured oocytes were denuded in 0.1% hyaluronidase in TALP medium containing 114 mM NaCl, 9.91 mM KCl, 0.3 mM Sodium Phosphate, 2 mM Sodium Bicarbonate, 10 mM HEPES, 0.3% PVA, 2.78 mM $CaCl_2$, 65.12 μM $MgCl_2$ $6H_2O$, 5 mM Glucose, 170 μM Kanamycin, and 0.3% BSA by gentle pipetting, and then washed three times with TALP medium. The denuded oocytes were fixed in 4% paraformaldehyde for 1 h before transferring to 5 μg/mL Hoechst-33342 for 8 min. After washing, the oocytes were mounted on a sliding glass with a coverslip and evaluated under UV light using a fluorescence microscope (TE2000-S; Nikon, Tokyo, Japan) to be classified as: “degenerate,”

“immature” (no extrusion of polar body), or “mature (metaphase II and first polar body extrusion)”. Each of the eight oocytes, were used for oocyte nuclear assessment.

2.4. Cumulus cell expansion assessment

The degree of cumulus expansion exhibited by the COCs was evaluated after 42-44 h of IVM as previously described (Vanderhyden, Caron et al. 1990; Kim, Lee *et al.* 2017a; Lee, Oh et al. 2019). Four replicas, with 40 oocytes in each group, were used for cumulus expansion assessment. Briefly, no expansion was observed at a degree of 0, which is characterized by a complete or partial detachment of the CCs from the oocyte, with a flattened monolayer of fibroblastic appearance. At degree 1, a spherical shape was observed in the CCs without any expansion. At degree 2, expansion of the CCs was only observed on the outermost layer, while degree 3 showed expansion of all layers of the cells, except for the cells that were most proximal to the oocyte, the corona radiata. Finally, at degree 4, full expansion of the CCs was observed, including the corona radiata.

2.5. *In vitro* fertilization

Procedures for IVF were described in general methodology.

2.6. Embryo evaluation and total cell count after IVF

On the first day of IVF, that is, when the zygotes with second polar bodies had

been transferred to PZM-5, was denoted as Day 0. After 48 h of IVF (Day 2), the cleaved embryos were monitored using a stereomicroscope. On Day 7 (168 h) after IVF, the rate of blastocyst formation was evaluated, and total cell numbers were counted. After washing in PBS, the Zona Pellucida was removed by digesting in 0.5% pronase to remove any remaining attached spermatozoa. The zona-free blastocysts were stained with 5 μg/mL Hoechst 33342 for 8 min after washing in TALP medium. The stained blastocysts were washed with TALP medium once more before mounting on glass slides with 100% glycerol drops. These were then covered with a coverslip and analyzed under a fluorescence microscope (Nikon Corp.) at a magnification of 400×.

2.7. Measurement of intracellular glutathione (GSH) and ROS levels

After 42-44 h of IVM, the matured oocytes were denuded in 0.1% hyaluronidase in TALP, and then were washed several times in TALP medium. To measure the intracellular levels of GSH and ROS in the oocytes, CellTracker Blue (4-chloromethyl-6.8-difluoro-7-hydroxycoumarin (CMF2HC); Invitrogen) and H2DCFDA (2',7'-dichlorodihydrofluorescein diacetate; Invitrogen) were used, respectively. After washing, the oocytes were transferred to 10 μM of CellTracker Blue or 10 μM of H2DCFDA, diluted with TALP medium, and incubated for 30 min in the dark. The stained oocytes were washed three times in TALP medium before transferring to a 4-μL droplet of TALP medium and then, covered with mineral oil. The fluorescence images were captured using an epifluorescence microscope

(TE2000-S; Nikon, Tokyo, Japan) attached to UV filters (370 nm for GSH and 460 nm for ROS). Analysis of fluorescence intensities was performed using Image J software (version 1.49q; National Institutes of Health, Bethesda, MD, USA). Three independent replicas with a total of 124 oocytes were used for this analysis.

2.8. Immunofluorescence staining

Indirect immunofluorescence staining was used to evaluate and compare the protein expression levels of PEX19 and PHYH among the experimental groups after IVM. Matured oocytes were denuded using 0.1% hyaluronidase in TALP, and were then washed with PBS containing 1% PVA. Oocyte fixation was performed using 4% paraformaldehyde (w/v) in PBS for 1 h. The oocytes were permeabilized with 1% Triton X-100 (v/v) in distilled water (DW) for 1 h at 39°C. Oocytes were then washed four times in 1% PVA droplets and incubated in 2% BSA in DW for 2 h to prevent nonspecific binding. The oocytes were then directly moved to 2% BSA containing primary antibody for phytanoyl-CoA 2-hydroxylase (PHYH) (1:400) (Anti-PHYH; Rabbit, Polyclonal; MBS3212923; MyBioSource, San Diego, USA), and peroxisomal biogenesis factor 19 (PEX19) (1:400) (Anti-PEX19; Rabbit, Polyclonal; MBS9605735; MyBioSource, San Diego, USA) and incubated overnight at 4°C. After incubation, the oocytes were washed three times with PBS containing 1% PVA and incubated with a secondary fluorescein isothiocyanate-conjugated anti-rabbit polyclonal antibody (1:200) (Goat Anti-Rabbit; IgG; ab6717; Abcam, Cambridge, UK) at 37°C for 2 h in the dark). Immediately after incubation with the

secondary antibody, the counterstaining of the oocytes was performed with 5 μg/mL Hoechst-33342 for 8 min. After washing, they were mounted on glass slides with 100% glycerol, covered with coverslips, and analyzed under a fluorescence microscope. The fluorescence intensity measurements were measured using ImageJ software. Three replicas of at least 20 oocytes from each group were used.

2.9.mRNA transcript expression analysis by quantitative real-time PCR

Procedures for Real time PCR were described in general methodology. Samples used in this experiment are porcine oocytes and at least 400 oocytes (from five biological replicas) from each group were used for RNA extraction. The primers used in this experiment are listed in Table 10-14.

2.10. Lipid droplet staining

The lipid droplet staining was performed as described previously (Dunning, Russell *et al.* 2014). 10 milligram of BODIPY-LD (D3922; Molecular Probes, Eugene, OR, USA) or BODIPY 493/503 was prepared by dissolving in absolute DMSO and diluting to a final concentration of 10 μg/mL in 1% PVA/PBS to prevent adhesion between the oocytes and dishes. More than 30 oocytes from different biological replica and three technical replicas were performed for this experiment. The denuded oocytes were fixed in 4% PFA in PBS for 2 h at room temperature and then washed three times with droplets of 1% PVA in PBS. The oocytes were incubated for 1 h at room temperature in the dark. After incubation, the oocytes were

washed with 1% PVA in PBS three times, and then mounted on glass slides with coverslips. Images were captured using a fluorescence microscope (TE2000-S; Nikon). The fluorescence intensities of the lipid droplets were measured using ImageJ software.

2.11. Fluorescent fatty acid analog assays

Fluorescent FA analog assays were performed according to Lolicato *et al.* (Lolicato, Brouwers *et al.* 2015). Briefly, the oocytes were denuded and fixed in 4% PFA in PBS for 2 h, and then washed three times in 1% PVA. The fixed oocytes were incubated in 6 μM BODIPY 558/568 C12 (BODIPY-FA; D3835; Molecular Probes, Eugene, OR, USA) diluted in PBS for 1 h at room temperature in the dark. After incubation, the oocytes were washed three times in 1% PVA in PBS before mounting on glass slides and covered with coverslips. Images were captured using an epifluorescence microscope (TE2000-S; Nikon). More than 30 oocytes from different biological replica of each experimental group were used, with three technical replicas performed for this experiment.

2.12. JC-1 mitochondrial membrane potential assays

A total of 30-40 oocytes were used for each group. The denuded matured oocytes were washed at least three times in PVA/PBS solution and fixed in 4% PFA for 1 h. Oocytes were then transferred to PVA/PBS solution to remove any remaining PFA, and were then incubated at 37°C in culture medium (PZM-5) mixed with 2 μL JC-

1 solution (ab113850, Abcam; Cambridge, UK) for 30 min. After incubation, the oocytes were washed with PVA/PBS solution at least three times before mounting on coverslips. Images for each oocyte were obtained using an epifluorescence microscope (TE2000-S; Nikon). The fluorescence ratio of the JC-1 aggregate and JC-1 monomer (590 nm/530 nm, respectively) was measured using ImageJ software. The intensities of the control group were arbitrarily set to 1.

2.13. ATP content assay

The ATP content assay was performed as described previously (Guo, Xuan et al. 2019). Denuded mature oocytes were washed with 1% PVA in PBS three times, and then fixed in 4% PFA in PBS for 2 h at room temperature. After fixation, the oocytes were washed with 1% PVA in PBS several times and then transferred to PBS supplemented with 0.5 μM BODIPY FL ATP (BODIPY-ATP; A12410; Molecular Probes, Eugene, OR, USA) for 1 h at room temperature in the dark. The stained oocytes were washed three times in 1% PVA in PBS, mounted on glass slides and covered with slips. An epifluorescence microscope (TE2000-S; Nikon) was used to capture images. The ATP content was measured using ImageJ software. The intensities of the control group were arbitrarily set to 1. More than 30 oocytes from different biological replica of each experimental group were used, with four technical replicas for this experiment.

2.14. Statistical analysis

Procedures for statistical analysis were described in general methodology.

Table 10. Primer sequences related to oocyte competence and cumulus expansion.

Genes	Primer sequences (5'- 3')	Product size (bp)	Accession No.
GAPDH	F: GTCGGTTGTGGATCTGACCT	207	NM_001206359
	R: TTGACGAAGTGGTCGTTGAG		
POU5F1	F: GGTGGAGGAAGCTGACAACA	119	NM_001113060.1
	R: TCTCCAGGTTGCCTCTCACT		
BMP15	F: CTGGGCTTGCCTGTTTGTTC	161	NM_001005155.2
	R: GCCCAGTTCCCATCACTTCA		
GDF9	F: ATCCTTCAGCCCCTAGTGGT	129	NM_001001909.1
	R: GGCTGCCAGAAGAGTCATGT		
PTGS2	F: CCAGCACTTCACCCATCAGT	203	NM_214321.1
	R: GAGTGTCTTTGGCTGTCGGA		
HAS2	F: ATGTACACGGCCTTCAGAGC	144	NM_214053.1
	R: ATCTCCTCCGACACCTCCAA		
TNFAIP6	F: GCTCACGGATGGGGATTCAA	246	NM_00159607.1
	R: AATGGGGTAGCCAACTCTGC		

F, Forward primer; R, Reverse Primer

Table 11. Primer sequences related to antioxidant and apoptosis.

Genes	Primer sequences (5'- 3')	Product size (bp)	Accession No.
CAT	F: AGGGAGAGGCGGTTTATTGC	117	NM_001206359
	R: GGACTCGTTGGTGAAGCTCA		
BCL-2	F: AATGTCTCAGAGCAACCGGG	193	NM_214285
	R: GGGGCCTCAGTTCTGTTCTC		
BAX	F: CATGAAGACAGGGGCCCTTT	181	XM_003127290
	R: CATCCTCTGCAGCTCCATGT		

F, Forward primer; R, Reverse Primer

Table 12. Primer sequences related to peroxisome activities

Genes	Primer sequences (5'- 3')	Product size (bp)	Accession No.
PHYH	F: CCCTTCAGGCCCAGCAATAA	102	NM_001113447.1
	R: GCCTTTGTGAGTTCCTGGGA		
PEX3	F: AATGCATCTTCCTGGGGACG	125	NM_001244185.1
	R: ATACTGTCGTCGTGCTTGGG		
PEX5	F: CAGGCGGAGAATGAGCAAGA	117	XM_013988424.2
	R: GGACTCGTTGGTGAAGCTCA		
PEX12	F: CTCCTAAACTCGATCGCCCC	127	XM_003131719.4
	R: CGGTTCCGATCTCTCTCTGC		
PEX19	F: CTCAATCTATCGGGCCCACC	144	XM_001928869.5
	R: TAGACGACACTCCTGCCTCA		
PPARα	F: AGGTCACGCTGCTGAAGTAC	243	NM_001044526.1
	R: CGCACCAAATGATAGCAGCC		
PPARγ	F: CCATTCCCGAGAGCTGATCC	192	XM_005669783.3
	R: TTTATCCCCACAGACACGGC		

F, Forward primer; R, Reverse Primer

Table 13. Primer sequences related to lipid metabolism

Genes	Primer sequences (5'- 3')	Product size (bp)	Accession No.
PLIN2	F: CTAAAGGGGCTGTGACTGGG	123	NM_214200.2
	R: CACTTCCGGTCACTGCTTCT		
ATGL	F: GACGGTGGCATCTCAGACAA	113	NM_001098605.1
	R: TGGATGTTGGTGGAGCTGTC		
HSL	F: GCCTTTCCTGCAGACCATCT	104	NM_214315.3
	R: CACTGGTGAAGAGGGAGCTG		
MGLL	F: ACCCCACAGAGTGTCCCATA	96	XM_013982013.2
	R: GGGTGTAGCTGAGGGTTTCC		
CGI58	F: TCTTGCTGGGACACAACCTG	220	NM_001012407.1
	R: CCAAAGGGTCCTGCAATCCT		

F, Forward primer; R, Reverse Primer

Table 14. Primer sequences related to mitochondria

Genes	Primer sequences (5'- 3')	Product size (bp)	Accession No.
PGC-1a	F: CACGGACAGAACTGAGGGAC	156	XM_021100442.1
	R: ACCTGCGCAAAGTGTATCCA		
NRF1	F: CAGCAAGTACAGCAGGTCCA	222	XM_021078993.1
	R: ATGAGGCCGTTTCCGTTTCT		
TFAM	F: GCTCTCCGTTCAGTTTTGCG	238	NM_001130211.1
	R: ACCTGCCAGTCTGCCCTATA		

F, Forward primer; R, Reverse Primer

3. Results

3.1. Effect of phytanic acid on oocyte maturation

Different concentrations of PA (control (0 μM), 20 μM, 40 μM, and 80 μM) were used to determine the optimal concentration of IVM. As shown in Figure 8c, a PA concentration of 40 μM significantly increased the maturation rate of porcine oocytes compared to the control (83.56% vs. 73.91%; $P < 0.05$). Additionally, 40 μM PA also showed the lowest degeneration rate of porcine oocytes (Fig. 8b) compared to the control (7.98% vs. 16.25%; $P < 0.05$). As shown in Figure 8d, 40 μM PA showed the highest cumulus expansion rate compared to the control, 20 μM, and 80 μM concentrations (degree 2.94 vs. degree 2.44, degree 2.66, and degree 2.65, respectively; $P < 0.05$). More than 200 oocytes per group were used for the maturation analysis. The expression of mRNAs related to oocyte competence (*bone morphogenetic protein 15* (*BMP15*), *growth differentiation factor 9* (*GDF9*), *and Octamer-binding transcription factor 4* (*POU5F1*)) and cumulus expansion (*hyaluronan synthase 2* (*HAS2*), *prostaglandin-endoperoxide synthase 2* (*PTGS2*), and *tumor necrosis factor-inducible gene 6* (*TNFAIP6*)) were examined. Figure 8e-g shows that the expression levels of *BMP15* and *POU5F1* in the oocytes were higher in the 40 μM PA group. Moreover, the level of *GDF9* was higher in the 80 μM PA group. In cumulus cells (CCs), the expression level of *PTGS2* was higher in the 40 μM PA group, and *HAS2* was higher in the 20 μM PA group than in the other

groups (Fig. 13d). Lastly, the expression of *TNFAIP6* was significantly increased in all PA-treated groups (Fig. 8h-j). As a result, 40 μM PA was used for subsequent experiments.

3.2. Effect of phytanic acid on embryonic development

Even though no differences were found in the cleavage rate (Fig. 9a), 40 μM PA showed a strong positive effect and significantly increased the blastocyst formation rate compared to the control group (21.98 % vs. 11.32 %; $P < 0.05$, Fig. 9b). Furthermore, the total number of cells in blastocysts was also significantly higher than that in the Control Group (64.63 vs. 51.15; $P < 0.05$, Fig. 9c). These results suggest that PA had a positive effect on porcine oocyte developmental competence.

3.3. Effect of phytanic acid on antioxidant and apoptotic mechanisms in oocytes

GSH was significantly increased in the 40 μM PA groups compared to the control (Fig. 9d), while the ROS level was significantly reduced in the 40 μM PA group compared to the control group (Fig. 9e). Additionally, *catalase* (*CAT*) expression showed a significant increase in the 40 μM PA group (almost 3-fold) (Fig. 9f) when compared with the control group. However, as shown in Figure 13b, the

relative expression of *CAT* in CCs did not show any differences between the groups. Furthermore, the relative expression of *B-cell lymphoma 2* (*BCL-2*) in the 40 μM PA group was significantly higher than that of the Control Group (Fig. 9g). Conversely, the relative expression of *BCL2-associated X* (*BAX*) in the 40 μM PA group showed a significant decrease ($P < 0.05$) (Fig. 9h). However, the relative expression level of *BAX* in the CCs treated with 40 μM PA was significantly lower than that in the control group (Fig. 13a). Therefore, I concluded that 40 μM PA affects the survival rates of oocytes.

3.4. Detection of peroxisomal and activities in oocytes

Figures 10a and 10b show the results of immunocytochemistry of PHYH and PEX19. Interestingly, the 40 μM PA group showed a significant increase in both PHYH and PEX19 levels when compared to the control group. ($P < 0.05$). For the oocyte mRNA levels, the expression of *PHYH, PEX3, PEX5, PEX12, PEX19, peroxisome proliferator-activated receptor* (*PPAR*)*α,* and *PPARγ* were significantly increased in the 40 μM PA group (Fig. 10c-g). For CC mRNA, *PEX5, PEX12*, and *PPARα* showed no differences between the groups (Fig. 13c). Consistent with the oocyte results, the expression levels of *PEX3* and *PHYH* in the 40 μM PA group were significantly higher than those in the Control Group (Fig. 13c). Additionally, the mRNA expression levels in the control group were significantly higher for *PPARγ* and *PEX19* than in the 40 μM PA group.

3.5. Effects of phytanic acid on lipid metabolism in oocytes

The fluorescent intensity of the lipid droplets showed a significant increase in the 40 μM PA group when compared with the control group ($P < 0.05$) (Fig. 11a). Moreover, the relative expression of the FA analog assay was significantly higher in the 40 μM PA group than in the control group ($P < 0.05$) (Fig. 11b). Interestingly, the relative expression levels of *adipose triglyceride lipase* (*ATGL*), *hormone-sensitive lipase* (*HSL*), *monoacylglycerol lipase* (*MGLL*), *comparative gene identification-58* (*CGI58*), and *Perilipin 2* (*PLIN2*) in the oocytes were significantly upregulated in the 40 μM PA group (Fig. 11c-g). However, the expression levels of the related genes were different from those in the CCs. In Fig. 13b, the relative expression level of *ATGL* did not differ between the two groups. The expression levels of *HSL, MGLL, CGI58,* and *PLIN2* were significantly lower in the 40 μM PA group than in the control group. This result suggests that PA has a positive effect on oocyte lipid metabolism, but not in CCs.

3.6. Effects of phytanic acid on mitochondria in oocytes

The 40 μM PA-treated group showed a significant increase in the JC-1 aggregate/JC-1 monomer ratio compared to the control group (Fig. 12a). Furthermore, the intensity of ATP content in the 40 μM PA-treated group was significantly higher

than that of the control group (Fig. 12b). Additionally, the relative expression of *nuclear respiratory factor 1* (*NRF1*) and *peroxisome proliferator-activated receptor gamma coactivator* (*PGC-1α*) were significantly increased in the 40 μM PA-treated group compared to that in the Control Group (Fig. 12c and 12d). However, there were no differences in the *transcription factor A, mitochondrial* (*TFAM*) expression levels between the two groups (Fig. 12e). Regarding the expression in CCs, no differences were observed in the expression of *NRF1*, while the expression level of *TFAM* was downregulated in the 40 μM PA-treated group compared to the control group (Fig. 13e). However, the expression level of *PGC-1α* was significantly increased in the 40 μM PA-treated group compared to that in the control group. These results are consistent with the results obtained in the oocytes and indicate that a 40 μM PA may also benefit the mitochondria in porcine oocytes.

3.7. Effects of phytanic acid on porcine embryos

Different concentrations of PA (control (0), 20, 40, and 80 μM) were also tested during porcine IVC to find an appropriate concentration. After 7 days of embryo culture, cleavage rate, blastocyst formation rate, and total cell number of blastocysts were evaluated. All experimental groups showed no differences of the cleavage rates (Fig. 14b), however, in the blastocyst formation rate, 20 μM PA was the highest compared to the control, 40, and 80 μM treated groups (26.48% vs. 20.00%, 20.00%, and 17.06%, respectively; $P < 0.05$) (Fig. 14c) and moreover, 20 μM PTA showed the highest total cell number of blastocysts compared to the control,

40, and 80 μM treated groups (58.50 vs. 43.31, 46.10%, and 44.57%, respectively; $P < 0.05$) (Fig. 14d). Therefore, 20 μM PA was considered to be the optimal concentration during porcine IVC. Total five biological replications were performed and more than 170 porcine embryos per experimental groups were used.

The protein expression of PEX19 and PHYH in porcine embryos was also tested. In blastocysts, the expression of PEX19 and PHYH was highly increased when PA was treated (Fig 14a and 15a). In PEX19, the highest expression was observed in 20 μM PA, however, 40 and 80 μM PA was lower than 20 μM, but still significantly higher than the control group ($P < 0.05$; Fig. 14e). In case of PHYH, the protein expression was the highest in 20 and 40 μM PA compared to the control and 80 μM PA and no difference was observed between them (Fig. 15b).

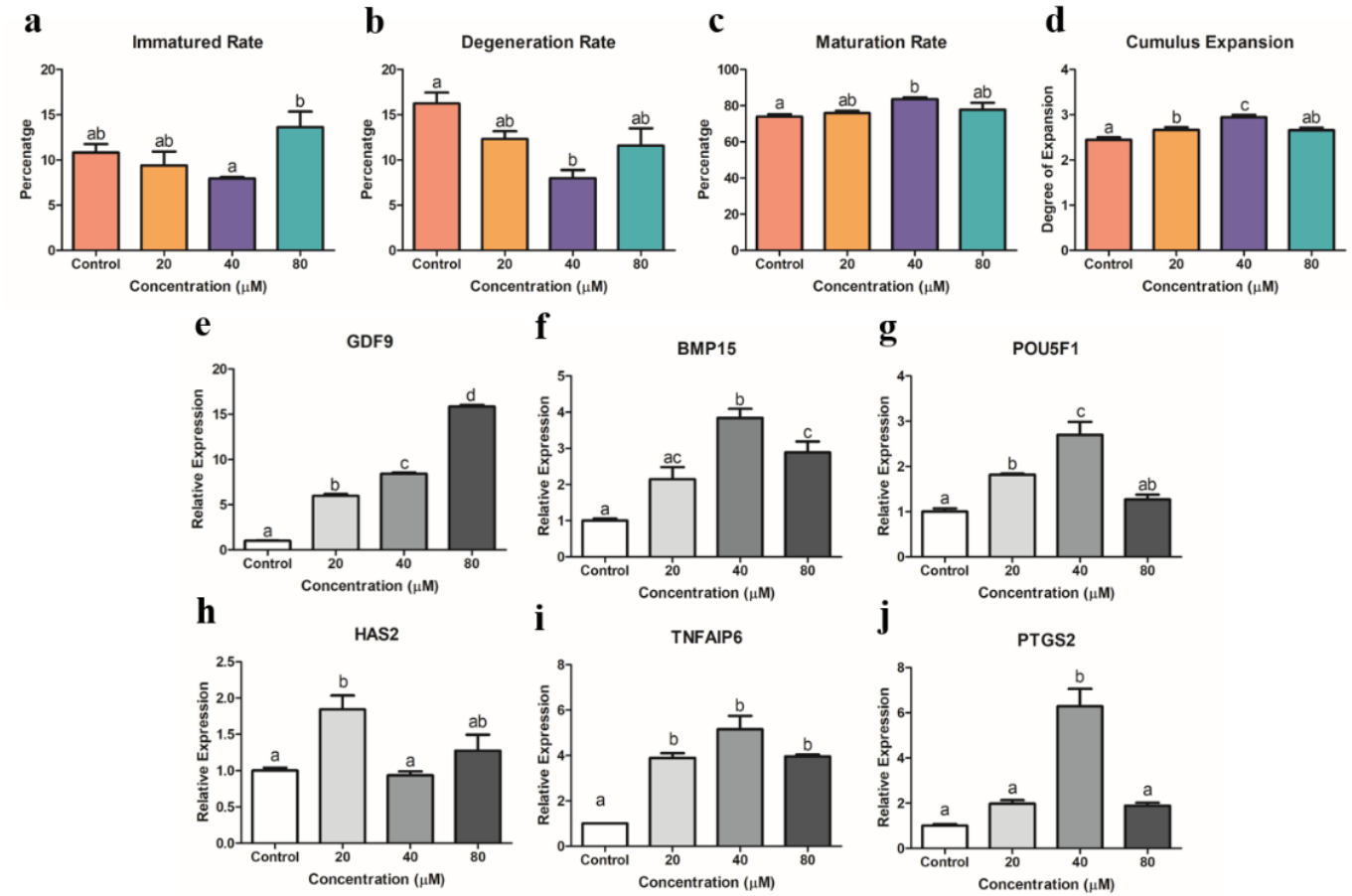
a
Immatured Rate
Percenatge
Control
20
40
80
Concentration (μM)
b
Degeneration Rate
Percenatge
Control
20
40
80
Concentration (μM)
c
Maturation Rate
Percenatge
Control
20
40
80
Concentration (μM)
d
Cumulus Expansion
Degree of Expansion
Control
20
40
80
Concentration (μM)
e
GDF9
Relative Expression
Control
20
40
80
Concentration (μM)
f
BMP15
Relative Expression
Control
20
40
80
Concentration (μM)
g
POU5F1
Relative Expression
Control
20
40
80
Concentration (μM)
h
HAS2
Relative Expression
Control
20
40
80
Concentration (μM)
i
TNFAIP6
Relative Expression
Control
20
40
80
Concentration (μM)
j
PTGS2
Relative Expression
Control
20
40
80
Concentration (μM)

Figure 8. Optimization of phytanic acid (PA) concentration through the assessment of oocyte maturation, cumulus expansion assessment, and mRNA transcript expressions. PA concentrations: 0, 20, 40, and 80 μM. Experiments were carried out at least in triplicates. (a-c) The oocytes were stained with Hoechst 33342 for the detection of the nucleus. Oocyte nuclear maturation was categorized as: mature oocytes, immature oocytes, and degenerated oocytes. (d) Degrees of the cumulus cell expansion were applied to optimize the PA concentration. (e-j). The expression levels in denuded oocytes of genes related to oocyte competence (*GDF9*, *BMP15*, and *POU5F1)* and cumulus expansion (*HAS2*, *TNFAIP6*, and *PTGS2*) were analyzed by qRT-PCR. Data are represented as mean ± SEM. Bars with different letters indicate significant differences ($P < 0.05$).

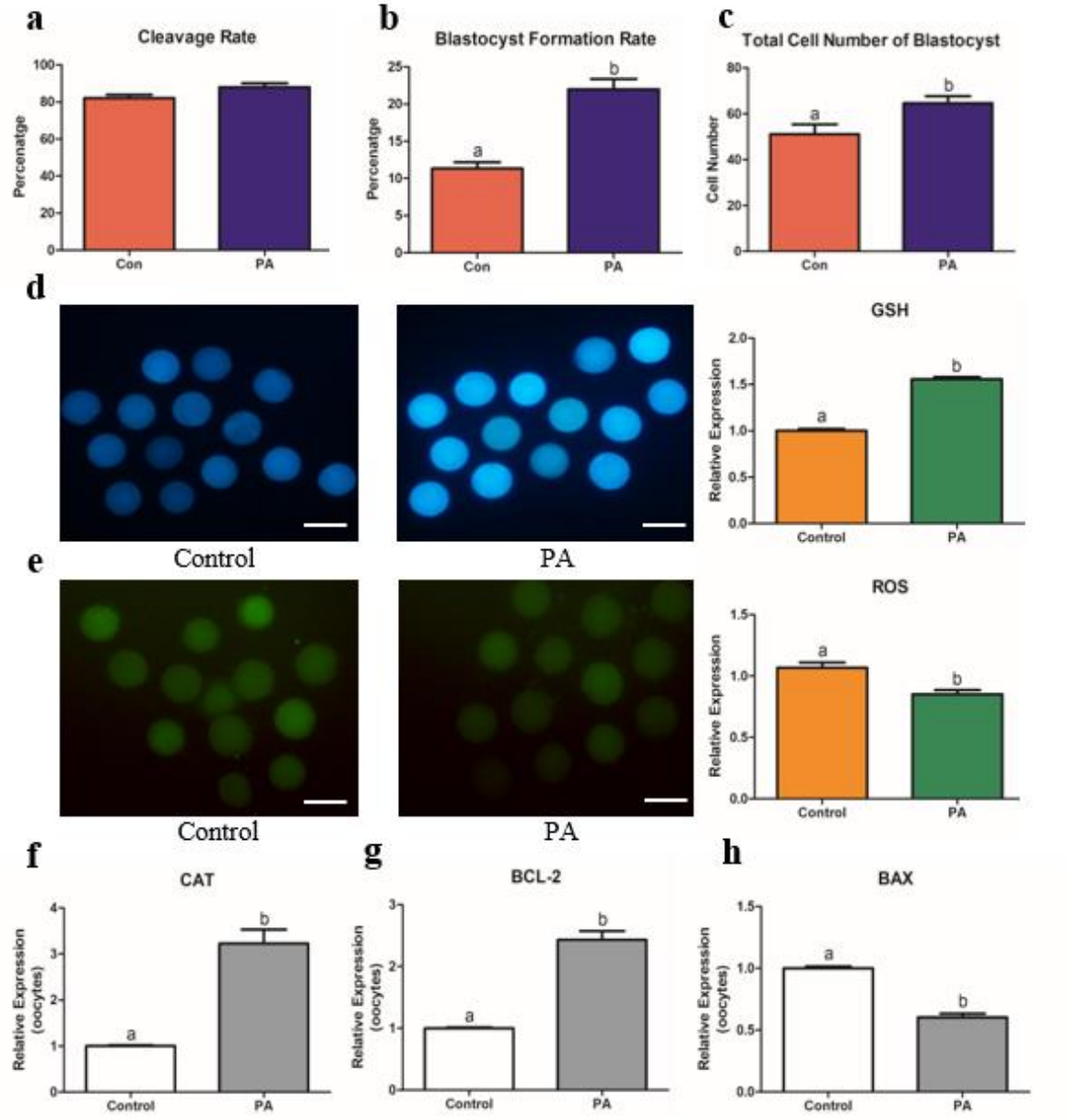
a
Cleavage Rate
Percenatge
100
80
60
40
20
0
Con
PA
b
Blastocyst Formation Rate
Percenatge
25
20
15
10
5
0
a
b
Con
PA
c
Total Cell Number of Blastocyst
Cell Number
80
60
40
20
0
a
b
Con
PA
d
Control
PA
GSH
Relative Expression
2.0
1.5
1.0
0.5
0.0
a
b
Control
PA
e
Control
PA
ROS
Relative Expression
1.5
1.0
0.5
0.0
a
b
Control
PA
f
CAT
Relative Expression (oocytes)
4
3
2
1
0
a
b
Control
PA
g
BCL-2
Relative Expression (oocytes)
3
2
1
0
a
b
Control
PA
h
BAX
Relative Expression (oocytes)
1.5
1.0
0.5
0.0
a
b
Control
PA

Figure 9. Assessment of the effect of 40 μM PA on IVF-derived embryonic development, oocyte antioxidant, and apoptosis level. Experiments were carried out at least in triplicate. (Costa, Peruzzo et al.) The serial assessments of IVF-derived embryonic development were categorized as cleavage rate (day 2), blastocyst formation rate (day 7), and total cell number of blastocysts. (d-e) Staining of porcine oocytes with GSH (blue) and ROS (green). Images were captured using an epifluorescence microscope. Original magnification: 100×; scale bar: 200μm. (f-h) The expression levels in denuded oocytes of genes related to antioxidant (Lolicato, Brouwers et al.) and apoptosis (*BCL-2* and *BAX*) were analyzed by qRT-PCR. Data are represented as mean ± SEM. Bars with different letters indicate significant differences ($P < 0.05$).

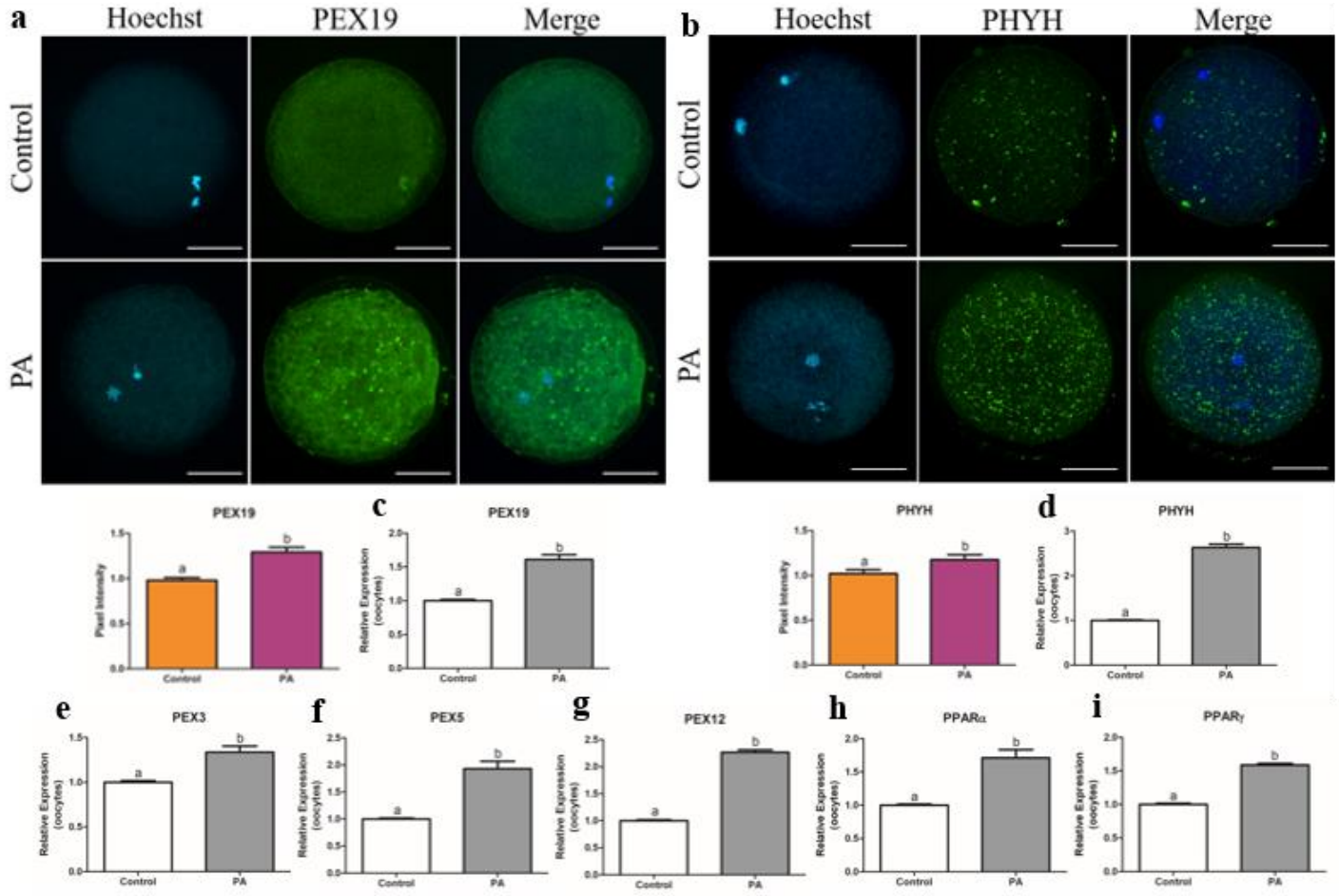
a
Hoechst
PEX19
Merge
Control
PA
b
Hoechst
PHYH
Merge
Control
PA
PEX19
Pixel Intensity
c
PEX19
Relative Expression (oocytes)
PHYH
Pixel Intensity
d
PHYH
Relative Expression (oocytes)
Control
PA
e
PEX3
f
PEX5
g
PEX12
h
PPARα
i
PPARγ
Relative Expression (oocytes)

Figure 10. Evaluation of the peroxisomal activities in matured porcine oocytes. (a-b) Immunocytochemical analysis of PHYH and PEX19. Representative matured oocytes from each group were stained with PHYH and PEX19, respectively. They were then counterstained with Hoechst 33342 for nucleus identification. More than 50 oocytes from different replica were used in each experiment. PA; 40 μM PA. Original magnification: 200×; scale bar: 100μm. (c-i) The expression levels in denuded oocytes of genes related to peroxisomal activities (*PHYH, PEX3, PEX5, PEX12, PEX19, PPARα,* and *PPARγ*) were analyzed by qRT-PCR. Data are represented as mean ± SEM. Bars with different letters indicate significant differences ($P < 0.05$). At least three independent experiments were performed.

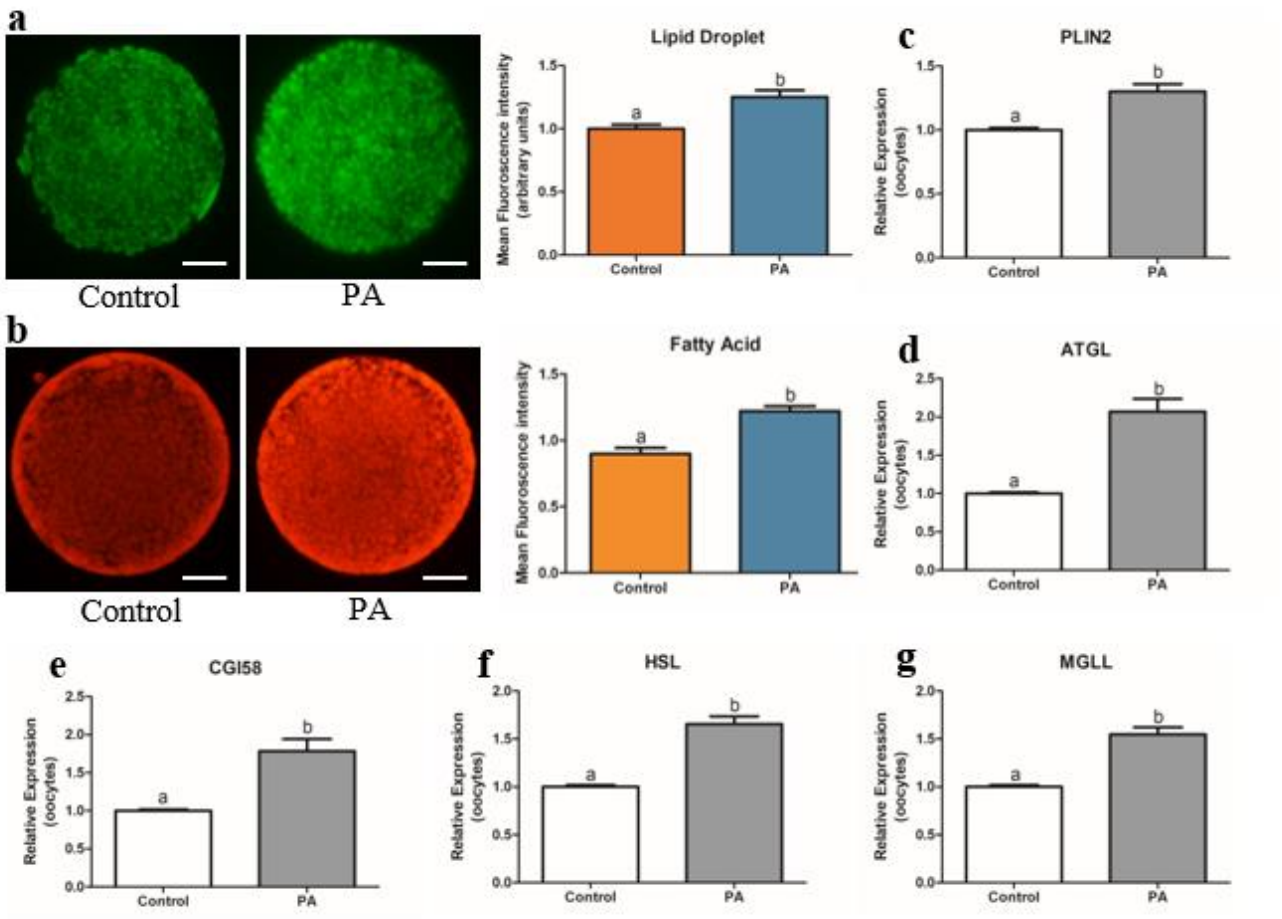
a
Control
PA
Lipid Droplet
Mean Fluorescence intensity (arbitrary units)
b
Fatty Acid
c
PLIN2
Relative Expression (oocytes)
d
ATGL
e
CGI58
f
HSL
g
MGLL

Figure 11. Assessment of lipid metabolism in porcine oocytes. (a) Staining of lipid droplets in porcine oocytes. More than 30 oocytes from different replica were used. Different letters indicate significant differences ($P < 0.05$). PA; 40 μM PA. Original magnification: 200×. (b) Staining of fatty acid in porcine oocytes. Over 30 oocytes from different replica were used. Different letters indicate significant differences ($P < 0.05$). PA; 40 μM PA. Original magnification: 200×; scale bar: 50μm. (c-g) The expression levels in denuded oocytes of genes related to lipid metabolism (*ATGL, HSL, MGLL, CGI58,* and *PLIN2*) were analyzed by qRT-PCR. Bars with different letters indicate significant differences ($P < 0.05$). At least three independent experiments were performed.

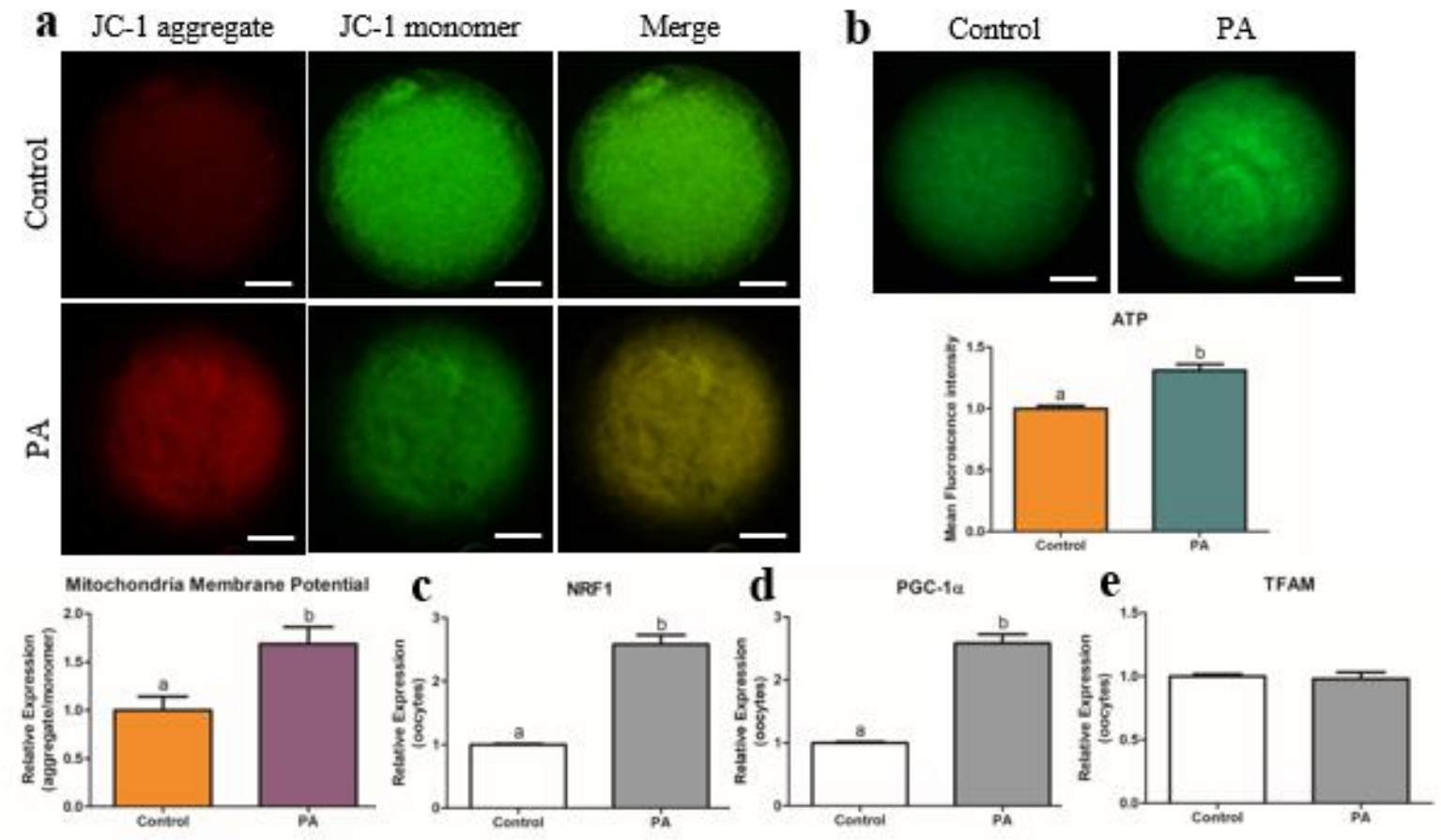
a
JC-1 aggregate
JC-1 monomer
Merge
Control
PA
b
Control
PA
ATP
Mean Fluorescence intensity
Control
PA
Mitochondria Membrane Potential
Relative Expression (aggregate/monomer)
c
NRF1
Relative Expression (oocytes)
d
PGC-1α
Relative Expression (oocytes)
e
TFAM
Relative Expression (oocytes)

Figure 12. Evaluation of mitochondrial potentials in porcine oocytes. (a) Staining of JC-1 mitochondrial membrane potentials in porcine oocytes was analyzed by the ration of JC-1 aggregate (red)/JC-1 monomer (green). Over 50 oocytes from different replica were used. PA, 40 μM PA. Original magnification: 200×; scale bar: 200μm. (b) Staining of ATP content in porcine oocytes. More than 30 oocytes from different replica were used. PA, 40 μM PA. (c-e) The expression levels in denuded oocytes of mRNAs related to mitochondrial potentials (*NRF1*, *PGC-1α,* and *TFAM*) were analyzed by qRT-PCR. Data are represented as mean ± SEM. Bars with different letters indicate significant differences ($P < 0.05$). At least three independent experiments were performed.

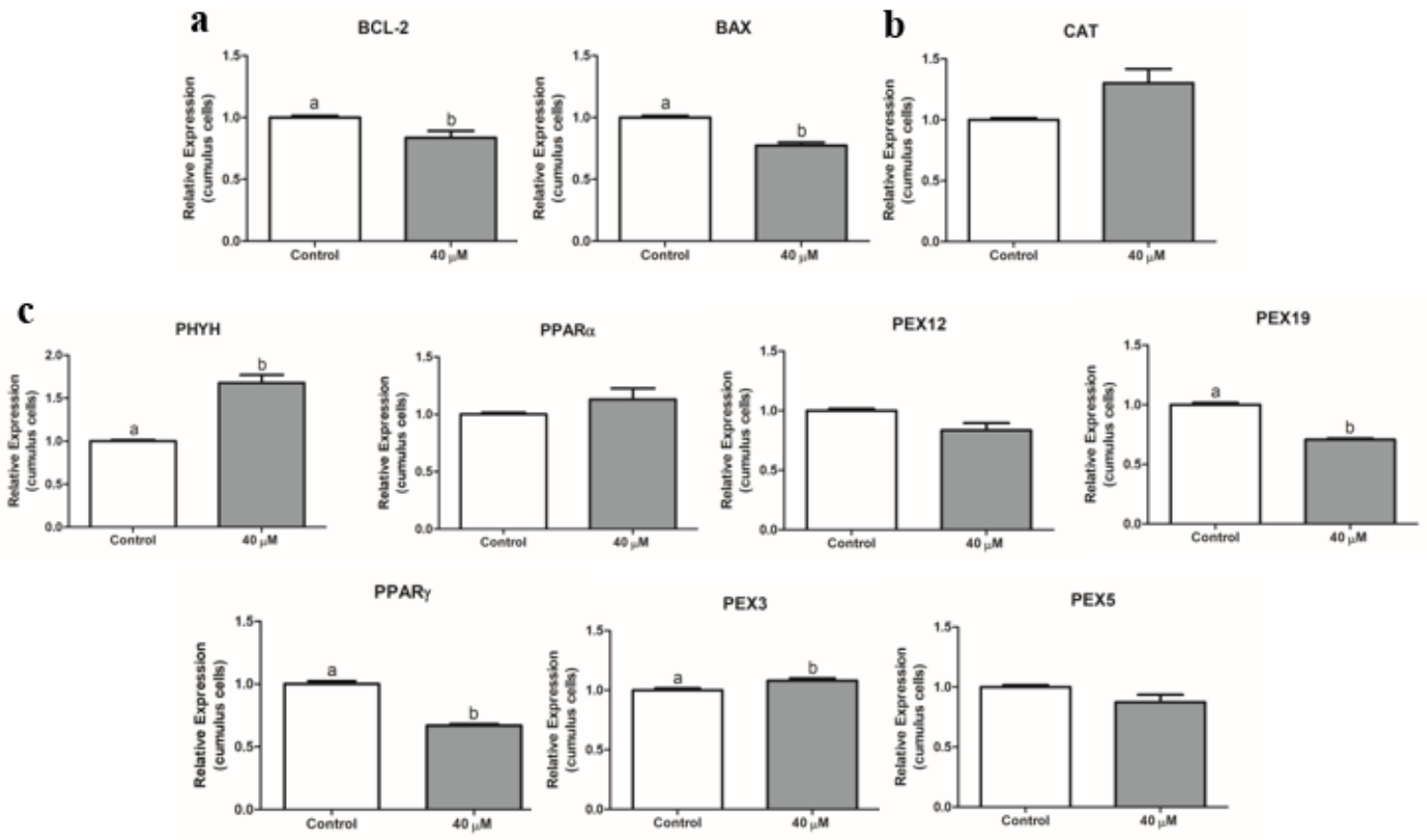
a
BCL-2
BAX
b
CAT
c
PHYH
PPARα
PEX12
PEX19
PPARγ
PEX3
PEX5
Relative Expression (cumulus cells)
Control
40 μM

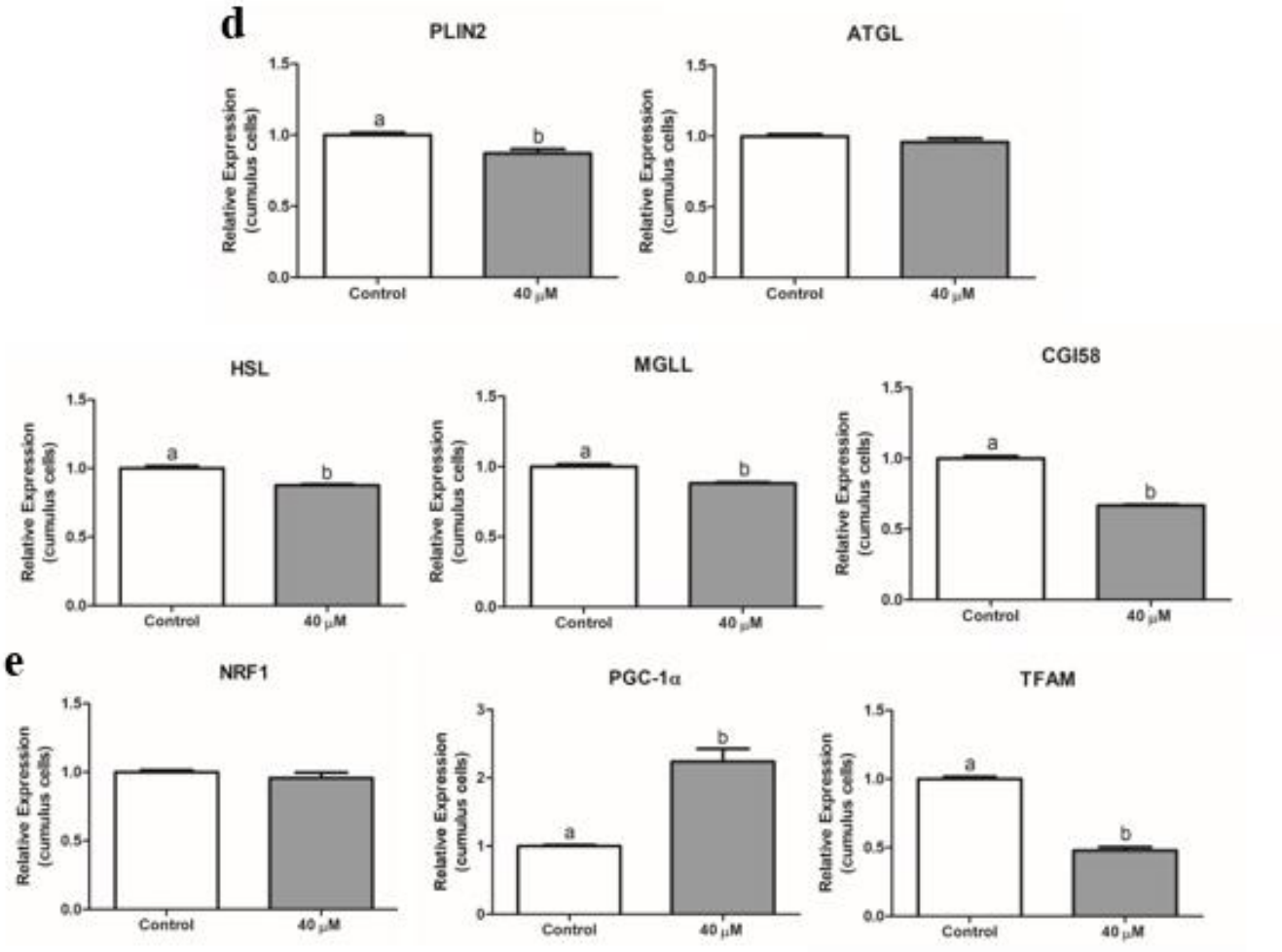
d
PLIN2
ATGL
HSL
MGLL
CGI58
e
NRF1
PGC-1α
TFAM
Relative Expression (cumulus cells)
Control
40 μM
a
b

Figure 13. Several genes related to (a) apoptosis (*BCL2* and *BAX*), (b) antioxidant (*CAT*), (c) peroxisomal activities (*PHYH, PEX3, PEX5, PEX12, PEX19, PPARα,* and *PPARγ*), (d) lipid metabolism (*ATGL, HSL, MGLL, CGI58,* and *PLIN2*), and (e) mitochondria (*NRF1, PGC-1α,* and *TFAM*) were analyzed in porcine CCs from two experimental groups (control vs. 40 μM PA) by real time PCR. The CCs from six biological replications were used for RNA extraction and subsequent real time PCR. Data are represented as mean ± S E M. Bars with different letters indicate significant differences ($P < 0.05$). At least three independent technical experiments were performed.

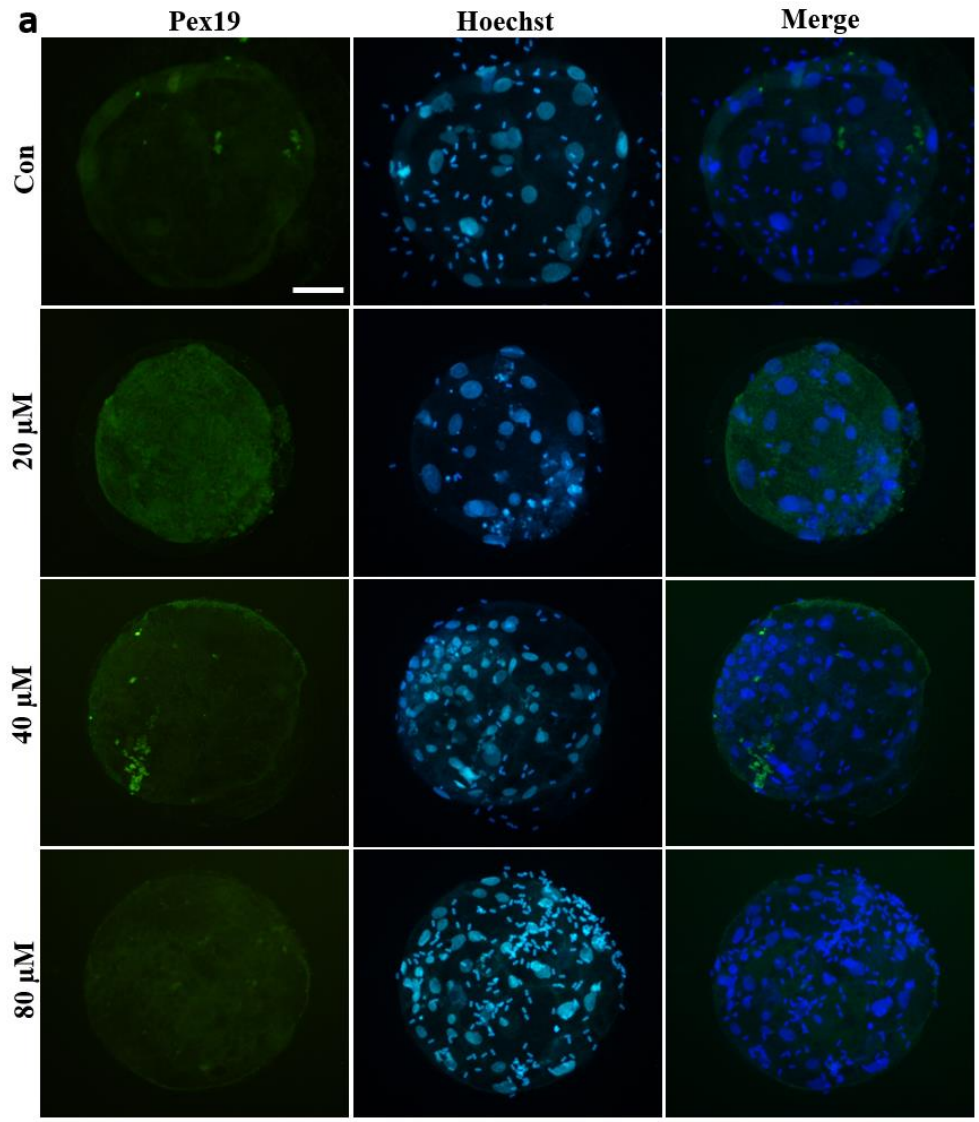
a
Pex19
Hoechst
Merge
Con
20 μM
40 μM
80 μM

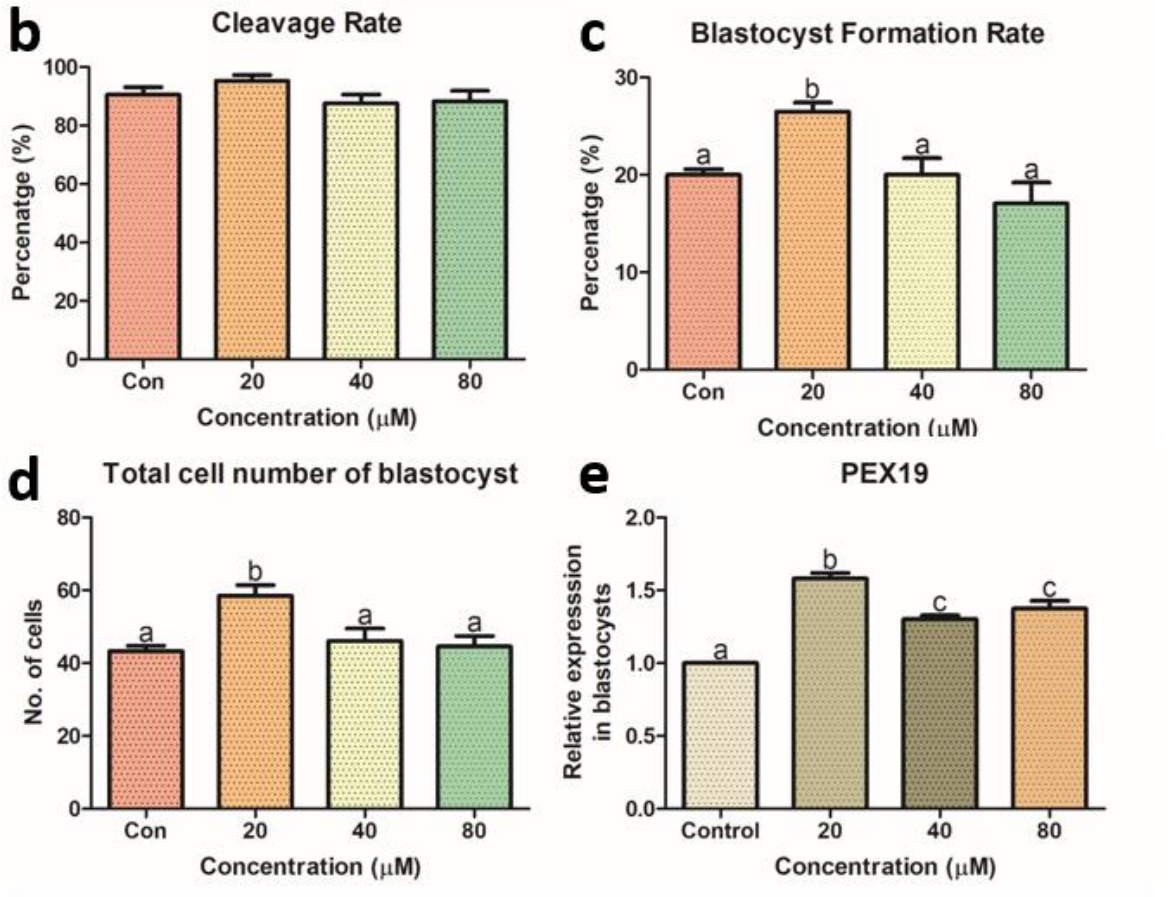
b
Cleavage Rate
Percenatge (%)
100
80
60
40
20
0
Con
20
40
80
Concentration (μM)
c
Blastocyst Formation Rate
Percenatge (%)
30
20
10
0
a
b
a
a
Con
20
40
80
Concentration (μM)
d
Total cell number of blastocyst
No. of cells
80
60
40
20
0
a
b
a
a
Con
20
40
80
Concentration (μM)
e
PEX19
Relative expresssion in blastocysts
2.0
1.5
1.0
0.5
0.0
a
b
c
c
Control
20
40
80
Concentration (μM)

Figure 14. The effect of PA was tested during IVC of porcine embryos and concentrations of PA was ranged 0, 20, 40, and 80 μM. During the embryo culture, (b) cleavage rate, (c) blastocyst formation rate, and (d) total cell number of blastocysts were evaluated. In addition, (a) the protein expressions of PEX19 in blastocysts were validated by immunocytochemistry. At least 15 blastocysts in each experimental group from six biological replications were used and the immunocytochemistry was performed three times technically. Data are represented as mean ± S.E.M. Bars with different alphabetical letters are significantly different among the groups ($P < 0.05$). Con, control; original magnification: 400X; The white bar indicates 50 μm.

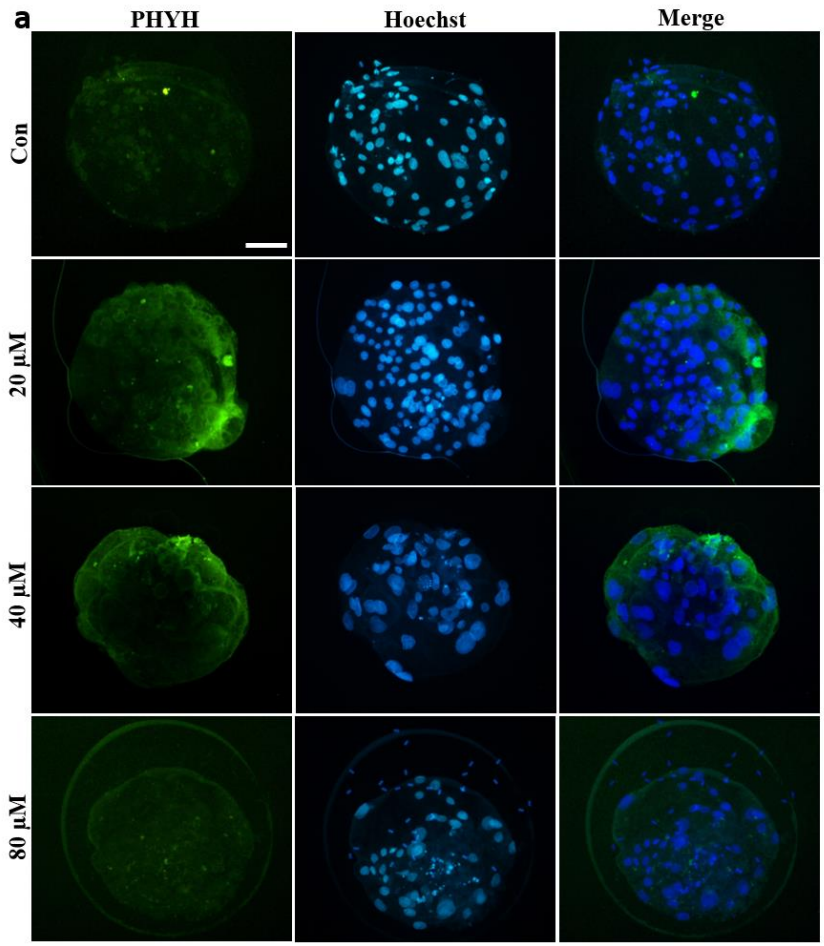
a
PHYH
Hoechst
Merge
Con
20 μM
40 μM
80 μM

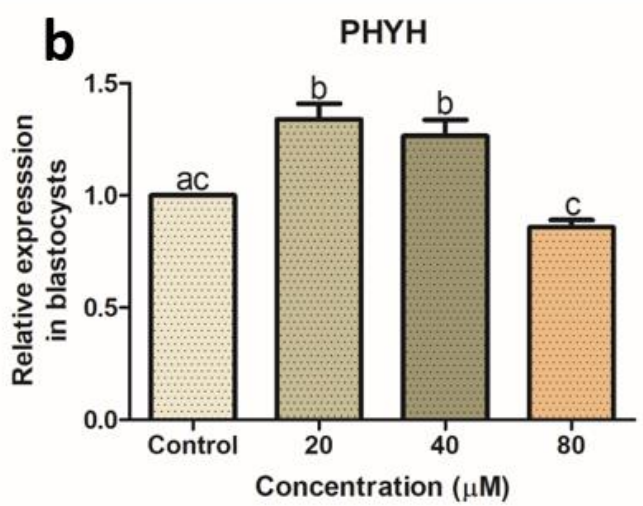
b
PHYH
Relative expresssion in blastocysts
1.5
1.0
0.5
0.0
ac
b
b
c
Control
20
40
80
Concentration (μM)

Figure 15. The effect of PA was tested during IVC of porcine embryos and (a) the influence of PA on PHYH was evaluated by immunocytochemistry with concentrations ranged 0, 20, 40, and 80 μM. (b) Statistic analysis was assessed through fluorescences. At least 15 blastocysts in each experimental group from six biological replications were used and the immunocytochemistry was performed three times technically. Data are represented as mean ± S.E.M. Bars with different alphabetical letters are significantly different among the groups ($P < 0.05$). Con, control; original magnification: 400X; The white bar indicates 50 μm.

4. Discussion

According to some studies, the effects of PA on muscle cells in rats (Dhaunsi, Alsaeid et al. 2017), satellite cells in pigs (Che, Oksbjerg et al. 2013), and numerous tests have been conducted on PA administration *in Vivo.* However, to my knowledge, this study is the first to investigate peroxisomal lipid metabolism in porcine oocytes and PA was used to increase peroxisomal activity and downstream metabolism. The results presented here indicate that the peroxisomes are crucial compartments for porcine oocyte developmental competence by providing energy, activation of the antioxidant mechanism, and reduction of apoptosis. The mRNA and protein expression levels related to alpha oxidation in the peroxisome and its subsequent mechanisms were found to be mostly upregulated by treatment with PA in the oocytes, implying that the peroxisome plays a significant role in porcine oocytes, in accordance with the hypothesis.

PA is known to activate alpha oxidation, as one of the ligands of the peroxisome proliferator-activated receptor (PPAR) α and 9-*cis*-retinoic acid receptor in eukaryotic cells, including mammalian oocytes and embryos (Lemotte, Keidel et al. 1996; Ellinghaus, Wolfrum et al. 1999; Huang 2008; Atikuzzaman, Koo et al. 2011). Additionally, PA is involved in alpha oxidation and the conversion of phytanoyl-CoA into 2-hydroxyphytanoyl-CoA via phytanoyl-CoA hydroxylase (PHYH), which exists solely in the peroxisomes (Mihalik, Rainville et al. 1995; Jansen, Mihalik et al. 1996). Therefore, it is speculated that PHYH may be a key mediator of alpha oxidation in porcine oocytes, using PA to activate peroxisome

activity. First, the concentration of PA before evaluating the peroxisomal activities at the mRNA and protein levels was optimized in oocytes. As the result, I found that treatment with 40 μM PA was optimal concentration for improving oocyte maturation and competence, based on the results of oocyte maturation rate, cumulus expansion, and the increased expression of *BMP15*, *GDF9*, and *POU5F1*, which are associated with oocyte competence (Belli & Shimasaki 2018). Additionally, *PTGS2*, and *TNFAIP6* were increased in the 40 μM PA group which are the main genes related to expansion and interaction in CCs (Marchal, Caillaud et al. 2003). Collectively, it was decided that IVM with 40 μM PA was the optimal concentration for subsequent experiments.

Results showed that the 40 μM PA-treated group exhibited a significant increase in the rate of blastocyst formation and the total cell number of IVF embryos. These findings indicate that the PA-alpha oxidation mechanism provides oocytes with the necessary amount of lipid-derived energy, potentiating them to develop more effectively. Further experiments were performed to elucidate this mechanism. Peroxisomes are also known to be involved in defense mechanisms against oxidative stress. Specifically, catalase in peroxisomes degrades H_2O_2 into water and oxygen, thereby protecting cells from ROS (Fransen, Nordgren et al. 2012). GSH is one of the representative molecules for measuring antioxidant activity (Forman, Zhang et al. 2009) and is involved in the antioxidant mechanism of peroxisomes (Rokka, Antonenkov et al. 2009). Furthermore, oxidative stress has been found to impair the developmental competence of bovine oocytes (Fatehi, Roelen et al. 2005), damage the nucleus, induce apoptosis, and reduce the rates of maturation and development

in porcine oocytes (Tatemoto, Sakurai et al. 2000; Tatemoto, Muto et al. 2004). Therefore, the assessment of the expression levels of GSH and ROS is crucial to determine the levels of oxidative stress in oocytes. Treatment with 40 μM PA significantly increased the expression of GSH, while reducing the expression of ROS. These results suggest that 40 μM PA positively affects the antioxidative defense in the peroxisomes of porcine oocytes.

Notably, alpha oxidation is thought to be only present in the peroxisomes, and hence I used PHYH as a marker for peroxisomes, including PEX19 (Jansen & Wanders 2006). PEX19, or Peroxin19, is a major peroxisomal membrane biogenesis factor that plays multiple roles in the functional assembly of the peroxisome (Agrawal, Shang et al. 2017). Briefly, when PA, a long branched fatty acid, is absorbed by peroxisomes, PA is broken down into pristanic acid, which is subsequently used for beta oxidation (Jansen & Wanders 2006).

These results indicate that short branched FAs (SBFAs) are formed, which are then transferred to the mitochondria for further energy metabolism (Dunning, Cashman et al. 2010). I further investigated the regulation of alpha oxidation and biogenesis of the peroxisome by ICC and qRT-PCR. As previously reported, *PEX3* and *PEX19* are found to be fundamental factors for peroxisomal membrane biogenesis and division (Agrawal, Shang et al. 2017). Moreover, *PEX5* and *PEX12* are believed to interact with each other during the process of peroxisome biogenesis (Chang, Warren et al. 1999). Furthermore, *PPARα* and *PPARγ* are known to be significant in lipolysis, lipogenesis, antioxidant mechanisms, and peroxisomal beta oxidation rates in eukaryotic cells, including mammalian oocytes (Lehmann, Moore

et al. 1995; Lefebvre, Chinetti et al. 2006; Sanchez-Lazo, Brisard et al. 2014). Additionally, *PPARγ* is strongly expressed in mammalian granulosa cells and ovarian follicles (Huang 2008). The results showed that 40 μM PA-treated group significantly increased the relative expression of *PHYH, PEX3, PEX5, PEX12, PEX19, PPARα,* and *PPARγ* transcripts as well as an increase in the intensity of PHYH and PEX19 protein expression. These results indicate that peroxisomes are activated by treatment with PA.

The lipid metabolism was also investigated in the oocytes. The expression levels of the lipid droplets and fatty acid were significantly increased in the 40 μM PA-treated group as indicated by the increased relative expression of *ATGL*, *HSL*, *MGLL*, *CGI58,* and *PLIN2* mRNA transcripts. Specifically, *ATGL* is involved in the first step of triglycerides breakdown. CGI58 is a key co-activator of ATGL. *HSL* and *MGLL* are involved in subsequent digestion (Zechner, Kienesberger et al. 2009; Morak, Schmidinger et al. 2012). PLIN2, also known as perilipin, is one of the main lipid droplet-associated proteins that facilitates the utilization and accumulation of lipids during porcine oocyte maturation (Zhang, Fu et al. 2014). It is presumed that it is phosphorylated by protein kinase A and then activates CGI-58, a co-activator of ATGL. The main purpose of these processes is to increase the efficacy and rate of lipolysis. It is found that lipid metabolism in porcine oocytes was upregulated by treatment with PA, which might be associated with the concurrent increase in peroxisomal activities.

The results of the peroxisome activities raised some questions concerning how SBFAs are utilized by mitochondria. To this end, the membrane potential of

mitochondria and ATP production were analyzed. The results showed that the 40 μM PA-treated group had a significantly increased ratio of JC-1 aggregate/JC-1 monomer (or high ΔΨm/low ΔΨm), which indicates the membrane potential of mitochondria. Moreover, the ATP content was significantly increased in the 40 μM PA-treated group. These results support the idea that the digested SBFAs derived from PA degradation in peroxisomes affect the mitochondrial potential and its subsequent ATP production via peroxisome activities in porcine oocytes. ATP is mainly synthesized in the mitochondria and is generally accepted to promote embryonic development during IVM (Ge, Tollner et al. 2012), allowing for the production of sufficient energy from the lipids that are abundantly stored in porcine oocytes and embryos (Sturmey & Leese 2003). Furthermore, several studies have proven that lipid metabolism-derived ATP production is fundamental for early embryonic development (Prates, Nunes et al. 2014; Jin, Lee et al. 2017). When the ATP content in the porcine oocytes was measured, the 40 μM PA group showed a significant increase in ATP content.

It is generally accepted that ATP is mainly produced in the mitochondria of oocytes (Yang, Park et al. 2018). Novin et al. stated that the mRNA expression levels of *TFAM* and *NRF1* increased from the germinal vesicle to metaphase II stages in human oocytes (Novin, Allahveisi et al. 2015). *NRF1* and *TFAM* are required for mitochondrial respiration, mtDNA transcription, and mitochondrial biogenesis (Jiang, Kunej et al. 2005; Wang, Li et al. 2006). PPARγ coactivator-1α (PGC-1α) has been proven to be involved in mitochondrial biogenesis, which is regarded as one of the key regulators of mitochondrial respiration (Liang & Ward 2006).

Therefore, these genes were selected as indicators of mitochondrial activity. The results showed that the 40 μM PA group increased the relative expression of *NRF1* and *PGC-1α* transcripts that were concomitantly associated with the increase in mitochondrial membrane potential.

It is known that CC uses large amounts of glucose and its byproducts are then transferred to the oocytes for subsequent metabolic reactions (Harris, Adriaens et al. 2007). A previous study reported that denuded oocytes showed lower glycolytic abilities than intact COCs (Cetica, Pintos et al. 2002). Another study showed that lipid metabolism in CCs is pivotal for maintaining metabolic homeostasis and increasing survival rates in oocytes (Sanchez-Lazo, Brisard et al. 2014). Therefore, I explored the differences in mRNA expression levels between oocytes and CCs (Fig. 13). Lastly, the effects of PA additionally analyzed in porcine embryos and the subsequent peroxisomal activities. Through previous experiments, I found that PA does influence PEX19 and PHYH in oocytes, which have significant roles in peroxisomal activities. The fact that accumulation of lipids and ATPs in oocytes would lead to a successful embryonic development (Ge, Tollner et al. 2012; Prates, Nunes et al. 2014; Jin, Lee et al. 2017), I hypothesized that the aftermath of PA treatment during IVM would affect up to embryonic development. As a result, the expressions of PEX19 and PHYH in embryos were the highest in 20 μM, including 40 μM compared to the control group. Therefore, it is speculated that PA improves porcine IVM system as well as the embryonic development, however, deeper investigation of PA during IVC is needed.

In conclusion, for the first time, peroxisomal activities were investigated in porcine oocytes in response to PA supplementation. Overall, the results showed that peroxisomes were significantly upregulated in the 40 μM PA-treated group in terms of energy production via lipid metabolism. This study provides a paradigm for cellular organelle research in mammalian oocytes, including embryos, particularly the pathways for lipid metabolism and it is expected to continue further research on the role of peroxisomes in porcine and mammalian oocytes.

PART IV

CROSS-TALK BETWEEN NRF2 SIGNALING AND PEROXISOMAL ACTIVITIES IN OOCYTES AND EMBRYOS

Abstract

In general, melatonin and Nrf2 signaling synergistically improve mammalian oocyte maturation and embryonic development. Furthermore, previous studies have suggested an interplay between peroxisomes and Nrf2 signaling in cells, but it is still unclear whether peroxisomes are involved in oocyte maturation. The aim of the chapter I was to identify the possible roles of peroxisomes in the melatonin-Nrf2 signaling pathway during IVM of porcine oocytes. Porcine oocytes were treated with melatonin (10^{-9} M) and brusatol, a Nrf2 specific inhibitor, in order to investigate the mechanism. Then, the rates of maturation and related gene and protein expression were analyzed. During oocyte maturation, melatonin upregulated the expression of gene and protein related to Nrf2 signaling and peroxisomal activities; RNA sequencing partially validated these results. The results demonstrate that melatonin can activate Nrf2 signaling by binding to melatonin receptor 2, resulting in the upregulation of catalase. Moreover, peroxisomes were also found to be activated in response to melatonin treatment, causing the activation of catalase; together with Nrf2 signaling, peroxisomes synergistically prevented the generation of reactive oxygen species and enhanced oocyte quality. Thus, it is suggested that a crosstalk might exist between Nrf2 signaling and peroxisomal activities in porcine oocytes.

In addition, melatonin and PA are known to be involved in lipid metabolism and β-oxidation, in which peroxisomal activities also significantly participate. In addition, other studies have reported that the Nrf2 signaling pathway mediates lipid

metabolism and its subsequent cascades. As these mechanisms are partially involved in porcine oocytes or embryonic development, I hypothesized that the factors governing these mechanisms could be interconnected. Therefore, in chapter II, it was aimed to investigate possible crosstalk between peroxisomal activities and Nrf2 signaling in porcine embryos following melatonin and PA treatment. Porcine embryos were cultured for seven days after parthenogenetic activation, and subsequently treated with melatonin and PA, or injected with *Pex19* (peroxisome biogenesis factor 19)-targeted siRNAs. Real-time PCR, immunocytochemistry, and BODIPY staining were used to evaluate peroxisomal activities, Nrf2 signaling, and subsequent lipid metabolism. It was found that melatonin/PA treatment enhanced embryonic development, while injection with *Pex19*-targeted siRNAs had the opposite effect. Moreover, melatonin/PA treatment upregulated peroxisomal activities, Nrf2 signaling, lipid metabolism, and mitochondrial membrane potentials, while most of these mechanisms were downregulated by *Pex19*-targeted siRNAs. Therefore, it was suggested that there is a connection between the action of melatonin and PA and the Nrf2 signaling pathway and peroxisomal activities, which positively influences porcine embryonic development.

Chapter I. Melatonin-induced Nrf2 signaling influences peroxisomal activities in porcine oocytes

1. Introduction

Melatonin (N-acetyl-5-methoxytryptamine) is a natural hormone produced by the pineal gland in mammals and is primarily known to be involved in the regulation of circadian rhythm (Stehle, Saade et al. 2011). However, melatonin was found to play additional roles in processes such as in steroidogenesis and mammalian reproduction (MacPhee, Cole et al. 1975; Tamarkin, Baird et al. 1985). Additionally, melatonin was also found to exhibit antioxidant effects against elevated levels of ROS (Nguyen, Nioi et al. 2009; Reiter, Mayo et al. 2016) that are known to be responsible for the development of several pathological conditions (Sanchez-Barcelo, Mediavilla et al. 2010). Several studies in the field of animal reproduction indicate that melatonin regulates antioxidant effects in porcine oocytes and embryos by preventing ROS-induced DNA damage. Further, melatonin is also known to crosstalk with signaling pathways related to oocyte maturation, embryo development, and activation of antioxidant-related factors (Lee, Jin et al. 2017; Liang, Jin et al. 2017; Kim, Kim et al. 2019); additionally, melatonin significantly upregulates lipid metabolism by increasing fatty acid content and lipid droplet size in porcine oocytes (Jin, Lee et al. 2017; Lee, Jin et al. 2017). Importantly, the

antioxidant mechanism of melatonin, is regulated by Nrf2 signaling (Trivedi, Jena et al. 2016; Shah, Khan et al. 2017; Kim, Kim et al. 2019).

Nrf2 mediates in several biological phenomenon such as lipid metabolism(Jin, Lee et al. 2017), aging (Sykiotis, Habeos et al. 2011), and defense against oxidative stress in mammalian cells (Lee & Johnson 2004; Wells 2015), including oocytes, and embryos (Amin, Gad et al. 2014; Lin, Sui et al. 2018). Nrf2 mediates its antioxidant activity by translocating into the nucleus, where it binds to antioxidant response elements (AREs) to regulate the expression of genes related to the detoxication and antioxidant mechanisms (Kansanen, Kuosmanen et al. 2013; Ma 2013). Nrf2 signaling has been proposed to be essential for oocyte maturation and embryo development in cows (Amin, Gad et al. 2014), mice (Lin, Sui et al. 2018), and pigs (Kim, Kim et al. 2019) because it counteracts conditions generated in response to ROS exposure. Additionally, some of these studies verified the role of the Nrf2 signaling pathway by administering brusatol - a quassinoid from Brucea javanica – that is recognized as a specific inhibitor of Nrf2, thereby preventing the activation of genes whose expression is driven by the AREs even in conditions of high oxidative stress (Ren, Villeneuve et al. 2011; Olayanju, Copple et al. 2015). Interestingly, peroxisome-related molecules have also been suggested to crosstalk with Nrf2 to protect against ROS-induced damage. Many publications indicate that Nrf2 and peroxisome-related molecules such as PPARγ function in a synergistic manner (Cho, Gladwell et al. 2010; Polvani, Tarocchi et al. 2012; Lee 2017). Some studies have proposed a strong relationship between PPARγ signaling and Nrf2 based on the fact that they exhibit synergistic effects against oxidative stress and

lung injuries in mice (Cho, Gladwell et al. 2010; Polvani, Tarocchi et al. 2012). However, no reports have investigated this crosstalk in mammalian oocytes, especially in pigs.

Peroxisomes are dynamic organelles that are present in most mammalian cells (Gabaldon 2010), and they are thought to play a significant role in mediating cellular defenses against ROS; this is attributed to the presence of catalase in these organelles (Antonenkov, Grunau *et al.* 2010; Walton & Pizzitelli 2012), and the role of these organelles in ATP synthesis, lipid metabolism, and apoptosis (Fransen, Lismont et al. 2017). Furthermore, Vázquez et al. suggested that melatonin induces peroxisome accumulation and enhances the activity of catalase (Vazquez, Grillitsch et al. 2018), an H_2O_2-hydrolzing enzyme (Farr, Lismont et al. 2016). These findings indicate that Nrf2 signaling as well as melatonin influence the activities of peroxisomes. However, the effects of peroxisomal activities in oocytes remain largely unknown, although their effects in cells were found to be dynamic. Therefore, this study aimed to demonstrate the activation and biogenesis of peroxisomes and their related regulators - that are influenced by melatonin-Nrf2 signaling - in COCs.

2. Materials and methods

2.1. Animals and chemicals

Procedures for animals and chemicals were described in general methodology.

2.2. *In vitro* maturation

Procedures for IVM and chemicals were described in general methodology.

2.3. Cumulus cell expansion assessment

The expansion rate of CC was evaluated after 42-44 h of IVM. In accordance with a previous study (Vanderhyden, Caron *et al.* 1990; Lee, Oh *et al.* 2019), CC expansion was assessed in the following manner: degree 0, the CCs are present as flattened monolayer with fibroblastic appearance and complete detachment from the oocyte; degree 1, CCs are spherical in shape and form a single layer; degree 2, expansion at only the outermost layer of the CCs; degree 3, expansion of all cell layers, except for the corona radiata, which are the most proximal to the oocyte; degree 4, complete expansion of the CCs, including the corona radiata.

2.4. Parthenogenetic Activation

Procedures for parthenogenetic activation and chemicals were described in general methodology.

2.5. Embryo evaluation and total cell count after parthenogenetic activation

The day on which the activated oocytes were transferred to the IVC medium was denoted as Day 0. On Day 2 (48 h), embryos with even cleavage were observed under a stereomicroscope. Blastocyst formation was evaluated and total cell numbers counted On Day 7 (168 h). The blastocysts from Day 7 were washed in PBS and then fixed for 1 h in 4% paraformaldehyde (w/v) in PBS at room temperature. Subsequently, the blastocysts were stained with 5 μg/mL of Hoechst 33342 for 8 min. After a washing process with PBS, the stained blastocysts were mounted on glass slides, covered with cover slips. The total cell numbers of the blastocysts were counted under a fluorescence microscope (Nikon Corp.) at 400× magnification.

2.6. Immunocytochemistry

Matured COCs were denuded with 0.1% hyaluronidase in TALP, then washed in 1% PVA/PBS. The denuded oocytes were fixed with 4% paraformaldehyde (w/v) in PBS for 1 h at room temperature. Permeabilization of the oocytes were performed with 1% Triton X-100 (v/v) in distilled water for 1 h at 39°C, washed 4 times in 1% PVA/PBS, and incubated in 2% BSA in 1% PVA/PBS for at 2 h to prevent non-

specific bindings. Then, the oocytes were directly transferred to 2% BSA containing primary antibody for BMP15 (1:200; PA5–34401; Thermo Fisher Scientific), as well as GDF9 (1:200; ab93892; Abcam), MT2 (1:200; ARP64072_P050; Aviva Systems Biology, San Diego, USA), catalase (1:200; 21260-1-AP; Proteintech, Rosemont, USA), NRF2 (1:200; 70R-50116; Fitzgerald Industries International, Acton, USA), PHYH (1:400; MBS3212923; MyBioSource, San Diego, USA), and PEX19 (1:400; MBS9605735; MyBioSource, San Diego, USA) and performed the overnight incubation at 4°C. After the incubation, the oocytes were washed several times in 1% PVA/PBS and incubated with a secondary fluorescein isothiocyanate-conjugated anti-rabbit polyclonal antibody (1:200; ab6717; Abcam, Cambridge, UK) and Goat Anti-Rabbit IgG H&L (Texas Red ®, 1:200; ab6719; Abcam, Cambridge, UK) at 37°C for 2 h (light avoided). After the secondary antibody incubation and washing with 1% PVA/PBS, the counterstaining of the oocytes was performed immediately with 5 μg/mL Hoechst-33342 for 8 min. After through washing, they were mounted on glass slides with 100 % glycerol droplets, covered with cover slips, and then analyzed under a fluorescence microscope. The fluorescence was evaluated using ImageJ software (version 1.46r; National Institute of Health, USA). Within three independent replications, at least 25 COCs from each group were used for the staining.

2.7. ATP Content Assay

Matured COCs were denuded and washed in 1 % PVA/PBS for three times, then fixed in 4 % PFA/PBS for 2 hours at room temperature. Subsequently, the fixed

oocytes were washed in 1 % PVA/PBS droplets for three times and they were transferred to 0.5 μM of BODIPY FL ATP (BODIPY-ATP; A12410; Molecular Probes, Eugene, OR, USA) in PBS for 1 hour at room temperature, light avoided. After the staining, the oocytes were again washed in PBS and mounted on glass slides, covered with slips. An epifluorescence microscope (TE2000-S; Nikon) was used for capturing images, and the intensities of ATP content was measured using ImageJ software (version 1.46r; National Institutes of Health, USA). The intensities of the control group were standardized to 1. At least 20 COCs from each experimental group were used for the staining.

2.8. Measurement of GSH and ROS levels

After 42-44 hours of IVM, the matured COCs were denuded and washed several times thoroughly in TALP medium. H2DCFDA (2', 7'-dichlorodihydrofluorescein diacetates; Invitrogen) and CellTracker Blue (4-chloromethyl- 6.8- difluoro- 7-hydroxycoumarin; CMF2HC; Invitrogen) were used for measuring intracellular ROS and GSH levels in oocytes, respectively. The oocytes were transferred to 10 μM of CellTracker Blue or 10 μM of H2DCFDA in TALP medium, and incubated for 30 min at room temperature, avoiding light. Stained oocytes were again washed several times in TALP medium, then they were transferred to a 4-μl droplet of TALP medium, covered with mineral oil. Epifluorescence microscope (TE2000-S; Nikon, Tokyo, Japan) was used for measuring the intensities of the fluorescence, observed through UV filters (460 nm for ROS and 370 nm for GSH), then images were

captured. Analysis was performed by Image J software and the intensities of the control group was standardized to 1. For three independent replications, at least 36 COCs from each experimental group were used in this experiment.

2.9. mRNA sequencing

In order to construct cDNA libraries with the TruSeq Stranded mRNA LT Sample Prep Kit, total RNA was used. The protocol consisted of poly A-selected RNA extraction, RNA fragmentation, random hexamer primed reverse transcription and 100nt paired-end sequencing by Illumina NovaSeq 6000. The libraries were quantified using qPCR according to the qPCR Quantification Protocol Guide and qualified using an Agilent Technologies 2100 Bioanalyzer. The raw reads were preprocessed from the sequencer to remove low quality and adapter sequence before analysis and aligned the processed reads to the *Sus scrofa (Sscrofa11.1)* using HISAT v2.1.0 (Kim, Langmead et al. 2015). HISAT utilizes two types of indexes for alignment (a global, whole-genome index and tens of thousands of small local indexes). These two types' indexes are constructed using the same BWT (Burrows–Wheeler transform)/ a graph FM index as Bowtie2. The reference genome sequence of *Sus scrofa (Sscrofa11.1)* and annotation data were downloaded from the NCBI. And then, transcript assembly of known transcripts was processed by StringTie v1.3.4d (Pertea, Pertea et al. 2015; Pertea, Kim et al. 2016). Base on the result of that, expression abundance of transcript and gene were calculated as read count or FPKM value (Fragments Per Kilobase of exon per Million fragments mapped) per sample. The expression profiles are used to do additional analysis such as DEG

(Differentially Expressed Genes). In groups with different conditions, differentially expressed genes or transcripts can be filtered through statistical hypothesis testing.

2.10. Analysis of gene expression by quantitative real-time PCR

Procedures for Real time PCR and chemicals were described in general methodology. A list of related genes is shown in Table 15.

2.11. Western blotting

More than 1000 COCs from each experimental group were sampled and stored at -80℃ until use, then they were used for protein extraction with PRO-PREP™ (Intron Biotechnology, gyeong-gi, Korea). The equal concentration of protein was determined by the Bradford reagent. SDS sample buffer was used for lysing the samples (Protein concentrations were set as 20μg/μl), and boiled for 10 min at 95℃, then SDS-PAGE was conducted using 12% SDS-polyacrylamide gel electrophoresis in running buffer at constant 120V for 70 min. Proteins were then electrically transferred onto polyvinylidene difluoride membranes (Thermo Fisher Scientific) using a blotting apparatus adjusted to 350 mA for 60 min. Membranes were blocked with 5% (w/vol) bovine serum albumin in Tris-buffered saline with 0.05% (vol/vol) Tween-20 (TBST) for 2 h at room temperature. The membranes were hybridized with first antibody against each of the proteins: Anti-β-actin (1:4000, ab6276; Abcam), NRF2 (1:500; 70R-50116; Fitzgerald Industries International), PEX19 (1:1000; MBS9605735; MyBioSource), and PHYH (1:1000; MBS3212923;

MyBioSource) overnight at 4℃ in TBST. Thereafter, the membranes were washed with TBST, then incubated with second antibodies: Rabbit antimouse immunoglobulin G (IgG; (1:5000, ab6728; Abcam) or Goat antirabbit IgG (1:5000, 6721; Abcam), for 2 h at room temperature. Subsequently, the membranes were washed three times by shaking in TBST for 30 min, then detected using the enhanced chemiluminescence reagent (West-Q ECL solution, GenDEPOT) according to the manufacturer's protocol. Images were developed with Fusion Solo software (Vilber Lourmat, France)

2.12. Statistical analysis

Procedures for Statistical analysis were described in general methodology. Additionally, we performed the statistical analysis to find differentially expressed genes using the estimates of abundances for each gene in samples. Genes with one more than zeroed read count values in the samples were excluded. Filtered data were log2-transformed and subjected to TMM Normalization. Statistical significance of the differential expression data was determined using edgeR exactTest (Robinson, McCarthy et al. 2010) and fold change in which the null hypothesis was that no difference exists among groups. False discovery rate was controlled by adjusting p value using Benjamini-Hochberg algorithm. For DEG set, hierarchical clustering analysis was performed using complete linkage and Euclidean distance as a measure of similarity. Enrichment of gene ontology analysis was performed for DEGs using g:Profiler (Raudvere, Kolberg et al. 2019).

Table 15. Primers used for quantification of differential expressed transcripts.

Genes	Primer sequences (5'- 3')	Product size (bp)	Accession No.
GAPDH	F: GTCGGTTGTGGATCTGACCT R: TTGACGAAGTGGTCGTTGAG	207	NM_001206359
MT2	F: AGCTGCCTTAACGCCATCAT R: ATTGTCGCCCAGTCAGTGAG	209	XM 021063941.1
catalase	F: AGGGAGAGGCGGTTTATTGC R: GGACTCGTTGGTGAAGCTCA	117	NM_214301.2
NRF2	F: GCCCAGTCTTCATTGCTCCT R: AGCTCCTCCCAAACTTGCTC	115	XM_013984303
PEX19	F: CCAGCACTTCACCCATCAGT R: TAGACGACACTCCTGCCTCA	144	XM_001928869.5
PEX3	F: AATGCATCTTCCTGGGGACG R: ATACTGTCGTCGTGCTTGGG	125	NM_001244185.1
PEX5	F: CAGGCGGAGAATGAGCAAGA R: GGACTCGTTGGTGAAGCTCA	117	XM_013988424.2
PPARγ	F: CTCAATCTATCGGGCCCACC R: TTTATCCCCACAGACACGGC	192	XM_005669783.3
PHYH	F: CCCTTCAGGCCCAGCAATAA R: GCCTTTGTGAGTTCCTGGGA	102	NM_001113447.1
BAX	F: CATGAAGACAGGGGCCCTTT R: CATCCTCTGCAGCTCCATGT	181	XM_003127290
BCL2	F: AATGTCTCAGAGCAACCGGG R: GGGGCCTCAGTTCTGTTCTC	193	NM_214285

F, Forward primer; R, Reverse Primer.

3. Results

3.1. Optimization of brusatol concentration and subsequent co-treatment with melatonin

To determine the appropriate concentration range of brusatol for IVM, the first concentration range was used in a previous study (Kim, Kim *et al.* 2019) (50, 200, and 400 nM); control COCs were treated with DMSO. Figure 16a shows morphological changes in CC expansion after 44 h of IVM and after parthenogenetic activation. A significant and sharp decrease in cleavage rate (24.84%, 17.39%, and 18.24% vs. 86.67%, respectively, $P<0.05$) and blastocyst formation rate (2.93%, 0.98%, and 0% vs. 20.95%, respectively, $P<0.05$) was observed upon treatment with 50, 200, and 400 nM brusatol (compared to the control group; Fig. 16b-16c). Moreover, a similar decrease was observed in CC expansion in the groups treated with 50, 200, and 400 nM brusatol compared to the control (Degree 1.07, 0.84, and 0.80 vs. Degree 3.094, respectively, $P<0.05$) (Fig. 16d).

Therefore, lower concentrations (0, 6, 12, and 25 nM; Fig. 16e) of brusatol were used and found that treatment with brusatol at concentrations of 12 and 25 nM resulted in a significant decrease in the cleavage rate (63.08% and 43.87% vs. 85.40% and 78.65%, respectively, $P<0.05$) and blastocyst formation rate (11.02% and 2.21% vs. 23.52% and 20.62%, respectively, $P<0.05$) compared with those observed in the control - 6 nM brusatol (Fig. 16f-16g). Furthermore, 25 nM brusatol significantly reduced the total cell number of blastocysts compared to that in the

control and 6 and 12 nM brusatol-treated group (35.40 vs. 56.10, 61.11, and 49.29, respectively, $P<0.05$). Figures 16h-16i show that 6, 12, and 25 nM brusatol caused significant decreases in the CC expansion rate compared to the control (Degree 2.23, 1.39, and 0.98 vs. Degree 3.01, respectively, $P<0.05$). Additionally, based on the CC expansion and blastocyst formation rates, the chosen concentration (12 nM) was confirmed by calculating IC_{50} with the rate of CC expansion and blastocyst formation, which was determined to be approximately 11.11 and 11.79 nM brusatol (r^2 value: 0.975 and 0.9404, respectively, $P< 0.05$) (Fig. 16j). As the IC_{50} values were close to the chosen concentration, 12 nM brusatol was selected as the optimal concentration for the subsequent experiments.

3.2. Effects of melatonin on oocyte maturation and subsequent embryo development

Along with the chosen concentration of brusatol (12 nM), 10^{-9} M melatonin was used for oocyte maturation. Four groups, the control, melatonin, brusatol, and co-treatment with melatonin and brusatol (co-treatment) groups, were created for subsequent experiments (Fig. 17a). First, the CC expansion rate in each experimental group was evaluated. As shown in Figure 17b, the melatonin-treated group showed the highest CC expansion rate compared to the control, brusatol, and co-treated groups (Degree 3.30 vs. Degree 2.92, 2.05, and 2.36, respectively, $P<0.05$). Notably, all experimental groups exhibited significant differences in the CC expansion rate. During embryo development, the control and melatonin-treated groups showed

higher cleavage rates compared to the brusatol and co-treated groups (89.16% and 90.96% vs. 75.25% and 81.44%, respectively, $P<0.05$) (Fig. 17c). Moreover, the melatonin-treated group showed higher blastocyst formation rate compared to the control, brusatol, and co-treated groups (30.36% vs. 19.71%, 10.35%, and 17.43%, respectively, $P<0.05$) (Fig. 17d), while the brusatol-treated group showed the lowest rate of blastocyst formation. Finally, the melatonin-treated group also exhibited the highest total cell number in blastocysts among the control, brusatol, and co-treated groups (81.20 vs. 61.60, 57.80, and 74.90, respectively, $P<0.05$) (Fig. 17e).

In addition, oocyte maturation-related factors (BMP15 and GDF9) that are expressed only in oocytes (Fig. 17f and 17g) were evaluated. BMP15 levels were the highest in the melatonin-treated group and lowest in the brusatol-treated group ($P<0.05$). Moreover, the co-treated group exhibited restored BMP15 protein expression compared to the brusatol-treated group. The same pattern was observed for the protein expression of GDF9, except for the co-treated group, which showed no significant difference compared to the brusatol-treated group ($P<0.05$). In summary, it is partially verified that melatonin positively affected on oocyte maturation and embryo development; this was in agreement with the results of previous studies.

3.3 ATP production, GSH/ROS levels, and gene expression patterns in COCs

ATP production, GSH/ROS levels, and gene expression patterns in porcine oocytes were assessed in subsequent analyses. Compared to that in the other groups, ATP expression was significantly increased in the melatonin group ($P<0.05$) and was lowest in the brusatol-treated group (Fig. 18a). As shown in Figure 18b, all experimental groups exhibited significant differences in GSH levels. In particular, compared to that in other groups, the GSH level was significantly increased in the melatonin-treated group and was the lowest in the brusatol-treated group; furthermore, the GSH level was recovered in the co-treated group compared to that in the brusatol-treated group ($P<0.05$). Figure 18c depicts the ROS levels in oocytes, which were lowest in the melatonin-treated group and highest in the brusatol-treated group ($P<0.05$). Lastly, the level of ROS in the co-treated group was significantly lower than that in the brusatol-treated group, indicating that melatonin could overcome the effect of brusatol ($P<0.05$).

Next, the overall gene expression patterns was analyzed in COCs. Total RNA was extracted from the COCs, purified, and trimmed (Table 16-18). Figure 19a shows raw data of read counts for each experimental group. To filter the data, a logarithm was applied, followed by trimming by TMM normalization. In addition, Figure 19d shows the correlation of each experimental group after normalization; notably, clear differences were observed between the control vs. brusatol treatment. Moreover, through multidimensional scaling, the closest relationship was observed

between the control and melatonin-treated groups, and the brusatol- and co-treated groups showed larger differences than expected (Fig. 19b). Prior to DEG analysis, quality control was performed, and it is found that 16,720 genes were mapped across all samples (Fig. 19c); these data were used for subsequent DEG analysis.

3.4. Analysis from DEG and Gene Ontology (GO) term in porcine COCs

In order to confirm differences of genetic expression levels among the experimental groups, DEG and GO term were analyzed with the trimmed data. Figure 20a to 20f show comparisons of gene expression levels of individual groups, respectively. Numeric interpretation is demonstrated in Figure 21b, and the biggest difference in DEGs was shown in control versus brusatol-treated group, consistent with Figure 21b. Furthermore, other Figures also showed significant differences. Figure 20g summarizes the overall DEG patterns among the groups. Interestingly, the co-treated group had the most diverse patterns compared to other experimental groups, and brusatol-treated group had an opposing DEG pattern compared to that of the control and melatonin-treated groups. With the normalized data, Pearson's coefficient was applied to verify reproducibility among the samples (Fig. 21a); looking at the correlation coefficients, it is found that control and melatonin-treated group versus brusatol-treated group had the least similarity and control and melatonin-treated groups were the most similar. Indeed, these values are verified in pigs as values below 0.70 indicate differences in species. Figures 21c, 21d, and 21e show significant changes in biological process, molecular function, and cellular

component within all experimental groups. In biological process, ‘metabolic process’ was the most significant enrichment term among the 10 terms and ‘developmental process’ also had a P-value less than 0.001 (Fig. 21c). As the result, the processes related to metabolism, biogenesis, or development had the most significant changes in COCs in accordance with Figure 21c-1. Interestingly, in ‘cellular component’ (Figure 21d and 21d-1), the most frequent and significant changes were observed in ‘organelle’ and ‘intracellular’ section and genes related to peroxisome and oocyte were detected ($P<0.05$). Finally, in ‘molecular function’, functions related to ‘binding’ were the most significant enrichment terms; in addition, genes related to oocyte maturation, embryo development, apoptosis, peroxisome, and antioxidant response were found. Subsequent analysis was performed with the genes of interest from these data.

3.5. Gene and protein expression related to melatonin-Nrf2 signaling and peroxisome mechanism

Factors related to melatonin-Nrf2 signaling and peroxisome were evaluated. MT2 had the highest gene expression level in melatonin-treated group (Fig. 22a) as well as protein expression level in Figure 22l. The protein expression level of MT2 in brusatol-treated group was significantly lower than the control, but not in gene expression. In case of catalase, the gene and protein expressions were the highest in melatonin-treated group (Fig. 22b, 22m). Results of immunocytochemistry of MT2

and catalase are shown in Figures 22k-22m. With regards to gene expression in PEX3, the co-treated group was significantly higher than other experimental groups, and the melatonin-treated group was also significantly higher than control and brusatol-treated groups (Fig. 22d). In PEX5, the gene expression levels of each experimental group showed significant differences. Melatonin group had the highest expression level among the groups and the co-treated group was significantly higher than brusatol-treated group (Fig. 22e). The gene expression of PPARγ in co-treated groups was the highest among the groups and the melatonin- and brusatol-treated groups were significantly higher than the control (Fig. 22g). Including the melatonin-treated group, the gene expression in BAX for all the groups were significantly lower than the control group, while the expression of BCL2 in the melatonin-treated group was more than 2-fold higher than the other groups (Fig. 22i and 22j). The melatonin-treated group was the highest gene expression in NRF2 compared to other experimental groups; the brusatol-treated group was significantly lower than the control. In addition, the co-treated group was significantly higher than brusatol-treated group (Fig. 22c). A similar pattern was observed in protein expression levels of NRF2, verified through western blot analysis and immunocytochemistry (Fig. 23a and 21c). Specifically, the result of western blotting in NRF2, the expression level of the co-treated group was the same as that of the melatonin-treated group (Fig. 23b). In PEX19, all experimental groups had significant differences except for brusatol-treated group and the highest expression level in the melatonin-treated group (Fig. 23b). Additionally, the expression level of co-treated group was significantly higher than that of brusatol-treated group. The protein expression of

PEX19, verified by immunocytochemistry, had the same pattern as the gene expression pattern shown in Figure 22f; however, western blot analysis showed that the co-treated group showed no difference compared to the melatonin-treated group. Lastly, gene and protein expression levels of PHYH had the same expression patterns (Fig. 22h and 23f), with the melatonin-treated group having the highest expression level compared to the other groups, and the co-treated group was significantly higher than the control and brusatol-treated groups.

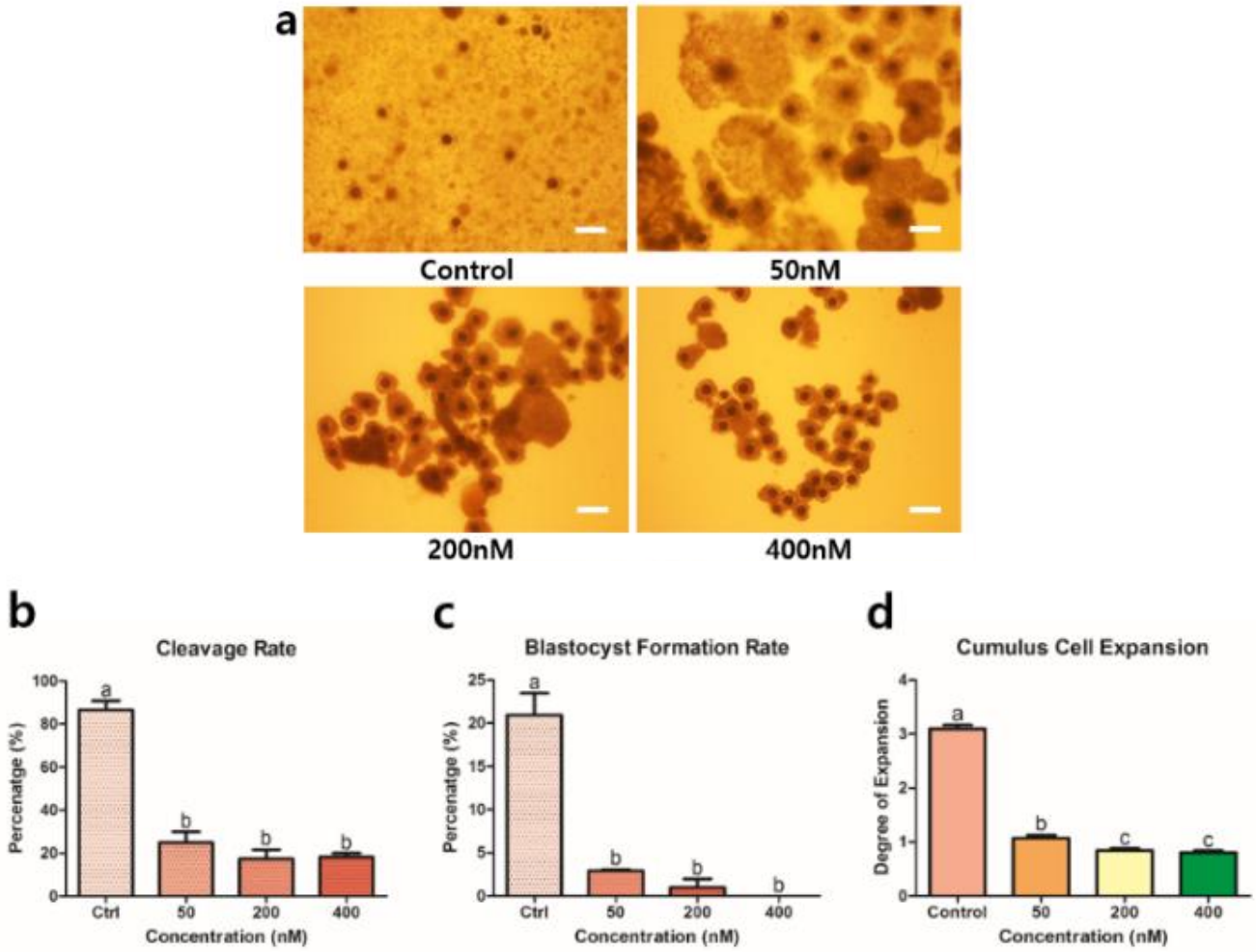
a
Control
50nM
200nM
400nM
b
Cleavage Rate
Percenatge (%)
Ctrl
50
200
400
Concentration (nM)
c
Blastocyst Formation Rate
Percenatge (%)
Ctrl
50
200
400
Concentration (nM)
d
Cumulus Cell Expansion
Degree of Expansion
Control
50
200
400
Concentration (nM)

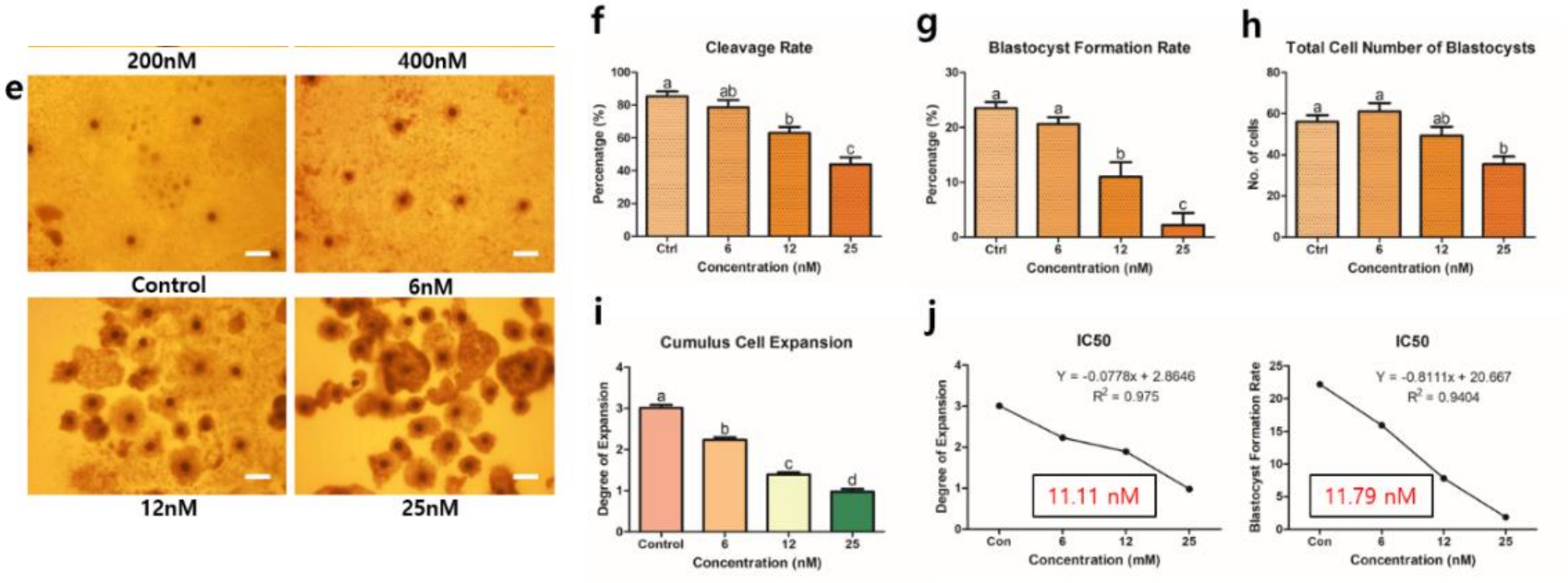
e
200nM
400nM
Control
6nM
12nM
25nM
f
Cleavage Rate
Percenatge (%)
Concentration (nM)
g
Blastocyst Formation Rate
Percenatge (%)
Concentration (nM)
h
Total Cell Number of Blastocysts
No. of cells
Concentration (nM)
i
Cumulus Cell Expansion
Degree of Expansion
Concentration (nM)
j
IC50
Y = -0.0778x + 2.8646
R2 = 0.975
11.11 nM
Degree of Expansion
Concentration (mM)
IC50
Y = -0.8111x + 20.667
R2 = 0.9404
11.79 nM
Blastocyst Formation Rate
Concentration (nM)

Figure 16. Selection of optimal brusatol concentration via the assessment of embryo development and cumulus expansion. Brusatol concentrations: 0, 50, 200, and 400 nM (first concentration range); 0, 6, 12, and 25 nM (second concentration range). (a) Microscopy-based images of cumulus cell expansion in porcine COCs treated with the first concentration range of brusatol are shown; (b-d) subsequently, embryo development and CC expansion rates were evaluated. (e) A subsequent analysis using the second concentration range of brusatol was performed. Acceptable results were observed for (f) cleavage rate, (g) blastocyst formation rate, (h) total cell number, and (i) CC expansion. (j) Lastly, the selected brusatol concentration (12 nM) was confirmed by calculating the IC_{50} (11.11 and 11.79 nM, respectively). Bars with letters indicate significant differences ($P < 0.05$). Original magnification: 20×; bars indicate 300 μm. Con: control. At least five replicates were performed for each experiment.

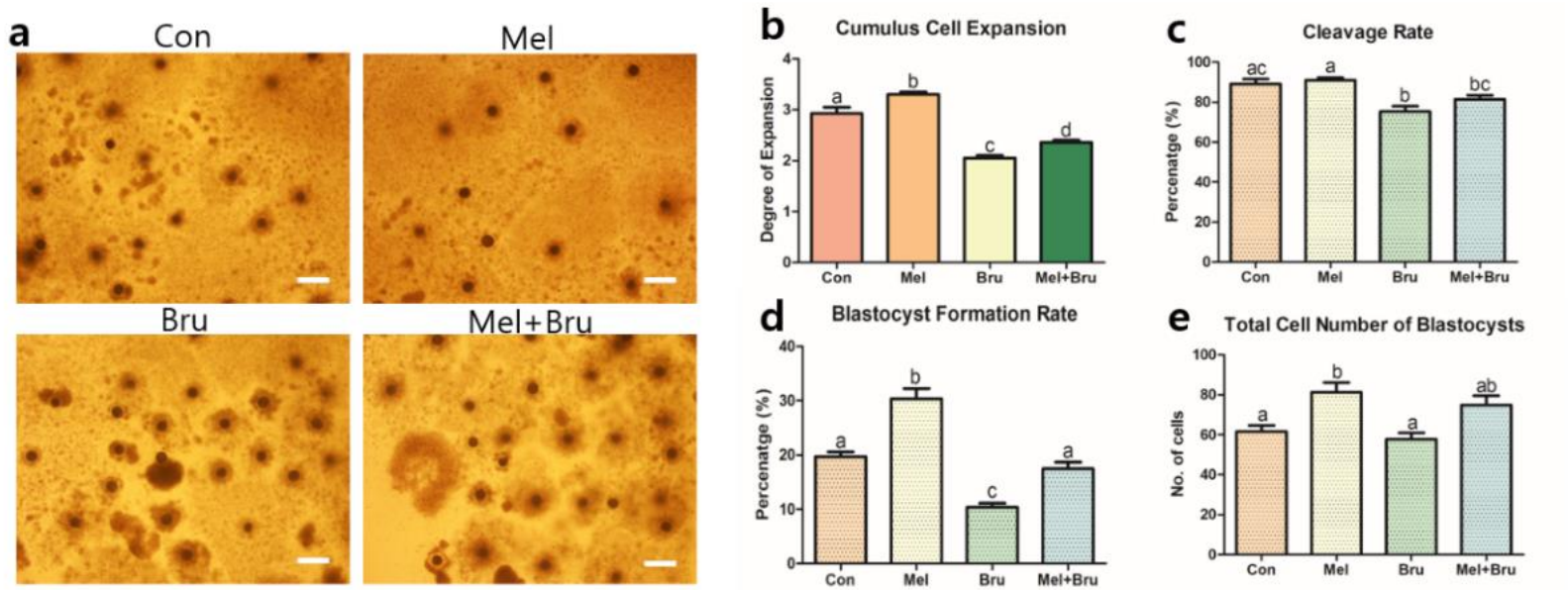
a
Con
Mel
Bru
Mel+Bru
b
Cumulus Cell Expansion
Degree of Expansion
a
b
c
d
Con
Mel
Bru
Mel+Bru
c
Cleavage Rate
Percenatge (%)
ac
a
b
bc
d
Blastocyst Formation Rate
Percenatge (%)
e
Total Cell Number of Blastocysts
No. of cells
ab

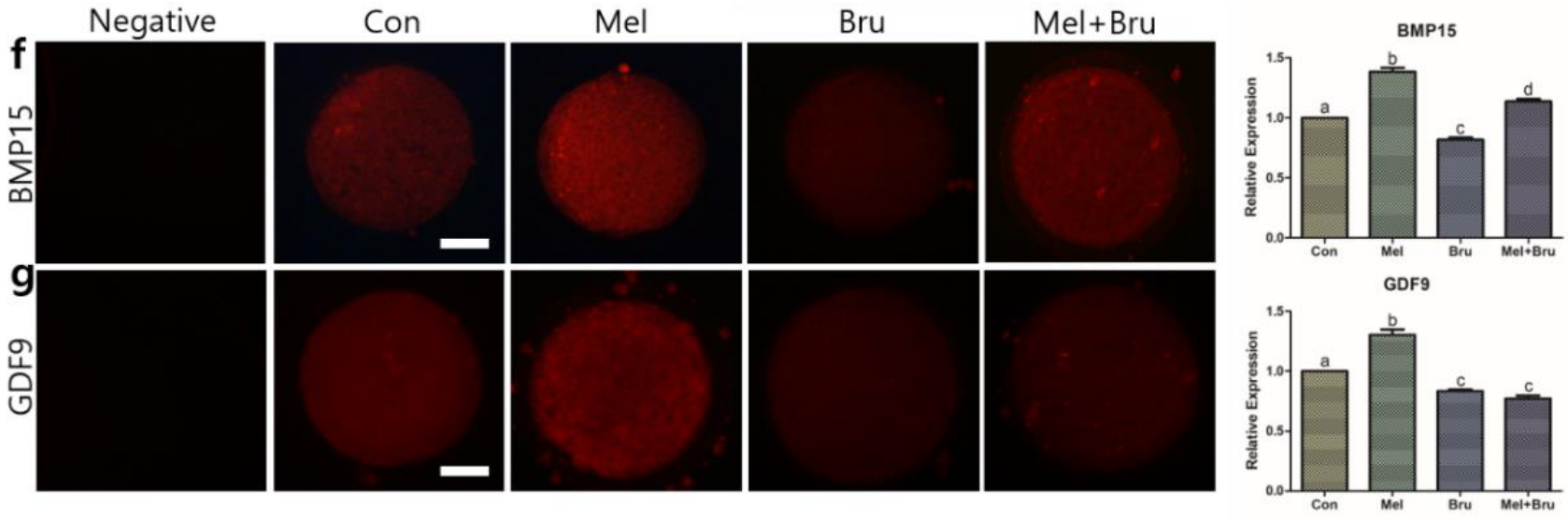
Negative
Con
Mel
Bru
Mel+Bru
f
BMP15
g
GDF9
BMP15
Relative Expression
a
b
c
d
Con
Mel
Bru
Mel+Bru
GDF9
Relative Expression
a
b
c
c
Con
Mel
Bru
Mel+Bru

Figure 17. Evaluation of treatments with melatonin and brusatol on porcine COCs and their competences. With the treatment of 10^{-9}M melatonin and 12 nM brusatol, their effects on the CC expansion and subsequent embryonic development were evaluated. The four experimental groups (control, melatonin, brusatol, and co-treatment) showed distinct differences in (a-b) the CC expansion, (c) cleavage rate, (d) blastocyst formation rate, and (e) total cell number. Additionally, protein expressions related to competence of the porcine COCs from each experimental group were evaluated by immunocytochemistry. The protein expression levels in (f) BMP15 and (g) GDF9 showed significant differences among the groups. Bars with letters indicate significant differences ($P < 0.05$). 20× magnification, bars indicate 300 μm in Figure 15a and 400× magnification, bars indicate 30μm in Figures 15f and 15g. At least three replicates were performed for each experiment.

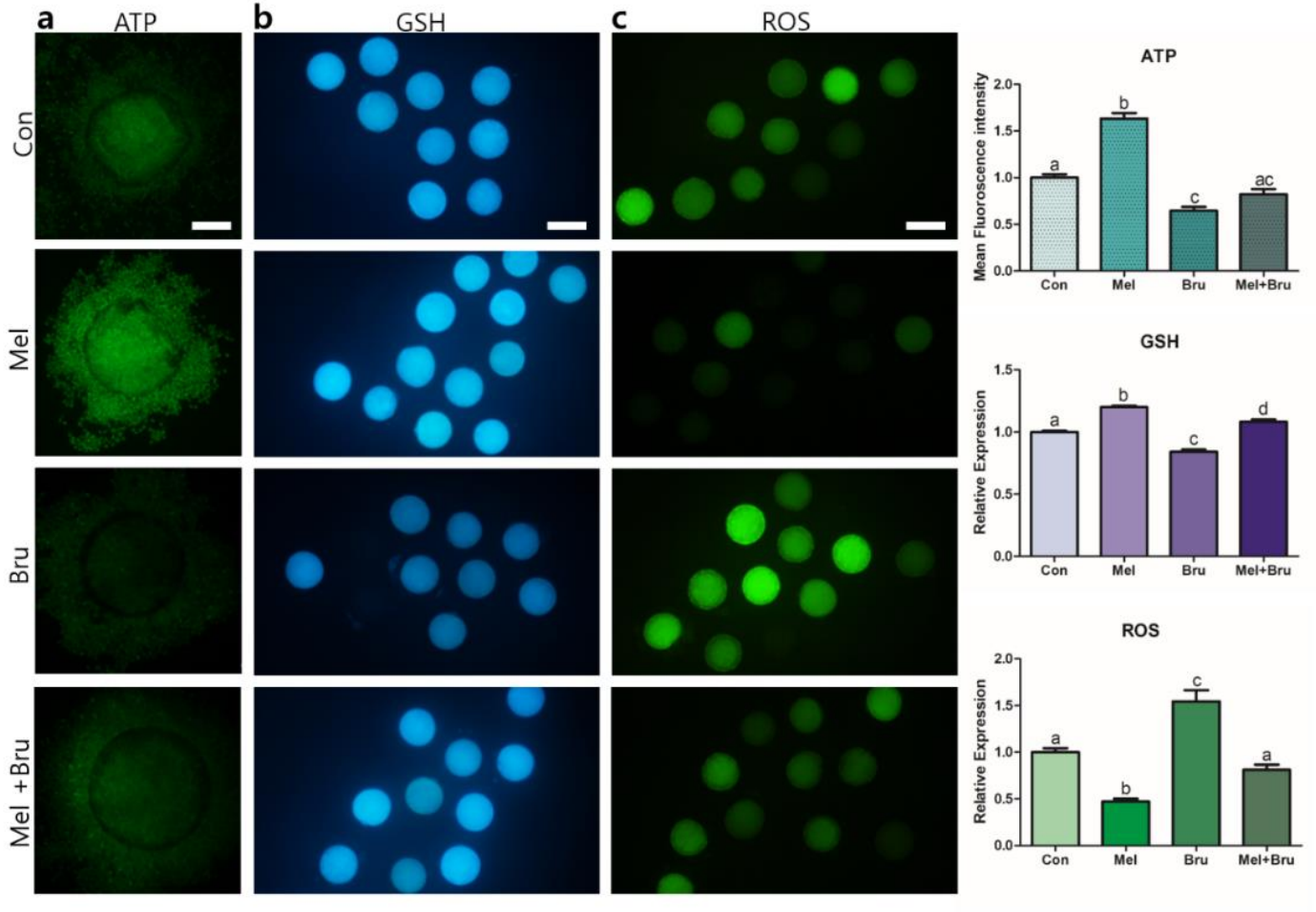
a
ATP
b
GSH
c
ROS
Con
Mel
Bru
Mel +Bru
ATP
Mean Fluoroscence intensity
2.0
1.5
1.0
0.5
0.0
a
b
c
ac
Con
Mel
Bru
Mel+Bru
GSH
Relative Expression
1.5
1.0
0.5
0.0
a
b
c
d
Con
Mel
Bru
Mel+Bru
ROS
Relative Expression
2.0
1.5
1.0
0.5
0.0
a
b
c
a
Con
Mel
Bru
Mel+Bru

Figure 18. Determination of ATP production and GSH and ROS levels in porcine oocytes. The four experimental groups (control, melatonin, brusatol, and co-treatment) showed significant differences in (a) ATP production (BODIPY staining), (b) GSH level (CellTracker Blue staining), and (c) ROS level (H2DCFDA fluorescence). Bars with letters indicate significant differences ($P < 0.05$). Figure 16a: 200× magnification; bars indicate 50 μm. Figure 16b and 16c: 100× magnification; bars indicate 100 μm. Con: control, Mel: melatonin, Bru: brusatol, and Mel+Bru: melatonin+brusatol. At least three replicates were performed for each experiment.

Table 16. Raw data of sequencing from mature COCs.

Group	Total Read Bases*	Total Reads	GC (%)	Q20 (%)	Q30* (%)
Control	8,351,726,158	82,690,358	52.03	97.95	94.27
Melatonin	6,910,083,872	68,416,672	51.83	98.21	94.93
Brusatol	7,250,491,242	71,787,042	48.24	98.29	94.80
Melatonin+Brusatol	6,150,647,904	60,897,504	51.65	98.23	94.81

* Total read bases - Calculated by 'Total reads × Read length'.

* Q30 (%) : Ratio of bases that have better quality than Phred quality score 30.

Table 17. Trimmed data of sequencing from mature COCs.

Group	Total Read Bases*	Total Reads	GC (%)	Q20 (%)	Q30* (%)
Control	8,136,781,932	81,169,626	52.02	98.58	95.12
Melatonin	6,746,869,394	67,271,268	51.84	98.80	95.72
Brusatol	7,121,678,665	70,894,536	48.24	98.71	95.39
Melatonin+Brusatol	6,027,897,479	60,032,956	51.66	98.72	95.49

* Total read bases - Calculated by 'Total reads × Read length'.

* Q30 (%) : Ratio of bases that have better quality than Phred quality score 30.

Table 18. Result of mapped data from cDNA fragments.

Group	Number of processed reads*	Number of mapped reads* (%)	Number of unmapped reads (%)
Control	81,169,626	79,230,444 (97.61)	1,939,537 (2.39)
Melatonin	67,271,268	65,674,842 (97.63)	1,596,426 (2.37)
Brusatol	70,894,536	69,635,999 (98.22)	1,258,537 (1.78)
Melatonin+Brusatol	60,032,956	58,858,650 (98.04)	1,174,306 (1.96)

* Processed reads : Number of cleaned reads after data trimming.

* Mapped reads : Number of mapped reads according to the genomic DNA reference (GCF_000003025.6_Sscrofa 11.1)

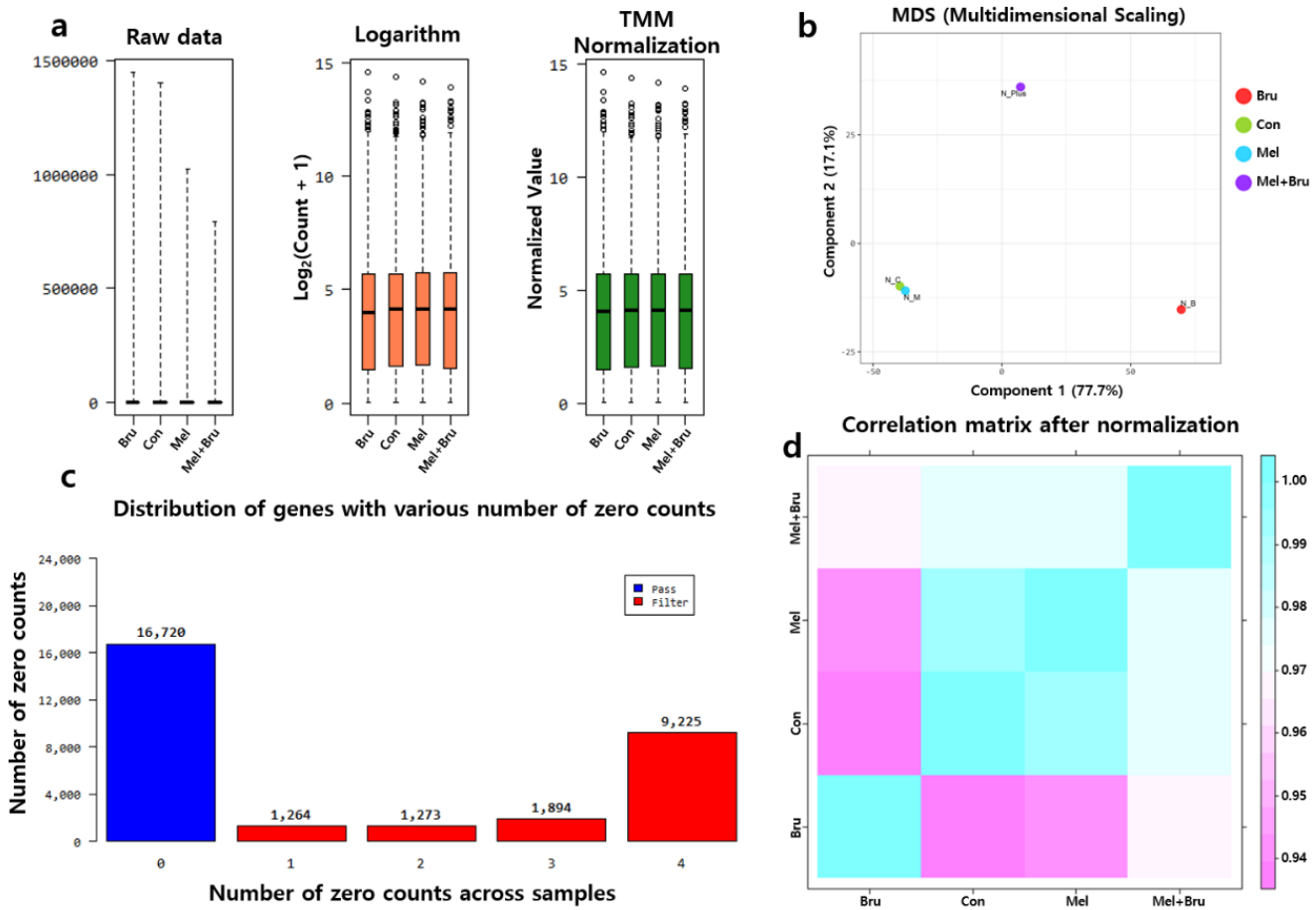
a
Raw data
Logarithm
TMM Normalization
Log2(Count + 1)
Normalized Value
Bru
Con
Mel
Mel+Bru
b
MDS (Multidimensional Scaling)
Component 2 (17.1%)
Component 1 (77.7%)
c
Distribution of genes with various number of zero counts
Number of zero counts
Number of zero counts across samples
Pass
Filter
16,720
1,264
1,273
1,894
9,225
d
Correlation matrix after normalization

Figure 19. Raw data and trimmed read counts in porcine COCs from RNA sequencing. (a) the raw data from the COCs were processed by a series of data trimming up to data normalization, applying logarithm and TMM normalization. (b) The normalized data was first used for multidimensional scaling and (c) the quality control was performed for analyzing DEGs, then as the result, total 16,720 genes were mapped. (d) Lastly, a correlation among the genes were demonstrated as a matrix after data normalization. Con; control, Mel; melatonin, Bru; brusatol, and Mel+Bru; melatonin+brusatol.

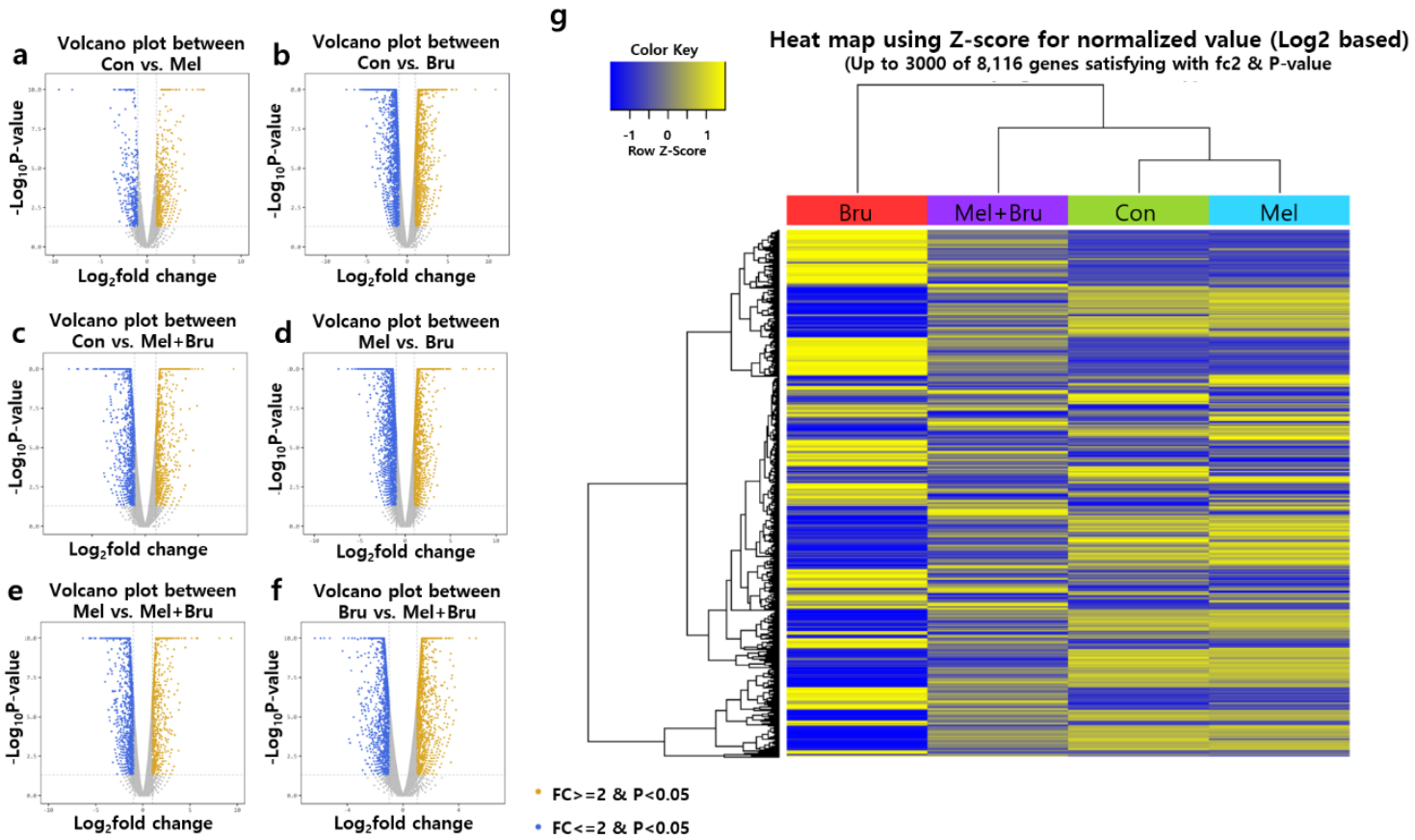
a
Volcano plot between Con vs. Mel
b
Volcano plot between Con vs. Bru
c
Volcano plot between Con vs. Mel+Bru
d
Volcano plot between Mel vs. Bru
e
Volcano plot between Mel vs. Mel+Bru
f
Volcano plot between Bru vs. Mel+Bru
-Log10P-value
Log2fold change
g
Color Key
-1 0 1
Row Z-Score
Heat map using Z-score for normalized value (Log2 based)
(Up to 3000 of 8,116 genes satisfying with fc2 & P-value
Bru
Mel+Bru
Con
Mel
FC>=2 & P<0.05
FC<=2 & P<0.05

Figure 20. General gene expressions in porcine COCs from the four experimental groups (control, melatonin, brusatol, and co-treatment). (a-f) Total of six cases of gene expression comparisons were compared: Con vs. Mel, Con vs. Bru, Con vs. Mel+Bru, Mel vs. Bru, Mel vs. Mel+Bru, and Bru vs. Mel+Bru. Yellow dots indicate expression changes of up-regulated genes that have more than 2-fold higher with $P < 0.05$, and blue dots indicate expression changes of down-regulated genes that have more than 2-fold lower with $P < 0.05$. (g) A heat map was generated using the normalized value from each experimental group, it showed up to 3,000 of 8,116 genes satisfying with 2-fold changes and $P < 0.05$. Con; control, Mel; melatonin, Bru; brusatol, and Mel+Bru; melatonin+brusatol. At least 1,100 porcine COCs per experimental group were collected from eight biological replications.

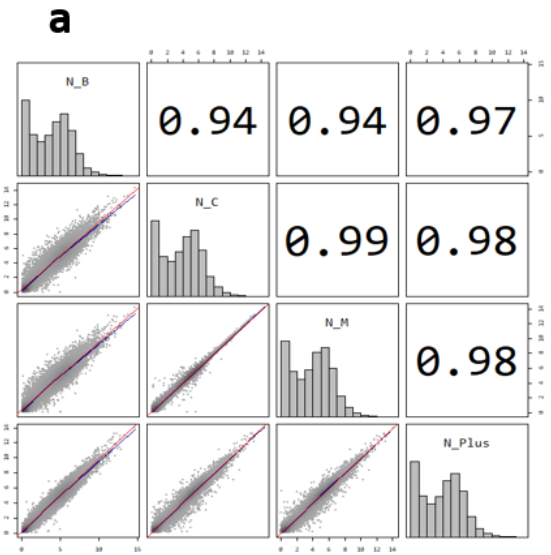
a
N_B
0.94
0.94
0.97
N_C
0.99
0.98
N_M
0.98
N_Plus

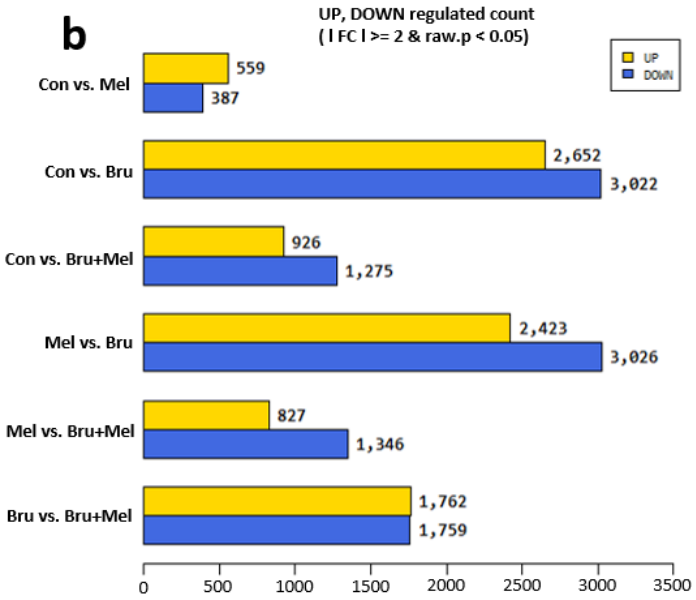
b
UP, DOWN regulated count
(| FC | >= 2 & raw.p < 0.05)
UP
DOWN
Con vs. Mel
559
387
Con vs. Bru
2,652
3,022
Con vs. Bru+Mel
926
1,275
Mel vs. Bru
2,423
3,026
Mel vs. Bru+Mel
827
1,346
Bru vs. Bru+Mel
1,762
1,759
0
500
1000
1500
2000
2500
3000
3500

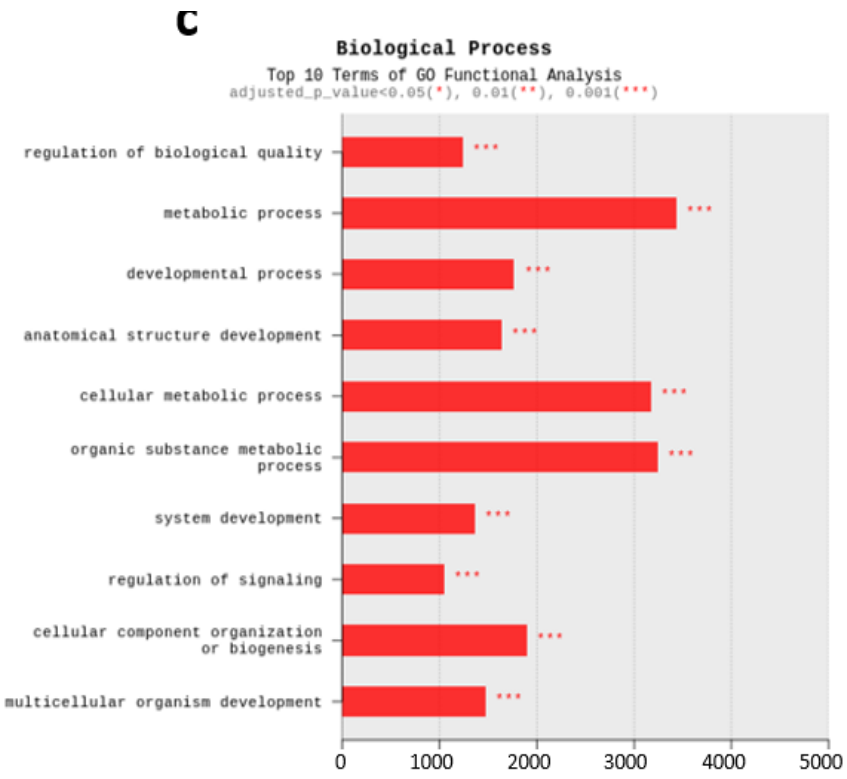
c
Biological Process
Top 10 Terms of GO Functional Analysis
adjusted_p_value<0.05(*), 0.01(**), 0.001(***)
regulation of biological quality
metabolic process
developmental process
anatomical structure development
cellular metabolic process
organic substance metabolic process
system development
regulation of signaling
cellular component organization or biogenesis
multicellular organism development
***
0
1000
2000
3000
4000
5000

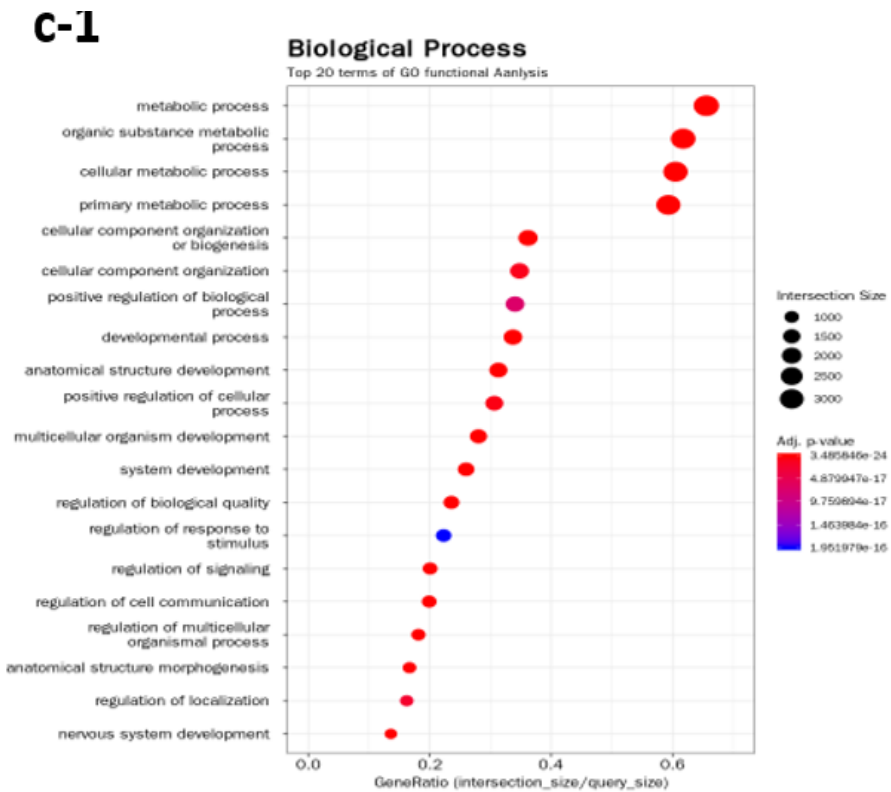
c-1
Biological Process
Top 20 terms of GO functional Aanlysis
metabolic process
organic substance metabolic process
cellular metabolic process
primary metabolic process
cellular component organization or biogenesis
cellular component organization
positive regulation of biological process
developmental process
anatomical structure development
positive regulation of cellular process
multicellular organism development
system development
regulation of biological quality
regulation of response to stimulus
regulation of signaling
regulation of cell communication
regulation of multicellular organismal process
anatomical structure morphogenesis
regulation of localization
nervous system development
0.0
0.2
0.4
0.6
GeneRatio (intersection_size/query_size)
Intersection Size
1000
1500
2000
2500
3000
Adj. p-value
3.485846e-24
4.879947e-17
9.759894e-17
1.463984e-16
1.951979e-16

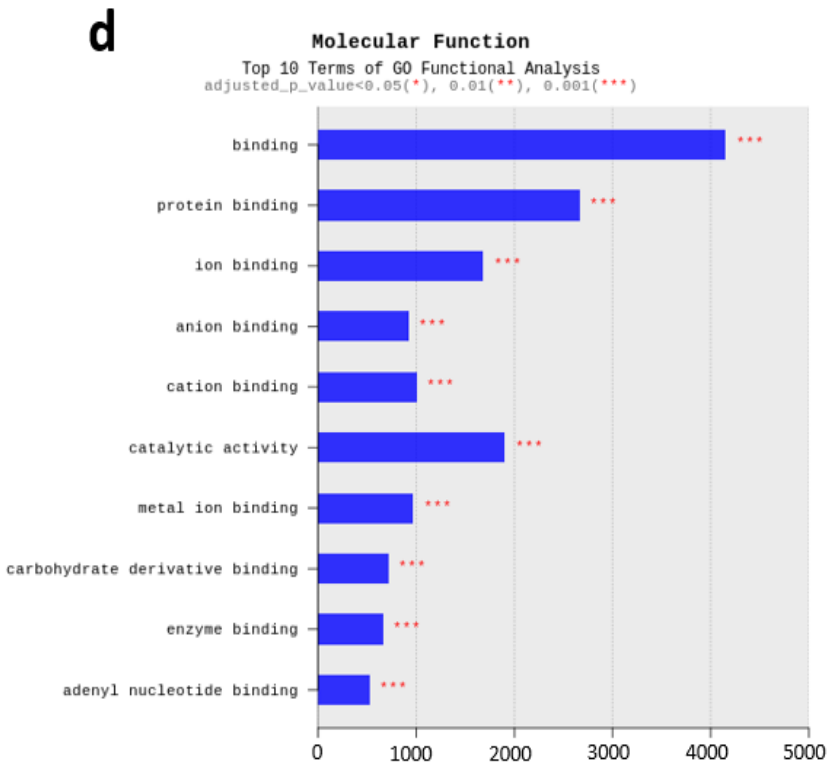
d
Molecular Function
Top 10 Terms of GO Functional Analysis
adjusted_p_value<0.05(*), 0.01(**), 0.001(***)
binding
protein binding
ion binding
anion binding
cation binding
catalytic activity
metal ion binding
carbohydrate derivative binding
enzyme binding
adenyl nucleotide binding
***
0
1000
2000
3000
4000
5000

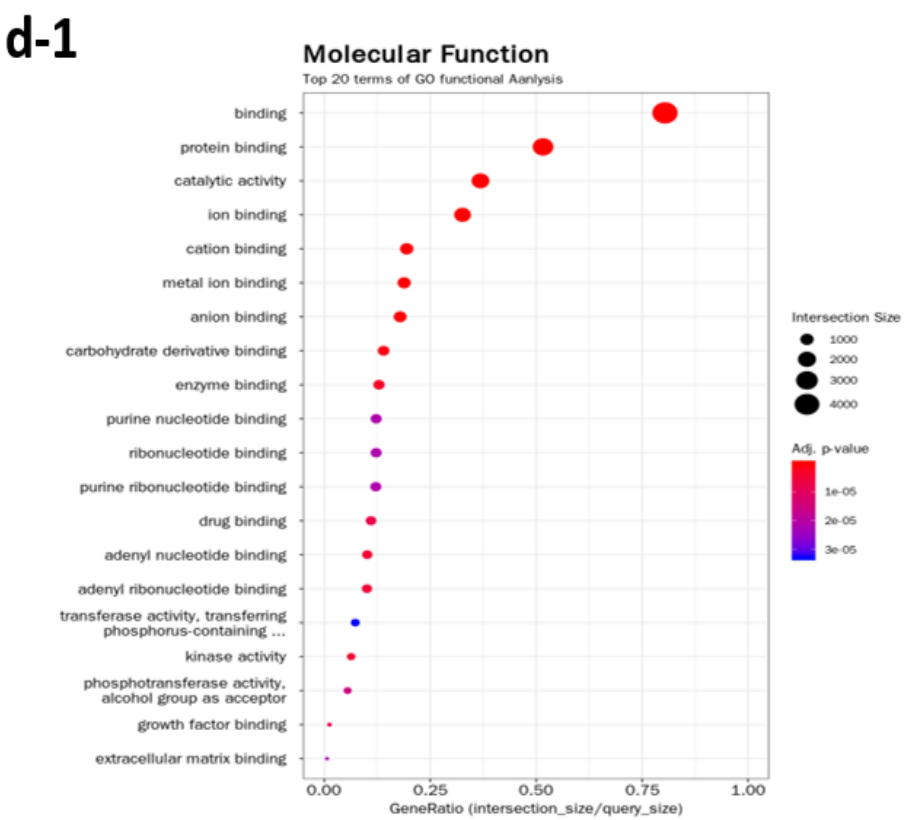
d-1
Molecular Function
Top 20 terms of GO functional Aanlysis
binding
protein binding
catalytic activity
ion binding
cation binding
metal ion binding
anion binding
carbohydrate derivative binding
enzyme binding
purine nucleotide binding
ribonucleotide binding
purine ribonucleotide binding
drug binding
adenyl nucleotide binding
adenyl ribonucleotide binding
transferase activity, transferring phosphorus-containing ...
kinase activity
phosphotransferase activity, alcohol group as acceptor
growth factor binding
extracellular matrix binding
0.00
0.25
0.50
0.75
1.00
GeneRatio (intersection_size/query_size)
Intersection Size
1000
2000
3000
4000
Adj. p-value
1e-05
2e-05
3e-05

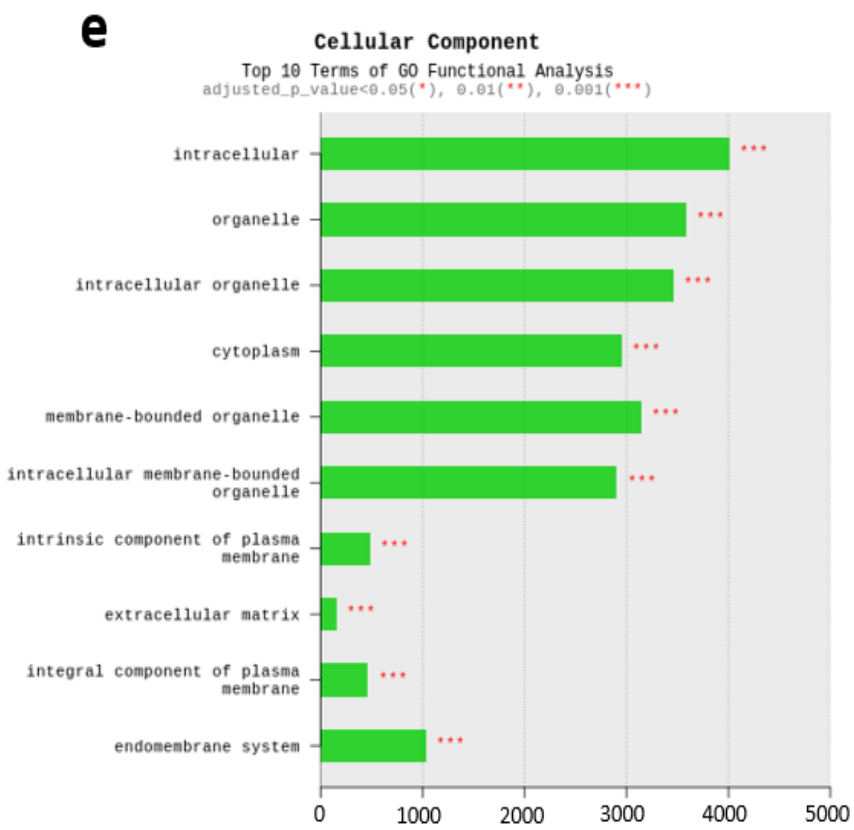
e
Cellular Component
Top 10 Terms of GO Functional Analysis
adjusted_p_value<0.05(*), 0.01(**), 0.001(***)
intracellular
organelle
intracellular organelle
cytoplasm
membrane-bounded organelle
intracellular membrane-bounded organelle
intrinsic component of plasma membrane
extracellular matrix
integral component of plasma membrane
endomembrane system
***
0
1000
2000
3000
4000
5000

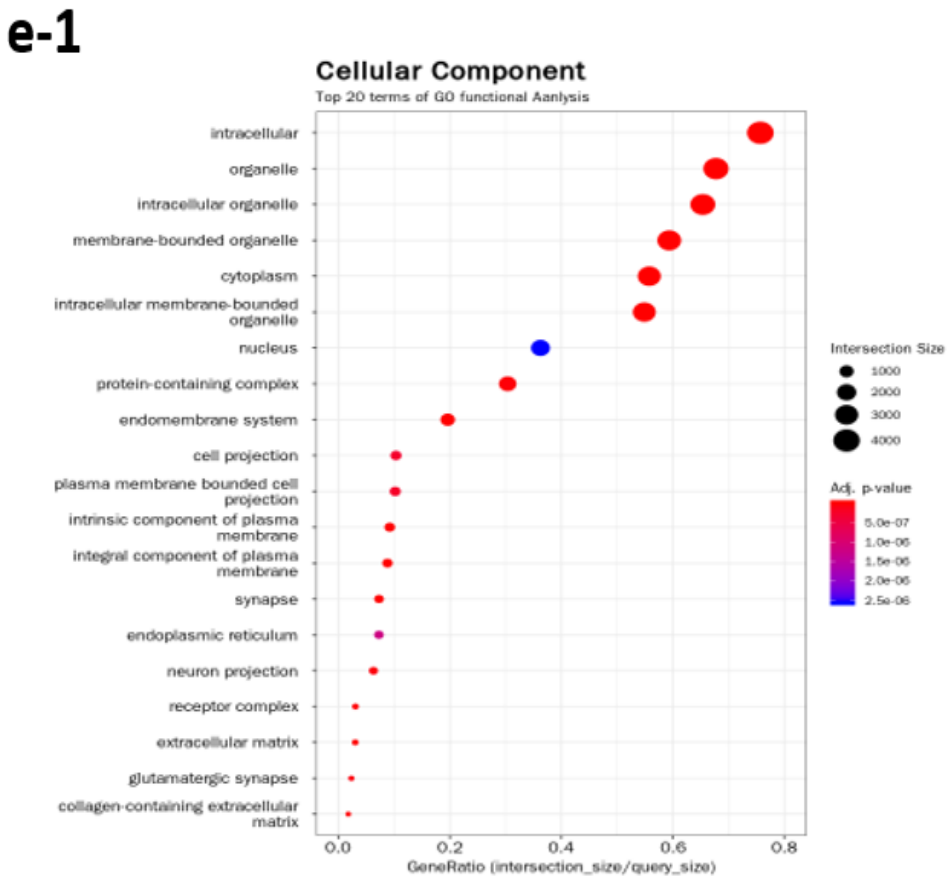
e-1
Cellular Component
Top 20 terms of GO functional Aanlysis
intracellular
organelle
intracellular organelle
membrane-bounded organelle
cytoplasm
intracellular membrane-bounded organelle
nucleus
protein-containing complex
endomembrane system
cell projection
plasma membrane bounded cell projection
intrinsic component of plasma membrane
integral component of plasma membrane
synapse
endoplasmic reticulum
neuron projection
receptor complex
extracellular matrix
glutamatergic synapse
collagen-containing extracellular matrix
0.0
0.2
0.4
0.6
0.8
GeneRatio (intersection_size/query_size)
Intersection Size
1000
2000
3000
4000
Adj. p-value
5.0e-07
1.0e-06
1.5e-06
2.0e-06
2.5e-06

Figure 21. Evaluation of sample reproducibility and results of the top 10 terms of GO functional analysis. (a) Pearson's coefficient was tested to validate the reproducibility among the samples and (b) numeric interpretations of differences in DEGs were demonstrated, compared to six cases within the experimental groups: Con vs. Mel, Con vs. Bru, Con vs. Mel+Bru, Mel vs. Bru, Mel vs. Mel+Bru, and Bru vs. Mel+Bru. (c-e) Top 10 GO terms were analyzed in 'biological process', 'molecular function', and 'cellular component', and (c-1-e-1) top 20 terms of GO functional analysis were demonstrated by the size of intersection. Con; control, Mel; melatonin, Bru; brusatol, and Mel+Bru; melatonin+brusatol.

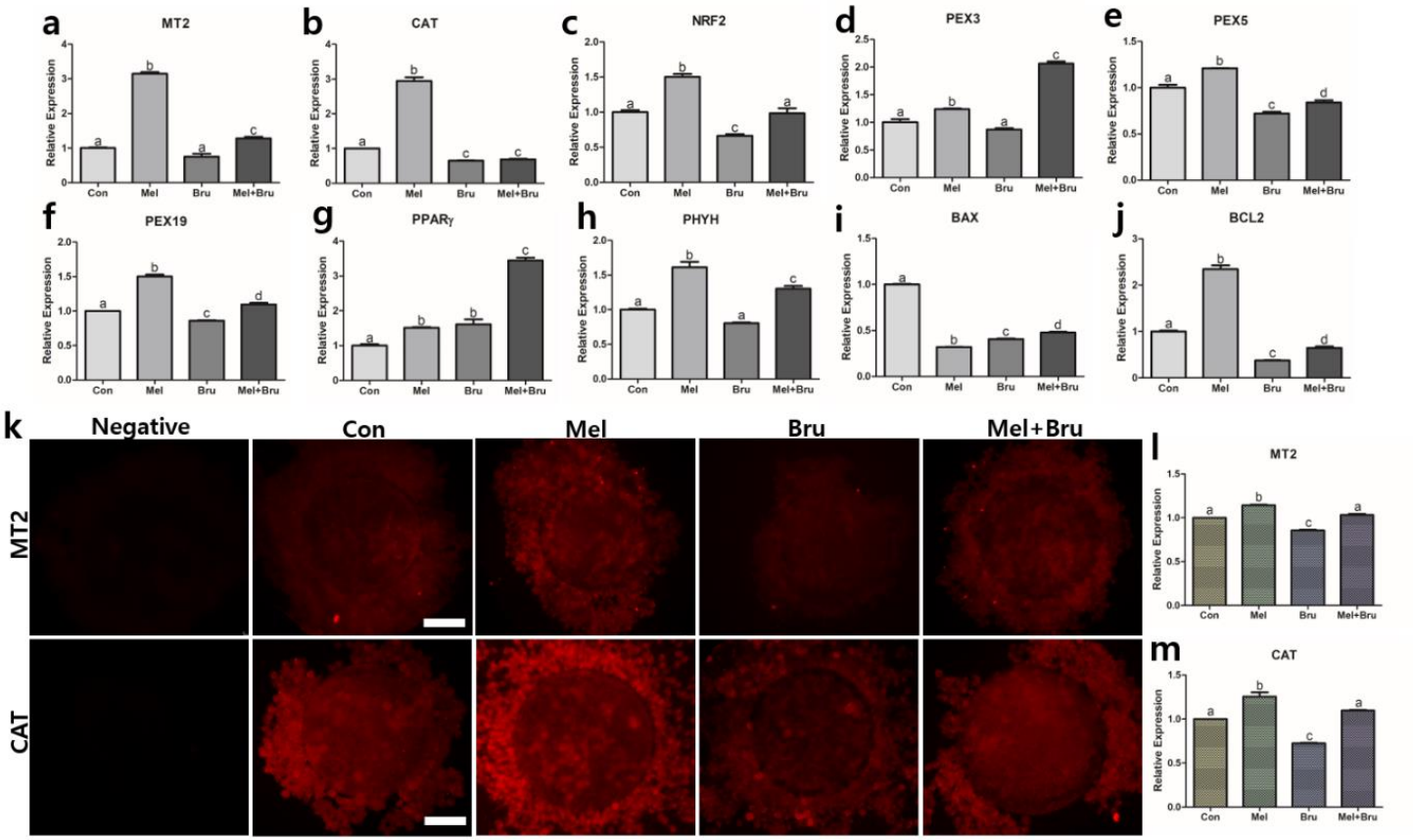
a
MT2
b
CAT
c
NRF2
d
PEX3
e
PEX5
f
PEX19
g
PPARγ
h
PHYH
i
BAX
j
BCL2
Relative Expression
Con
Mel
Bru
Mel+Bru
k
Negative
Con
Mel
Bru
Mel+Bru
MT2
CAT
l
MT2
m
CAT

Figure 22. Assessments of genes of interest by qRT-PCR and protein expression analysis by immunocytochemistry in porcine COCs. (a) Gene expressions related to (a-b) melatonin and antioxidant (*MT2* and *CATALASE*), (c) Nrf2 signaling (*NRF2*), (d-h) peroxisomal activities (*PEX3*, *PEX5*, *PEX19*, *PPARγ*, and *PHYH*), and (i-j) apoptosis (*BAX* and *BCL2*) were tested. The protein expression of MT2 and CATALASE in porcine COCs were evaluated by immunocytochemistry. Bars with letters indicate significant differences ($P < 0.05$). Original magnification: 400×, bars indicate 30μm Con; control, Mel; melatonin, Bru; brusatol, and Mel+Bru; melatonin+brusatol. At least three technical and biological replicates were performed.

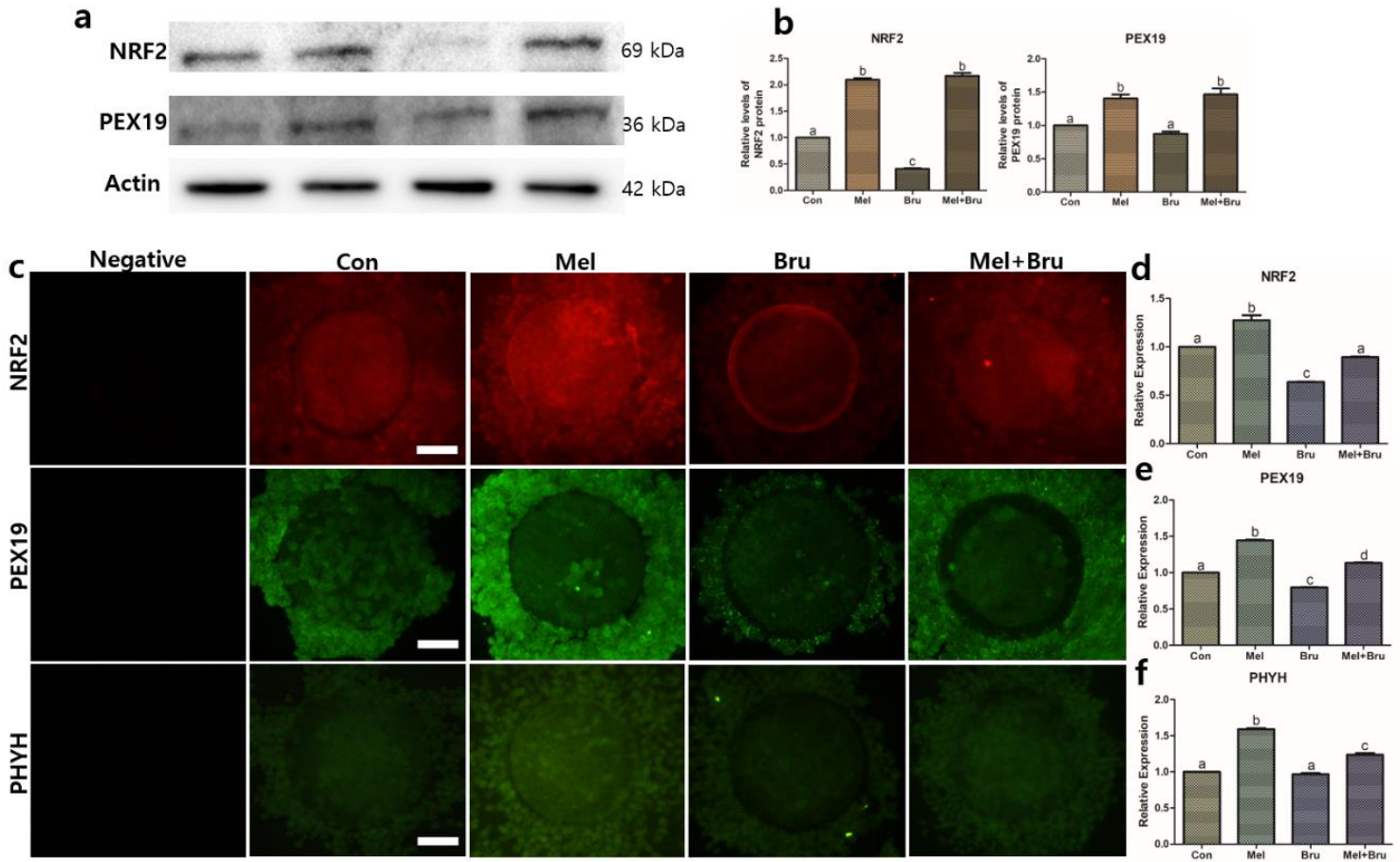
a
NRF2
PEX19
Actin
69 kDa
36 kDa
42 kDa
b
NRF2
PEX19
Relative levels of NRF2 protein
Relative levels of PEX19 protein
Con
Mel
Bru
Mel+Bru
c
Negative
Con
Mel
Bru
Mel+Bru
NRF2
PEX19
PHYH
d
NRF2
e
PEX19
f
PHYH
Relative Expression

Figure 23. Protein analysis of protein of interest in porcine COCs by immunocytochemistry and western blotting. (a-b) Western blot was performed to analyze and quantify NRF2 and PEX19 proteins in the porcine COCs. Beta-actin was used as the reference protein. (c-f) In order to re-validate the proteins expressed in the COCs, immunocytochemistry was performed. Bars with letters indicate significant differences ($P < 0.05$). Original magnification: 400×, bars indicate 30 μm Con; control, Mel; melatonin, Bru; brusatol, and Mel+Bru; melatonin+brusatol. At least three technical and biological replicates were performed.

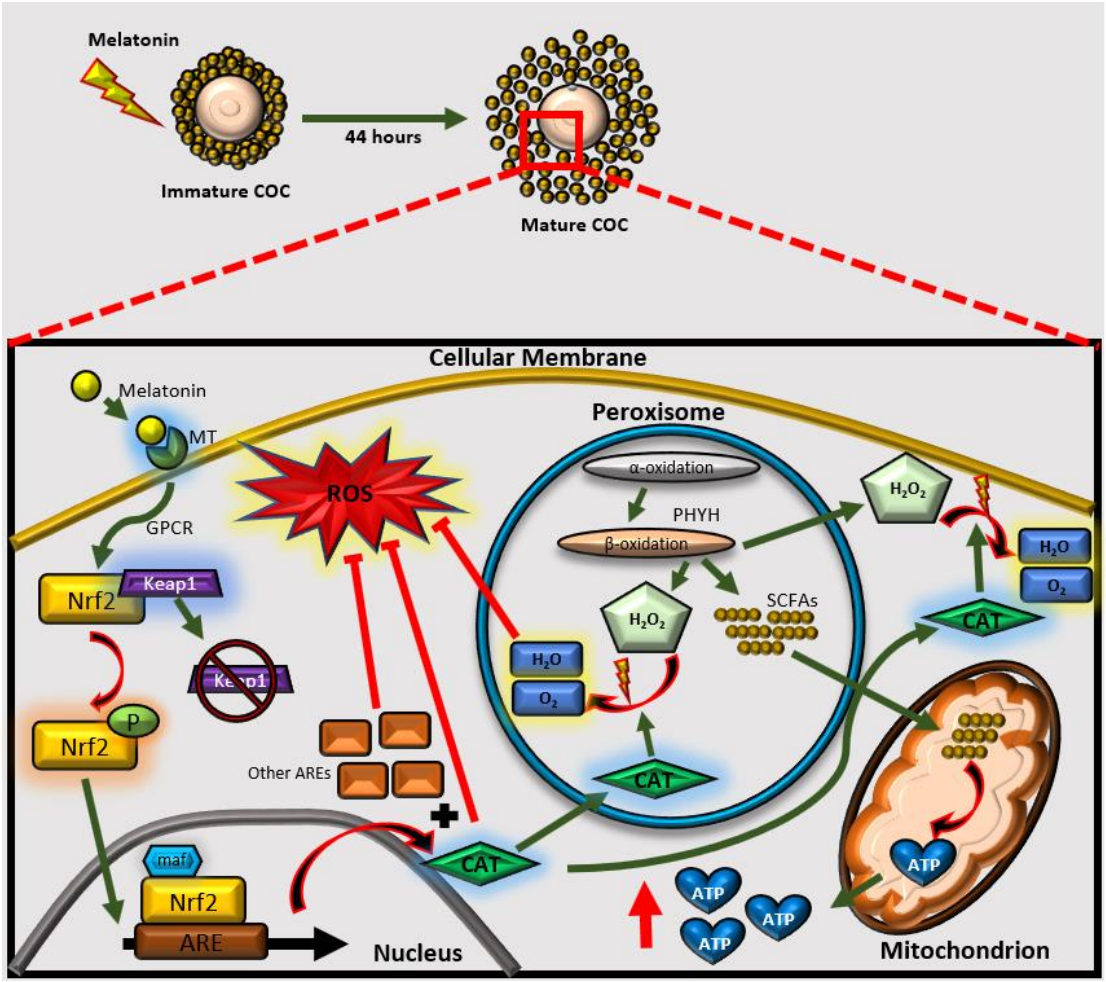
Melatonin
44 hours
Immature COC
Mature COC
Cellular Membrane
Melatonin
MT
GPCR
ROS
Peroxisome
α-oxidation
PHYH
β-oxidation
SCFAs
Nrf2
Keap1
P
Other AREs
CAT
maf
ARE
Nucleus
ATP
Mitochondrion

Figure 24. A schematic illustration of the cross-talk between Nrf2 signaling and peroxisomes activated by melatonin in porcine COCs. When melatonin binds to melatonin receptor 2, a series of cascades is activated via the GPCRs. Nrf2 is subsequently activated by the detachment of Keap1, which is later targeted for degradation. Activated Nrf2 is translocated to the nucleus, and transcription is initiated in conjunction with maf. Catalase is produced that prevents ROS accumulation, hydrolyzes H_2O_2, and also work in peroxisomes. Through α- and β- oxidation, Short-chained fatty acids (SCFAs) and H_2O_2 are produced in the peroxisome. The SCFAs are transferred to mitochondria for energy production. In addition, catalases are also stored in the peroxisome to hydrolyze H_2O_2 generated during peroxisomal activities. MT: melatonin receptor.

4. Discussion

To my knowledge, it is have demonstrated for the first time the possibility of a cross-talk between melatonin-Nrf2 signaling and peroxisomal activities in porcine COCs and partially validated these findings using RNA sequencing. The results suggest that peroxisomes may crosstalk with melatonin via the Nrf2/ARE signaling pathway, as most of the related mRNA and protein expression levels were significantly up- or down-regulated, and the expansion of CCs and embryo development altered in response to treatment with melatonin and brusatol in the porcine COCs. In addition, catalase activity and ATP production were also differently regulated by the treatments, implying that the antioxidant mechanism and energy metabolism were influenced by the crosstalk between NRF2 signaling and peroxisomes in accordance with the hypothesis.

A schematic of this study is shown in Figure 24. The study shows that melatonin can improve porcine oocyte quality and subsequent embryonic development through its various biological activities (Jin, Lee et al. 2017; Lee, Jin et al. 2018b; Park, Park et al. 2018). Melatonin is thought to mediate its effect by binding to receptors on the membrane, i.e., MTs (Mayo, Aguado et al. 2018), which constitute a superfamily of guanine nucleotide binding protein (G-protein)-coupled receptors (Reppert 1997; Cho, Kim et al. 2007). Specifically, MT2 was found to be fundamentally involved in oocyte maturation, embryo development, and activation of antioxidant-related signaling in porcine oocytes and embryos (Lee, Jin et al. 2018b; Kim, Kim et al. 2019); accordingly, the results showed that regulation of MT2 resulted in differences

in mRNA and protein levels among the treatment groups. As demonstrated in many studies, melatonin is known to regulate the Nrf2/ARE signaling pathway (Trivedi, Jena et al. 2016; Shah, Khan et al. 2017; Kim, Kim et al. 2019); therefore, brusatol, a Nrf2 inhibitor, was employed in order to verify the mechanism.

No CC expansion was observed with high concentrations of brusatol (50, 200, and 400nM) and lower concentrations (12 and 25nM) also showed negative effects on CC expansion (Fig 16). This corroborated the hypothesis that brusatol can specifically inhibit Nrf2 signaling and could influence the CC expansion in COCs. Kwak et al. suggested that the down-regulation of Nrf2 in oocytes may decrease CC expansion (Kwak, Yoon et al. 2014), which supported the results in that visible reductions in CC expansion, including the reduction in subsequent embryonic development, were clearly observed.

Upon evaluating embryonic development in the control, melatonin treatment, brusatol treatment, and co-treatment groups, it is found that the brusatol-treated group had the lowest developmental potential during the embryonic stage. This result is supported by a study by Ma and Lin et al., who demonstrated a significant decrease in the maturation of mouse oocytes and embryonic development following brusatol treatment (Ma, Li et al. 2017; Lin, Sui et al. 2018). In addition, the results are similar to those obtained in previous studies (Jin, Lee et al. 2017; Lee, Jin et al. 2017; Lee, Jin et al. 2018b) in that melatonin not only increased subsequent embryo development, but also increased the maturation rates of porcine COCs. Moreover, the expression levels of GDF9 and BMP15, which are related to oocyte competence (Belli & Shimasaki 2018), were also significantly influenced in each experimental

group. Various studies also suggested that melatonin is associated with ROS mechanisms in oocytes (Li, Wang et al. 2016; Zhao, Wang et al. 2018; Yang, Wang et al. 2020), and the results corroborated these findings. Additionally, negative effects of brusatol on GSH and ROS levels were observed. This may be due to the fact that brusatol, a Nrf2 inhibitor, could affect not only embryonic development, but also oxidative stress. In other words, embryonic development can also be decreased due to a negative redox imbalance due to brusatol, which is supported by the report by Guerin et al. that generation of ROS impairs embryonic development in various ways (Guerin, El Mouatassim *et al.* 2001). In summary, it is partially demonstrated the actions of melatonin and brusatol via Nrf2 signaling in pigs; therefore, subsequent experiments were conducted intracellular studies in the COCs.

Interestingly, the expression pattern of DEGs showed drastic differences in the brusatol- and co-treated groups compared to that in the control and melatonin-treated groups. This may imply that various causes are responsible for the impairment of COC morphology. First, as brusatol was confirmed to decrease CC expansion and hamper embryo development, the Nrf2 signaling pathway may strongly affect the morphological changes and developmental potential in porcine COCs; this is similar to the results obtained in previous studies (Ma, Li et al. 2017; Lin, Sui et al. 2018). Second, ATP content was significantly decreased in the brusatol-treated group and was increased in response to melatonin treatment in the COCs. As ATP is produced in the mitochondria and peroxisomes mainly though lipid β-oxidation (Fransen, Lismont et al. 2017), I hypothesized that melatonin and brusatol can also affect peroxisomes and mitochondria via the Nrf2 signaling pathway. The results of GO

term analysis revealed meaningful functions such as ‘in the peroxisome’, ‘peroxisomal fission’, ‘the PPAR signaling pathway’, ‘mitochondrion’, ‘mitochondrial membrane’, ‘mitochondrial translational elongation’, etc., which were all included in the top 10 GO terms in cellular components (Fig. 21e and 21e-1). Moreover, I found significant differences in ‘ATP synthesis coupled electron transport’, ‘ATP metabolic process’, ‘ATPase activity’, and ‘antioxidant activity’, all of which were also included in top 10 GO terms in molecular functions. It has been suggested that SCFAs produced during α- or β- oxidation in peroxisomes are transferred to the mitochondria for subsequent ATP production (Jansen & Wanders 2006). Furthermore, considering the fact that ATP can be produced by the peroxisomes themselves (Wanders, Jansen et al. 2001) and that ATP from FA oxidation enhances oocyte competence (Dunning, Cashman et al. 2010; Dunning, Russell et al. 2014), the study was narrowed to examine the effects of peroxisomes and their relationship with the Nrf2 signaling pathway.

In order to track the enzymatic activities in peroxisomes, PHYH and PEX19 were used. PHYH is involved in α-oxidation, which is thought to occure only in the peroxisomes (Jansen & Wanders 2006). Therefore, it is surmised that PHYH would serve as a useful peroxisome marker. More specifically, PEX19 is one of the major factors associated with peroxisomal membrane biogenesis, and plays numerous roles in the functional assembly of the peroxisome (Agrawal, Shang *et al.* 2017). The data showed that peroxisomal activities were significantly increased in the melatonin-treated group and decreased in the co-treated group, which was verified by the levels of PHYH and PEX19. This may suggest that melatonin could increase peroxisomal

activities, which could be reduced upon co-treatment with brusatol. In other words, it is suggested that the possibility that peroxisomal activities can be regulated by Nrf2 signaling. This is corroborated by a study by You et al., which showed that knockdown of *PEX19* caused a reduction in peroxisome number, resulting in increased apoptosis and simultaneous reduction in the activation of Nrf2 signaling and facilitation of ROS accumulation (You, Chen et al. 2020). The results regarding NRF2 expression levels support the findings of You et al. in that similar expression patterns were observed for NRF2 compared to those of PHYH and PEX19.

Another connection between Nrf2 signaling and peroxisomes can be explained by catalase activation. Catalase exists within and outside of the peroxisome, and plays a major role in maintaining the oxidative balance of the organelle by breaking down hydrogen peroxide produced in the peroxisome (Schrader & Fahimi 2006; Walton & Pizzitelli 2012). Catalase is also known as a peroxisomal marker protein that is associated with PEX19 activity (Sacksteder, Jones et al. 2000). Miller et al. demonstrated that a significant reduction in catalase levels occurred in *Nrf2* knockout mice (Miller, Gounder et al. 2012) and a similar phenomenon was observed in pigs (Yang, Zhao et al. 2017). Together with previous reports, the data also showed that the protein expression pattern of catalase was similar to that of Nrf2 and PEX19 in that the melatonin-treated group, which exhibited significantly increased the expression of catalase; additionally, catalase expression in the co-treated group was significantly lower than that in the melatonin-treated group, demonstrating an alternative connection between Nrf2 signaling and peroxisomes.

In conclusion, that the upregulation of Nrf2 signaling and peroxisomes by melatonin treatment followed by their downregulation by brusatol imply a strong relationship between them; this is depicted in Figure 24. To my knowledge, this is the first study to examine the collaborative roles and functions in porcine oocytes activated by melatonin. As antioxidant mechanisms and energy production are involved in oocyte maturation and subsequent embryonic development in mammals, further studies are essential to uncover the intricate cross-talk between Nrf2 signaling and the peroxisomes.

Chapter II. Peroxisome-derived lipid metabolism influences Nrf2 signaling via the co-treatment of melatonin and phytanic acid in porcine embryos

1. Introduction

The production of transgenic pigs and xenotransplantation are pivotal processes in translational biomedical research (Prather, Hawley et al. 2003; Aigner, Renner et al. 2010), and the development of optimal procedures for embryo production are essential (Wu, Vilarino et al. 2017). However, overcoming the four-cell block and maximizing the developmental potentials of porcine embryos still remains an unsolvable assignment for researchers (Brussow, Torner et al. 2000; Dang-Nguyen, Wells et al. 2020). Therefore, attempts to improve the porcine IVC system and transgenic pig production using either chemical treatment or ARTs (Chuang, Chen et al. 2017; Kim, Kim et al. 2019; Lee, Lee et al. 2019; Taweechaipaisankul, Kim et al. 2019) have been continuously reported. Interestingly, both PA (a branched FA) and melatonin (a mammalian pineal gland- and peripheral reproductive organ-derived natural hormone) are suggested to be involved in lipid metabolism in mammalian cells (Schluter, Yubero et al. 2002; Ekthuwapranee, Sotthibundhu et al. 2015), oocytes (Lee, Jin et al. 2017; Kim, Kim et al. 2020; Lan, Zhang et al. 2020), and embryos (Kim, Kim et al. 2019; Niu, Zhou et al. 2020; Qu, Sun et al. 2020). Although there has been a study of their inverse effects in cells (Chaudhary & Parvez

2017), there have been no reports on their synergistic effect on lipid metabolism, specifically in mammalian oocytes or embryos.

It is widely accepted that the Nrf2 signaling pathway is involved in cellular defense mechanisms against OS. Under cellular oxidative stress conditions, Nrf2 detaches from Keap1 through the breakage of disulfide bonds, stabilizes itself, and translocates into the nucleus to facilitate ARE activation (Tonelli, Chio et al. 2018; Li, Jia et al. 2019). The action of this pathway in mammalian oocytes (Lin, Sui et al. 2018; Ma, Liang et al. 2018; Jiang, Xing et al. 2020) and embryos (Amin, Gad et al. 2014; Lin, Sui et al. 2018; Kim, Kim et al. 2019) has previously been proven; moreover, some of these studies suggested that the potential for embryonic development and maturation also increased with pathway activation. In addition, the study of Van Den Brink and Wanders et al. suggested that α-oxidation from the digestion of PA occurs soley in peroxisomes (van den Brink & Wanders 2006). Because of the branched structure of PA, it undergoes a series of shortening-processes via PHYH-mediated α- and β-oxidation, and the subsequent short-chained FAs are transferred to the mitochondria to facilitate ATP production via the citric acid cycle (Wanders, Waterham et al. 2015). Interestingly, there have been some studies on the role of β-oxidation in mammalian oocytes or embryos, which claim that FA is one of the most pivotal sources of energy for the development of oocyte competence and embryonic developmental potentials (Dunning, Cashman et al. 2010; Dunning, Russell et al. 2014; Sanchez-Lazo, Brisard et al. 2014).

Pex19 is a peroxisome biogenesis factor that collaborates with Pex3. This collaboration is known to participate in the categorization of membrane proteins for

transportation to other organelles, such as lipid droplets and mitochondria (Jansen & van der Klei 2019). Sunyer-Figueres et al. reported that melatonin significantly increased the expression of Pex19, suggesting that melatonin upregulates β-oxidation of FAs in peroxisomes through the regulation of *Pex19* (Sunyer-Figueres, Vazquez et al. 2020). Here, some studies raised an interesting suggestion that the Nrf2 signaling pathway not only plays a role in the maintenance of cellular redox homeostasis, but also mediates the β-oxidation of FAs, MMP, and production of ATP. Moreover, it has been reported that the Nrf2 signaling pathway has a beneficial effect on compromised mitochondria (Dinkova-Kostova & Abramov 2015; Holmstrom, Kostov et al. 2016).

To date, there have been numerous emerging suggestions on the co-regulation of the Nrf2 signaling pathway and peroxisomal activity via the activities of Pex19 and PHYH; however, we could not find any studies on their relationship in porcine embryos. Since both the Nrf2 signaling pathway and peroxisomal activities are found to be involved in β-oxidation and lipid metabolism in eukaryotic cells, we suggest that their crosstalk in porcine embryos needs to be investigated, as it may prove to be a significant key to improving porcine IVC. Therefore, the aim of this study was to investigate whether the regulation of peroxisomal activities would affect the Nrf2 signaling pathway and subsequent lipid metabolism in porcine embryos treated with melatonin and PA.

2. Materials and methods

2.1. Research ethics and chemicals

Procedures for research ethics and chemical administration were described in general methodology

2.2. COC retrieval and IVM

Procedures for IVM were described in general methodology.

2.3. Parthenogenetic activation

Procedures for parthenogenetic activation were described in general methodology

2.4. Microinjection

Matured oocytes were denuded with 0.1% hyaluronidase, and then parthenogenetically activated. After 1 h of culture, potential embryos were microinjected into 4 μL droplets of 7.5 μg/mL cytochalasin B using an Eppendorf

FemtoJet microinjector. Candidate (Cnd) siRNAs targeting *Pex19* and scramble siRNA(Bou, Liu et al. 2017) for the negative control were designed and synthesized by Bioneer Co. (Daejeon, Korea). Information on these siRNAs is shown in Table 19. For injection, 25 μmol/L siRNA was loaded onto FemtoTip II (Eppendorf) using a microloader (Eppendorf), and injection of the siRNA was confirmed by visualization of the distinct expansion of droplets within the cytoplasm of the embryo. Immediately after microinjection, the embryos were washed several times in PZM-5 droplets and cultured for 7 days.

2.5. Chemical administration during IVC and embryo evaluation

After parthenogenetic activation or microinjection, cells were treated with a series of PA concentrations during IVC: 0 (control), 20, 40, and 80 μM, to determine the optimum concentration. For melatonin, we used concentrations of 10^{-7} M melatonin, as this was demonstrated to be the optimal concentration in a previous study. Both PA and melatonin were dissolved in DMSO, and for exact comparison, the control and microinjected groups were also treated with DMSO. The day on which the activated or microinjected oocytes were transferred to the IVC medium was denoted as day 0. The number of embryos with even cleavage was counted under a stereomicroscope on day 2 (at 48 h). On day 7, the number of blastocysts and total cell numbers were counted (168 h). The blastocysts from day 7 were washed in PVA/PBS and then fixed for 1 h in 4% paraformaldehyde (w/v) in PBS at room

temperature. Subsequently, the day 2 embryos and blastocysts were stained with 5 μg/mL Hoechst 33342 for 8 min. After washing with PVA/PBS, the stained embryos were mounted on glass slides and covered with cover slips. The total cell numbers of the day 2 and day 7 embryos were determined under a fluorescence microscope (Nikon Corp.). In each group, at least 15 embryos from five biological replications were used for staining.

2.6. Immunofluorescence staining

Day 2 and 7 (2-cell and blastocyst, respectively) embryos were washed in PVA/PBS and then fixed with 4% paraformaldehyde (PFA) (w/v) in PBS for 1 h at room temperature. The embryos were permeabilized with 1% Triton X-100 (v/v) in distilled water (DW) for 1 h at 39°C, washed three times in 1% PVA/PBS, and then incubated in 2% BSA in PVA/PBS for 2 h to prevent non-specific binding. The embryos were then directly transferred to 2% BSA containing the primary antibody for NRF2 (1:200; 70R-50116; Fitzgerald Industries International, Acton, USA), PHYH (1:400; MBS3212923; MyBioSource, San Diego, USA), and PEX19 (1:400; MBS9605735; MyBioSource, San Diego, USA) and incubated overnight at 4°C. After incubation, the embryos were washed several times in PVA/PBS and incubated with secondary fluorescein isothiocyanate-conjugated anti-rabbit polyclonal antibody (1:200; ab6717; Abcam, Cambridge, UK) and goat anti-rabbit IgG H&L (Texas Red ®, 1:200; ab6719; Abcam, Cambridge, UK) at 37°C for 2 h in the dark.

After the secondary antibody incubation, the embryos were washed in PVA/PBS and the counterstaining was directly performed with 5 μg/mL Hoechst-33342 for 8 min. After washing, embryos were mounted on glass slides with 100 % glycerol droplets, covered with cover slips, and then analyzed under a fluorescence microscope. Assessment of the fluorescence was performed using ImageJ software (version 1.46r; National Institute of Health, USA). The intensities of the control group were standardized to 1. Staining was performed at least three times, and in each group, at least 15 embryos from eight biological replications were used for the staining.

2.7. Fluorescent FA analog assays

The fluorescent FA analog assay was performed in accordance with a study by Lolicato et al (Lolicato, Brouwers *et al.* 2015). In brief, day 2 and day 7 embryos were fixed in 4% PFA/PBS for 1 h at room temperature, and then washed three times in PVA/PBS. The fixed embryos were then incubated in 6 μM BODIPY 558/568 C12 (BODIPY-FA; D3835; Molecular Probes, Eugene, OR, USA) diluted in PBS for 1 h at room temperature (avoiding light). After incubation, the embryos were again washed three times in PVA/PBS before mounting on glass slides with cover slips. Images were captured using an epifluorescence microscope (TE2000-S; Nikon), and the fluorescence intensities of the FA were evaluated using ImageJ software. The intensities of the control group were standardized to 1. Staining was technically performed at least three times, and in each group, at least 15 embryos from eight biological replications were used for the staining.

2.8. JC-1 MMP assays

The entire procedure of the JC-1 MMP assay was previously described (Kim, Kim *et al.* 2020). Day 2 and 7 embryos were fixed and washed in PVA/PBS, and then incubated at 37°C in JC-1 solution mixed with culture medium (PZM-5) for 30 min. After incubation, the embryos were washed with PVA/PBS several times before mounting on cover slips. Images of each embryo were obtained using an epifluorescence microscope (TE2000-S; Nikon). The fluorescence ratio of the JC-1 aggregate and JC-1 monomer (590 nm and 530 nm, respectively) was measured using ImageJ software (version 1.46r; National Institutes of Health, USA). The intensities of the control group were standardized to 1. Staining was technically performed at least three times, and in each group, at least 17 embryos from five biological replications were used for the staining.

2.9. ATP Content Assay

Day 2 and 7 embryos were washed in PVA/PBS three times, and then fixed in 4 % PFA/PBS for 1 h at room temperature. The fixed embryos were washed three times in PVA/PBS droplets, and then transferred to 0.5 μM of BODIPY FL ATP (BODIPY-ATP; A12410; Molecular Probes, Eugene, OR, USA) diluted in PBS for 1 h at room temperature. Subsequently, the embryos were washed again in PVA/PBS and mounted on glass slides, covered with slips. Images were captured using an epifluorescence microscope, and the ATP content was measured using ImageJ

software. The staining was technically performed three times, and in each group, at least 21 embryos from five biological replicates were used for the staining.

2.10. Analysis of gene expression by quantitative real-time PCR

Procedures for real-time PCR were described in general methodology. A list of primers is shown in Table 20. More than 200 2-cell embryos and 50 blastocysts from at least five replications were used for total RNA extraction, then proceeded for cDNA synthesis and real time PCR

2.11. Statistical analysis

Procedures for statistical analysis were described in general methodology.

Table 19. List of candidate siRNAs targeting *Pex19* and scramble siRNA.

Candidate (Cnds)	Target gene	Sequences (5'- 3') RNA : [A, C, G, U], DNA : [a, c, g, t]	GC content	Tm	NGIC score
-	Scramble	CGAACAGAUAAAGCCGCUGUAAGUA UACUUACAGCGGCUUUAUCUGUUCG	-	-	-
Cnd1	*PEX19*	GAGAUCUCCAGGAGACACU=tt AGUGUCUCCUGGAGAUCUC=tt	0.53	59.96	98
Cnd2	*PEX19*	CGUGACUUUCCCUCAGGUU=tt AACCUGAGGGAAAGUCACG=tt	0.53	59.51	98
Cnd3	*PEX19*	CACUACACCCUCUUACCUU=tt AAGGUAAGAGGGUGUAGUG=tt	0.47	58.66	91.9

Table 20. Sequence-specific primers used for quantification of differential expressed transcripts.

Genes	Primer sequences (5'- 3')	Product size (bp)	Accession No.
GAPDH	F: GTCGGTTGTGGATCTGACCT	207	NM_001206359
	R: TTGACGAAGTGGTCGTTGAG		
NRF2	F: GCCCAGTCTTCATTGCTCCT	115	XM_013984303
	R: AGCTCCTCCCAAACTTGCTC		
PEX3	F: AATGCATCTTCCTGGGGACG	125	NM_001244185.1
	R: ATACTGTCGTCGTGCTTGGG		
PEX19	F: CTCAATCTATCGGGCCCACC	144	XM_001928869.5
	R: TAGACGACACTCCTGCCTCA		
PPARγ	F: CCATTCCCGAGAGCTGATCC	192	XM_005669783.3
	R: TTTATCCCCACAGACACGGC		
ATGL	F: GACGGTGGCATCTCAGACAA	113	NM_001098605.1
	R: TGGATGTTGGTGGAGCTGTC		
HSL	F: GCCTTTCCTGCAGACCATCT	104	NM_214315.3

	R: CACTGGTGAAGAGGGAGCTG		
MGLL	F: ACCCCACAGAGTGTCCCATA	96	XM_013982013.2
	R: GGGTGTAGCTGAGGGTTTCC		
CGI58	F: TCTTGCTGGGACACAACCTG	220	NM_001012407.1
	R: CCAAAGGGTCCTGCAATCCT		
BAX	F: CATGAAGACAGGGGCCCTTT	181	XM_003127290
	R: CATCCTCTGCAGCTCCATGT		
BCL2	F: AATGTCTCAGAGCAACCGGG	193	NM_214285
	R: GGGGCCTCAGTTCTGTTCTC		

F, Forward primer; R, Reverse Primer

3. Results

3.1. Optimization of phytanic acid and co-treatment with melatonin

Treatment with 20 μM PA was used in subsequent experiments in which the embryos were co-treated with melatonin and PA. There were no differences in the rates of embryo cleavage among the experimental groups (Fig. 25a). However, the individually treated melatonin and PA groups had significantly higher blastocyst formation rates than the control group (26.96% and 24.02% vs. 18.63%, respectively; $P < 0.05$) (Fig. 25b). Furthermore, the melatonin and PA co-treated group showed the highest blastocyst formation rate (31.35%, $P < 0.05$). As shown in Figure 25c, the total cell number of blastocysts in the melatonin-, PA-, and co-treated groups were significantly higher than that of the control group (61.30, 57.08, 60.31, and 44.30%, respectively; $P < 0.05$). More than 180 embryos were used per experimental group, with six biological replications each. Presumably, this result might indicate that co-treatment with melatonin and PA was more effective than either individual treatment

3.2. *Pex19* siRNA selection and application

To select an appropriate *Pex19*-targeting siRNA, three Cnds were designed and used for microinjection. In Figure 25d, differences in cleavage rates were observed between the scramble siRNA and all Cnds (Cnd1, 2, and 3); rates in the Cnd-treated

groups were significantly lower than those in the control and scramble siRNA groups (82.76%, 81.16%, and 84.82% vs. 96.10% and 94.48%, respectively; $P < 0.05$). All Cnd-injected embryos (Cnd1, 2, and 3) had significantly lower blastocyst formation rates than either in the control or scramble siRNA groups (6.52%, 9.45%, and 15.40% vs. 20.42% and 17.59%, and 17.06%, respectively; $P < 0.05$) (Fig. 25e). However, there were no differences between the scrambled siRNA and Cnd3. In addition, I analyzed the gene expression of *Pex19* in porcine 2-cell embryos and found that all Cnds significantly reduced *Pex19* expression compared to the control and scramble siRNA (Fig. 25f) ($P < 0.05$). From this experiment, Cnd3 was selected as the appropriate siRNA for subsequent experiments because it significantly reduced the expression of *Pex19*, but had the highest blastocyst formation rate, indicating that Cnd3 was the least harmful to embryonic development. At least 180 embryos were used for each experimental group, and six biological replications were performed. For gene (*Pex19*) expression analysis, a total of 844 2-cell embryos from five biological replications were used for total RNA extraction, and real time PCR was performed in triplicate.

With the selected siRNA, the last test for IVC was performed and the experimental groups were as follows: control (DMSO treated), melatonin/PA, Cnd3, and Cnd3 with melatonin/PA (combination group). In Figure 25g, the cleavage rates in the Cnd3 and combination groups were significantly lower than those of the control and melatonin/PA-treated groups (85.77% and 85.67% vs. 92.74% and 93.52%, respectively; $P < 0.05$). The melatonin/PA-treated group showed the highest blastocyst formation rates compared to the control, Cnd3 and the combination group

(31.62% vs. 20.29%, 13.60%, and 19.19%, respectively; $P < 0.05$), and Cnd3 had the lowest blastocyst formation rate among all groups ($P < 0.05$) (Fig. 25h). Similarly, the melatonin/PA-treated group also showed the highest blastocyst cell numbers compared to the control, Cnd3, and the combination group (63.58 vs. 46.08, 37.15, and, 39.58, respectively; $P < 0.05$) (Fig. 25i). At least 200 embryos from each experimental group from six biological replications were used.

3.3. Gene expression analysis in 2-cell embryos and blastocysts

Figure 26 and 27 show the gene expression of components of the Nrf2 signaling, peroxisomal activities, lipid metabolism, and apoptosis pathways in porcine 2-cell embryos and blastocysts. In 2-cell embryos, the expression of *Nrf2* was highly increased when melatonin/PA was applied regardless of Cnd3 injection ($P < 0.05$), and there was no significant difference in the Cnd3-injected group (Fig. 26a). In contrast, in blastocysts, no difference was observed between the control and melatonin/PA-treated groups; however, gene expression in the Cnd3-injected and combination group showed a significant decrease compared to the other groups ($P < 0.05$; Fig. 27a). In the case of *Pex19* (Fig. 26b and 27b), melatonin/PA-treatment significantly upregulated gene expression and the Cnd3-injected group showed decreased expression in 2-cell embryos ($P < 0.05$). In blastocysts, a similar tendency in expression was observed in the melatonin/PA-treated group ($P < 0.05$), and downregulation was observed in the Cnd3-injected group ($P < 0.05$). In *PHYH* (Fig. 26c and 27c), the melatonin/PA-treated group showed significantly increased

expression in both types of embryos; however, expression was decreased in the Cnd3 and combination groups compared to the control group in blastocysts ($P < 0.05$). In addition, an increase in the expression was observed in the combination group compared to the control in 2-cell embryos ($P < 0.05$).

In 2-cell embryos, melatonin/PA treatment significantly upregulated the expression of *Pex3*, *PPARγ*, *ATGL*, *HSL*, *MGLL*, *CGI58*, and *Bcl2*, while the expression of *PPARγ*, *HSL*, *MGLL*, and *Bcl2* were the lowest in the Cnd3-injected group ($P < 0.05$). Interestingly, expression of *Pex3*, *PPARγ*, HSL, *MGLL*, and *Bcl2* was recovered in the combination group compared to the Cnd3-injected group ($P < 0.05$). The gene expression of *Bax* was opposite to that of *Bcl2* in Cnd3 and the combination group ($P < 0.05$) (Fig. 26d-26k). The gene expression signatures in blastocysts (Fig. 27d-27k), were similar to those observed in the 2-cell embryos; melatonin/PA treatment significantly increased the expression of *Pex3*, *PPARγ*, *ATGL*, *HSL*, *MGLL*, *CGI58*, and *Bcl2*, whereas only *ATGL*, *CGI58*, and *Bcl2* showed a significant decrease in gene expression in the Cnd3-injected group ($P < 0.05$). Moreover, recovery of the gene expression of *PPARγ*, *ATGL*, *HSL*, and *Bcl2* was observed in the combination group compared to the Cnd3-injected group ($P < 0.05$).

3.4. Immunocytochemistry, BODIPY and JC-1 MMP staining in porcine embryos

Immunocytochemistry of the protein of interest was performed on porcine 2-cells and blastocysts. Figure 28, 29, and 30 show that the protein expression of NRF2, PEX19, and PHYH 2-cell embryos; expression was significantly increased in the melatonin/PA-treated group, whereas a decrease was observed in the Cnd3-injected group compared to the control group ($P < 0.05$). The expression was again significantly improved in the combination group compared to the Cnd3-injected group (a and a' in the figures indicate results from 2-cell embryos). Similarly, in blastocysts, melatonin/PA-treatment significantly upregulated protein expression. However, only PEX19 and PHYH protein expression were significantly decreased in the Cnd3-injected group compared to the control group, and recovery of protein expression was observed in the combination group compared to the Cnd3 alone-injected group ($P < 0.05$). In addition, the expression of NRF2 in the combination group was significantly higher than that in the control group ($P < 0.05$), and no difference was observed between Cnd3 and the combination groups (b and b' in the figures indicate the results from blastocysts).

Subsequently, ATP, FA, and JC-1 MMP were analyzed in porcine 2-cell embryos and blastocysts. The intensity of ATP content was higher in the melatonin/PA-treated group than in the other experimental groups ($P < 0.05$), and Cnd3-injection significantly decreased the intensity in the embryos compared to the control. Lastly, intensity was again increased in the combination group compared to

the Cnd3-injected group ($P < 0.05$; Fig. 31a and 31a'). I next investigated the fluorescence of FAs in blastocysts, and found no significant difference in the intensities between the control and melatonin/PA-treated group; however, differences were observed in the Cnd3-injected and combination groups compared to the control and melatonin/PA-treated group (Fig. 31b and 31b'). In addition, JC-1 MMP analysis was performed in blastocysts, and the intensities were calculated from the ratios of JC-1 aggregates/JC-1 monomer. Although there was no difference observed between the control and Cnd3-injected groups, the intensities of the melatonin/PA-treated group and the combination group were significantly higher than those of the control group, melatonin/PA treatment resulted in the highest intensity among the groups ($P < 0.05$; Fig. 32a and 32b).

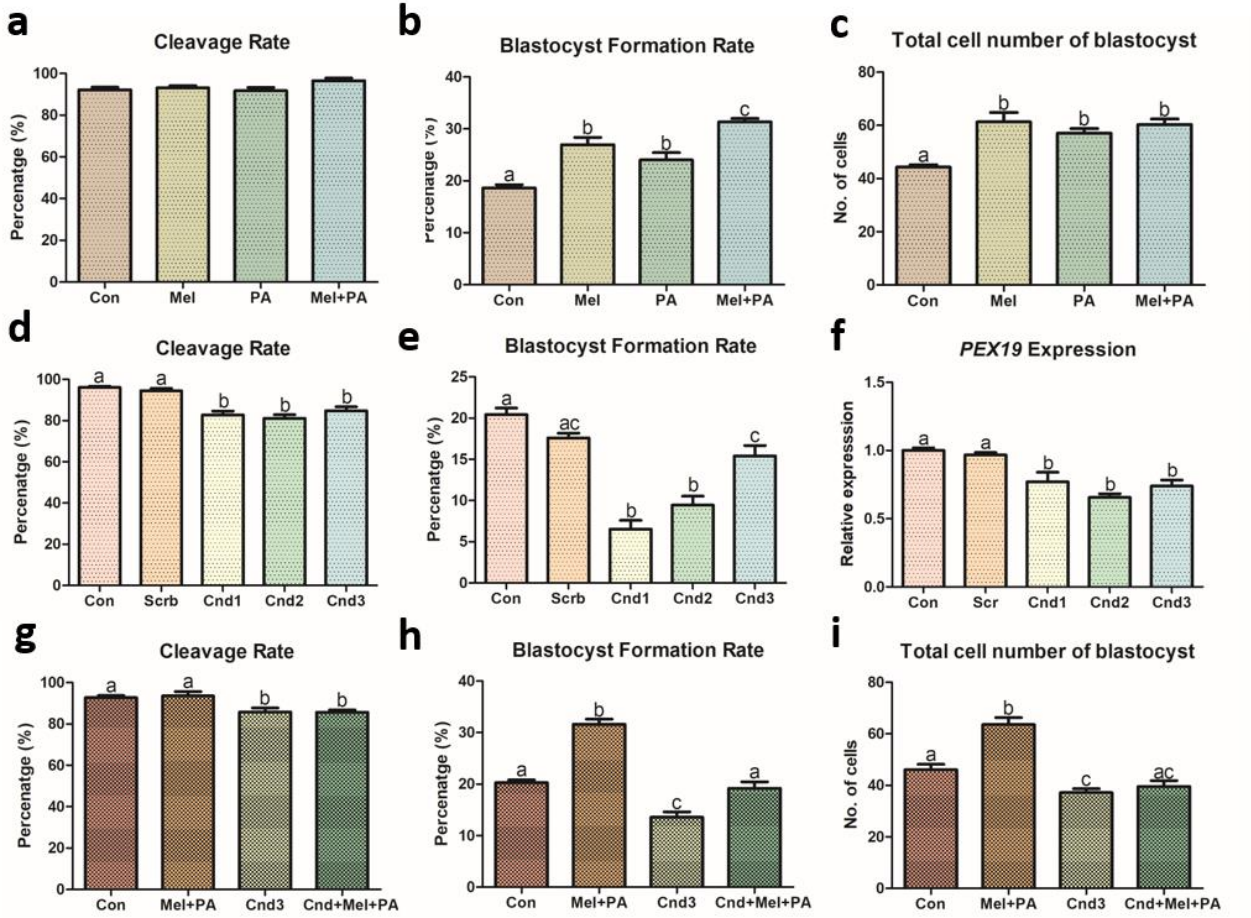
a
Cleavage Rate
Percenatge (%)
Con
Mel
PA
Mel+PA
b
Blastocyst Formation Rate
c
Total cell number of blastocyst
No. of cells
d
Cleavage Rate
Con
Scrb
Cnd1
Cnd2
Cnd3
e
Blastocyst Formation Rate
f
PEX19 Expression
Relative expresssion
Scr
g
Cleavage Rate
Mel+PA
Cnd3
Cnd+Mel+PA
h
Blastocyst Formation Rate
i
Total cell number of blastocyst

Figure 25. Assessments of porcine embryonic development treated with melatonin, phytanic acid (PA), and injected with *Pex19*-targeted siRNAs. (a-c) Assessment of co-treatment effect by melatonin and PA. (g-h) Selection of *Pex19*-targeted siRNAs through embryonic development and (i) verification of *Pex19* knockdown by real-time PCR. (j-l) Assessment of melatonin/PA treatment and siRNA on porcine embryos through rates of cleavage, blastocyst formation, and total cell numbers of blastocysts. At least five biological replications were performed and more than 170 embryos from each experimental group were used. Data are shown as the means ± S.E.M. Groups marked with different alphabetical letters are significantly different ($P < 0.05$). Con, control; mel, melatonin; PA, phytanic acid; Cnd, candidate.

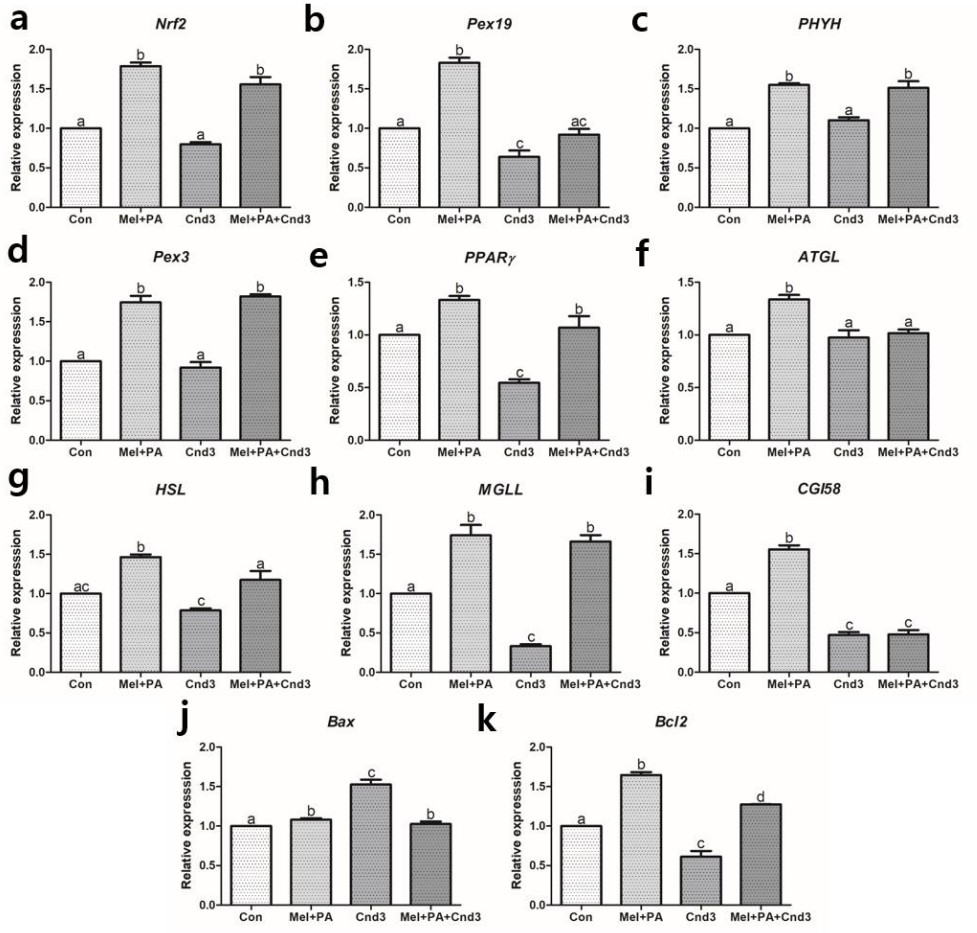
a
Nrf2
b
Pex19
c
PHYH
d
Pex3
e
PPARγ
f
ATGL
g
HSL
h
MGLL
i
CGI58
j
Bax
k
Bcl2
Relative expresssion
Con
Mel+PA
Cnd3
Mel+PA+Cnd3

Figure 26. Gene expression evaluations of melatonin/PA treatment and Cnd3-injection on porcine 2-cell embryos. The gene expressions of (a) Nrf2, the main factor in the Nrf2 signaling pathway, (b-e) factors that are related to peroxisomal activities, (f-i) lipid metabolism, and (j-k) apoptosis in the embryos were analyzed within the four groups. More than 200 embryos in each experimental group from six biological replications were used and real time PCR was performed three times technically. Within the same mRNA, bars with different alphabetical letters are significantly different among the groups ($P < 0.05$). Con, control; mel, melatonin, PA, phytanic acid; Cnd3, siRNA candidate 3.

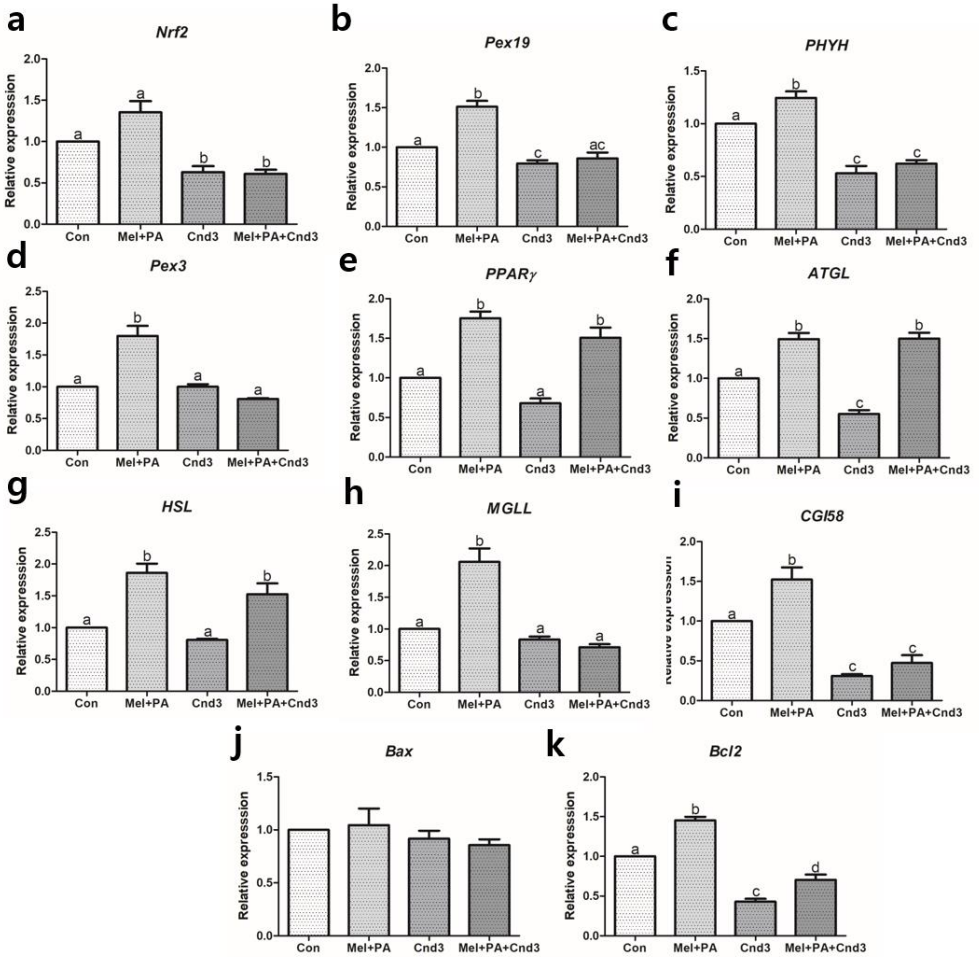
a
Nrf2
Relative expresssion
Con
Mel+PA
Cnd3
Mel+PA+Cnd3
b
Pex19
c
PHYH
d
Pex3
e
PPARγ
f
ATGL
g
HSL
h
MGLL
i
CGI58
j
Bax
k
Bcl2

Figure 27. Gene expression evaluations of melatonin/PA treatment and Cnd3-injection on porcine blastocysts. The gene expressions of (a) Nrf2, the main factor in the Nrf2 signaling pathway, (b-e) factors that are related to peroxisomal activities, (f-i) lipid metabolism, and (j-k) apoptosis in the embryos were analyzed within the four groups. More than 50 blastocysts in each experimental group from six biological replications were used and real time PCR was performed three times technically. Within the same mRNA, bars with different alphabetical letters are significantly different among the groups ($P < 0.05$). Con, control; mel, melatonin, PA, phytanic acid; Cnd3, siRNA candidate 3.

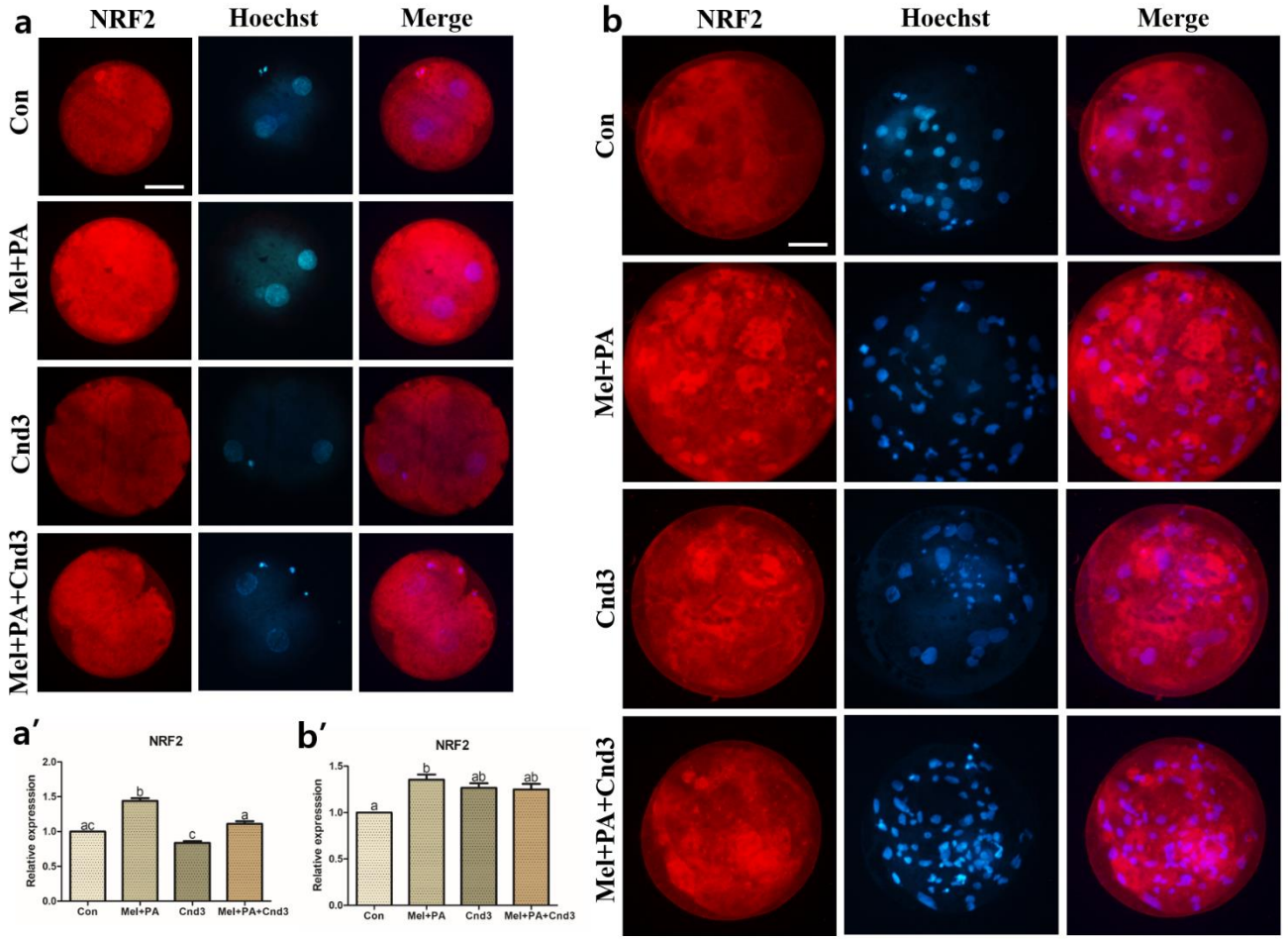
a
NRF2
Hoechst
Merge
Con
Mel+PA
Cnd3
Mel+PA+Cnd3
b
NRF2
Hoechst
Merge
Con
Mel+PA
Cnd3
Mel+PA+Cnd3
a′
NRF2
Relative expresssion
2.0
1.5
1.0
0.5
0.0
ac
b
c
a
Con
Mel+PA
Cnd3
Mel+PA+Cnd3
b′
NRF2
Relative expresssion
1.5
1.0
0.5
0.0
a
b
ab
ab
Con
Mel+PA
Cnd3
Mel+PA+Cnd3

Figure 28. Immunocytochemical analysis of NRF2 in porcine 2-cell embryos blastocysts. Fluorescence microscopy was applied to obtain images of embryos. (a and b) Representative 2-cell embryos in each group were stained with NRF2 rabbit-derived antibody and counterstained with Hoechst 33342. (a' and b') Analysis of intensities from NRF2-stained 2-cell embryos and blastocysts. At least 20 2-cell embryos and 15 blastocysts from five biological replications in each group were used for the staining and immunocytochemistry was performed three times technically. Data are shown as the means ± S.E.M. Bars with different alphabetical letters are significantly different ($P < 0.05$). Con, control; mel, melatonin, PTA, phytanic acid; Cnd3, siRNA candidate 3. White bars in the images indicate 50 μm; 400× magnification.

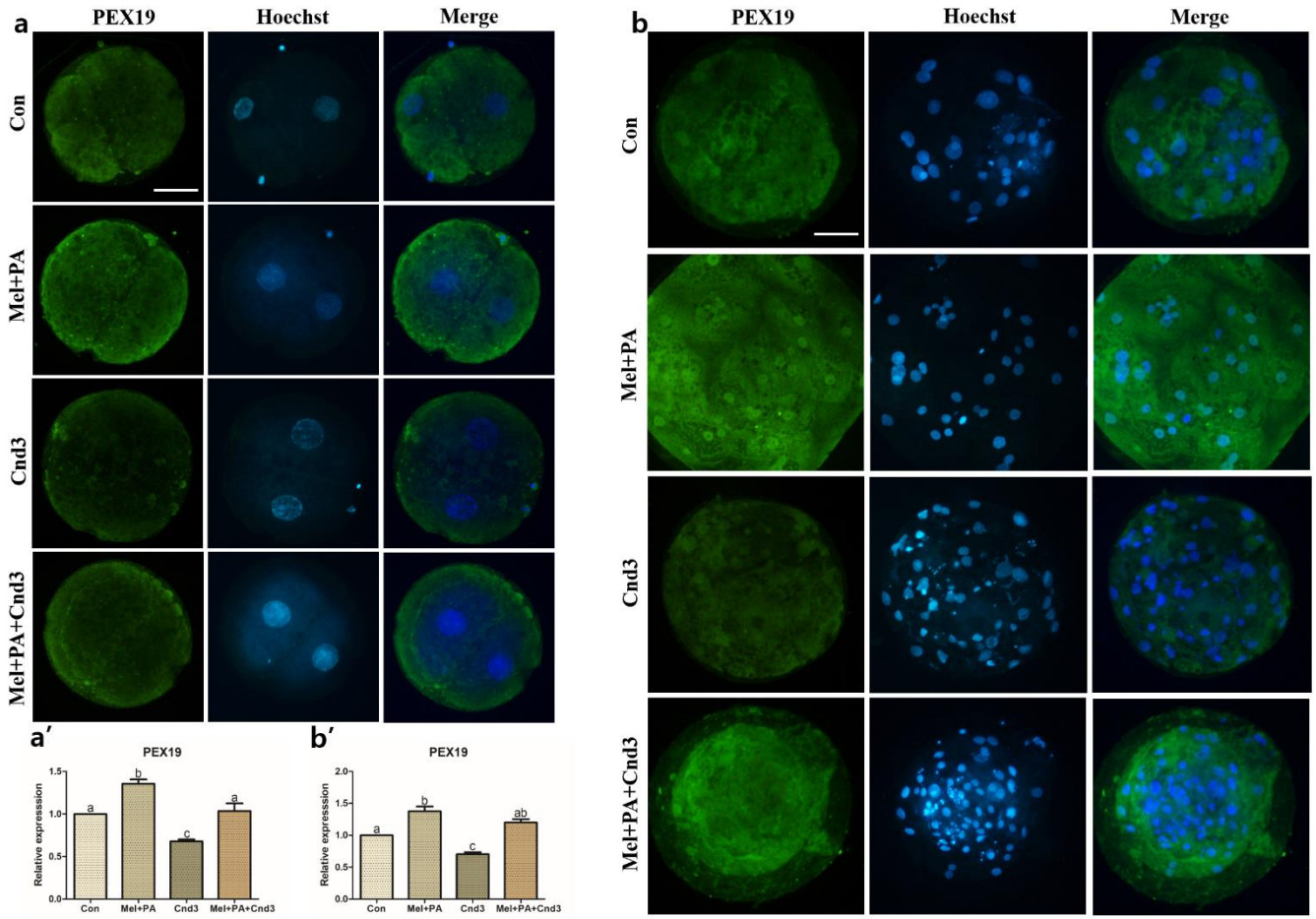
a
PEX19
Hoechst
Merge
Con
Mel+PA
Cnd3
Mel+PA+Cnd3
a'
PEX19
Relative expresssion
1.5
1.0
0.5
0.0
a
b
c
a
Con
Mel+PA
Cnd3
Mel+PA+Cnd3
b'
PEX19
Relative expresssion
2.0
1.5
1.0
0.5
0.0
a
b
c
ab
Con
Mel+PA
Cnd3
Mel+PA+Cnd3
b
PEX19
Hoechst
Merge
Con
Mel+PA
Cnd3
Mel+PA+Cnd3

Figure 29. Immunocytochemical analysis of PEX19 in porcine 2-cell embryos blastocysts. Fluorescence microscopy was applied to obtain images of embryos. (a and b) Representative 2-cell embryos in each group were stained with PEX19 rabbit-derived antibody and counterstained with Hoechst 33342. (a' and b') Analysis of intensities from PEX19-stained 2-cell embryos and blastocysts. At least 20 2-cell embryos and 15 blastocysts from five biological replications in each group were used for the staining and immunocytochemistry was performed three times technically. Data are shown as the means ± S.E.M. Bars with different alphabetical letters are significantly different ($P < 0.05$). Con, control; mel, melatonin, PTA, phytanic acid; Cnd3, siRNA candidate 3. White bars in the images indicate 50 μm; 400× magnification.

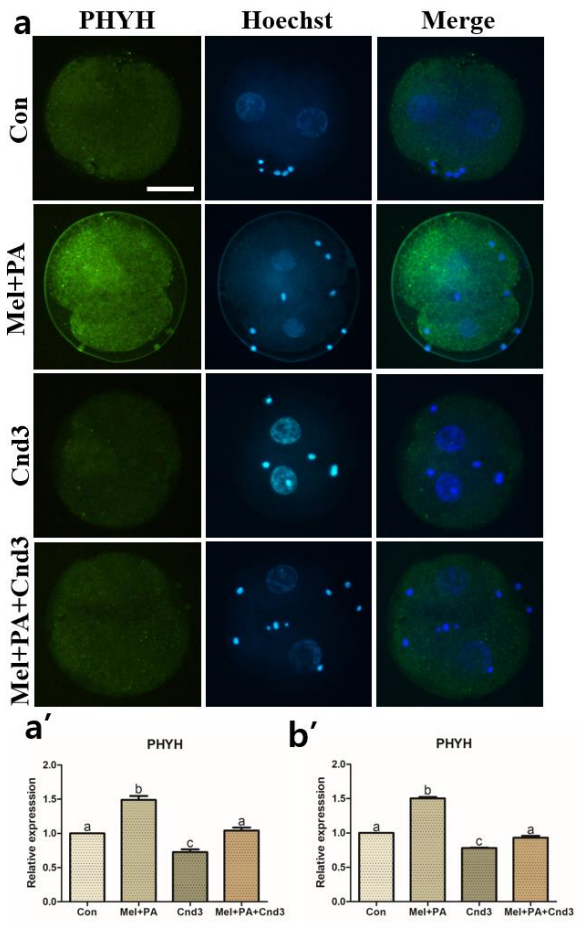
a
PHYH
Hoechst
Merge
Con
Mel+PA
Cnd3
Mel+PA+Cnd3
a′
PHYH
Relative expression
2.0
1.5
1.0
0.5
0.0
a
b
c
a
Con
Mel+PA
Cnd3
Mel+PA+Cnd3
b′
PHYH
Relative expression
2.0
1.5
1.0
0.5
0.0
a
b
c
a
Con
Mel+PA
Cnd3
Mel+PA+Cnd3

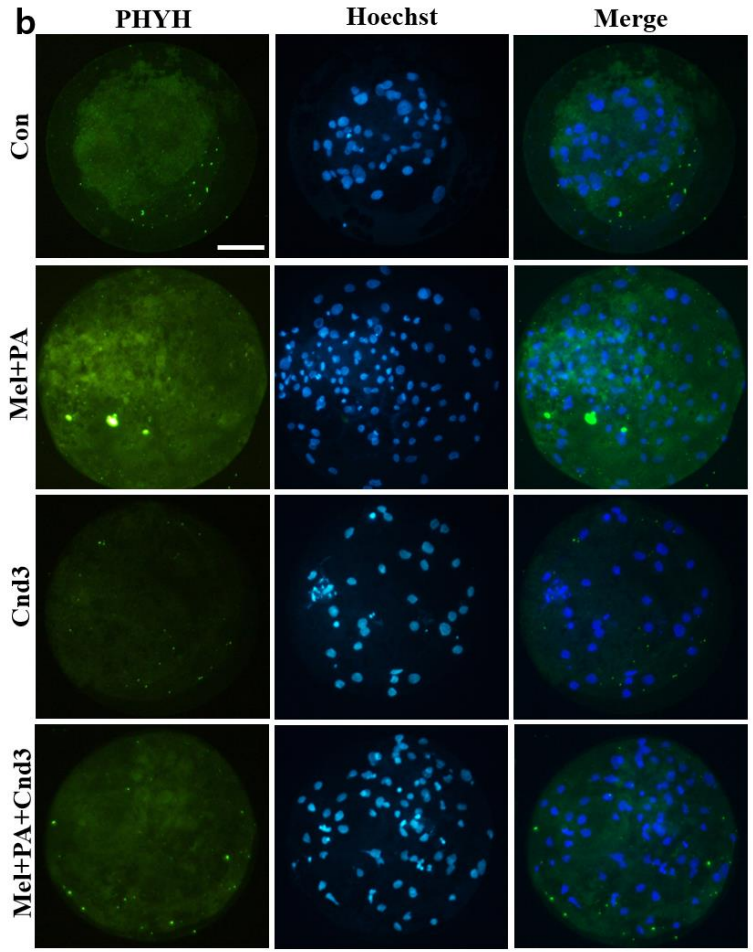
b
PHYH
Hoechst
Merge
Con
Mel+PA
Cnd3
Mel+PA+Cnd3

Figure 30. Immunocytochemical analysis of PHYH in porcine 2-cell embryos blastocysts. Fluorescence microscopy was applied to obtain images of embryos. (a and b) Representative 2-cell embryos in each group were stained with PHYH rabbit-derived antibody and counterstained with Hoechst 33342. (a' and b') Analysis of intensities from PHYH-stained 2-cell embryos and blastocysts. At least 20 2-cell embryos and 15 blastocysts from five biological replications in each group were used for the staining and immunocytochemistry was performed three times technically. Data are shown as the means ± S.E.M. Bars with different alphabetical letters are significantly different ($P < 0.05$). Con, control; mel, melatonin, PTA, phytanic acid; Cnd3, siRNA candidate 3. White bars in the images indicate 50 μm; 400× magnification.

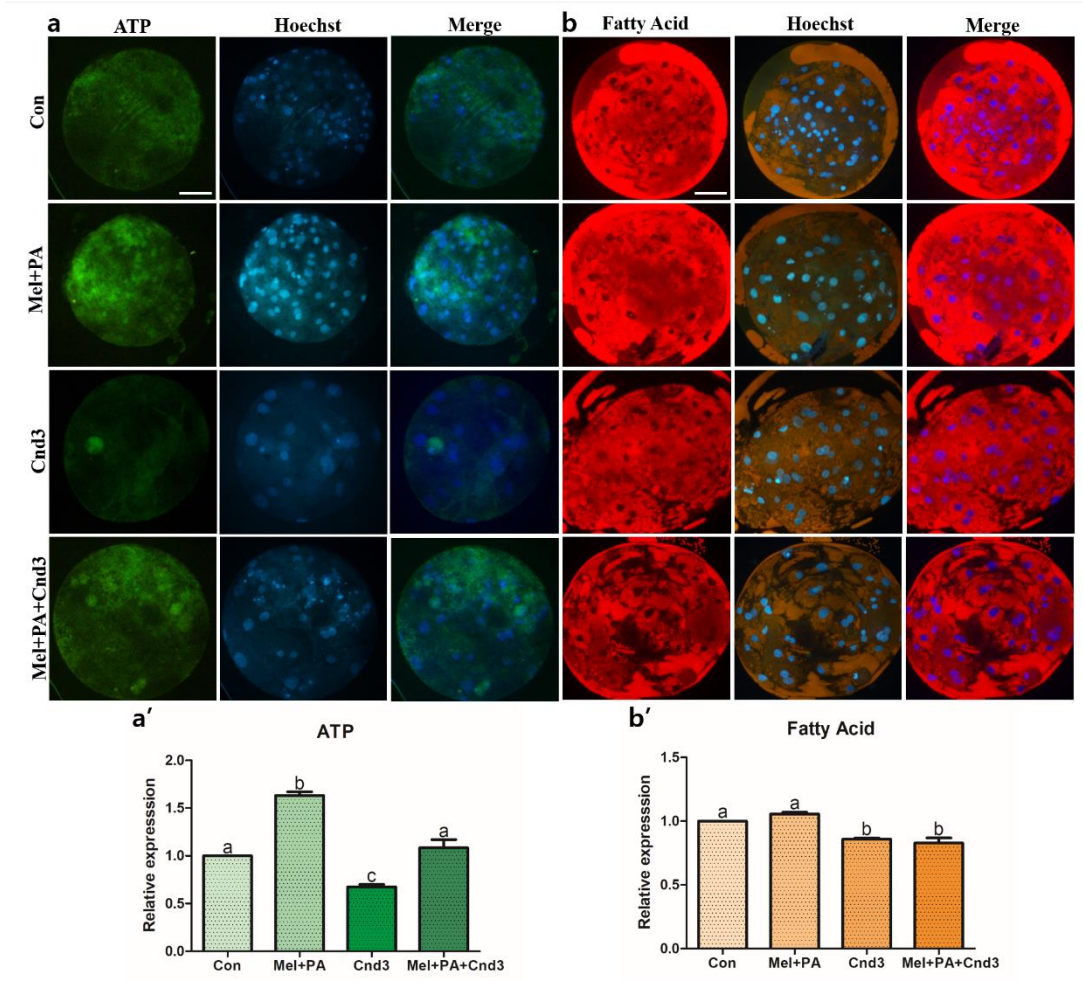
a
ATP
Hoechst
Merge
b
Fatty Acid
Hoechst
Merge
Con
Mel+PA
Cnd3
Mel+PA+Cnd3
a′
ATP
Relative expresssion
2.0
1.5
1.0
0.5
0.0
a
b
c
a
Con
Mel+PA
Cnd3
Mel+PA+Cnd3
b′
Fatty Acid
Relative expresssion
1.5
1.0
0.5
0.0
a
a
b
b
Con
Mel+PA
Cnd3
Mel+PA+Cnd3

Figure 31. BODIPY staining analysis of ATP contents and fatty acids in blastocysts. Fluorescence microscopy was applied to obtain images of the blastocysts. (a and b) Representative blastocysts in each group were stained BODIPY FL ATP and BODIPY 558/568 C^{12}, respectively, then counter stained with Hoechst 33342 (a' and b') Analysis of intensities from BODIPY FL ATP- and BODIPY 558/568 C^{12}-stained blastocysts. At least 15 blastocysts from four biological replications in each group were used for the staining and it was performed three times technically. Data are shown as the means ± S.E.M. Bars with different alphabetical letters are significantly different ($P < 0.05$). Con, control; mel, melatonin, PTA, phytanic acid; Cnd3, siRNA candidate 3. White bars in the images indicate 50 μm; 400× magnification.

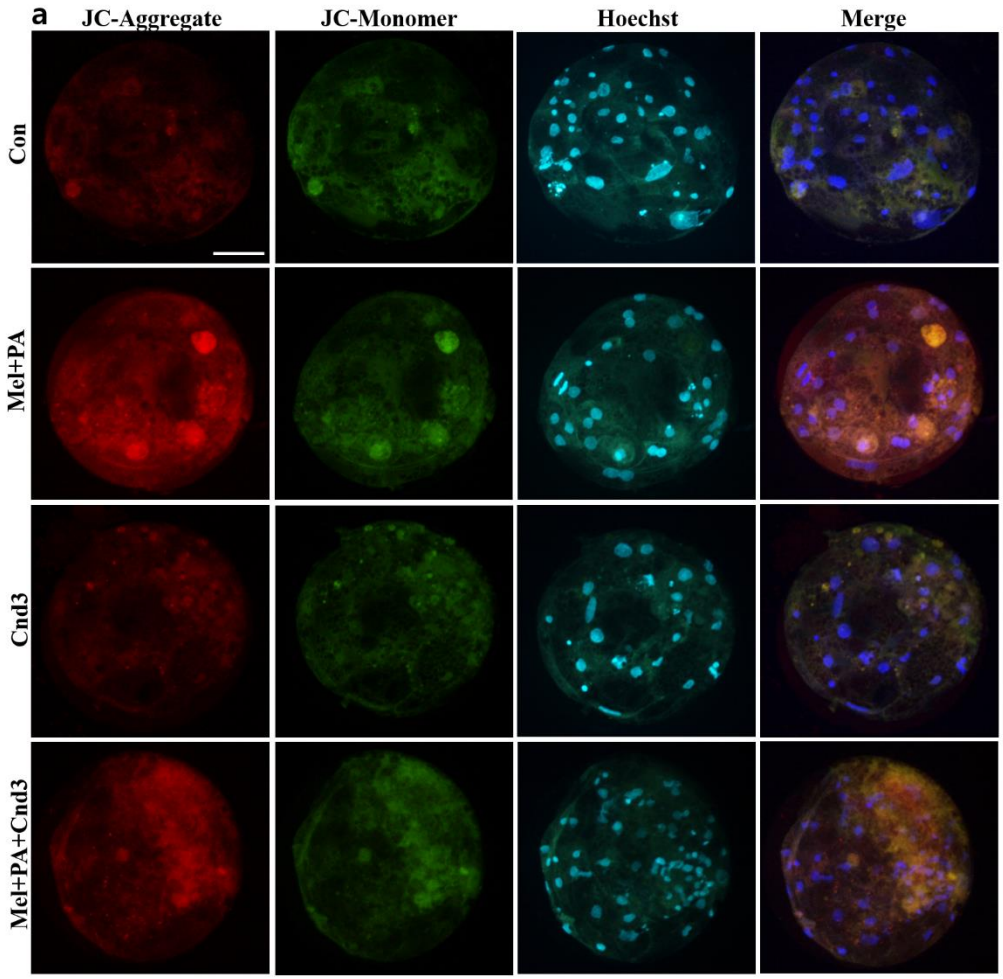
a
JC-Aggregate
JC-Monomer
Hoechst
Merge
Con
Mel+PA
Cnd3
Mel+PA+Cnd3

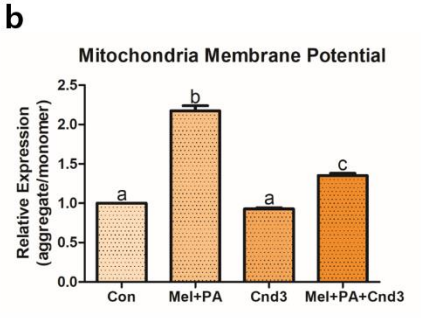
b
Mitochondria Membrane Potential
Relative Expression (aggregate/monomer)
2.5
2.0
1.5
1.0
0.5
0.0
a
b
a
c
Con
Mel+PA
Cnd3
Mel+PA+Cnd3

Figure 32. JC-1 mitochondrial membrane potential (MMP) staining in blastocysts. Fluorescence microscopy was applied to obtain images of the blastocysts. (a) Representative blastocysts in each group were stained JC-1 aggregate and JC-1 monomer, then counter stained with Hoechst 33342. (a' and b') Analysis of intensities from JC-1 MMP-stained blastocysts. At least 15 blastocysts from four biological replications in each group were used for the staining and it was performed three times technically. Data are shown as the means ± S.E.M. Bars with different alphabetical letters are significantly different ($P < 0.05$). Con, control; mel, melatonin, PTA, phytanic acid; Cnd3, siRNA candidate 3. White bars in the images indicate 50 μm; 400× magnification.

4. Discussion

Many studies have shown the significance of different signaling pathways in mammalian embryonic development. It is generally accepted that the culture conditions and environmental factors must be well-controlled when culturing *in vitro* embryos (Hamdoun & Epel 2007), however, the signaling pathways involved significantly in the embryonic development cannot be negligible. It is presumed that this is the first study to investigate a possible cross-talk between the Nrf2 signaling pathway and peroxisomal activities in porcine embryos which artificially regulated by co-treatment with melatonin and PA and *Pex19*-targeted siRNAs. The results suggest that the regulation of peroxisomal activities with melatonin, PA, and the Cnd3 influenced porcine embryonic development possibly via the Nrf2 signaling pathway. Moreover, the treatments and siRNA injections also regulated the Nrf2 signaling pathway, peroxisomal activities, lipid metabolism, and ATP production. Thus, these results suggest that the communication between the Nrf2 signaling pathway and peroxisomal activities might be significant to porcine embryo development and subsequent metabolisms.

Melatonin is frequently suggested to play a fundamental role in enhancing mammalian oocyte maturation, embryo development, and antioxidant mechanisms, including lipid metabolism and the Nrf2 signaling pathway (Amin, Gad et al. 2014; Jin, Lee et al. 2017; Lee, Jin et al. 2017; Kim, Kim et al. 2019), while PA has been suggested to influence β-oxidation in peroxisomes, lipid metabolism, and ATP production (Wanders, Jansen et al. 2001; van den Brink & Wanders 2006).

Additionally, the effect of PA on β-oxidation in mammalian gametes and embryos has also been reported (Figueroa, Kawada et al. 2000; Brauns, Heine et al. 2019; Kim, Kim et al. 2020). Therefore, porcine embryos were co-treated with melatonin and PA during IVC. We found that co-treatment with melatonin and PA resulted in a higher blastocyst formation rate compared to individual treatment and that there was significant upregulation in expression of genes related to lipid metabolism, including MMP, FA, and ATP content. This result may be supported by the study of Dunning et al., which found that shortened FAs derived from long or branched FAs such as PA initiate lipid metabolism and cause energy metabolism (Dunning, Cashman et al. 2010). Moreover, the results may also be supported by some studies demonstrating that lipid-derived ATP synthesis from the mitochondria promotes porcine embryonic development (Sturmey & Leese 2003; Prates, Nunes et al. 2014). Therefore, it might be speculated that melatonin and PA exert a synergistic effect during embryonic development, potentiating the embryos to more lipid metabolism-derived energy production.

It is found that melatonin/PA treatment improved embryonic development and increased expression of several genes related to the Nrf2 signaling pathway, peroxisome activities, lipid metabolism, and apoptosis. As is widely known, the Nrf2 signaling pathway is involved in the defense mechanism against oxidative stress; however, some studies suggest additional roles of the pathway, such as embryonic cell cycle progression (Lin, Sui et al. 2018), anti-aging in embryos (Ma, Liang et al. 2018). Lastly, Amin et al. suggested the possibility of an involvement in lipid metabolism in embryos (Amin, Gad et al. 2014). Gene expression of Nrf2 and lipid

metabolism were found to be upregulated in 2-cell embryos and blastocysts; this is supported by the claims from Ludtmann et al. that Nrf2 has a relationship with the β-oxidation of FAs (Ludtmann, Angelova et al. 2014), and it has been demonstrated that ATP production correlates with FA oxidation (Schafer, Grassian et al. 2009), which may possibly be connected with the actions of Nrf2. The results have proven that the Nrf2 signaling pathway and lipid metabolism are interconnected in porcine embryos.

In the current study, the peroxisome activities and the Nrf2 signaling pathway were upregulated by the combination treatment of melatonin and PA. In order to prove that the combination group affected the activities of Nrf2 and the peroxisome, *Pex19*-targeted siRNA microinjection was applied in this study. Pex19 and Pex3 function in tandem to modulate peroxisome membrane biogenesis, lipid droplet transportation (Schrul & Kopito 2016), and the functioning of matured peroxisomes (Dimitrov, Lam et al. 2013; Hua & Kim 2016; Mayerhofer 2016). In addition, PPARs are involved in lipid detection, peroxisomal gene activators (Dubois, Eeckhoute et al. 2017) and β-oxidation (Pawlak, Lefebvre et al. 2015). PPARγ is also involved in peroxisomal biogenesis (Lodhi & Semenkovich 2014) and mediates embryo implantation and survival (Lord, Murphy et al. 2006). Sunyer-Figueres et al. stated that *Pex19* is regulated by melatonin, implying that melatonin can mediate FA β-oxidation in peroxisomes by *Pex19* regulation (Sunyer-Figueres, Vazquez et al. 2020). This was corroborated by the result that the content of FAs in the Cnd3-injected group was significantly lower than that in the control and melatonin/PA-

treated groups (Fig. 31b'). Moreover, *Pex19* and *PPARγ* are strongly suggested to have a close relationship with Nrf2 signaling (Ishii, Itoh et al. 2004; Ganguli, Pattanaik et al. 2020). Similar gene and protein expression patterns were primarily observed in peroxisomal activities and lipid metabolism in 2-cell embryos and blastocysts. This result is corroborated by my hypothesis that *Pex19*-targeted siRNA would decrease such actions and metabolism. Interestingly, the levles of ATP and Nrf2 gene and protein expression were also partially decreased, which may also be supported by previous reports.

According to some of the results, expression of some genes in the Cnd3-injected group were increased or recovered in the blastocyst stage compared to the 2-cell embryo stage. I surmised that these results could be due to several reasons; firstly, several studies have shown siRNAs to have a maximum effect duration of seven days (Dorsett & Tuschl 2004; Bartlett & Davis 2006; Zeng, Apte et al. 2007); however, duration may differ depending on the cell type. Moreover, it has been reported that 24-96 h is the ideal period to evaluate the effects of knockdown and functioning of siRNAs in general (Han 2018). For example, Dadi et al. observed that the knockdown effects of growth factor-related siRNAs were significant in early stage mouse embryos, and that these effects were reduced during the late blastocyst stage (Dadi, Li et al. 2009), which is corroborated by some of the results in this study. It would be affordable if the *Pex19*-targeted siRNA could last seven days without diminishing its effects, and the study partially demonstrates the influence of peroxisomal activity knock down ability. However, it is suggested that permanent

knockdown techniques, such as the use of shRNAs should also be applied for further studies.

In this study, I hypothesized that co-treatment with melatonin and PA not only would upregulate the developmental potentials of porcine embryos but also increase the activities of the Nrf2 signaling pathway and peroxisomes. In addition, combination treatment upregulated lipid metabolism, ATP production, and MMP. In order to verify these connections, I applied Pex19-targeted siRNA injection into porcine embryos to determine whether downregulation of Pex19 affects the Nrf2 signaling pathway and subsequent lipid metabolism and ATP production, and found drastic changes in these pathways. Altogether, I suggest a plausible crosstalk between the activities of the Nrf2 signaling pathway and peroxisome in the process of lipid metabolism and ATP production during the development of porcine embryos. To my knowledge, this is the first report on this crosstalk in porcine embryos. Further investigations and assessments should be conducted in other species and cell types in order to elucidate the intricacies of peroxisomal activity and its influence on Nrf2 signaling and lipid metabolism.

General conclusion

In order to generate transgenic pig models for biomedical research purposes, embryo transfer to surrogates and appropriate control of gestation are pivotal to the successful delivery. However, ahead of this, providing favorable *in vitro* conditions for embryonic development and oocyte maturation would be the first priority. Therefore, a number of researchers in this field have gone through numerous tests and analyses to improve IVM and IVC systems, because major problems such as oxidative or heat stress, gauche skills of researchers, compositions of culture media, and gas compositions in the incubator are still impairing oocytes and embryos. On the other hand, there are also many reports on making breakthroughs of the mentioned problems occurring in *in vitro* experiments. Some of the representative solutions were to reduce ROS levels, prevent any stresses from culture environments, and potentiate the oocytes or embryos for better survival. Nonetheless, there still are a few reports or suggestions on how exactly the improvement or success of their survival was processed. Therefore, it is now necessary to investigate detailed mechanisms that intervene the improvement of IVM and IVC systems.

According to studies, signaling pathways and intracellular energizing mechanisms in mammalian oocytes and embryos were reported and among them, the Nrf2 signaling pathway and peroxisomal activity-derived lipid metabolism were suggested to have potential roles in the survival of oocytes and embryos. Thus, this thesis was designed and aimed to find the exact roles of the Nrf2 signaling pathway

and the peroxisomal activity in oocytes and embryos respectively, then the cross talk, or interactions, of the two mechanisms were validated during porcine oocyte maturation, embryonic development, and subsequent lipid metabolism and antioxidant mechanism. For proper investigation, gene and protein level analysis such as real-time PCR, RNA sequencing, western blot, and immunocytochemistry including strict evaluations of maturation of porcine oocytes and subsequent development of porcine embryos were employed in every chapter. In addition, staining for ROS, glutathione (GSH), BODIPY, and mitochondrial membrane potential (MMP) were also employed in order to investigate and evaluate subsequent antioxidant mechanisms and lipid metabolisms in the oocytes and embryos.

Therefore, in Part III, the involvement of the Nrf2 signaling pathway via the treatment of melatonin in porcine embryos was investigated. With evaluations of embryonic development, real-time PCR and immunocytochemistry, gene and protein expressions in porcine embryos were analyzed. As a result, melatonin induced upregulation of Nrf2 signaling and antioxidant-related gene and protein expression, along with the regulation of embryonic development. In summary, it was found that Nrf2 signaling does work significantly in porcine embryonic development. Next, supplementation of phytanic acid (PA) during IVM of porcine oocytes showed significant regulations in peroxisomal activities and subsequent lipid metabolism, which was verified through gene, protein, and lipid metabolism-related expressions employing real-time PCR, immunocytochemistry, as well as ATP, FA, MMP, and BODIPY staining. Moreover, the PA treatment during IVC was also effective on embryonic development and protein expression of PEX19 and PHYH in porcine

blastocysts. Therefore, these results demonstrate that PA can support the peroxisomal activities and subsequent lipid metabolism in porcine oocytes and embryos. In Part III, it was verified that both the Nrf2 signaling and the peroxisomal activities respectively have conspicuous roles in porcine oocyte maturation and embryonic development. Through these findings, the aim of the research was narrowed to an idea that these two mechanisms may have connections to each other and give mutual or synergistic effects on the oocytes and embryos, in addition to the antioxidant mechanism and the metabolism of lipids.

Thus, Part IV, the first aim was to find the connection between the Nrf2 signaling pathway and the peroxisomal activities in porcine oocytes. It was hypothesized that the Nrf2 signaling would affect activities of peroxisomes depending on chemical treatments. Melatonin was used to induce the Nrf2 signaling and in the oocytes and brusatol, the *Nrf2*-specific inhibitor, was used to verify the pathway. As significant results were observed by analyses from real-time PCR, immunocytochemistry, western blot, BODIPY staining, and oocyte maturation, it was verified that the peroxisomal activities were regulated by the activation and inhibition of Nrf2 signaling, which suggest a possible mutual communication between them in porcine oocytes. In addition, the connection was re-confirmed by RNA sequencing which showed a similar tendency with the demonstrated results. Lastly, their cross talk was also investigated during porcine embryonic development. According to significant results from *PEX19* knockdown, real-time PCR, immunocytochemistry, and BODIPY staining, it was proven that the cross talk was strongly regulated by the co-treatment of melatonin and PA and *Pex19*-targeted

siRNA injection. Significant changes were observed in lipid metabolism, ATP, FA, and MMP. In brief, the connection, or the cross talk between the Nrf2 signaling pathway and the peroxisomal activities were mutually and synergistically regulated by the treatment of melatonin and PA in porcine oocytes and embryos.

In conclusion, regarding the fact that the improvements of IVM and IVC systems is pivotal for biomedical research, this thesis was designed to identify specific roles of the Nrf2 signaling and the peroxisomal activities respectively in oocytes and embryos and subsequently, the connection of the two mechanisms were investigated within the oocytes and embryos. Therefore, it was found that the respective involvements of the Nrf2 signaling pathway and peroxisomal activities in porcine embryos and oocytes were distinctively fundamental in oocyte maturation, embryonic development, antioxidant mechanisms, and lipid metabolisms. Subsequently, the cross talk between the two mechanisms in oocytes and embryos was discovered by synergistic collaborations of regulations in lipid metabolism and antioxidant mechanisms, and then re-confirmed by RNA sequencing. Based on the results of the present study, thorough research on intracellular signaling and mechanisms in mammalian oocytes and embryos may be conducted. Especially with focus on the Nrf2 signaling and melatonin, as they are widely acknowledged to be involved in mammalian reproduction, with their roles possibly achieving delivery of transgenic litters. Finally, the cross talk between the Nrf2 signaling pathway and the peroxisomal activities may start shedding light on intracellular signaling of mammalian gametes and embryos, including those that occur during mammalian reproduction.

REFERENCES

Agrawal G., Shang H.H., Xia Z.J. & Subramani S. (2017) Functional regions of the peroxin Pex19 necessary for peroxisome biogenesis. J Biol Chem 292, 11547-60.

Aigner B., Renner S., Kessler B., Klymiuk N., Kurome M., Wunsch A. & Wolf E. (2010) Transgenic pigs as models for translational biomedical research. J Mol Med (Berl) 88, 653-64.

Akino N., Wada-Hiraike O., Terao H., Honjoh H., Isono W., Fu H., Hirano M., Miyamoto Y., Tanikawa M., Harada M., Hirata T., Hirota Y., Koga K., Oda K., Kawana K., Fujii T. & Osuga Y. (2018) Activation of Nrf2 might reduce oxidative stress in human granulosa cells. Mol Cell Endocrinol 470, 96-104.

Alminana C., Gil M.A., Cuello C., Caballero I., Roca J., Vazquez J.M., Gomez E. & Martinez E.A. (2008) In vitro maturation of porcine oocytes with retinoids improves embryonic development. Reprod Fertil Dev 20, 483-9.

Alvarez G.M., Ferretti E.L., Gutnisky C., Dalvit G.C. & Cetica P.D. (2013) Modulation of glycolysis and the pentose phosphate pathway influences porcine oocyte in vitro maturation. Reprod Domest Anim 48, 545-53.

Amin A., Gad A., Salilew-Wondim D., Prastowo S., Held E., Hoelker M., Rings F., Tholen E., Neuhoff C., Looft C., Schellander K. & Tesfaye D. (2014) Bovine embryo survival under oxidative-stress conditions is associated with activity of the NRF2-mediated oxidative-stress-response pathway. Mol Reprod Dev 81, 497-513.

Andrade G.M., da Silveira J.C., Perrini C., Del Collado M., Gebremedhn S., Tesfaye D., Meirelles F.V. & Perecin F. (2017) The role of the PI3K-Akt signaling pathway in the developmental competence of bovine oocytes. PLoS One 12, e0185045.

Antonenkov V.D., Grunau S., Ohlmeier S. & Hiltunen J.K. (2010) Peroxisomes are oxidative organelles. Antioxid Redox Signal 13, 525-37.

Appeltant R., Somfai T., Maes D., A V.A.N.S. & Kikuchi K. (2016) Porcine oocyte maturation in vitro: role of cAMP and oocyte-secreted factors - A practical approach. J Reprod Dev 62, 439-49.

Ashry M., Rajput S.K., Folger J.K., Knott J.G., Hemeida N.A., Kandil O.M., Ragab R.S. & Smith G.W. (2018) Functional role of AKT signaling in bovine early embryonic development: potential link to embryotrophic actions of follistatin. Reprod Biol Endocrinol 16, 1.

Atikuzzaman M., Koo O.J., Kang J.T., Kwon D.K., Park S.J., Kim S.J., Gomez M.N., Oh H.J., Hong S.G., Jang G. & Lee B.C. (2011) The 9-cis retinoic acid signaling pathway and its regulation of prostaglandin-endoperoxide synthase 2 during in vitro maturation of pig cumulus cell-oocyte complexes and effects on parthenogenetic embryo production. Biol Reprod 84, 1272-81.

Bartlett D.W. & Davis M.E. (2006) Insights into the kinetics of siRNA-mediated gene silencing from live-cell and live-animal bioluminescent imaging. Nucleic Acids Res 34, 322-33.

Batista M.R., Diniz P., Torres A., Murta D., Lopes-da-Costa L. & Silva E. (2020) Notch signaling in mouse blastocyst development and hatching. BMC Dev Biol 20, 9.

Beall S., Brenner C. & Segars J. (2010) Oocyte maturation failure: a syndrome of bad eggs. Fertil Steril 94, 2507-13.

Belli M. & Shimasaki S. (2018) Molecular Aspects and Clinical Relevance of GDF9 and BMP15 in Ovarian Function. Vitam Horm 107, 317-48.

Bou G., Liu S., Sun M., Zhu J., Xue B., Guo J., Zhao Y., Qu B., Weng X., Wei Y., Lei L. & Liu Z. (2017) CDX2 is essential for cell proliferation and polarity in porcine blastocysts. Development 144, 1296-306.

Brauns A.K., Heine M., Todter K., Baumgart-Vogt E., Luers G.H. & Schumacher U. (2019) A defect in the peroxisomal biogenesis in germ cells induces a spermatogenic arrest at the round spermatid stage in mice. Sci Rep 9, 9553.

Brussow K.P., Torner H., Kanitz W. & Ratky J. (2000) In vitro technologies related to pig embryo transfer. Reprod Nutr Dev 40, 469-80.

Bush E.L., Barbas A.S., Holzknecht Z.E., Byrne G.W., McGregor C.G., Parker W., Davis R.D. & Lin S.S. (2011) Coagulopathy in alpha-galactosyl transferase knockout pulmonary xenotransplants. Xenotransplantation 18, 6-13.

Cetica P., Pintos L., Dalvit G. & Beconi M. (2002) Activity of key enzymes involved in glucose and triglyceride catabolism during bovine oocyte maturation in vitro. Reproduction 124, 675-81.

Chang C.C., Warren D.S., Sacksteder K.A. & Gould S.J. (1999) PEX12 interacts with PEX5 and PEX10 and acts downstream of receptor docking in peroxisomal matrix protein import. J Cell Biol 147, 761-74.

Chaudhary S. & Parvez S. (2017) Phytanic acid induced neurological alterations in rat brain synaptosomes and its attenuation by melatonin. Biomed Pharmacother 95, 37-46.

Che B.N., Oksbjerg N., Hellgren L.I., Nielsen J.H. & Young J.F. (2013) Phytanic acid stimulates glucose uptake in a model of skeletal muscles, the primary porcine myotubes. Lipids Health Dis 12, 14.

Chen L.Y., Renn T.Y., Liao W.C., Mai F.D., Ho Y.J., Hsiao G., Lee A.W. & Chang H.M. (2017) Melatonin successfully rescues hippocampal bioenergetics and

improves cognitive function following drug intoxication by promoting Nrf2-ARE signaling activity. J Pineal Res 63.

Cho B., Kim S.J., Lee E.J., Ahn S.M., Lee J.S., Ji D.Y., Lee K. & Kang J.T. (2018) Generation of insulin-deficient piglets by disrupting INS gene using CRISPR/Cas9 system. Transgenic Res 27, 289-300.

Cho H.Y., Gladwell W., Wang X., Chorley B., Bell D., Reddy S.P. & Kleeberger S.R. (2010) Nrf2-regulated PPAR{gamma} expression is critical to protection against acute lung injury in mice. Am J Respir Crit Care Med 182, 170-82.

Cho M.K., Kim W.D., Ki S.H., Hwang J.I., Choi S., Lee C.H. & Kim S.G. (2007) Role of Galpha12 and Galpha13 as novel switches for the activity of Nrf2, a key antioxidative transcription factor. Mol Cell Biol 27, 6195-208.

Choi J., Park S.M., Lee E., Kim J.H., Jeong Y.I., Lee J.Y., Park S.W., Kim H.S., Hossein M.S., Jeong Y.W., Kim S., Hyun S.H. & Hwang W.S. (2008) Anti-apoptotic effect of melatonin on preimplantation development of porcine parthenogenetic embryos. Mol Reprod Dev 75, 1127-35.

Chuang C.K., Chen C.H., Huang C.L., Su Y.H., Peng S.H., Lin T.Y., Tai H.C., Yang T.S. & Tu C.F. (2017) Generation of GGTA1 Mutant Pigs by Direct Pronuclear Microinjection of CRISPR/Cas9 Plasmid Vectors. Anim Biotechnol 28, 174-81.

Cibelli J., Emborg M.E., Prockop D.J., Roberts M., Schatten G., Rao M., Harding J. & Mirochnitchenko O. (2013) Strategies for improving animal models for regenerative medicine. Cell Stem Cell 12, 271-4.

Conti M. & Franciosi F. (2018) Acquisition of oocyte competence to develop as an embryo: integrated nuclear and cytoplasmic events. Hum Reprod Update 24, 245-66.

Cooper D.K.C. Ye Y., Rolf L.L., Zuhdi N. (1991) The Pig as Potential Organ Donor for Man. Xenotransplantation, Springer. Chapter 30.

Costa R., Peruzzo R., Bachmann M., Monta G.D., Vicario M., Santinon G., Mattarei A., Moro E., Quintana-Cabrera R., Scorrano L., Zeviani M., Vallese F., Zoratti M., Paradisi C., Argenton F., Brini M., Cali T., Dupont S., Szabo I. & Leanza L. (2019) Impaired Mitochondrial ATP Production Downregulates Wnt Signaling via ER Stress Induction. Cell Rep 28, 1949-60 e6.

Crespo F.L. & Moeller S.J. (2009) Overview of world swine and pork production. Encyclopedia of Life Systems, Agricultural Sci, Vol 1

Cullinan S.B., Gordan J.D., Jin J., Harper J.W. & Diehl J.A. (2004) The Keap1-BTB protein is an adaptor that bridges Nrf2 to a Cul3-based E3 ligase: oxidative stress sensing by a Cul3-Keap1 ligase. Mol Cell Biol 24, 8477-86.

Dadi T.D., Li M.W. & Lloyd K.C. (2009) Decreased growth factor expression through RNA interference inhibits development of mouse preimplantation embryos. Comp Med 59, 331-8.

Dang-Nguyen T.Q., Wells D., Haraguchi S., Men N.T., Nguyen H.T., Noguchi J., Kaneko H. & Kikuchi K. (2020) Combined refinements to somatic cell nuclear transfer methods improve porcine embryo development. J Reprod Dev 66, 281-6.

Danilova N., Krupnik V.E., Sugden D. & Zhdanova I.V. (2004) Melatonin stimulates cell proliferation in zebrafish embryo and accelerates its development. FASEB J 18, 751-3.

Del Rio L.A. & Lopez-Huertas E. (2016) ROS Generation in Peroxisomes and its Role in Cell Signaling. Plant Cell Physiol 57, 1364-76.

Denicol A.C., Dobbs K.B., McLean K.M., Carambula S.F., Loureiro B. & Hansen P.J. (2013) Canonical WNT signaling regulates development of bovine embryos to the blastocyst stage. Sci Rep 3, 1266.

Dennery P.A. (2007) Effects of oxidative stress on embryonic development. Birth Defects Res C Embryo Today 81, 155-62.

Dhaunsi G.S., Alsaeid M. & Akhtar S. (2017) Phytanic acid attenuates insulin-like growth factor-1 activity via nitric oxide-mediated gamma-secretase activation in rat aortic smooth muscle cells: possible implications for pathogenesis of infantile Refsum disease. Pediatr Res 81, 531-6.

Dimitrov L., Lam S.K. & Schekman R. (2013) The role of the endoplasmic reticulum in peroxisome biogenesis. Cold Spring Harb Perspect Biol 5, a013243.

Dinkova-Kostova A.T. & Abramov A.Y. (2015) The emerging role of Nrf2 in mitochondrial function. Free Radic Biol Med 88, 179-88.

Do L.T., Shibata Y., Taniguchi M., Nii M., Nguyen T.V., Tanihara F., Takagi M. & Otoi T. (2015) Melatonin Supplementation During In Vitro Maturation and Development Supports the Development of Porcine Embryos. Reprod Domest Anim 50, 1054-8.

Dong J., Sulik K.K. & Chen S.Y. (2008) Nrf2-mediated transcriptional induction of antioxidant response in mouse embryos exposed to ethanol in vivo: implications for the prevention of fetal alcohol spectrum disorders. Antioxid Redox Signal 10, 2023-33.

Dorsett Y. & Tuschl T. (2004) siRNAs: applications in functional genomics and potential as therapeutics. Nat Rev Drug Discov 3, 318-29.

Du X., Pan Z., Li Q., Liu H. & Li Q. (2018) SMAD4 feedback regulates the canonical TGF-β signaling pathway to control granulosa cell apoptosis. Cell Death Dis 9, 151.

Dubois V., Eeckhoute J., Lefebvre P. & Staels B. (2017) Distinct but complementary contributions of PPAR isotypes to energy homeostasis. J Clin Invest 127, 1202-14.

Dunning K.R., Cashman K., Russell D.L., Thompson J.G., Norman R.J. & Robker R.L. (2010) Beta-oxidation is essential for mouse oocyte developmental competence and early embryo development. Biol Reprod 83, 909-18.

Dunning K.R., Russell D.L. & Robker R.L. (2014) Lipids and oocyte developmental competence: the role of fatty acids and beta-oxidation. Reproduction 148, R15-27.

Ekthuwapranee K., Sotthibundhu A., Tocharus C. & Govitrapong P. (2015) Melatonin ameliorates dexamethasone-induced inhibitory effects on the proliferation of cultured progenitor cells obtained from adult rat hippocampus. J Steroid Biochem Mol Biol 145, 38-48.

El Sheikh M., Mesalam A., Mesalam A.A., Idrees M., Lee K.L. & Kong I.K. (2019) Melatonin Abrogates the Anti-Developmental Effect of the AKT Inhibitor SH6 in Bovine Oocytes and Embryos. Int J Mol Sci 20, 2956.

Ellinghaus P., Wolfrum C., Assmann G., Spener F. & Seedorf U. (1999) Phytanic acid activates the peroxisome proliferator-activated receptor alpha (PPARalpha) in sterol carrier protein 2-/ sterol carrier protein x-deficient mice. J Biol Chem 274, 2766-72.

Ericsson A.C., Crim M.J. & Franklin C.L. (2013) A brief history of animal modeling. Mo Med 110, 201-5.

Farr R.L., Lismont C., Terlecky S.R. & Fransen M. (2016) Peroxisome biogenesis in mammalian cells: The impact of genes and environment. Biochim Biophys Acta 1863, 1049-60.

Fatehi A.N., Roelen B.A., Colenbrander B., Schoevers E.J., Gadella B.M., Beverst M.M. & van den Hurk R. (2005) Presence of cumulus cells during in vitro fertilization protects the bovine oocyte against oxidative stress and improves first cleavage but does not affect further development. Zygote 13, 177-85.

Ferguson E.M. & Leese H.J. (2006) A potential role for triglyceride as an energy source during bovine oocyte maturation and early embryo development. Mol Reprod Dev 73, 1195-201.

Ferreira D.W. & Allard P. (2015) Models of germ cell development and their application for toxicity studies. Environ Mol Mutagen 56, 637-49.

Figueroa C., Kawada M.E., Veliz L.P., Hidalgo U., Barros C., Gonzalez S. & Santos M.J. (2000) Peroxisomal proteins in rat gametes. Cell Biochem Biophys 32 Spring, 259-68.

Forman H.J., Zhang H. & Rinna A. (2009) Glutathione: overview of its protective roles, measurement, and biosynthesis. Mol Aspects Med 30, 1-12.

Fransen M., Lismont C. & Walton P. (2017) The Peroxisome-Mitochondria Connection: How and Why? Int J Mol Sci 18.

Fransen M., Nordgren M., Wang B. & Apanasets O. (2012) Role of peroxisomes in ROS/RNS-metabolism: implications for human disease. Biochim Biophys Acta 1822, 1363-73.

Gabaldon T. (2010) Peroxisome diversity and evolution. Philos Trans R Soc Lond B Biol Sci 365, 765-73.

Gad A., Abu Hamed S., Khalifa M., Amin A., El-Sayed A., Swiefy S.A. & El-Assal S. (2018) Retinoic acid improves maturation rate and upregulates the expression of antioxidant-related genes in in vitro matured buffalo (Bubalus bubalis) oocytes. Int J Vet Sci Med 6, 279-85.

Galsgaard K.D., Pedersen J., Knop F.K., Holst J.J. & Wewer Albrechtsen N.J. (2019) Glucagon Receptor Signaling and Lipid Metabolism. Front Physiol 10, 413.

Ganguli G., Pattanaik K.P., Jagadeb M. & Sonawane A. (2020) Mycobacterium tuberculosis Rv3034c regulates mTORC1 and PPAR-gamma dependant pexophagy mechanism to control redox levels in macrophages. Cell Microbiol 22, e13214.

Ge H., Tollner T.L., Hu Z., Dai M., Li X., Guan H., Shan D., Zhang X., Lv J., Huang C. & Dong Q. (2012) The importance of mitochondrial metabolic activity and mitochondrial DNA replication during oocyte maturation in vitro on oocyte quality and subsequent embryo developmental competence. Mol Reprod Dev 79, 392-401.

Ghimire S., Heindryckx B., Van der Jeught M., Neupane J., O'Leary T., Lierman S., De Vos W.H., Chuva de Sousa Lopes S., Deroo T. & De Sutter P. (2015) Inhibition of transforming growth factor β signaling promotes epiblast formation in mouse embryos. Stem Cells Dev 24, 497-506.

Gil M.A., Cuello C., Parrilla I., Vazquez J.M., Roca J. & Martinez E.A. (2010) Advances in swine in vitro embryo production technologies. Reprod Domest Anim 45 Suppl 2, 40-8.

Goldfischer S., Moore C.L., Johnson A.B., Spiro A.J., Valsamis M.P., Wisniewski H.K., Ritch R.H., Norton W.T., Rapin I. & Gartner L.M. (1973) Peroxisomal and mitochondrial defects in the cerebro-hepato-renal syndrome. Science 182, 62-4.

Guerin P., El Mouatassim S. & Menezo Y. (2001) Oxidative stress and protection against reactive oxygen species in the pre-implantation embryo and its surroundings. Hum Reprod Update 7, 175-89.

Guo J., Zhang T., Guo Y., Sun T., Li H., Zhang X., Yin H., Cao G., Yin Y., Wang H., Shi L., Guo X., Sha J., Eppig J.J. & Su Y.Q. (2018) Oocyte stage-specific effects of MTOR determine granulosa cell fate and oocyte quality in mice. Proc Natl Acad Sci U S A 115, E5326-e33.

Guo Q., Xuan M.F., Luo Z.B., Wang J.X., Jin S.S., Yin X.J. & Kang J.D. (2019) Baicalin improves IVM of pig oocytes and subsequent preimplantation embryo development by inhibiting apoptosis. Reprod Fertil Dev 31, 983-92.

Guo Y., Sun J., Li T., Zhang Q., Bu S., Wang Q. & Lai D. (2017) Melatonin ameliorates restraint stress-induced oxidative stress and apoptosis in testicular cells via NF-kappaB/iNOS and Nrf2/ HO-1 signaling pathway. Sci Rep 7, 9599.

Gupta S.K., Bansal P., Ganguly A., Bhandari B. & Chakrabarti K. (2009) Human zona pellucida glycoproteins: functional relevance during fertilization. J Reprod Immunol 83, 50-5.

Hamdoun A. & Epel D. (2007) Embryo stability and vulnerability in an always changing world. Proc Natl Acad Sci U S A 104, 1745-50.

Hammer R.E., Pursel V.G., Rexroad C.E., Jr., Wall R.J., Bolt D.J., Ebert K.M., Palmiter R.D. & Brinster R.L. (1985) Production of transgenic rabbits, sheep and pigs by microinjection. Nature 315, 680-3.

Han H. (2018) RNA Interference to Knock Down Gene Expression. Methods Mol Biol 1706, 293-302.

Han L., Wang H., Li L., Li X., Ge J., Reiter R.J. & Wang Q. (2017) Melatonin protects against maternal obesity-associated oxidative stress and meiotic defects in oocytes via the SIRT3-SOD2-dependent pathway. J Pineal Res 63.

Harris S.E., Adriaens I., Leese H.J., Gosden R.G. & Picton H.M. (2007) Carbohydrate metabolism by murine ovarian follicles and oocytes grown in vitro. Reproduction 134, 415-24.

Hassa H., Aydin Y. & Taplamacioglu F. (2014) The role of perivitelline space abnormalities of oocytes in the developmental potential of embryos. J Turk Ger Gynecol Assoc 15, 161-3.

Hauschild J., Petersen B., Santiago Y., Queisser A.L., Carnwath J.W., Lucas-Hahn A., Zhang L., Meng X., Gregory P.D., Schwinzer R., Cost G.J. & Niemann H. (2011) Efficient generation of a biallelic knockout in pigs using zinc-finger nucleases. Proc Natl Acad Sci U S A 108, 12013-7.

He J., Ye J., Li Q., Feng Y., Bai X., Chen X., Wu C., Yu Z., Zhao Y., Hu X. & Li N. (2013) Construction of a transgenic pig model overexpressing polycystic kidney disease 2 (PKD2) gene. Transgenic Res 22, 861-7.

Heinritz S.N., Mosenthin R. & Weiss E. (2013) Use of pigs as a potential model for research into dietary modulation of the human gut microbiota. Nutr Res Rev 26, 191-209.

Holmstrom K.M., Kostov R.V. & Dinkova-Kostova A.T. (2016) The multifaceted role of Nrf2 in mitochondrial function. Curr Opin Toxicol 1, 80-91.

Hryhorowicz M., Zeyland J., Slomski R. & Lipinski D. (2017) Genetically Modified Pigs as Organ Donors for Xenotransplantation. Mol Biotechnol 59, 435-44.

Hu X., Roberts J.R., Apopa P.L., Kan Y.W. & Ma Q. (2006) Accelerated ovarian failure induced by 4-vinyl cyclohexene diepoxide in Nrf2 null mice. Mol Cell Biol 26, 940-54.

Hua R. & Kim P.K. (2016) Multiple paths to peroxisomes: Mechanism of peroxisome maintenance in mammals. Biochim Biophys Acta 1863, 881-91.

Huang J.C. (2008) The role of peroxisome proliferator-activated receptors in the development and physiology of gametes and preimplantation embryos. PPAR Res 2008, 732303.

Huang Y., Ouyang H., Xie W., Chen X., Yao C., Han Y., Han X., Song Q., Pang D. & Tang X. (2013) Moderate expression of Wnt signaling genes is essential for porcine parthenogenetic embryo development. Cell Signal 25, 778-85.

Huang Y., Yuan L., Li T., Liu X., Yu Y., Ouyang H. & Wang B. (2017) IWP2 impairs the development of porcine somatic cell nuclear transfer embryos via Wnt signaling pathway inactivation. Biomed Rep 7, 36-40.

Hubbard N., Prasasya R.D. & Mayo K.E. (2019) Activation of Notch Signaling by Oocytes and Jag1 in Mouse Ovarian Granulosa Cells. Endocrinology 160, 2863-76.

Ishii T., Itoh K., Ruiz E., Leake D.S., Unoki H., Yamamoto M. & Mann G.E. (2004) Role of Nrf2 in the regulation of CD36 and stress protein expression in murine macrophages: activation by oxidatively modified LDL and 4-hydroxynonenal. Circ Res 94, 609-16.

Iwamoto M., Onishi A., Fuchimoto D., Somfai T., Takeda K., Tagami T., Hanada H., Noguchi J., Kaneko H., Nagai T. & Kikuchi K. (2005) Low oxygen tension during in vitro maturation of porcine follicular oocytes improves parthenogenetic activation and subsequent development to the blastocyst stage. Theriogenology 63, 1277-89.

Iwase H., Hara H., Ezzelarab M., Li T., Zhang Z., Gao B., Liu H., Long C., Wang Y., Cassano A., Klein E., Phelps C., Ayares D., Humar A., Wijkstrom M. & Cooper D.K.C. (2017) Immunological and physiological observations in baboons with life-supporting genetically engineered pig kidney grafts. Xenotransplantation 24.

Jansen G.A., Mihalik S.J., Watkins P.A., Moser H.W., Jakobs C., Denis S. & Wanders R.J. (1996) Phytanoyl-CoA hydroxylase is present in human liver, located in peroxisomes, and deficient in Zellweger syndrome: direct, unequivocal evidence for the new, revised pathway of phytanic acid alpha-oxidation in humans. Biochem Biophys Res Commun 229, 205-10.

Jansen G.A. & Wanders R.J. (2006) Alpha-oxidation. Biochim Biophys Acta 1763, 1403-12.

Jansen R.L.M. & van der Klei I.J. (2019) The peroxisome biogenesis factors Pex3 and Pex19: multitasking proteins with disputed functions. FEBS Lett 593, 457-74.

Jeon Y., Yoon J.D., Cai L., Hwang S.U., Kim E., Zheng Z., Jeung E., Lee E. & Hyun S.H. (2015) Zinc deficiency during in vitro maturation of porcine oocytes causes meiotic block and developmental failure. Mol Med Rep 12, 5973-82.

Jeong P.S., Lee S., Park S.H., Kim M.J., Kang H.G., Nanjidsuren T., Son H.C., Song B.S., Koo D.B., Sim B.W. & Kim S.U. (2020) Butylparaben Is Toxic to Porcine Oocyte Maturation and Subsequent Embryonic Development Following In Vitro Fertilization. Int J Mol Sci 21.

Jeong P.S., Yoon S.B., Choi S.A., Song B.S., Kim J.S., Sim B.W., Park Y.H., Yang H.J., Mun S.E., Kim Y.H., Kang P., Jeong K.J., Lee Y., Jin Y.B., Huh J.W., Lee S.R., Koo D.B., Park Y.I., Kim S.U. & Chang K.T. (2017) Iloprost supports early development of in vitro-produced porcine embryos through activation of the phosphatidylinositol 3-kinase/AKT signalling pathway. Reprod Fertil Dev 29, 1306-18.

Jiang X., Xing X., Zhang Y., Zhang C., Wu Y., Chen Y., Meng R., Jia H., Cheng Y., Zhang Y. & Su J. (2020) Lead exposure activates the Nrf2/Keap1 pathway, aggravates oxidative stress, and induces reproductive damage in female mice. Ecotoxicol Environ Saf 207, 111231.

Jiang Z., Kunej T., Michal J.J., Gaskins C.T., Reeves J.J., Busboom J.R., Dovc P. & Wright R.W., Jr. (2005) Significant associations of the mitochondrial transcription factor A promoter polymorphisms with marbling and subcutaneous fat depth in Wagyu x Limousin F2 crosses. Biochem Biophys Res Commun 334, 516-23.

Jiao Y., Zhu S., Li J., Jam Zaheer A., Li M. & Huang B. (2020) PS48 promotes in vitro maturation and developmental competence of porcine oocytes through activating PI3K/Akt signalling pathway. Reprod Domest Anim.

Jin J.X., Lee S., Khoirinaya C., Oh A., Kim G.A. & Lee B.C. (2016) Supplementation with spermine during in vitro maturation of porcine oocytes improves early embryonic development after parthenogenetic activation and somatic cell nuclear transfer. J Anim Sci 94, 963-70.

Jin J.X., Lee S., Taweechaipaisankul A., Kim G.A. & Lee B.C. (2017) Melatonin regulates lipid metabolism in porcine oocytes. J Pineal Res 62.

Johnson J., Espinoza T., McGaughey R.W., Rawls A. & Wilson-Rawls J. (2001) Notch pathway genes are expressed in mammalian ovarian follicles. Mech Dev 109, 355-61.

Kajdasz A., Warzych E., Derebecka N., Madeja Z.E., Lechniak D., Wesoly J. & Pawlak P. (2020) Lipid Stores and Lipid Metabolism Associated Gene Expression in Porcine and Bovine Parthenogenetic Embryos Revealed by Fluorescent Staining and RNA-seq. Int J Mol Sci 21.

Kalous J., Kubelka M. & Motlík J. (2003) The effect of PD98059 on MAPK regulation in cumulus-enclosed and cumulus-free mouse oocytes. Zygote 11, 61-8.

Kannan K. & Jain S.K. (2000) Oxidative stress and apoptosis. Pathophysiology 7, 153-63.

Kansanen E., Kuosmanen S.M., Leinonen H. & Levonen A.L. (2013) The Keap1-Nrf2 pathway: Mechanisms of activation and dysregulation in cancer. Redox Biol 1, 45-9.

Kao Y.T., Gonzalez K.L. & Bartel B. (2018) Peroxisome Function, Biogenesis, and Dynamics in Plants. Plant Physiol 176, 162-77.

Kararli T.T. (1995) Comparison of the gastrointestinal anatomy, physiology, and biochemistry of humans and commonly used laboratory animals. Biopharm Drug Dispos 16, 351-80.

Kaspar J.W., Niture S.K. & Jaiswal A.K. (2009) Nrf2:INrf2 (Keap1) signaling in oxidative stress. Free Radic Biol Med 47, 1304-9.

Keffer J., Probert L., Cazlaris H., Georgopoulos S., Kaslaris E., Kioussis D. & Kollias G. (1991) Transgenic mice expressing human tumour necrosis factor: a predictive genetic model of arthritis. EMBO J 10, 4025-31.

Kikuchi K., Onishi A., Kashiwazaki N., Iwamoto M., Noguchi J., Kaneko H., Akita T. & Nagai T. (2002) Successful piglet production after transfer of blastocysts produced by a modified in vitro system. Biol Reprod 66, 1033-41.

Kim D., Langmead B. & Salzberg S.L. (2015) HISAT: a fast spliced aligner with low memory requirements. Nat Methods 12, 357-60.

Kim D.H., Lee H.R., Kim M.G., Lee J.S., Jin S.J. & Lee H.T. (2017a) The effect of poly(ADP-ribosyl)ation inhibition on the porcine cumulus-oocyte complex during in vitro maturation. Biochem Biophys Res Commun 483, 752-8.

Kim E.H., Kim G.A., Taweechaipaisankul A., Lee S.H., Muhammad Q., Ahn C. & Lee B.C. (2019) Melatonin enhances porcine embryo development via the Nrf2/ARE signaling pathway. J Mol Endocrinol 63(3), 175-185.

Kim E.H., Kim G.A., Taweechaipaisankul A., Ridlo M.R., Lee S.H., Ra K., Ahn C. & Lee B.C. (2020) Phytanic acid-derived peroxisomal lipid metabolism in porcine oocytes. Theriogenology 157, 276-85.

Kim E.H., Ridlo M.R., Lee B.C. & Kim G.A. (2020) Melatonin-Nrf2 Signaling Activates Peroxisomal Activities in Porcine Cumulus Cell-Oocyte Complexes. Antioxidants (Basel) 9.

Kim E.H., Taweechaipaisankul A., Ridlo M.R., Kim G.A. & Lee B.C. (2020) Effect of Klotho protein during porcine oocyte maturation via Wnt signaling. Aging (Albany NY) 12.

Kim G.A., Lee E.M., Cho B., Alam Z., Kim S.J., Lee S., Oh H.J., Hwang J.I., Ahn C. & Lee B.C. (2019) Generation by somatic cell nuclear transfer of GGTA1 knockout pigs expressing soluble human TNFRI-Fc and human HO-1. Transgenic Res 28, 91-102.

Kim G.A., Lee E.M., Jin J.X., Lee S., Taweechaipaisankul A., Hwang J.I., Alam Z., Ahn C. & Lee B.C. (2017b) Generation of CMAHKO/GTKO/shTNFRI-Fc/HO-1 quadruple gene modified pigs. Transgenic Res 26, 435-45.

Kim S., Kim J.H., Lee E., Jeong Y.W., Hossein M.S., Park S.M., Park S.W., Lee J.Y., Jeong Y.I., Kim H.S., Kim Y.W., Hyun S.H. & Hwang W.S. (2010) Establishment and characterization of embryonic stem-like cells from porcine somatic cell nuclear transfer blastocysts. Zygote 18, 93-101.

Knijn H.M., Gjorret J.O., Vos P.L., Hendriksen P.J., van der Weijden B.C., Maddox-Hyttel P. & Dieleman S.J. (2003) Consequences of in vivo development and subsequent culture on apoptosis, cell number, and blastocyst formation in bovine embryos. Biol Reprod 69, 1371-8.

Kobayashi A., Kang M.I., Okawa H., Ohtsuji M., Zenke Y., Chiba T., Igarashi K. & Yamamoto M. (2004) Oxidative stress sensor Keap1 functions as an adaptor for Cul3-based E3 ligase to regulate proteasomal degradation of Nrf2. Mol Cell Biol 24, 7130-9.

Kordowitzki P., Hamdi M., Derevyanko A., Rizos D. & Blasco M. (2020) The effect of rapamycin on bovine oocyte maturation success and metaphase telomere length maintenance. Aging (Albany NY) 12, 7576-84.

Kragh P.M., Nielsen A.L., Li J., Du Y., Lin L., Schmidt M., Bøgh I.B., Holm I.E., Jakobsen J.E., Johansen M.G., Purup S., Bolund L., Vajta G. & Jørgensen A.L. (2009) Hemizygous minipigs produced by random gene insertion and handmade

cloning express the Alzheimer's disease-causing dominant mutation APPsw. Transgenic Res 18, 545-58.

Kwak S.S., Yoon J.D., Cheong S.A., Jeon Y., Lee E. & Hyun S.H. (2014) The new system of shorter porcine oocyte in vitro maturation (18 hours) using >/=8 mm follicles derived from cumulus-oocyte complexes. Theriogenology 81, 291-301.

Lan M., Han J., Pan M.H., Wan X., Pan Z.N. & Sun S.C. (2018) Melatonin protects against defects induced by deoxynivalenol during mouse oocyte maturation. J Pineal Res 65, e12477.

Lan M., Zhang Y., Wan X., Pan M.H., Xu Y. & Sun S.C. (2020) Melatonin ameliorates ochratoxin A-induced oxidative stress and apoptosis in porcine oocytes. Environ Pollut 256, 113374.

Lee C. (2017) Collaborative Power of Nrf2 and PPARgamma Activators against Metabolic and Drug-Induced Oxidative Injury. Oxid Med Cell Longev 2017, 1378175.

Lee G.K., Shin H. & Lim H.J. (2016) Rapamycin Influences the Efficiency of In vitro Fertilization and Development in the Mouse: A Role for Autophagic Activation. Asian-Australas J Anim Sci 29, 1102-10.

Lee J., Lee Y., Lee G.S., Lee S.T. & Lee E. (2019) Comparative study of the developmental competence of cloned pig embryos derived from spermatogonial stem cells and fetal fibroblasts. Reprod Domest Anim 54, 1258-64.

Lee J., Park J.I., Yun J.I., Lee Y., Yong H., Lee S.T., Park C.K., Hyun S.H., Lee G.S. & Lee E. (2015) Rapamycin treatment during in vitro maturation of oocytes improves embryonic development after parthenogenesis and somatic cell nuclear transfer in pigs. J Vet Sci 16, 373-80.

Lee J.M. & Johnson J.A. (2004) An important role of Nrf2-ARE pathway in the cellular defense mechanism. J Biochem Mol Biol 37, 139-43.

Lee K., Wang C., Chaille J.M. & Machaty Z. (2010) Effect of resveratrol on the development of porcine embryos produced in vitro. J Reprod Dev 56, 330-5.

Lee S., Jin J.X., Taweechaipaisankul A., Kim G.A., Ahn C. & Lee B.C. (2017) Melatonin influences the sonic hedgehog signaling pathway in porcine cumulus oocyte complexes. J Pineal Res 63.

Lee S., Jin J.X., Taweechaipaisankul A., Kim G.A., Ahn C. & Lee B.C. (2018a) Sonic hedgehog signaling mediates resveratrol to improve maturation of pig oocytes in vitro and subsequent preimplantation embryo development. J Cell Physiol 233, 5023-33.

Lee S., Jin J.X., Taweechaipaisankul A., Kim G.A. & Lee B.C. (2018b) Stimulatory Effects of Melatonin on Porcine In Vitro Maturation Are Mediated by MT2 Receptor. Int J Mol Sci 19.

Lee S., Jin J.X., Taweechaipaisankul A., Kim G.A. & Lee B.C. (2018c) Synergistic effects of resveratrol and melatonin on in vitro maturation of porcine oocytes and subsequent embryo development. Theriogenology 114, 191-8.

Lee S.E., Hyun H., Park M.R., Choi Y., Son Y.J., Park Y.G., Jeong S.G., Shin M.Y., Ha H.J., Hong H.S., Choi M.K., Im G.S., Park E.W., Kim Y.H., Park C., Kim E.Y. & Park S.P. (2017) Production of transgenic pig as an Alzheimer's disease model using a multi-cistronic vector system. PLoS One 12, e0177933.

Lee S.E., Kim E.Y., Choi H.Y., Moon J.J., Park M.J., Lee J.B., Jeong C.J. & Park S.P. (2014) Rapamycin rescues the poor developmental capacity of aged porcine oocytes. Asian-Australas J Anim Sci 27, 635-47.

Lee S.H., Oh H.J., Kim M.J., Kim G.A., Choi Y.B., Jo Y.K., Setyawan E.M.N. & Lee B.C. (2018) Effect of co-culture canine cumulus and oviduct cells with porcine

oocytes during maturation and subsequent embryo development of parthenotes in vitro. Theriogenology 106, 108-16.

Lee S.H., Oh H.J., Kim M.J., Setyawan E.M.N. & Lee B.C. (2019) Interaction of the EGFR signaling pathway with porcine cumulus oocyte complexes and oviduct cells in a coculture system. J Cell Physiol 234, 4030-43.

Leem J., Bai G.Y., Kim J.S. & Oh J.S. (2019) Melatonin protects mouse oocytes from DNA damage by enhancing nonhomologous end-joining repair. J Pineal Res 67, e12603.

Lefebvre P., Chinetti G., Fruchart J.C. & Staels B. (2006) Sorting out the roles of PPAR alpha in energy metabolism and vascular homeostasis. J Clin Invest 116, 571-80.

Lehmann J.M., Moore L.B., Smith-Oliver T.A., Wilkison W.O., Willson T.M. & Kliewer S.A. (1995) An antidiabetic thiazolidinedione is a high affinity ligand for peroxisome proliferator-activated receptor gamma (PPAR gamma). J Biol Chem 270, 12953-6.

Lemotte P.K., Keidel S. & Apfel C.M. (1996) Phytanic acid is a retinoid X receptor ligand. Eur J Biochem 236, 328-33.

Leung L., Kwong M., Hou S., Lee C. & Chan J.Y. (2003) Deficiency of the Nrf1 and Nrf2 transcription factors results in early embryonic lethality and severe oxidative stress. J Biol Chem 278, 48021-9.

Li L.Y., Li M.M., Yang S.F., Zhang J., Li Z., Zhang H., Zhu L., Zhu X., Verma V., Liu Q., Shi D. & Huang B. (2016) Inhibition of FGF Signalling Pathway Augments the Expression of Pluripotency and Trophoblast Lineage Marker Genes in Porcine Parthenogenetic Blastocyst. Reprod Domest Anim 51, 649-56.

Li R., Jia Z. & Zhu H. (2019) Regulation of Nrf2 Signaling. React Oxyg Species (Apex) 8, 312-22.

Li Y., Liu H., Wu K., Liu H., Huang T., Chen Z.J., Zhao S., Ma J. & Zhao H. (2019) Melatonin promotes human oocyte maturation and early embryo development by enhancing clathrin-mediated endocytosis. J Pineal Res 67, e12601.

Li Y., Wang J., Zhang Z., Yi J., He C., Wang F., Tian X., Yang M., Song Y., He P. & Liu G. (2016) Resveratrol compares with melatonin in improving in vitro porcine oocyte maturation under heat stress. J Anim Sci Biotechnol 7, 33.

Liang H. & Ward W.F. (2006) PGC-1alpha: a key regulator of energy metabolism. Adv Physiol Educ 30, 145-51.

Liang S., Jin Y.X., Yuan B., Zhang J.B. & Kim N.H. (2017) Melatonin enhances the developmental competence of porcine somatic cell nuclear transfer embryos by preventing DNA damage induced by oxidative stress. Sci Rep 7, 11114.

Lin Y., Sui L.C., Wu R.H., Ma R.J., Fu H.Y., Xu J.J., Qiu X.H. & Chen L. (2018) Nrf2 inhibition affects cell cycle progression during early mouse embryo development. J Reprod Dev 64, 49-55.

Liu L., Locascio L.M. & Dore S. (2019) Critical Role of Nrf2 in Experimental Ischemic Stroke. Front Pharmacol 10, 153.

Liu L., Wang Y. & Yu Q. (2014) The PI3K/Akt signaling pathway exerts effects on the implantation of mouse embryos by regulating the expression of RhoA. Int J Mol Med 33, 1089-96.

Liu M.J., Sun A.G., Zhao S.G., Liu H., Ma S.Y., Li M., Huai Y.X., Zhao H. & Liu H.B. (2018) Resveratrol improves in vitro maturation of oocytes in aged mice and humans. Fertil Steril 109, 900-7.

Liu X., Xu H., Zhang Y., Wang P. & Gao W. (2019) Brusatol inhibits amyloid-beta-induced neurotoxicity in U-251 cells via regulating the Nrf2/HO-1 pathway. J Cell Biochem.

Liu Y., Wei Z., Huang Y., Bai C., Zan L. & Li G. (2014) Cyclopamine did not affect mouse oocyte maturation in vitro but decreased early embryonic development. Anim Sci J 85, 840-7.

Lodhi I.J. & Semenkovich C.F. (2014) Peroxisomes: a nexus for lipid metabolism and cellular signaling. Cell Metab 19, 380-92.

Logan J.S. & Martin M.J. (1994) Transgenic swine as a recombinant production system for human hemoglobin. Methods Enzymol 231, 435-45.

Lolicato F., Brouwers J.F., de Lest C.H., Wubbolts R., Aardema H., Priore P., Roelen B.A., Helms J.B. & Gadella B.M. (2015) The cumulus cell layer protects the bovine maturing oocyte against fatty acid-induced lipotoxicity. Biol Reprod 92, 16.

Lord E., Murphy B.D., Desmarais J.A., Ledoux S., Beaudry D. & Palin M.F. (2006) Modulation of peroxisome proliferator-activated receptor delta and gamma transcripts in swine endometrial tissue during early gestation. Reproduction 131, 929-42.

Lorson M.A., Spate L.D., Samuel M.S., Murphy C.N., Lorson C.L., Prather R.S. & Wells K.D. (2011) Disruption of the Survival Motor Neuron (SMN) gene in pigs using ssDNA. Transgenic Res 20, 1293-304.

Lowe J.L., Bathgate R. & Grupen C.G. (2019) Effect of carbohydrates on lipid metabolism during porcine oocyte IVM. Reprod Fertil Dev 31, 557-69.

Ludtmann M.H., Angelova P.R., Zhang Y., Abramov A.Y. & Dinkova-Kostova A.T. (2014) Nrf2 affects the efficiency of mitochondrial fatty acid oxidation. Biochem J 457, 415-24.

Luo Y., Li J., Liu Y., Lin L., Du Y., Li S., Yang H., Vajta G., Callesen H., Bolund L. & Sørensen C.B. (2011) High efficiency of BRCA1 knockout using rAAV-

mediated gene targeting: developing a pig model for breast cancer. Transgenic Res 20, 975-88.

Ma Q. (2013) Role of nrf2 in oxidative stress and toxicity. Annu Rev Pharmacol Toxicol 53, 401-26.

Ma R., Li H., Zhang Y., Lin Y., Qiu X., Xie M. & Yao B. (2017) The toxic effects and possible mechanisms of Brusatol on mouse oocytes. PLoS One 12, e0177844.

Ma R., Liang W., Sun Q., Qiu X., Lin Y., Ge X., Jueraitetibaike K., Xie M., Zhou J., Huang X., Wang Q. & Chen L. (2018) Sirt1/Nrf2 pathway is involved in oocyte aging by regulating Cyclin B1. Aging (Albany NY) 10, 2991-3004.

Machaty Z., Day B.N. & Prather R.S. (1998) Development of early porcine embryos in vitro and in vivo. Biol Reprod 59, 451-5.

MacPhee A.A., Cole F.E. & Rice B.F. (1975) The effect of melatonin on steroidogenesis by the human ovary in vitro. J Clin Endocrinol Metab 40, 688-96.

Magesh S., Chen Y. & Hu L. (2012) Small molecule modulators of Keap1-Nrf2-ARE pathway as potential preventive and therapeutic agents. Med Res Rev 32, 687-726.

Manivannan S., Scheckhuber C.Q., Veenhuis M. & van der Klei I.J. (2012) The impact of peroxisomes on cellular aging and death. Front Oncol 2, 50.

Mannaerts G.P. & van Veldhoven P.P. (1996) Functions and organization of peroxisomal beta-oxidation. Ann N Y Acad Sci 804, 99-115.

Mao J., Zhao M.T., Whitworth K.M., Spate L.D., Walters E.M., O'Gorman C., Lee K., Samuel M.S., Murphy C.N., Wells K., Rivera R.M. & Prather R.S. (2015) Oxamflatin treatment enhances cloned porcine embryo development and nuclear reprogramming. Cell Reprogram 17, 28-40.

Marchal R., Caillaud M., Martoriati A., Gerard N., Mermillod P. & Goudet G. (2003) Effect of growth hormone (GH) on in vitro nuclear and cytoplasmic oocyte maturation, cumulus expansion, hyaluronan synthases, and connexins 32 and 43 expression, and GH receptor messenger RNA expression in equine and porcine species. Biol Reprod 69, 1013-22.

Mattioli M., Bacci M.L., Galeati G. & Seren E. (1989) Developmental competence of pig oocytes matured and fertilized in vitro. Theriogenology 31, 1201-7.

Matz-Soja M., Rennert C., Schonefeld K., Aleithe S., Boettger J., Schmidt-Heck W., Weiss T.S., Hovhannisyan A., Zellmer S., Kloting N., Schulz A., Kratzsch J., Guthke R. & Gebhardt R. (2016) Hedgehog signaling is a potent regulator of liver lipid metabolism and reveals a GLI-code associated with steatosis. Elife 5.

Mayerhofer P.U. (2016) Targeting and insertion of peroxisomal membrane proteins: ER trafficking versus direct delivery to peroxisomes. Biochim Biophys Acta 1863, 870-80.

Mayo J.C., Aguado A., Cernuda-Cernuda R., Alvarez-Artime A., Cepas V., Quiros-Gonzalez I., Hevia D. & Sainz R.M. (2018) Melatonin Uptake by Cells: An Answer to Its Relationship with Glucose? Molecules 23(8), 1999.

McVicar J.W., Eisner R.J., Johnson L.A. & Pursel V.G. (1977) Foot-and-mouth disease and swine vesicular disease viruses in boar semen. Proc Annu Meet U S Anim Health Assoc, 221-30.

Miao Y.L., Kikuchi K., Sun Q.Y. & Schatten H. (2009) Oocyte aging: cellular and molecular changes, developmental potential and reversal possibility. Hum Reprod Update 15, 573-85.

Mihalik S.J., Rainville A.M. & Watkins P.A. (1995) Phytanic acid alpha-oxidation in rat liver peroxisomes. Production of alpha-hydroxyphytanoyl-CoA and formate is enhanced by dioxygenase cofactors. Eur J Biochem 232, 545-51.

Miller C.J., Gounder S.S., Kannan S., Goutam K., Muthusamy V.R., Firpo M.A., Symons J.D., Paine R., 3rd, Hoidal J.R. & Rajasekaran N.S. (2012) Disruption of Nrf2/ARE signaling impairs antioxidant mechanisms and promotes cell degradation pathways in aged skeletal muscle. Biochim Biophys Acta 1822, 1038-50.

Mohiuddin M.M., Singh A.K., Corcoran P.C., Thomas Iii M.L., Clark T., Lewis B.G., Hoyt R.F., Eckhaus M., Pierson Iii R.N., Belli A.J., Wolf E., Klymiuk N., Phelps C., Reimann K.A., Ayares D. & Horvath K.A. (2016) Chimeric 2C10R4 anti-CD40 antibody therapy is critical for long-term survival of GTKO.hCD46.hTBM pig-to-primate cardiac xenograft. Nat Commun 7, 11138.

Morak M., Schmidinger H., Riesenhuber G., Rechberger G.N., Kollroser M., Haemmerle G., Zechner R., Kronenberg F. & Hermetter A. (2012) Adipose triglyceride lipase (ATGL) and hormone-sensitive lipase (HSL) deficiencies affect expression of lipolytic activities in mouse adipose tissues. Mol Cell Proteomics 11, 1777-89.

Mukherjee. (1972) Normal progeny from fertilization in vitro of mouse oocytes matured in culture and spermatozoa capacitated in vitro. Nature 237, 397-8.

Muñoz-Descalzo S., Hadjantonakis A.K. & Arias A.M. (2015) Wnt/ß-catenin signalling and the dynamics of fate decisions in early mouse embryos and embryonic stem (ES) cells. Semin Cell Dev Biol 47-48, 101-9.

Nagai T., Funahashi H., Yoshioka K. & Kikuchi K. (2006) Up date of in vitro production of porcine embryos. Front Biosci 11, 2565-73.

Nakano M., Kato Y. & Tsunoda Y. (2012) Effect of melatonin treatment on the developmental potential of parthenogenetic and somatic cell nuclear-transferred porcine oocytes in vitro. Zygote 20, 199-207.

Nasiri E., Mahmoudi R., Bahadori M.H. & Amiri I. (2011) The Effect of Retinoic Acid on in vitro Maturation and Fertilization Rate of Mouse Germinal Vesicle Stage Oocytes. Cell J 13, 19-24.

Negi G., Kumar A. & Sharma S.S. (2011) Melatonin modulates neuroinflammation and oxidative stress in experimental diabetic neuropathy: effects on NF-kappaB and Nrf2 cascades. J Pineal Res 50, 124-31.

Nguyen N.T., Lo N.W., Chuang S.P., Jian Y.L. & Ju J.C. (2011) Sonic hedgehog supplementation of oocyte and embryo culture media enhances development of IVF porcine embryos. Reproduction 142, 87-97.

Nguyen T., Nioi P. & Pickett C.B. (2009) The Nrf2-antioxidant response element signaling pathway and its activation by oxidative stress. J Biol Chem 284, 13291-5.

Niemann H. & Rath D. (2001) Progress in reproductive biotechnology in swine. Theriogenology 56, 1291-304.

Niu Y.J., Zhou W., Nie Z.W., Shin K.T. & Cui X.S. (2020) Melatonin enhances mitochondrial biogenesis and protects against rotenone-induced mitochondrial deficiency in early porcine embryos. J Pineal Res 68, e12627.

Nomura M., Iwase A., Furui K., Kitagawa T., Matsui Y., Yoshikawa M. & Kikkawa F. (2007) Preferable correlation to blastocyst development and pregnancy rates with a new embryo grading system specific for day 3 embryos. J Assist Reprod Genet 24, 23-8.

Novin M.G., Allahveisi A., Noruzinia M., Farhadifar F., Yousefian E., Fard A.D. & Salimi M. (2015) The relationship between transcript expression levels of nuclear

encoded (TFAM, NRF1) and mitochondrial encoded (MT-CO1) genes in single human oocytes during oocyte maturation. Balkan J Med Genet 18, 39-46.

Olayanju A., Copple I.M., Bryan H.K., Edge G.T., Sison R.L., Wong M.W., Lai Z.Q., Lin Z.X., Dunn K., Sanderson C.M., Alghanem A.F., Cross M.J., Ellis E.C., Ingelman-Sundberg M., Malik H.Z., Kitteringham N.R., Goldring C.E. & Park B.K. (2015) Brusatol provokes a rapid and transient inhibition of Nrf2 signaling and sensitizes mammalian cells to chemical toxicity-implications for therapeutic targeting of Nrf2. Free Radic Biol Med 78, 202-12.

Pala D., Lodola A., Bedini A., Spadoni G. & Rivara S. (2013) Homology models of melatonin receptors: challenges and recent advances. Int J Mol Sci 14, 8093-121.

Paredes S.D., Terron M., Cubero J., Valero V., Barriga C., Reiter R.J. & Rodriguez A.B. (2007) Tryptophan increases nocturnal rest and affects melatonin and serotonin serum levels in old ringdove. Physiol Behav 90, 576-82.

Park H.J., Park J.Y., Kim J.W., Yang S.G., Jung J.M., Kim M.J., Kang M.J., Cho Y.H., Wee G., Yang H.Y., Song B.S., Kim S.U. & Koo D.B. (2018) Melatonin improves the meiotic maturation of porcine oocytes by reducing endoplasmic reticulum stress during in vitro maturation. J Pineal Res 64(2), e12458.

Pavelka M., Goldenberg H., Huttinger M. & Kramar R. (1976) Enzymic and morphological studies on catalase positive particles from brown fat of cold adapted rats. Histochemistry 50, 47-55.

Pawlak M., Lefebvre P. & Staels B. (2015) Molecular mechanism of PPARalpha action and its impact on lipid metabolism, inflammation and fibrosis in non-alcoholic fatty liver disease. J Hepatol 62, 720-33.

Perleberg C., Kind A. & Schnieke A. (2018) Genetically engineered pigs as models for human disease. Dis Model Mech 11(1), dmm030783.

Pertea M., Kim D., Pertea G.M., Leek J.T. & Salzberg S.L. (2016) Transcript-level expression analysis of RNA-seq experiments with HISAT, StringTie and Ballgown. Nat Protoc 11, 1650-67.

Pertea M., Pertea G.M., Antonescu C.M., Chang T.C., Mendell J.T. & Salzberg S.L. (2015) StringTie enables improved reconstruction of a transcriptome from RNA-seq reads. Nat Biotechnol 33, 290-5.

Phillips R.M., Foley C.W. & Lukert P.D. (1972) Isolation and characterization of viruses from semen and the reproductive tract of male swine. J Am Vet Med Assoc 161, 1306-16.

Polejaeva I.A. & Campbell K.H. (2000) New advances in somatic cell nuclear transfer: application in transgenesis. Theriogenology 53, 117-26.

Polvani S., Tarocchi M. & Galli A. (2012) PPARgamma and Oxidative Stress: Con(beta) Catenating NRF2 and FOXO. PPAR Res 2012, 641087.

Powell M.D., Manandhar G., Spate L., Sutovsky M., Zimmerman S., Sachdev S.C., Hannink M., Prather R.S. & Sutovsky P. (2010) Discovery of putative oocyte quality markers by comparative ExacTag proteomics. Proteomics Clin Appl 4, 337-51.

Prates E.G., Nunes J.T. & Pereira R.M. (2014) A role of lipid metabolism during cumulus-oocyte complex maturation: impact of lipid modulators to improve embryo production. Mediators Inflamm 2014, 692067.

Prather R.S., Hawley R.J., Carter D.B., Lai L. & Greenstein J.L. (2003) Transgenic swine for biomedicine and agriculture. Theriogenology 59, 115-23.

Prather R.S., Sims M.M. & First N.L. (1989) Nuclear transplantation in early pig embryos. Biol Reprod 41, 414-8.

Qu J., Sun M., Wang X., Song X., He H. & Huan Y. (2020) Melatonin Enhances the Development of Porcine Cloned Embryos by Improving DNA Methylation Reprogramming. Cell Reprogram 22, 156-66.

Ramirez P., Chavez R., Majado M., Munitiz V., Munoz A., Hernandez Q., Palenciano C.G., Pino-Chavez G., Loba M., Minguela A., Yelamos J., Gago M.R., Vizcaino A.S., Asensi H., Cayuela M.G., Segura B., Marin F., Rubio A., Fuente T., Robles R., Bueno F.S., Sansano T., Acosta F., Rodriguez J.M., Navarro F., Cabezuelo J., Cozzi E., White D.J., Calne R.Y. & Parrilla P. (2000) Life-supporting human complement regulator decay accelerating factor transgenic pig liver xenograft maintains the metabolic function and coagulation in the nonhuman primate for up to 8 days. Transplantation 70, 989-98.

Raudvere U., Kolberg L., Kuzmin I., Arak T., Adler P., Peterson H. & Vilo J. (2019) g:Profiler: a web server for functional enrichment analysis and conversions of gene lists (2019 update). Nucleic Acids Res 47, W191-W8.

Reiter R.J., Mayo J.C., Tan D.X., Sainz R.M., Alatorre-Jimenez M. & Qin L. (2016) Melatonin as an antioxidant: under promises but over delivers. J Pineal Res 61, 253-78.

Ren D., Villeneuve N.F., Jiang T., Wu T., Lau A., Toppin H.A. & Zhang D.D. (2011) Brusatol enhances the efficacy of chemotherapy by inhibiting the Nrf2-mediated defense mechanism. Proc Natl Acad Sci U S A 108, 1433-8.

Renner S., Fehlings C., Herbach N., Hofmann A., von Waldthausen D.C., Kessler B., Ulrichs K., Chodnevskaja I., Moskalenko V., Amselgruber W., Göke B., Pfeifer A., Wanke R. & Wolf E. (2010) Glucose intolerance and reduced proliferation of pancreatic beta-cells in transgenic pigs with impaired glucose-dependent insulinotropic polypeptide function. Diabetes 59, 1228-38.

Renner S., Martins A.S., Streckel E., Braun-Reichhart C., Backman M., Prehn C., Klymiuk N., Bähr A., Blutke A., Landbrecht-Schessl C., Wünsch A., Kessler B., Kurome M., Hinrichs A., Koopmans S.J., Krebs S., Kemter E., Rathkolb B., Nagashima H., Blum H., Ritzmann M., Wanke R., Aigner B., Adamski J., Hrabě de Angelis M. & Wolf E. (2019) Mild maternal hyperglycemia in INS (C93S) transgenic pigs causes impaired glucose tolerance and metabolic alterations in neonatal offspring. Dis Model Mech 12(8), dmm039156.

Reppert S.M. (1997) Melatonin receptors: molecular biology of a new family of G protein-coupled receptors. J Biol Rhythms 12, 528-31.

Reppert S.M., Weaver D.R. & Godson C. (1996) Melatonin receptors step into the light: cloning and classification of subtypes. Trends Pharmacol Sci 17, 100-2.

Ribarov S.R. & Benov L.C. (1981) Relationship between the hemolytic action of heavy metals and lipid peroxidation. Biochim Biophys Acta 640, 721-6.

Robinson M.D., McCarthy D.J. & Smyth G.K. (2010) edgeR: a Bioconductor package for differential expression analysis of digital gene expression data. Bioinformatics 26, 139-40.

Rodriguez-Osorio N., Kim I.J., Wang H., Kaya A. & Memili E. (2007) Melatonin increases cleavage rate of porcine preimplantation embryos in vitro. J Pineal Res 43, 283-8.

Rokka A., Antonenkov V.D., Soininen R., Immonen H.L., Pirila P.L., Bergmann U., Sormunen R.T., Weckstrom M., Benz R. & Hiltunen J.K. (2009) Pxmp2 is a channel-forming protein in Mammalian peroxisomal membrane. PLoS One 4, e5090.

Ross J.W., Fernandez de Castro J.P., Zhao J., Samuel M., Walters E., Rios C., Bray-Ward P., Jones B.W., Marc R.E., Wang W., Zhou L., Noel J.M., McCall M.A.,

DeMarco P.J., Prather R.S. & Kaplan H.J. (2012) Generation of an inbred miniature pig model of retinitis pigmentosa. Invest Ophthalmol Vis Sci 53, 501-7.

Russell M.C., Cowan R.G., Harman R.M., Walker A.L. & Quirk S.M. (2007) The hedgehog signaling pathway in the mouse ovary. Biol Reprod 77, 226-36.

Saadeldin I.M., Swelum A.A., Elsafadi M., Mahmood A., Yaqoob S.H., Alfayez M. & Alowaimer A.N. (2019) Effects of all-trans retinoic acid on the in vitro maturation of camel (Camelus dromedarius) cumulus-oocyte complexes. J Reprod Dev 65, 215-21.

Sacksteder K.A., Jones J.M., South S.T., Li X., Liu Y. & Gould S.J. (2000) PEX19 binds multiple peroxisomal membrane proteins, is predominantly cytoplasmic, and is required for peroxisome membrane synthesis. J Cell Biol 148, 931-44.

Sanchez-Barcelo E.J., Mediavilla M.D., Tan D.X. & Reiter R.J. (2010) Clinical uses of melatonin: evaluation of human trials. Curr Med Chem 17, 2070-95.

Sanchez-Diaz P.C., Chang J.C., Moses E.S., Dao T., Chen Y. & Hung J.Y. (2017) Ubiquitin carboxyl-terminal esterase L1 (UCHL1) is associated with stem-like cancer cell functions in pediatric high-grade glioma. PLoS One 12, e0176879.

Sanchez-Lazo L., Brisard D., Elis S., Maillard V., Uzbekov R., Labas V., Desmarchais A., Papillier P., Monget P. & Uzbekova S. (2014) Fatty acid synthesis and oxidation in cumulus cells support oocyte maturation in bovine. Mol Endocrinol 28, 1502-21.

Schafer Z.T., Grassian A.R., Song L., Jiang Z., Gerhart-Hines Z., Irie H.Y., Gao S., Puigserver P. & Brugge J.S. (2009) Antioxidant and oncogene rescue of metabolic defects caused by loss of matrix attachment. Nature 461, 109-13.

Schier A.F. (2007) The maternal-zygotic transition: death and birth of RNAs. Science 316, 406-7.

Schluter A., Yubero P., Iglesias R., Giralt M. & Villarroya F. (2002) The chlorophyll-derived metabolite phytanic acid induces white adipocyte differentiation. Int J Obes Relat Metab Disord 26, 1277-80.

Schmitt A. & Nebreda A.R. (2002) Signalling pathways in oocyte meiotic maturation. J Cell Sci 115, 2457-9.

Schrader M. & Fahimi H.D. (2006) Peroxisomes and oxidative stress. Biochim Biophys Acta 1763, 1755-66.

Schrader M., Grille S., Fahimi H.D. & Islinger M. (2013) Peroxisome interactions and cross-talk with other subcellular compartments in animal cells. Subcell Biochem 69, 1-22.

Schrul B. & Kopito R.R. (2016) Peroxin-dependent targeting of a lipid-droplet-destined membrane protein to ER subdomains. Nat Cell Biol 18, 740-51.

Shah J.A., Navarro-Alvarez N., DeFazio M., Rosales I.A., Elias N., Yeh H., Colvin R.B., Cosimi A.B., Markmann J.F., Hertl M., Sachs D.H. & Vagefi P.A. (2016) A Bridge to Somewhere: 25-day Survival After Pig-to-Baboon Liver Xenotransplantation. Ann Surg 263, 1069-71.

Shah S.A., Khan M., Jo M.H., Jo M.G., Amin F.U. & Kim M.O. (2017) Melatonin Stimulates the SIRT1/Nrf2 Signaling Pathway Counteracting Lipopolysaccharide (LPS)-Induced Oxidative Stress to Rescue Postnatal Rat Brain. CNS Neurosci Ther 23, 33-44.

Shai N., Yifrach E., van Roermund C.W.T., Cohen N., Bibi C., L I.J., Cavellini L., Meurisse J., Schuster R., Zada L., Mari M.C., Reggiori F.M., Hughes A.L., Escobar-Henriques M., Cohen M.M., Waterham H.R., Wanders R.J.A., Schuldiner M. & Zalckvar E. (2018) Systematic mapping of contact sites reveals

tethers and a function for the peroxisome-mitochondria contact. Nat Commun 9, 1761.

Shi J.M., Tian X.Z., Zhou G.B., Wang L., Gao C., Zhu S.E., Zeng S.M., Tian J.H. & Liu G.S. (2009) Melatonin exists in porcine follicular fluid and improves in vitro maturation and parthenogenetic development of porcine oocytes. J Pineal Res 47, 318-23.

Shimokawa H., Tomoike H., Nabeyama S., Yamamoto H., Araki H., Nakamura M., Ishii Y. & Tanaka K. (1983) Coronary artery spasm induced in atherosclerotic miniature swine. Science 221, 560-2.

Shin J., Torrison J., Choi C.S., Gonzalez S.M., Crabo B.G. & Molitor T.W. (1997) Monitoring of porcine reproductive and respiratory syndrome virus infection in boars. Vet Microbiol 55, 337-46.

Somfai T., Kaneda M., Akagi S., Watanabe S., Haraguchi S., Mizutani E., Dang-Nguyen T.Q., Geshi M., Kikuchi K. & Nagai T. (2011) Enhancement of lipid metabolism with L-carnitine during in vitro maturation improves nuclear maturation and cleavage ability of follicular porcine oocytes. Reprod Fertil Dev 23, 912-20.

Stehle J.H., Saade A., Rawashdeh O., Ackermann K., Jilg A., Sebesteny T. & Maronde E. (2011) A survey of molecular details in the human pineal gland in the light of phylogeny, structure, function and chronobiological diseases. J Pineal Res 51, 17-43.

Sturmey R.G. & Leese H.J. (2003) Energy metabolism in pig oocytes and early embryos. Reproduction 126, 197-204.

Sugden D., Davidson K., Hough K.A. & Teh M.T. (2004) Melatonin, melatonin receptors and melanophores: a moving story. Pigment Cell Res 17, 454-60.

Sunyer-Figueres M., Vazquez J., Mas A., Torija M.J. & Beltran G. (2020) Transcriptomic Insights into the Effect of Melatonin in Saccharomyces cerevisiae in the Presence and Absence of Oxidative Stress. Antioxidants (Basel) 9(10), 947.

Sykiotis G.P., Habeos I.G., Samuelson A.V. & Bohmann D. (2011) The role of the antioxidant and longevity-promoting Nrf2 pathway in metabolic regulation. Curr Opin Clin Nutr Metab Care 14, 41-8.

Tamarkin L., Baird C.J. & Almeida O.F. (1985) Melatonin: a coordinating signal for mammalian reproduction? Science 227, 714-20.

Tamura H., Takasaki A., Miwa I., Taniguchi K., Maekawa R., Asada H., Taketani T., Matsuoka A., Yamagata Y., Shimamura K., Morioka H., Ishikawa H., Reiter R.J. & Sugino N. (2008) Oxidative stress impairs oocyte quality and melatonin protects oocytes from free radical damage and improves fertilization rate. J Pineal Res 44, 280-7.

Tao S., Wang S., Moghaddam S.J., Ooi A., Chapman E., Wong P.K. & Zhang D.D. (2014) Oncogenic KRAS confers chemoresistance by upregulating NRF2. Cancer Res 74, 7430-41.

Tatemoto H., Muto N., Sunagawa I., Shinjo A. & Nakada T. (2004) Protection of porcine oocytes against cell damage caused by oxidative stress during in vitro maturation: role of superoxide dismutase activity in porcine follicular fluid. Biol Reprod 71, 1150-7.

Tatemoto H., Sakurai N. & Muto N. (2000) Protection of porcine oocytes against apoptotic cell death caused by oxidative stress during In vitro maturation: role of cumulus cells. Biol Reprod 63, 805-10.

Taweechaipaisankul A., Kim G.A., Jin J.X., Lee S., Qasim M., Kim E.H. & Lee B.C. (2019) Enhancement of epigenetic reprogramming status of porcine cloned embryos with zebularine, a DNA methyltransferase inhibitor. Mol Reprod Dev 86, 1013-22.

Terret M.E., Lefebvre C., Djiane A., Rassinier P., Moreau J., Maro B. & Verlhac M.H. (2003) DOC1R: a MAP kinase substrate that control microtubule organization of metaphase II mouse oocytes. Development 130, 5169-77.

Tian X., Wang F., He C., Zhang L., Tan D., Reiter R.J., Xu J., Ji P. & Liu G. (2014) Beneficial effects of melatonin on bovine oocytes maturation: a mechanistic approach. J Pineal Res 57, 239-47.

Tian X., Wang F., Zhang L., He C., Ji P., Wang J., Zhang Z., Lv D., Abulizi W., Wang X., Lian Z. & Liu G. (2017) Beneficial Effects of Melatonin on the In Vitro Maturation of Sheep Oocytes and Its Relation to Melatonin Receptors. Int J Mol Sci 18.

Titorenko V.I. & Terlecky S.R. (2011) Peroxisome metabolism and cellular aging. Traffic 12, 252-9.

Tonelli C., Chio I.I.C. & Tuveson D.A. (2018) Transcriptional Regulation by Nrf2. Antioxid Redox Signal 29, 1727-45.

Tripathi D.N. & Jena G.B. (2010) Effect of melatonin on the expression of Nrf2 and NF-kappaB during cyclophosphamide-induced urinary bladder injury in rat. J Pineal Res 48, 324-31.

Trivedi P.P., Jena G.B., Tikoo K.B. & Kumar V. (2016) Melatonin modulated autophagy and Nrf2 signaling pathways in mice with colitis-associated colon carcinogenesis. Mol Carcinog 55, 255-67.

Tseng Y.L., Kuwaki K., Dor F.J., Shimizu A., Houser S., Hisashi Y., Yamada K., Robson S.C., Awwad M., Schuurman H.J., Sachs D.H. & Cooper D.K. (2005)

alpha1,3-Galactosyltransferase gene-knockout pig heart transplantation in baboons with survival approaching 6 months. Transplantation 80, 1493-500.

Uchida M., Shimatsu Y., Onoe K., Matsuyama N., Niki R., Ikeda J.E. & Imai H. (2001) Production of transgenic miniature pigs by pronuclear microinjection. Transgenic Res 10, 577-82.

Umeyama K., Watanabe M., Saito H., Kurome M., Tohi S., Matsunari H., Miki K. & Nagashima H. (2009) Dominant-negative mutant hepatocyte nuclear factor 1alpha induces diabetes in transgenic-cloned pigs. Transgenic Res 18, 697-706.

Uysal K.T., Wiesbrock S.M., Marino M.W. & Hotamisligil G.S. (1997) Protection from obesity-induced insulin resistance in mice lacking TNF-alpha function. Nature 389, 610-4.

van den Brink D.M. & Wanders R.J. (2006) Phytanic acid: production from phytol, its breakdown and role in human disease. Cell Mol Life Sci 63, 1752-65.

Van Veldhoven P.P. (2010) Biochemistry and genetics of inherited disorders of peroxisomal fatty acid metabolism. J Lipid Res 51, 2863-95.

Vanderhyden B.C., Caron P.J., Buccione R. & Eppig J.J. (1990) Developmental pattern of the secretion of cumulus expansion-enabling factor by mouse oocytes and the role of oocytes in promoting granulosa cell differentiation. Dev Biol 140, 307-17.

Vazquez J., Grillitsch K., Daum G., Mas A., Torija M.J. & Beltran G. (2018) Melatonin Minimizes the Impact of Oxidative Stress Induced by Hydrogen Peroxide in Saccharomyces and Non-conventional Yeast. Front Microbiol 9, 1933.

Walton P.A. & Pizzitelli M. (2012) Effects of peroxisomal catalase inhibition on mitochondrial function. Front Physiol 3, 108.

Wanders R.J., Jansen G.A. & Skjeldal O.H. (2001) Refsum disease, peroxisomes and phytanic acid oxidation: a review. J Neuropathol Exp Neurol 60, 1021-31.

Wanders R.J. & Waterham H.R. (2006) Biochemistry of mammalian peroxisomes revisited. Annu Rev Biochem 75, 295-332.

Wanders R.J., Waterham H.R. & Ferdinandusse S. (2015) Metabolic Interplay between Peroxisomes and Other Subcellular Organelles Including Mitochondria and the Endoplasmic Reticulum. Front Cell Dev Biol 3, 83.

Wang C., Li Z., Lu Y., Du R., Katiyar S., Yang J., Fu M., Leader J.E., Quong A., Novikoff P.M. & Pestell R.G. (2006) Cyclin D1 repression of nuclear respiratory factor 1 integrates nuclear DNA synthesis and mitochondrial function. Proc Natl Acad Sci U S A 103, 11567-72.

Wang F., Tian X., Zhang L., Gao C., He C., Fu Y., Ji P., Li Y., Li N. & Liu G. (2014a) Beneficial effects of melatonin on in vitro bovine embryonic development are mediated by melatonin receptor 1. J Pineal Res 56, 333-42.

Wang F., Tian X., Zhang L., He C., Ji P., Li Y., Tan D. & Liu G. (2014b) Beneficial effect of resveratrol on bovine oocyte maturation and subsequent embryonic development after in vitro fertilization. Fertil Steril 101, 577-86.

Wang H. & Dey S.K. (2005) Lipid signaling in embryo implantation. Prostaglandins Other Lipid Mediat 77, 84-102.

Wang X., Zhu X., Liang X., Xu H., Liao Y., Lu K. & Lu S. (2019) Effects of resveratrol on in vitro maturation of porcine oocytes and subsequent early embryonic development following somatic cell nuclear transfer. Reprod Domest Anim 54, 1195-205.

Waterham H.R. & Wanders R.J. (2012) Metabolic functions and biogenesis of peroxisomes in health and disease. Biochim Biophys Acta 1822, 1325.

Wei J., Ouyang H., Wang Y., Pang D., Cong N.X., Wang T., Leng B., Li D., Li X., Wu R., Ding Y., Gao F., Deng Y., Liu B., Li Z., Lai L., Feng H., Liu G. & Deng X. (2012) Characterization of a hypertriglyceridemic transgenic miniature pig model expressing human apolipoprotein CIII. Febs j 279, 91-9.

Wells G. (2015) Peptide and small molecule inhibitors of the Keap1-Nrf2 protein-protein interaction. Biochem Soc Trans 43, 674-9.

Whyte J. & Laughlin M.H. (2010) Placentation in the pig visualized by eGFP fluorescence in eNOS over-expressing cloned transgenic swine. Mol Reprod Dev 77, 565.

Whyte J.J., Samuel M., Mahan E., Padilla J., Simmons G.H., Arce-Esquivel A.A., Bender S.B., Whitworth K.M., Hao Y.H., Murphy C.N., Walters E.M., Prather R.S. & Laughlin M.H. (2011) Vascular endothelium-specific overexpression of human catalase in cloned pigs. Transgenic Res 20, 989-1001.

Wierzbicki A.S. (2007) Peroxisomal disorders affecting phytanic acid alpha-oxidation: a review. Biochem Soc Trans 35, 881-6.

Wright R.W., Jr. (1977) Successful culture in vitro of swine embryos to the blastocyst stage. J Anim Sci 44, 854-8.

Wu J., Vilarino M., Suzuki K., Okamura D., Bogliotti Y.S., Park I., Rowe J., McNabb B., Ross P.J. & Belmonte J.C.I. (2017) CRISPR-Cas9 mediated one-step disabling of pancreatogenesis in pigs. Sci Rep 7, 10487.

Wu T., Harder B.G., Wong P.K., Lang J.E. & Zhang D.D. (2015) Oxidative stress, mammospheres and Nrf2-new implication for breast cancer therapy? Mol Carcinog 54, 1494-502.

Xie D., Chen C.C., Ptaszek L.M., Xiao S., Cao X., Fang F., Ng H.H., Lewin H.A., Cowan C. & Zhong S. (2010) Rewirable gene regulatory networks in the

preimplantation embryonic development of three mammalian species. Genome Res 20, 804-15.

Xu X., Li H., Hou X., Li D., He S., Wan C., Yin P., Liu M., Liu F. & Xu J. (2015) Punicalagin Induces Nrf2/HO-1 Expression via Upregulation of PI3K/AKT Pathway and Inhibits LPS-Induced Oxidative Stress in RAW264.7 Macrophages. Mediators Inflamm 2015, 380218.

Yan S., Tu Z., Liu Z., Fan N., Yang H., Yang S., Yang W., Zhao Y., Ouyang Z., Lai C., Yang H., Li L., Liu Q., Shi H., Xu G., Zhao H., Wei H., Pei Z., Li S., Lai L. & Li X.J. (2018) A Huntingtin Knockin Pig Model Recapitulates Features of Selective Neurodegeneration in Huntington's Disease. Cell 173, 989-1002.e13.

Yang D., Wang C.E., Zhao B., Li W., Ouyang Z., Liu Z., Yang H., Fan P., O'Neill A., Gu W., Yi H., Li S., Lai L. & Li X.J. (2010) Expression of Huntington's disease protein results in apoptotic neurons in the brains of cloned transgenic pigs. Hum Mol Genet 19, 3983-94.

Yang D., Yang H., Li W., Zhao B., Ouyang Z., Liu Z., Zhao Y., Fan N., Song J., Tian J., Li F., Zhang J., Chang L., Pei D., Chen Y.E. & Lai L. (2011) Generation of PPARγ mono-allelic knockout pigs via zinc-finger nucleases and nuclear transfer cloning. Cell Res 21, 979-82.

Yang L., Wang Q., Cui M., Li Q., Mu S. & Zhao Z. (2020) Effect of Melatonin on the In Vitro Maturation of Porcine Oocytes, Development of Parthenogenetically Activated Embryos, and Expression of Genes Related to the Oocyte Developmental Capability. Animals (Basel) 10.

Yang S.G., Park H.J., Kim J.W., Jung J.M., Kim M.J., Jegal H.G., Kim I.S., Kang M.J., Wee G., Yang H.Y., Lee Y.H., Seo J.H., Kim S.U. & Koo D.B. (2018) Mito-TEMPO improves development competence by reducing superoxide in preimplantation porcine embryos. Sci Rep 8, 10130.

Yang T., Zhao Z., Liu T., Zhang Z., Wang P., Xu S., Lei X.G. & Shan A. (2017) Oxidative stress induced by Se-deficient high-energy diet implicates neutrophil dysfunction via Nrf2 pathway suppression in swine. Oncotarget 8, 13428-39.

Yen S.Y., Tseng J.K., Chuang S.M., Chen S.E. & Ju J.C. (2014) Expression and activation of mitogen-activated protein kinases in matured porcine oocytes under thermal stress. J Reprod Dev 60, 388-94.

You L., Chen J., Liu W., Xiang Q., Luo Z., Wang W., Xu W., Wu K., Zhang Q., Liu Y. & Wu J. (2020) Enterovirus 71 induces neural cell apoptosis and autophagy through promoting ACOX1 downregulation and ROS generation. Virulence 11, 537-53.

Yuan B., Liang S., Kwon J.W., Jin Y.X., Park S.H., Wang H.Y., Sun T.Y., Zhang J.B. & Kim N.H. (2016) The Role of Glucose Metabolism on Porcine Oocyte Cytoplasmic Maturation and Its Possible Mechanisms. PLoS One 11, e0168329.

Yuan R., Peters L.L. & Paigen B. (2011) Mice as a mammalian model for research on the genetics of aging. ILAR J 52, 4-15.

Yuan Y., Spate L.D., Redel B.K., Tian Y., Zhou J., Prather R.S. & Roberts R.M. (2017) Quadrupling efficiency in production of genetically modified pigs through improved oocyte maturation. Proc Natl Acad Sci U S A 114, E5796-E804.

Zabihi A., Shabankareh H.K., Hajarian H. & Foroutanifar S. (2019) Resveratrol addition to in vitro maturation and in vitro culture media enhances developmental competence of sheep embryos. Domest Anim Endocrinol 68, 25-31.

Zechner R., Kienesberger P.C., Haemmerle G., Zimmermann R. & Lass A. (2009) Adipose triglyceride lipase and the lipolytic catabolism of cellular fat stores. J Lipid Res 50, 3-21.

Zeng G., Apte U., Cieply B., Singh S. & Monga S.P. (2007) siRNA-mediated beta-catenin knockdown in human hepatoma cells results in decreased growth and survival. Neoplasia 9, 951-9.

Zhang D.D., Lo S.C., Cross J.V., Templeton D.J. & Hannink M. (2004) Keap1 is a redox-regulated substrate adaptor protein for a Cul3-dependent ubiquitin ligase complex. Mol Cell Biol 24, 10941-53.

Zhang K. & Ealy A.D. (2012) Disruption of fibroblast growth factor receptor signaling in bovine cumulus-oocyte complexes during in vitro maturation reduces subsequent embryonic development. Domest Anim Endocrinol 42, 230-8.

Zhang R.N., Fu X.W., Jia B.Y., Liu C., Cheng K.R. & Zhu S.E. (2014) Expression of perilipin 2 (PLIN2) in porcine oocytes during maturation. Reprod Domest Anim 49, 875-80.

Zhang Y.L., Liu X.M., Ji S.Y., Sha Q.Q., Zhang J. & Fan H.Y. (2015) ERK1/2 activities are dispensable for oocyte growth but are required for meiotic maturation and pronuclear formation in mouse. J Genet Genomics 42, 477-85.

Zhao X.M., Hao H.S., Du W.H., Zhao S.J., Wang H.Y., Wang N., Wang D., Liu Y., Qin T. & Zhu H.B. (2016) Melatonin inhibits apoptosis and improves the developmental potential of vitrified bovine oocytes. J Pineal Res 60, 132-41.

Zhao X.M., Wang N., Hao H.S., Li C.Y., Zhao Y.H., Yan C.L., Wang H.Y., Du W.H., Wang D., Liu Y., Pang Y.W. & Zhu H.B. (2018) Melatonin improves the fertilization capacity and developmental ability of bovine oocytes by regulating cytoplasmic maturation events. J Pineal Res 64.

Zhou J., Tan L., Xie J., Lai Z., Huang Y., Qu C., Luo D., Lin Z., Huang P., Su Z. & Xie Y. (2017) Characterization of brusatol self-microemulsifying drug delivery

system and its therapeutic effect against dextran sodium sulfate-induced ulcerative colitis in mice. Drug Deliv 24, 1667-79.

Zipper L.M. & Mulcahy R.T. (2002) The Keap1 BTB/POZ dimerization function is required to sequester Nrf2 in cytoplasm. J Biol Chem 277, 36544-52.

국문초록

멜라토닌과 피탄산 처리에 따른 돼지 난자 및 배아 내 Nuclear factor erythroid-2-related factor 2 기전 및 퍼옥시좀 활성의 관계 분석

김의현

(지도교수: 윤 화 영)

서울대학교 대학원

수의학과 임상수의학(수의산과·생물공학) 전공

돼지는 장기의 크기 및 생리학적 부분에서 인간과 매우 흡사하여 질병모델 및 이종장기 이식에 있어서 필수불가결한 종으로 꼽히고 있다. 또한 돼지는 다태종으로서, 연구자들에게 비교적 쉬운 접근성을 제공한다. 이러한 연구에 있어서 돼지의 체외생산은 중추적이고, 세분화 시 난자의 체외성숙과 배아의 체외배양으로 나뉘게 된다. 이미 여러 차례 보고된 바 대로, 돼지의 난자 및 배아 배양 시 여러 배양조건과 환경을 통제하여 배양효율을 높이고자 하지만, 아직도 돼지의 생식세포 배양에 있어서의 산화적 스트레스 문제는 완전히

해결되지 못한 상황이다. 이에, 생식세포 배양에 여러 기전들을 작용시키는 방법에 관한 연구가 집중되고 있으며, 그 중 Nrf2 는 산화적 스트레스에 특화된 기전으로 알려져 있다.

또 다른 관점으로는, 돼지 생식세포의 배양효율을 높이기 위해 지질대사의 조절이 중요하다는 보고들이 있다. 그리고 멜라토닌과 피탄산은 지질대사를 조절하는 화학물로 알려져 있다. 지질 대사를 통해, 퍼옥시좀 내 존재하는 베타지질 산화가 긴 지방산 또는 지질 방울들을 산화시켜 짧은 지방산으로 만든 뒤, 이를 미토콘드리아로 보내어 최종적으로 ATP가 생산된다. 또한 이 과정에서 Nrf2 기전이 관여한다는 연구가 종종 발표되고 있다.

하여 본 연구는, 돼지 생식세포 내에서의 Nrf2 기전과 퍼옥시좀 활성의 관계와 영향을 알아보고자 수행되었다.

첫 번째로, Nrf2 기전을 활성화하기 위해 멜라토닌을 돼지 배아 배양단계에서 처리하여 배아 내 항산화 메커니즘에 Nrf2 기전의 관여 여부를 조사하였다. 체외 성숙된 난자를 사용하여 체외 수정을 시킨 뒤, 멜라토닌을 배양 배지에 처리하여 배아의 발달을 보고, 면역염색법과 real time PCR 을 통해 유전자 및 단백질 수준의 변화를 연구하였다. 그 결과 10^{-7} M 의 멜라토닌이 돼지 배아발달 증진에 있어서 유의적 효과가 있음을 확인하였고 ($P < 0.05$), 유전자 및 단백질 수준에서 멜라토닌에 인한 Nrf2 기전의 조절이 확인되었다.

이를 통해 멜라토닌이 Nrf2 signaling 을 통하여 배양과정에서의 산화를 억제하여 배아발달을 증진시킨다는 사실을 확인하였다.

두 번째로, 피탄산을 이용한 돼지 난자 내 퍼옥시좀 활성을 알아보고자 하였다. 이 실험에서는 돼지 난자에 피탄산을 첨가하여 난자의 체외 성숙과 체외 수정 유래 배아를 생산하고, real time PCR, 면역염색, 그리고 BODIPY 염색을 통하여 퍼옥시좀 활성을 검증하였다. 그 결과, 40μM 의 피탄산이 난자의 성숙뿐만 아니라, 난구세포의 확장률 증가와 배아의 발달에도 유의적 효과를 준다는 것을 확인하였다 ($P < 0.05$). 추가로, 피탄산은 퍼옥시좀 활성에 관련된 유전자, 단백질, 그리고 BODIPY 염색을 통한 지질대사를 유의적으로 증진시킨 것도 확인할 수 있었다 ($P < 0.05$). 또한 피탄산을 체외배양 시 첨가한 결과, 돼지 배아의 발달률 증가 및 퍼옥시좀의 활성에 유의적인 결과가 나타났다 ($P < 0.05$). 그러므로 위 연구에서는, 피탄산을 통해 난자의 성숙 및 발달 잠재능력을 유의적으로 증가시킬 수 있으며, 그 과정에서 퍼옥시좀이 중추적으로 관여한다는 것을 밝혀냈다.

세 번째로, 돼지 난자에서 Nrf2 기전의 조절과 이에 대한 퍼옥시좀 활성에 대한 변화를 조사하였다. Nrf2 기의 특이적 억제자인 brusatol 의 적정농도를 체외성숙 동안 처리하여 선정하고, 그 후 멜라토닌과 함께 체외성숙 과정에서 다시 한번 공동 처리하였다.

이 실험에서 멜라토닌과 brusatol 을 돼지 난자의 체외성숙 단계에서 처리하여, 난구세포 확장률을 검증하고 단일생식 유래 배아를 생산하였다. intracellular 적인 검증을 위해 면역염색, real time PCR, RNA sequencing, ATP/GSH/ROS 염색, 그리고 Western blot을 적용하였다. 그 결과, 12nM brusatol이 적정농도로 선정되어 멜라토닌과 함께 처리하였고, 성숙률 및 배아 발달 평가를 통해 각각의 화학물들에 대한 효과들을 유의적으로 확인하였다 ($P < 0.05$). 이 후, 유전자 및 단백질적 분석을 통해 Nrf2 기전과 퍼옥시좀의 활성이 난자 내에서 활발하게 조절되었음을 확인했을 뿐만 아니라 ($P < 0.05$), 항산화 기전도 유의적으로 조절되었다. 또한 RNA sequencing 을 통하여 보다 정확한 관계성을 난자 내에서 확인하였다. 결과적으로, Nrf2 기전과 퍼옥시좀 간의 상호 관계성이 분명히 있고, 난자의 성숙에 있어서 유의적인 영향을 끼친다는 것을 밝혀내었다.

마지막으로, 돼지 배아에서 Nrf2 기전과 퍼옥시좀의 활성에 대한 관계와 이에 따른 지질대사에 대해 조사하였다. 본 연구에서는 체외성숙, 단일생식, real time PCR, 면역염색, 그리고 BODIPY 염색법을 도입하였다. 최종적인 적용을 위해 멜라토닌과 피탄산을 돼지 체외배양 동안 함께 처리하였고, 확실한 확인을 위하여 siRNA 를 통한 퍼옥시좀 활성 관련 유전자인 *Pex19* 을

knockdown 하였다. 그 결과, 공동처리군에서는 유의적으로 높은 배아발달률을 보였고 (P < 0.05), siRNA 처리군에서는 유의적으로 낮은 배아 발달률을 보였다. 또한 위의 두 처리군을 기준으로, Nrf2 기전과 퍼옥시좀 활성관련 유전자 및 단백질 발현이 조절되었음을 확인하였다 (P < 0.05). 결과적으로, 위 연구를 통해 Nrf2 기전과 퍼옥시좀 활성이 돼지 배아 발달에 유의적 영향을 끼치는 것을 밝혀내었다.

결론적으로, 본 연구를 통해 Nrf2 기전과 퍼옥시좀 활성이 각각 돼지 배아 및 난자에 영향을 준다는 것을 확인하였다 (P < 0.05). 그 후, 이 둘의 상호적 관계를, 난자와 배아 내에서 체외성숙, 체외발달, 유전자 및 단백질적 발현을 통해 밝혀내었고, 난자 성숙 및 배아 발달 증진과정에서 중요한 역할을 한다는 것을 제시하였다.

.....

주요어: 항산화, 배아 발달, 지질 대사, Nrf2 기전, 퍼옥시좀 활성, 돼지, 난자 성숙

학번: 2018-25700